North Pacific Acoustic Laboratory CTD Data: R/V *Moana Wave* Cruise IW98 (August 15–30, 1998) and R/V *Melville* Cruise IW99 (June 18–July 3, 1999)

by S. Dickinson,[1] B.M. Howe,[1] and J.A. Colosi[2]

[1]*Applied Physics Laboratory, University of Washington, Seattle*

[2]*Naval Postgraduate School, Monterey, California*

Technical Memorandum

APL-UW TM 1-07

April 2007

Applied Physics Laboratory University of Washington

1013 NE 40th Street Seattle, Washington 98105-6698

Contract N00014-97-1-0259

Acknowledgments

We wish to thank the captains and crew of the R/V *Moana Wave* and R/V *Melville* for their help and hard work to make these cruises successful. We appreciate the excellent work from Le Olson (APL-UW) for setting the moorings and Lisa Day (Scripps Institution of Oceanography), Mitch Elend (APL-UW), and Bruce Cornuelle (Scripps) for data acquisition and analysis during the IW98 cruise. From the IW99 science team we wish to thank Mitch Elend (APL-UW), Matt Dzieciuch (Scripps), Americo Rivera (Scripps), Anna Teeter (Garfield High School, Seattle), and Mike Wolfson (Washington State University) for their exceptional work. This document was ultimately brought to completion by Rex Andrew (APL-UW).

The North Pacific Acoustic Laboratory project is sponsored by the Office of Naval Research (321OA) under grant number N00014-97-1-0259.

Contents

1. Introduction 1

2. Cruises 1

3. Instrumentation 4

4. Calibration 4

5. Data Processing 7

6. Pressure to Depth Conversion 8

7. Discussion 8

7.1 Data from IW98 8

7.2 Data from IW99 10

7.3 Comparison between IW98 and IW99 11

7.4 Comparison to Levitus Climatology 12

Sound Speed 12

Temperature 13

Salinity 13

7.5 Individual Cast Data 14

References 15

Figures 17

Appendix 147

1. Introduction

Two research cruises were conducted in the summers of 1998 and 1999 as part of the North Pacific Acoustic Laboratory (NPAL) project. The cruises' objective was to test the theory that predicts acoustic fluctuations from the internal wave sound speed or temperature fluctuations. Here we discuss the *in situ* profile measurements of temperature, salinity, and derived sound speed taken with conductivity temperature density (CTD) instruments dropped off the side of the ships as they steamed between the NPAL Acoustic Thermometry of Ocean Climate source off Kauai and a billboard receiving array on Sur Ridge off Point Sur, California. The first cruise, IW98, was aboard the University of Hawaii research vessel *Moana Wave*. The second cruise, IW99, was aboard the R/V *Melville*.

2. Cruises

On August 15, 1998, the R/V *Moana Wave* left Honolulu arriving in San Francisco on August 30. Thirty-two CTD casts were deployed along this cruise path (Figure 1a). The IW99 cruise began from Honolulu, on June 18, 1999, aboard the R/V *Melville*. Thirteen deep CTD casts to the ocean bottom and eleven shallow CTD casts to 1500 m were performed (Figure 1b). Seventeen shallow CTD casts were planned, but due to unusually strong trade winds, progress was slowed, and six shallow CTD casts were scrubbed, leaving some gaps mid-cruise.

Table 1 details the CTD profiles for IW98, giving the cast number, file name, maximum depth, date, time, latitude, and longitude of cast deployment. File name has the format of `jjjhhmm`, where `jjj` is the year day, `hh` and `mm` are the approximate hour and minute, respectively, local time. Longitudes are west of the dateline. All latitude and longitude values came from the `names.txt` file, except for Cast #31. Those values were obtained from the `2421143.HDR` file. Actual date and time values, which may differ slightly from the file name, came from the individual `<>.HDR` files (where `<>` refers to the file name). Maximum depths were obtained after data processing. Table 2 presents the same information for the IW99 cruise.

Table 1. R/V *Moana Wave* cruise IW98

Cast	File name	Depth	Date	Time	Latitude	W Longitude
1	2280551	1222.44	16-Aug-98	5:53	22.3575	159.5715
2	2281355	4762.75	16-Aug-98	13:55	22.9195	158.5731
3	2282327	1481.06	16-Aug-98	23:29	23.4837	157.5722
4	2290939	1498.82	17-Aug-98	9:40	24.0318	156.5715
5	2291846	4578.04	17-Aug-98	18:47	24.6900	155.3462
6	2300405	1496.85	18-Aug-98	4:06	25.1711	154.4185
7	2301309	5385.77	18-Aug-98	13:10	25.8101	153.1827
8	2310026	1481.06	19-Aug-98	0:28	26.4407	151.9241
9	2310936	5492.35	19-Aug-98	9:37	27.0567	150.6447
10	2312011	1512.63	19-Aug-98	20:13	27.6568	149.3694
11	2320951	5343.12	20-Aug-98	9:52	28.2416	148.2312
12	2331127	1506.71	21-Aug-98	11:28	28.7242	146.9968
13	2332143	4984.20	21-Aug-98	21:46	29.4141	145.3852
14	2340750	1516.57	22-Aug-98	7:52	29.9284	144.1420
15	2341703	5155.01	22-Aug-98	17:04	30.5165	142.6875
16	2350129	1465.28	23-Aug-98	1:31	30.8633	141.7723
17	2351111	4741.37	23-Aug-98	11:31	31.4534	140.5608
18	2352157	1500.79	23-Aug-98	21:58	31.9902	138.6494
19	2360705	1544.19	24-Aug-98	7:06	32.5063	137.1362
20	2362029	1500.79	24-Aug-98	20:30	33.2624	134.7774
21	2370050	1504.74	25-Aug-98	0:48	33.4367	134.1929
22	2371313	4830.76	25-Aug-98	13:15	33.5207	133.9373
22.5	2380134	2955.72	26-Aug-98	1:35	33.8569	132.7680
23	2380955	3006.66	26-Aug-98	9:55	34.1599	131.6669
24	2381921	5065.74	26-Aug-98	19:23	34.6440	130.2314
25	2390650	3002.74	27-Aug-98	6:47	34.9222	128.7619
26	2391658	4719.99	27-Aug-98	16:59	35.2769	127.2867
27	2400036	3030.16	28-Aug-98	0:37	35.4681	126.4517
28	2401051	3012.53	28-Aug-98	10:52	35.7970	124.9118
29	2401956	3708.81	28-Aug-98	19:57	36.0552	123.6654
30	2410551	1936.34	29-Aug-98	5:53	36.2820	122.5049
31	2421143	2590.95	30-Aug-98	11:44	37.3619	123.4939

Table 2. R/V *Melville* cruise IW99

Cast	File name	Depth	Date	Time	Latitude	W Longitude
1	1701235	916.02	19-Jun-99	12:36	22.3503	159.5769
2	1702114	4737.48	19-Jun-99	21:15	22.9828	158.4605
3	1710733	1520.52	20-Jun-99	7:36	23.6110	157.3365
4	1711653	1520.52	20-Jun-99	16:55	24.2285	156.2033
5	1720131	4811.33	21-Jun-99	1:32	24.8380	155.0595
6	1721556	1520.52	21-Jun-99	15:58	25.5735	153.6358
7	1722233	5385.77	21-Jun-99	22:34	26.0304	152.7384
8	1731008	1520.52	22-Jun-99	10:10	26.6122	151.5605
9	1731830	5440.03	22-Jun-99	18:32	27.1846	150.3716
10	1740409	1550.11	23-Jun-99	4:11	27.7466	149.1688
11	1741143	5296.59	23-Jun-99	11:45	28.2198	148.2409
12	1750626	1520.52	24-Jun-99	6:29	28.8383	146.7280
13	1751511	4970.61	24-Jun-99	15:12	29.3674	145.4888
15	1760815	4993.91	25-Jun-99	8:16	30.8830	141.6942
17	1770016	4334.76	26-Jun-99	0:18	31.3617	140.4030
20	1772306	5017.21	26-Jun-99	23:07	32.7232	136.6203
22	1781404	4986.15	27-Jun-99	14:05	33.4897	133.9753
24	1791204	5259.75	28-Jun-99	12:46	34.3358	131.0069
25	1792250	1686.16	28-Jun-99	22:53	34.6996	129.6139
26.5	1800748	4741.37	29-Jun-99	7:49	35.0481	128.2100
27	1801641	1520.52	29-Jun-99	16:42	35.3807	126.7929
28	1810030	4589.71	30-Jun-99	0:33	35.6958	125.3648
29	1810946	1522.49	30-Jun-99	9:47	35.9948	123.9255
30	1811715	1859.54	30-Jun-99	17:17	36.2733	122.4920

3. Instrumentation

Sea-Bird Electronics (SBE) 9plus CTD Underwater Unit, serial number 91685-87, was used for both cruises. This unit contains two temperature sensors (SBE model 3-02/F, serial numbers 843, primary and 848, secondary), two conductivity sensors (SBE model 4-02/O, serial numbers 484, primary and 485, secondary), one pressure sensor, (model Digiquartz 410K-023, serial number 26451), and a submersible pump (model SBE-5-02, serial number 128). During IW99 the secondary conductivity sensor, serial number 485, failed. It was replaced with a spare conductivity sensor, serial number 1880, of the same model number.

The CTD deck unit (model SBE 11, serial number 111685) performed 24 scans/s. The deck unit and the acquisition of data were controlled by a personal computer aboard the ship.

4. Calibration

Laboratory calibrations for the conductivity, temperature, and pressure sensors were performed by Sea-Bird Electronics before and after each cruise (Table 3). The secondary conductivity sensor, serial number 485, failed during the IW99 cruise and was replaced by serial number 1880 on June 28 before cast #24, file name 1791204.

Table 3. Calibration dates and number of days between calibrations

Sensor	S/N	pre-IW98	post-IW98	n	pre-IW99	post-IW99	N
Conductivity, primary	484	15-May-98	17-Sep-98	124	06-May-99	13-Jul-99	67
Conductivity, secondary	485	15-May-98	17-Sep-98	124	11-May-99	13-Jul-99	62
Conductivity, secondary	1880				25-Nov-98	13-Jul-99	229
Temperature, primary	843	14-May-98	17-Sep-98	125	05-May-99	13-Jul-99	68
Temperature, secondary	844	14-May-98	17-Sep-98	125	05-May-99	13-Jul-99	68
Pressure	26451	12-May-98	29-Sep-98	139	06-May-99	12-Jul-99	66

Many parameters are recorded during calibration at Sea-Bird Electronics, including what are known as the *g*, *h*, *i*, and *j* coefficients. These coefficients are part of non-linear

equations used to compute the measured variables of conductivity, temperature, or pressure. The *g*, *h*, *i*, and *j* values are unique for each sensor and change between calibrations. The sensor reading (computed measurement) changes slightly with time, by a slope and an offset, according to

$$corrected = slope \times computed + offset \tag{1}$$

Slope and offset values are also determined during calibration for each sensor. These values are interpolated to the day of sensor use by equations provided by Sea-Bird Electronics (Application Note No. 31, 2001). This operation is done after the cruise. The same pre-cruise *g*, *h*, *i*, and *j* coefficients are used and entered into the <>.con file for all CTD casts of a cruise (although different for each sensor). Post-cruise slope and offset values are modified to correct for sensor drift between the pre-cruise and post-cruise calibrations to the day of the cast. A linear drift is assumed.

Nominally the slope is set to 1.0 and the offset to 0.0. Offset values for the conductivity sensors are always set to this nominal value (personal communication, Norge Larsen, Sea-Bird Electronics, 2002). The slope for the conductivity sensors, however, is interpolated using the "post slope" value recorded on the calibration sheet. When this "post slope" is less than (greater than) one, the conductivity sensor has read a value too low (high). Equation (2) interpolates the slope to the day of the measurement.

$$islope = 1 + \frac{b}{n}\left(\frac{1}{postslope} - 1\right), \tag{2}$$

where *islope* is the interpolated slope to be entered into the `<>.con` file, *b* is the number of days since pre-cruise calibration, *n* is the total number of days between calibrations, and *postslope* is the post-cruise calibrated slope. The *islope* is different for each cast.

Temperature sensors also drift by an offset. Again the pre-cruise *g*, *h*, *i*, and *j* coefficients are used in the <>.con file, the same for each cast throughout the cruise. The post-cruise offset recorded on the calibration sheets is called '*delta T*'. The '*delta T*' is pre-cruise minus post-cruise, so if the '*delta T*' is positive, the temperatures after the pre-cruise calibration measure lower than the actual temperature. Therefore the measured temperature is added:

$$ioffset = deltaT\left(\frac{b}{n}\right), \tag{3}$$

where *ioffset* is the interpolated offset, *deltaT* is that reported on the calibration sheets (converted from m°C to °C) and *b* and *n* are as above. The *ioffset* value is entered into

the <>.con file, a different value for each cast. The slope values for the temperature sensors are always set to 1.0 in the <>.con file.

The slope and offset changes for the pressure sensor are so small that we can easily use either the pre-cruise, post-cruise, or the nominal values of 1.0 and 0.0, respectively (personal communication, Rick Bowman, Sea-Bird Electronics, 2002). The interpolated slopes for the conductivity sensors and the interpolated offsets for the temperature sensors used for IW98 and IW99 data processing are shown in tables in the Appendix.

The importance of interpolating slope values for the conductivity calibration and offset values for the temperature calibrations can be assessed with two cases. For cast #1, file name 2280551 on August 16 of IW98, we compute the derived variables using the interpolated values for slope and offset and the post-cruise values (Table 4). There are 32 days between day of cast and post-cruise calibration.

Table 4. Slope and offset values

Case 1: 2280551	Value		b/n
Conductivity (slope)	1.0001291	interpolated	92/124
Temperature (offset)	0.0005	interpolated	93/125
Conductivity (slope)	1.0001740	post-cruise	124/124
Temperature (offset)	0.0007	post-cruise	125/125

Case 2: 2351111	Value		b/n
Conductivity (slope)	1.0001389	interpolated	99/124
Temperature (offset)	0.00055	interpolated	100/125
Conductivity (slope)	1.0	pre-cruise	0/124
Temperature (offset)	0.0	pre-cruise	0/125

The differences in the derived variables (sound speed, temperature, salinity, and potential density) are shown in Figure 2a. The upper left panel shows that differences in sound speed are either zero or –0.01 m/s. (This discretization is due to the fact that the sound speed values are saved with two decimal places.) We compare these values to the differences between the measured sound speed and the Levitus climatology (see section 7.4), which is of order 10^{-2} as well. The interpolation may be important for sound speed. The differences in the temperature (Fibure 2a upper right panel) are close to –2e–4°C for the entire depth, with the range around that smaller than the range allowed by machine precision (hence the abnormal abscissa). The difference of the measured temperature from Levitus climatology at depth is of order 10^{-2}. The impact on salinity values is of the order of 10^{-3} psu, which is about one-tenth that of the difference between the measured salinity and Levitus climatological salinity. Potential density errors from not interpolating the slope and offset are of order 10^{-3} kg/m^3.

Figure 2b shows the effect of not interpolating the slope and offset for cast #17, file name 2351111 on August 23 of IW98, and using the pre-cruise values (Table 4) about 100 days prior to day of use. The effect is greater as the drift time is greater. Figure 2b shows the impact of interpolating these values.

5. Data Processing

There are many steps involved in the post-cruise data processing (Sea-Bird Electronics, 1998). Using SEASOFT subroutines or modules, the raw data are converted to engineering units using the module DATCNV. The data then go through three cycles of editing to remove wild data points (WILDEDIT). The casts are split into upcast and downcast (SPLIT module); only the downcasts are saved and analyzed. The CELLTM module removes conductivity cell thermal mass effects from the measured conductivity with a recursive filter. The conductivity and the pressure data are low-pass filtered (FILTER module) with the nominal time constants of 0.03 s and 0.15 s for the conductivity and pressure, respectively. LOOPEDIT removes data when the cast has slowed down (to less than 0.250 m/s) or reversed. Finally, the data are bin averaged in two-decibar pressure bins (BINAVG module) before being saved to ascii output files (ASCIIOUT module).

These processing steps eliminate noise. Here we examine three data files; each represented by four figures. The first figure shows the raw data and the final processed data overlaid. The three figures following show the profiles after each processing step for sound speed, density, primary and secondary temperature, and primary and secondary salinity profiles.

Figure 2 represents the raw and final data from cast #1 (file name 2280551, IW98). Figure 3 through 6 show the effect of the processing steps. There are no obvious problems in the data.

Figure 6 represents the raw and final data from cast #17 (file name 2351111, IW98). This is a deep profile. The effects of the data processing steps are shown in Figure 7 through Figure 9. Although these data contained bad values, the WILDEDIT processing seems to have improved the data.

Figure 10 represents the raw and final data from cast#11 (file 1741143, IW99). Figure 11 through Figure 13 show the effects of the data processing. There were major problems with the secondary salinity profile (primary salinity only is shown in Figure 10). The secondary salinity profile still contained bad data at the end of the processing. The entire profile of secondary salinity from this cast was discarded from the dataset.

A few data files contained a couple obviously wrong data points even after the processing. These were edited manually from the profile. The bulk of the profile remained in the data set.

6. Pressure to Depth Conversion

The conversion of pressure to depth is discussed in Sea-Bird Electronics, Inc., Application Note No. 69, and is repeated here for completeness. The ocean water column is assumed to be 0°C and 35 psu. Gravity is expressed as a function of pressure and latitude:

$$g = 9.780318 \cdot \left[1.0 + (5.2788 \times 10^{-3} + 2.36 \times 10^{-5} \cdot x) \cdot x\right] + 1.092 \times 10^{-6} \cdot p \,,$$

where g is in m/s^2, $x = \left[\sin(latitude)/57.29578)\right]^2$, and p is pressure in decibars. A latitude value of 25° was used for all casts regardless of location so that there is an easy method to return to pressure from depth. Depth is then calculated from pressure with

$$depth = \left[\left(\left(\left(-1.82 \times 10^{-15} \cdot p + 2.279 \times 10^{-10}\right) \cdot p - 2.2512 \times 10^{-5}\right) \cdot p + 9.72659\right) \cdot p\right] / g \,,$$

where *depth* is in meters.

7. Discussion

The data from the IW98 and IW99 cruises are discussed and compared, particularly at depth. A comparison between the data and Levitus (*Levitus*, 1998) climatology follows.

7.1 Data from IW98

Figure 14 represents range-averaged profiles of sound speed, temperature, salinity, and potential density for IW98. Range is the distance along the cruise path. Range was computed using the latitude and longitude of each cast, relative to that of the first cast assuming a spherical earth. The data were then interpolated in range to the 40-km grid spacing of the Levitus data along the same transect. A simple arithmetic mean was then computed. The measurements of all casts were not taken at exactly the same depths along the profile, so we matched the depths prior to interpolation and computation of the mean.

Individual profiles are plotted sequentially and rotate through the following seven colors; black, yellow, blue, magenta, cyan, red, and green. Each cast has the same color throughout the plots for IW98.

Sound speed profiles (Figure 15) are divided into those from the surface down to 2200 m (Figure 16) and those from 2000 m to the ocean bottom (Figure 17). The colors of the casts can be seen more clearly in the related figure, Figure 36.

Primary temperature profiles (Figure 18) are divided into those from the surface down to 2200 m (Figure 19) and from 2000 m to the ocean bottom (Figure 20). Similarly, secondary temperature profiles are shown in Figure 21 through Figure 23, and primary salinity profiles are shown in Figure 24 through Figure 26.

Secondary salinity profiles (Figure 27) from the surface down to 2200 m (Figure 28) and at depth, from 2000 m down to the ocean bottom (Figure 29), are shown. The secondary salinity profiles at depth are not bundled as the primary salinity profiles (Figure 26). The first four deep casts are labeled on the figure. The secondary salinity from Cast #2 was larger than that measured from the primary sensor (compare to Figure 26). The salinity from the next three deep casts show the values increasing, suggesting that the measured salinity increased with time or in an eastward direction across the Pacific Ocean. This was not observed in the primary salinity data. This issue is examined in more detail in the comparison of the two cruises.

Potential density profiles (Figure 30) are divided into those from the surface down to 2000 m (Figure 31) and those from 2000 m down to the ocean bottom (Figure 32).

Temperature-salinity plots are shown for the primary (Figure 34) and the secondary (Figure 34) sensors. Temperature-salinity plots for below 2000 m are shown in Figure 35a for the primary sensors and Figure 36b for the secondary sensor. The issue of the secondary salinities, discussed above, is evident in panel (b).

To aid viewing the profiles they are plotted with a separation between each. Sound speed profiles (Figure 36) are plotted with a separation of 10 m/s between profiles. The entire profile (Figure 36a) and the top 1000 m (Figure 36b) of the profile are shown.

Temperature profiles from the surface to the ocean bottom (Figure 37) for both (a) the primary and (b) the secondary temperature profiles are separated by 10°C. The difference between the primary and secondary temperature profiles ranges from +/–0.1°C (Figure 37c). Figure 38 is similar to Figure 37, except it shows the top 1000 m.

Salinity profiles from the surface to the ocean bottom (Figure 39) for both (a) the primary and (b) the secondary salinity profiles are separated by 10 psu. The difference between the primary and secondary salinity profiles are on the order of a few hundredths of one psu (Figure 39c). As in Figure 29, the first four deep casts are labeled. Figure 40 is similar to Figure 39, except it shows the top 1000 m. The first five casts are labeled.

Potential density profiles (Figure 41) are each shifted by 10 kg/m^3. Panel (a) shows entire profiles and panel (b) the top 1000 m.

7.2 Data from IW99

The range-averaged profiles of sound speed, temperature, salinity, and potential density for IW99 (Figure 42) were computed the same as for the IW98 cruise. The range averaging was particularly important for these data as the physical spacing between casts was quite large in the middle of the cruise (Figure 1). As with the profiles from IW98, the IW99 profiles are color coded with one of seven colors; black, yellow, blue, magenta, cyan, red, and green, and plotted sequentially. Each cast retains the same color throughout this section.

Sound speed profiles (Figure 43) are divided into those from the surface down to 2200 m (Figure 44) and at depth, from 2000 m to the ocean bottom (Figure 45). The colors of the casts can be seen more clearly in the related figure (Figure 64). Primary temperature profiles (Figure 46, Figure 47, and Figure 48), secondary temperature profiles (Figure 49, Figure 50, and Figure 51), and primary salinity profiles (Figure 52, Figure 53, and Figure 54) are similarly represented.

Secondary salinity profiles (Figure 55) are divided into those from the surface down to 2200 m (Figure 56) and those from 2000 m down to the ocean bottom (Figure 57). Many of the secondary salinity profiles were removed. During the deep portion of Cast #7, the salinity measurement spiked. Subsequent casts (#8, 9, 10, 11, 12, 13, 15, 17, 20, and 22) were plagued by bad data from the secondary conductivity sensor; these data were not removed or resolved in the processing so they were removed manually. Eventually, this sensor, serial number 485, was replaced with a spare, serial number 1880, on cast #24 (there was no cast #23).

Potential density profiles (Figure 58) are divided into those from the surface down to 2200 m (Figure 59) and those from 2000 m down to the ocean bottom (Figure 60).

Temperature-salinity plots are shown for the primary (Figure 61) and the secondary (Figure 62) sensors. Temperature-salinity plots for below 2000 m are shown in Figure 63a for the primary sensors and Figure 64b for the secondary sensors. The difference in salinity between secondary conductivity sensor number 485 and sensor number 1880 is evident in panel (b). The salinity values from sensor number 1880 correspond well with those from the primary sensor.

Sound speed profiles are plotted with a 10 m/s separation between profiles (Figure 64). The entire profile (Figure 64a) and the top 1000 m (Figure 64b) are shown.

Temperature profiles from the surface to the ocean bottom (Figure 65) for both (a) the primary and (b) the secondary temperature profiles are separated by 10°C. The difference between the primary and secondary temperature profiles ranges from +/–0.1°C (Figure 66c). Figure 66 is similar to Figure 65, except it shows the top 1000 m.

Salinity profiles from the surface to the ocean bottom (Figure 67) for both (a) the primary and (b) the secondary salinity profiles are separated by 10 psu. The missing profiles in panel (b) were removed (casts #8, 9, 10, 11, 12, 13, 15, 17, 20, and 22) as discussed above. The difference between the primary and secondary salinity profiles (Figure 67c) again shows the difference between data from the secondary conductivity sensors. Figure 68 is similar to Figure 67, except it shows the top 1000 m.

Potential density profiles (Figure 69) are each shifted by 10 kg/m^3. Entire profiles (panel a) and the top 1000 m (panel b) are shown.

7.3 Comparison between IW98 and IW99

The range-averaged means of sound speed, primary temperature, primary salinity, and potential density are plotted in Figure 70 with IW98 in blue and IW99 in red. Figure 71 shows these means from 2000 m down to the ocean bottom. The range-averaged primary salinity from IW98 is larger than that from IW99 for the entire profile. The same is true for the range-averaged potential density; larger for IW98 than for IW99.

Differences in the range-averaged means (IW98 cruise minus IW99 cruise) are shown in Figure 72 for the top 1000 m and in Figure 73 for below 1000 m. Panels (a) and (b) in Figure 73 have very similar profiles, showing the strong sound speed dependence on temperature. Salinity and potential density difference profiles in Figure 73 (c) and (d), respectively, are also quite similar. The near zero differences in temperature leave the potential density difference profile (d) looking very much like that of the salinity (c). The rather large difference in salinity, almost 0.01 psu, does not seem realistic.

Sound speed profiles at depth are shown for both cruises in Figure 74. This figure is not very illuminating. Figure 75 shows the demeaned sound speed profiles for each cruise. There is more variance in the IW98 cruise, although the differences are quite small for both, less than 0.5 m/s.

Primary temperature profiles at depth are shown for both cruises in Figure 76. Secondary temperature profiles at depth are shown in Figure 77. The temperatures at depth changed very little over the year.

Primary salinity profiles at depth are shown for both cruises in Figure 78. The salinity profiles for each year are nicely bundled, but the difference of almost 0.01 psu between the two bundles is not thought to be physically realistic. We look to the secondary salinity profiles (Figure 79) to help determine which year has the better salinity data. In panel (a) of Figure 79, we see that the IW98 secondary salinity measurements (from sensor number 485) are larger than those from the primary sensor (panel (a) of Figure 78.) The secondary salinity profiles are not nicely bundled, increasing rapidly during the cruise. In

panel (b) of Figure 79, we see the first three deep salinity profiles from IW99 taken with sensor 485 and the last three deep salinity profiles taken with sensor number 1880. Again the measurements from sensor number 485 are larger than those from the primary sensor (panel (b) of Figure 78.) The measurements from sensor number 1880 lie right on top of those from the primary sensor. This suggests that the primary salinity measurements from IW99 are more accurate than those from the IW98 cruise. The comparison to Levitus data is made in section 7.4 Comparison to Levitus Climatology.

Potential density profiles at depth are shown for both cruises in Figure 80. The shift to lower potential densities from IW98 to IW99 is due to the density dependence on salinity.

Temperature-salinity profiles from the primary sensors at depth are shown in Figure 81. The IW98 salinity measurements are again larger than those from IW99. Temperature-salinity profiles from the secondary sensors at depth are shown in Figure 82. The problem with the secondary conductivity sensor number 485 is again evident.

7.4 Comparison to Levitus Climatology

Levitus climatology data (courtesy of B. Cornuelle) for sound speed, temperature, and salinity from August were used for the IW98 comparison and the Levitus data from June for the IW99 comparison. Below about 700 m there are no monthly means in the Levitus data, only an annual mean. All figures are presented in the same manner. The color images in the left two panels of each figure show sound speed as a function of depth and range. Range is the distance in km from the first cast of the cruise. The two panels on the right show the range-averaged profiles. Levitus data are available at thirty-three depths. They are interpolated to the depths from the CTD data, which are on a much finer grid. The cruise data, however, are coarse in range and thus are interpolated to that of the Levitus climatology, which is on a 40-km grid.

Sound Speed

Sound speed data from Levitus for August (Figure 83) and from IW98 (Figure 84), as well as the sound speed differences, IW98 data minus Levitus for August, are shown (Figure 85). The range-averaged differences in the upper ocean (above 700 m) are 0–2 m/s, with the IW98 values smaller than the Levitus climatology. The range-averaged differences in the deeper ocean (below 700 m) are less than 0.1 m/s for most of the profile. We neglect the very deepest portion of the profile due to small sample size.

Sound speed data from Levitus for June (Figure 86) and from IW99 (Figure 87), as well as the sound speed differences, IW99 data minus Levitus for June (Figure 88), are shown. The range-averaged differences for both the upper ocean and the deeper ocean are of the same order as they are for IW98/Levitus August differences (Figure 85). Considering

Figure 72(a) for the upper ocean and Figure 73(a) for the deeper ocean, it is apparent that the differences between the two cruises are of the same order as either differs from Levitus.

Temperature

Temperature data from Levitus for August (Figure 89) and IW98 temperature data (Figure 90), as well as the temperature differences, IW98 data minus Levitus for August (Figure 91), are shown. The range-averaged differences in the upper ocean temperature are less than 1°C; the IW98 temperature values are lower than the Levitus climatology. The differences in the deeper ocean are less than 0.1°C.

Levitus temperature data for June (Figure 92) and from IW99 (Figure 93), as well as the temperature differences, IW99 data minus Levitus for June (Figure 94), are shown. The range-averaged differences in the upper ocean are less than 1°C. The differences in the deeper ocean are very similar to the differences between the IW98 cruise and August Levitus data (Figure 91). Considering Figure 72(b) the differences in the range-averaged temperature between cruises are of the same order as either cruise differs from the other. In the deeper ocean the differences between cruises is less than either cruise differs from Levitus.

Salinity

Levitus salinity data for August (Figure 95), IW98 salinity data (Figure 96), and the salinity differences, IW98 data minus Levitus for August (Figure 97), are shown. The range-averaged differences in the upper ocean are about 0.1 psu. The differences in the deeper ocean are about 0.01 psu, with the IW98 data showing greater salinity values than Levitus.

Levitus salinity data for June (Figure 98), IW99 salinity data (Figure 99), and the salinity differences, IW99 data minus Levitus data for June (Figure 100), are shown. The range-averaged differences in the upper ocean are about 0.1 psu, similar to that of IW98/Levitus August. The differences in the deeper ocean are less than half those of the IW98/Levitus August differences.

Acknowledging that the salinity across the entire range for the entire depth of the ocean cannot change by 0.01 psu in one year, which cruise had the more accurate data? The IW99 primary salinity data are corroborated by the three secondary salinity profiles from the spare conductivity sensor (serial number 1880). The IW99 salinity data are more similar to Levitus climatological salinity data. It has been suggested to remove the IW98 primary salinity bias by subtracting the difference in the means of the primary salinity data (mean of IW98 data minus mean of IW99 data). Or because the salinity measurements are perhaps suspect in general, users may wish to merge the Levitus salinity data at depth to the measured salinity data in the shallower water.

7.5 Individual Cast Data

The data from all of the individual casts are plotted in Figures 101–129.

References

Levitus, S., T.P. Boyer, M.E. Conkright, T. O'Brien, J. Antonov, C. Stephens, L. Stathoplos, D. Johnson, and R. Gelfeld, *World Ocean Database 1998 Volume 1: Introduction*, NOAA Atlas NESDIS 18, U.S. Government Printing Office, Washington, D.C., 1998, 346 pp.

Sea-Bird Electronics, Inc., *Computing Temperature and Conductivity Slope and Offset Correction Coefficients from Laboratory Coefficients and Salinity Bottle Samples*, Application Note No. 31, September 2001, 5 pp.

Sea-Bird Electronics, Inc., *Conversion of Pressure to Depth*, Application Note No. 69, July 2002, 1 p.

Sea-Bird Electronics, Inc., *CTD Data Acquisition Software SEASOFT, v. 4.233*, May 1998, 141 pp.

Figures

(a)

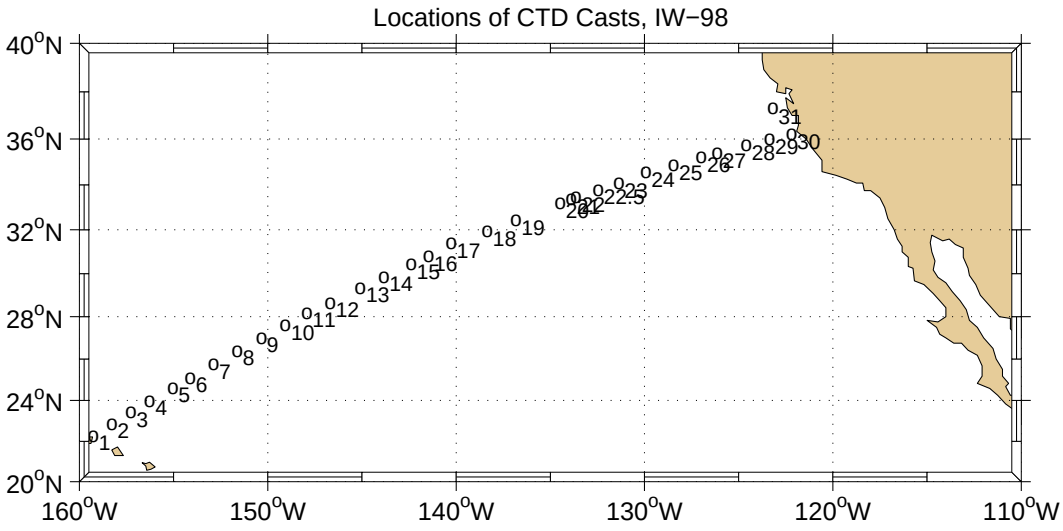

(b)

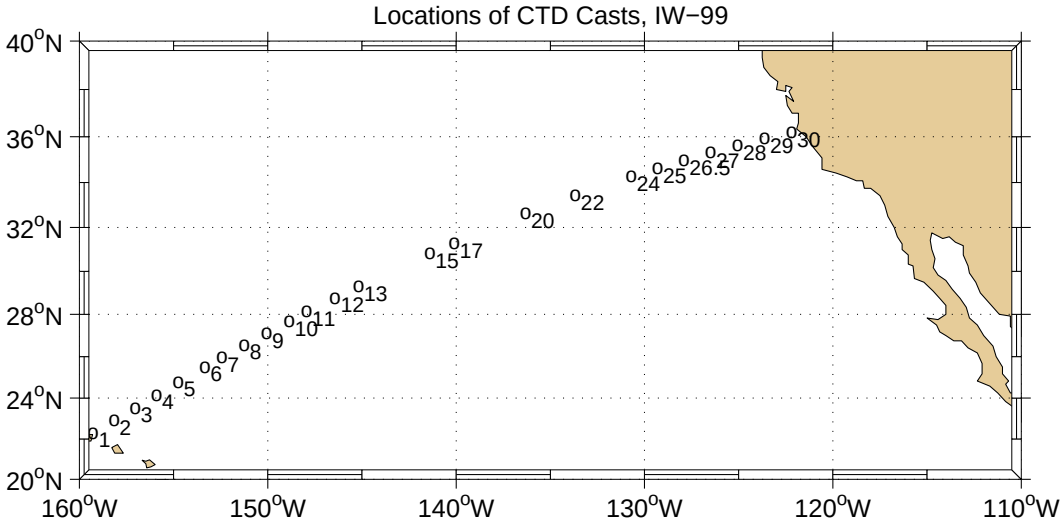

Figure 1. (a) Locations and numbers of the CTD casts from the IW98 cruise, August 15 – 30, 1998. (b) Same as in (a), except for the CTD casts from the IW99 cruise, June 18 – July 3, 1999.

(a)

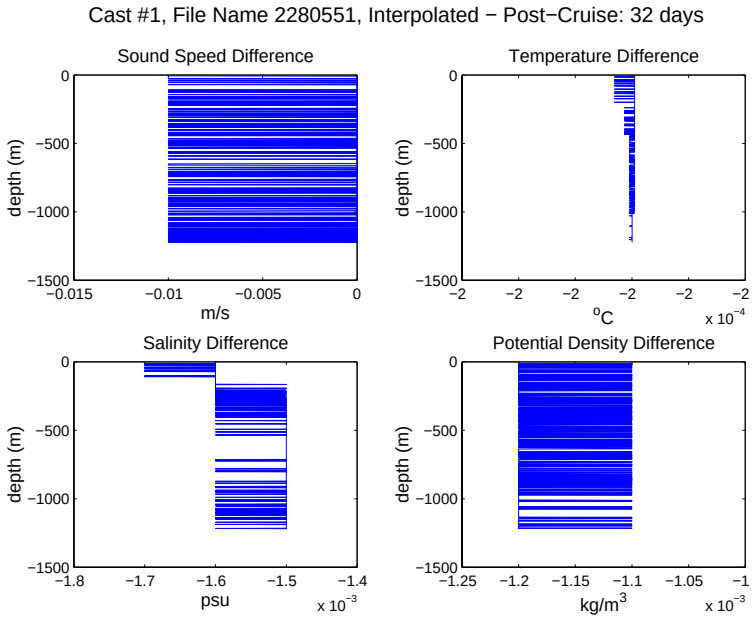

(b)

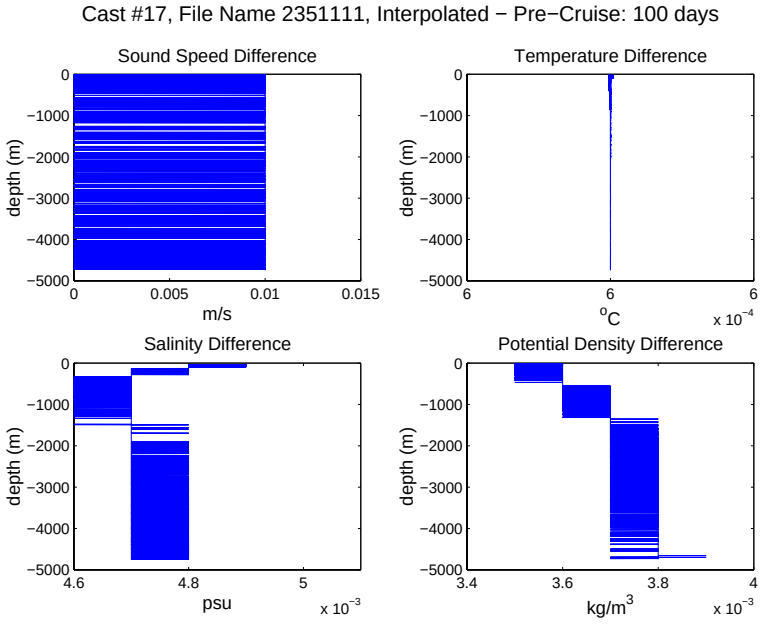

Figure 2. (a) Differences in the derived variables (sound speed, temperature, salinity and potential density profiles) with interpolated calibration values minus post-cruise calibration values for Cast #1 on IW98. (b) Differences in the same variables with interpolated calibration values minus post-cruise calibration values for Cast #17 of IW98.

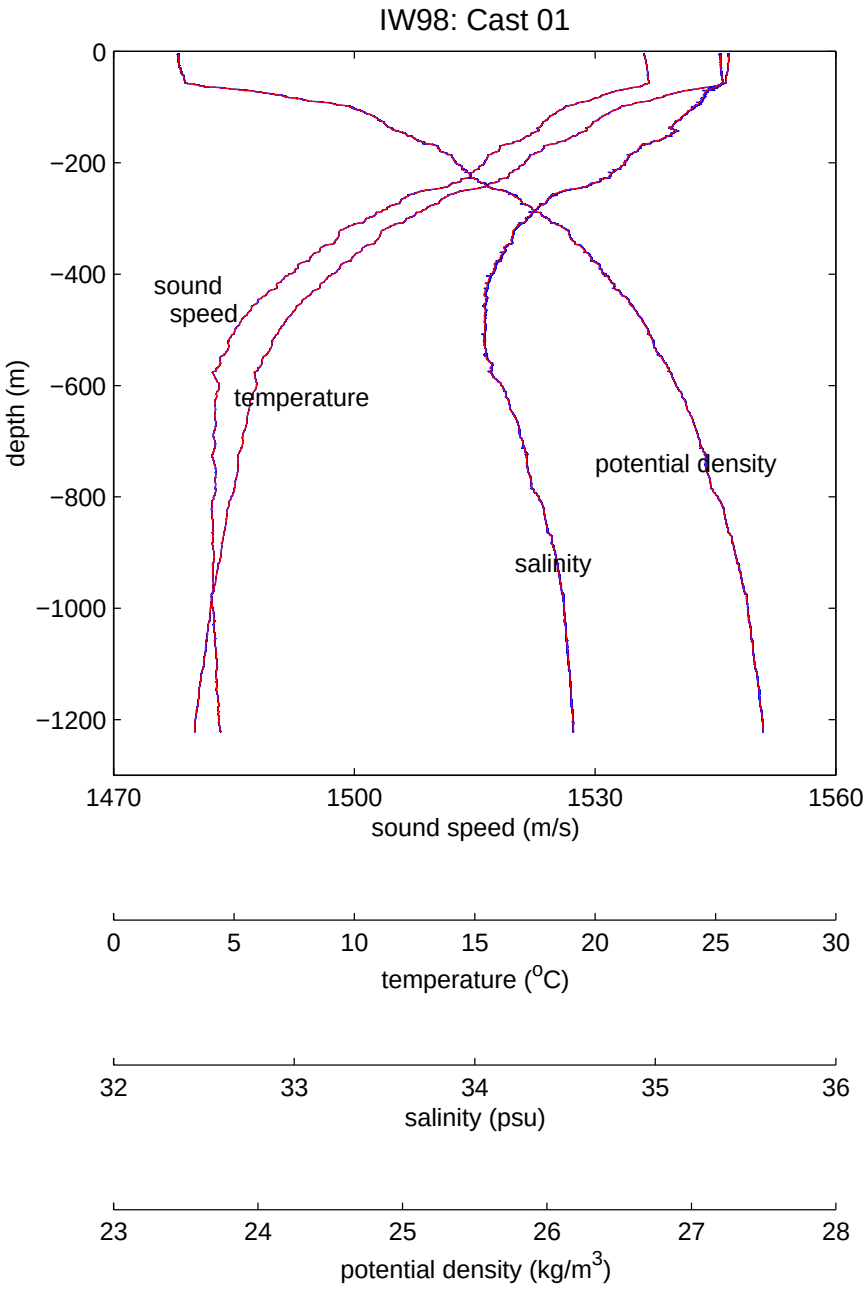

Figure 2. Sound speed, temperature, salinity, and potential density profiles for Cast#1, file name 2280551 on IW98 pre-processing (blue) and post-processing (red).

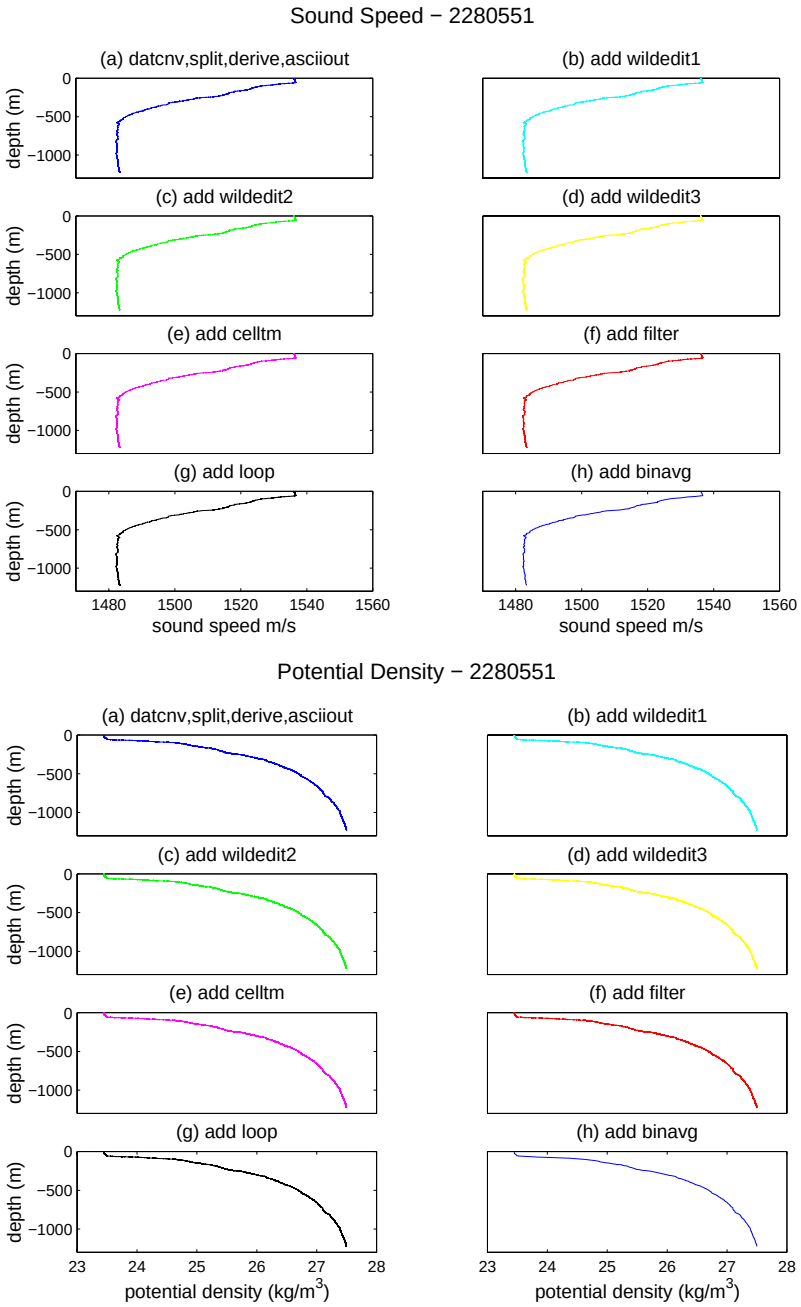

Figure 3. Sound speed and potential density profiles for Cast #1, file name 2280551 of IW98 for each step of the data processing. Top and bottom panels are similar. (a) Raw data after conversion to engineering units. (b), (c), and (d) Data after screening for wild data points, once, twice, and three times, respectively. (e) Data corrected for thermal mass effects. (f) Effect of a low-pass filter, (g) data after removal of slow or reversed downward motion, and (h) data after averaging into two-decibar pressure bins.

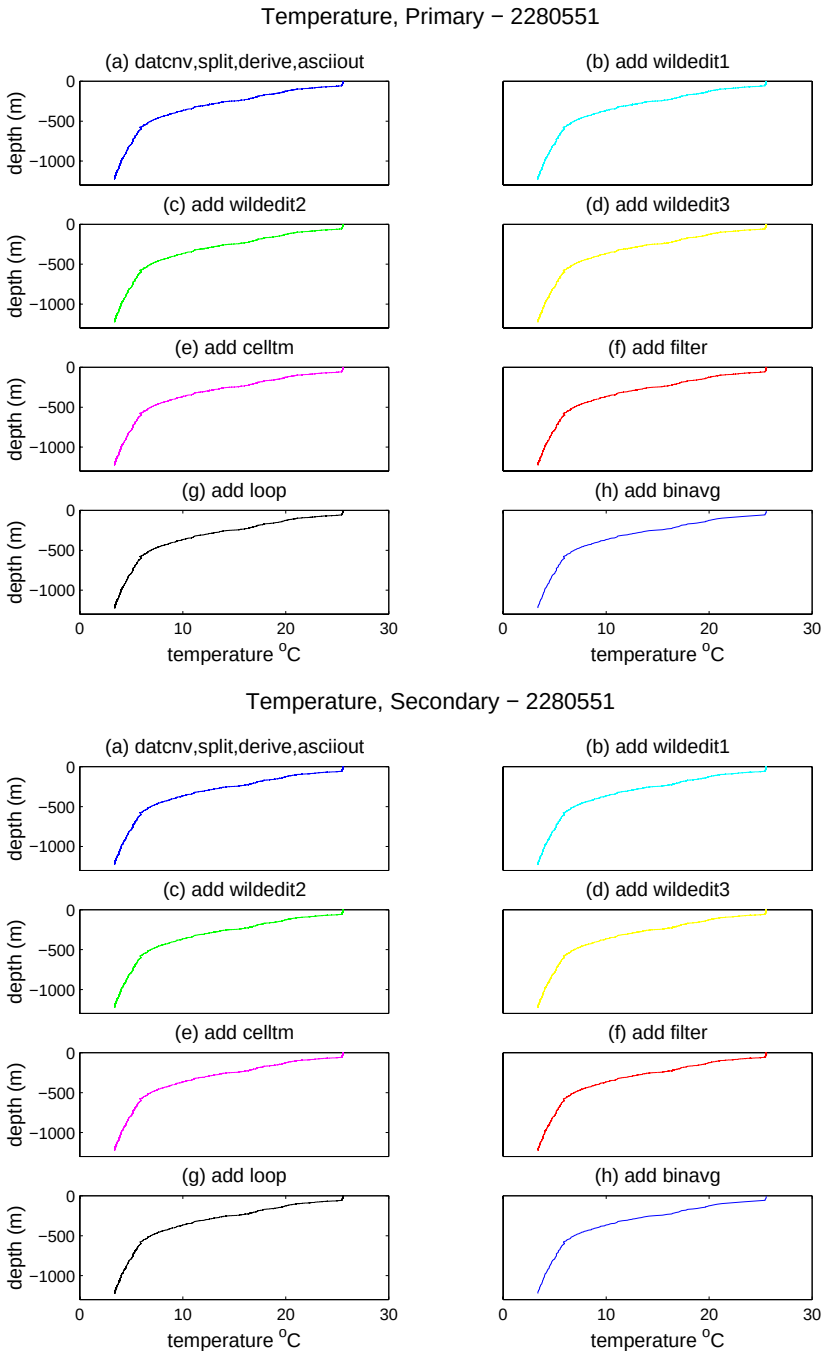

Figure 4. Same as in Figure 3, except for the primary temperature profile (top) and secondary temperature profile (bottom).

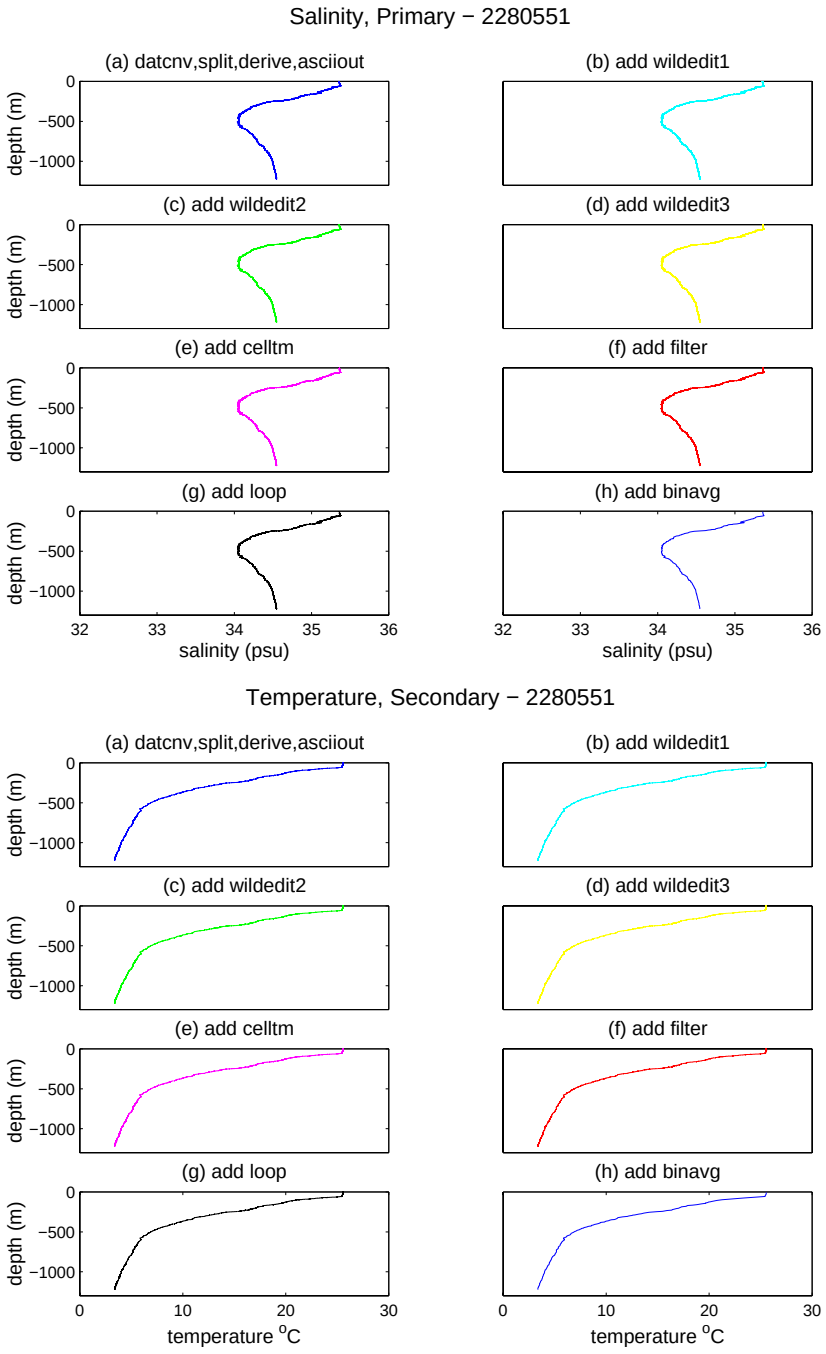

Figure 5. Same as in Figure 3, except for primary salinity profile (top) and secondary salinity profile (bottom).

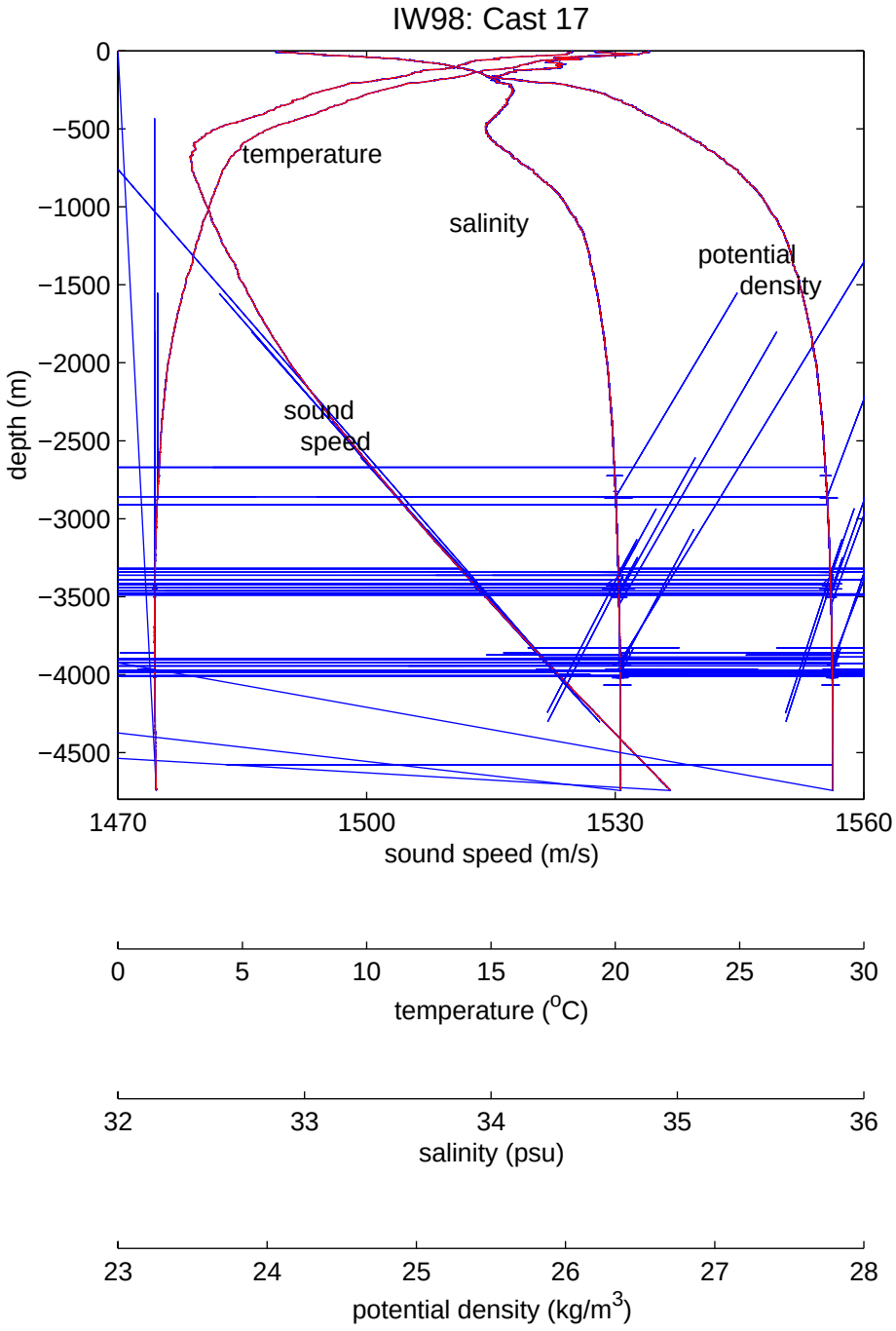

Figure 6. Sound speed, temperature, salinity, and potential density profiles for Cast #17, file name 2351111 on IW98, pre-processing (blue) and post-processing (red).

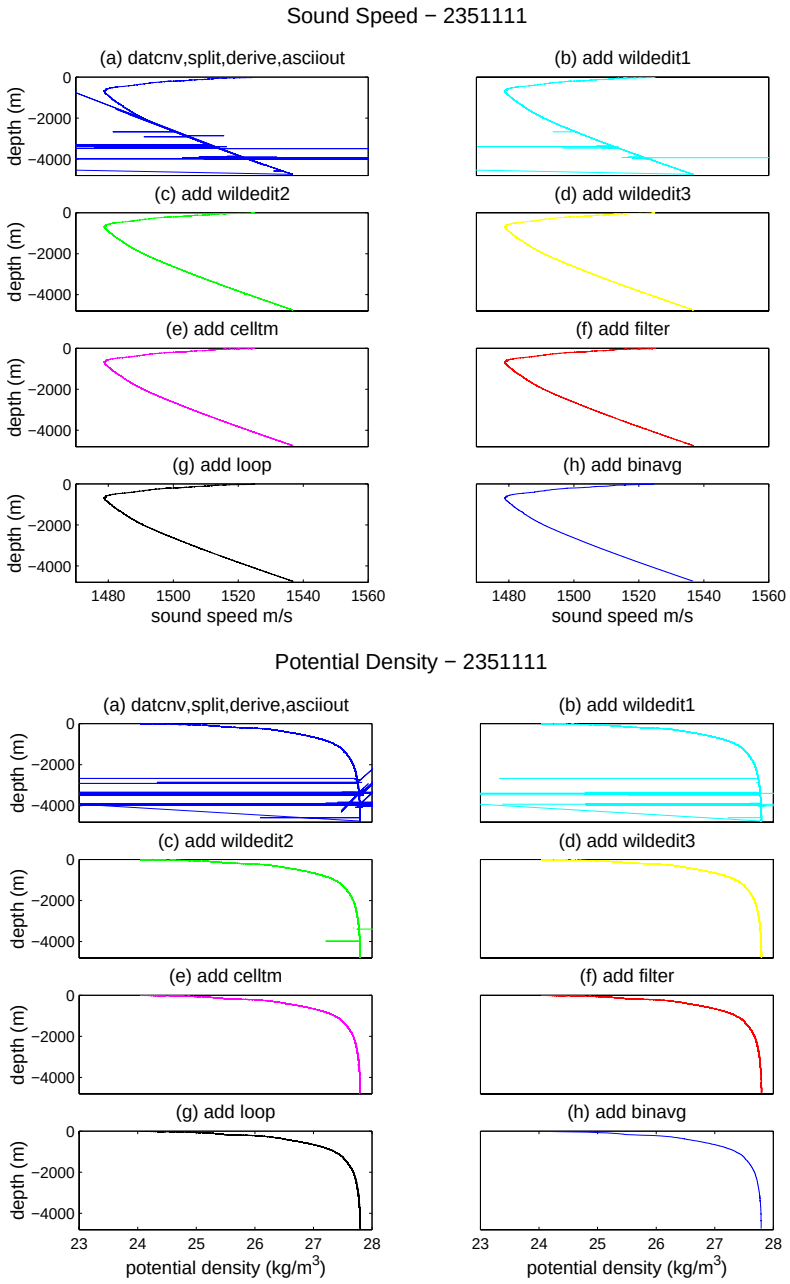

Figure 7. Sound speed and potential density profiles for Cast #17, file name 2351111 of IW98 for each step of the data processing. Top and bottom panels are similar. (a) Raw data after conversion to engineering units. (b), (c), and (d) Data after screening for wild data points, once, twice, and three times, respectively. (e) Data corrected for thermal mass effects. (f) Effect of a low-pass filter, (g) data after removal of slow or reversed downward motion, and (h) data after averaging into two-decibar pressure bins.

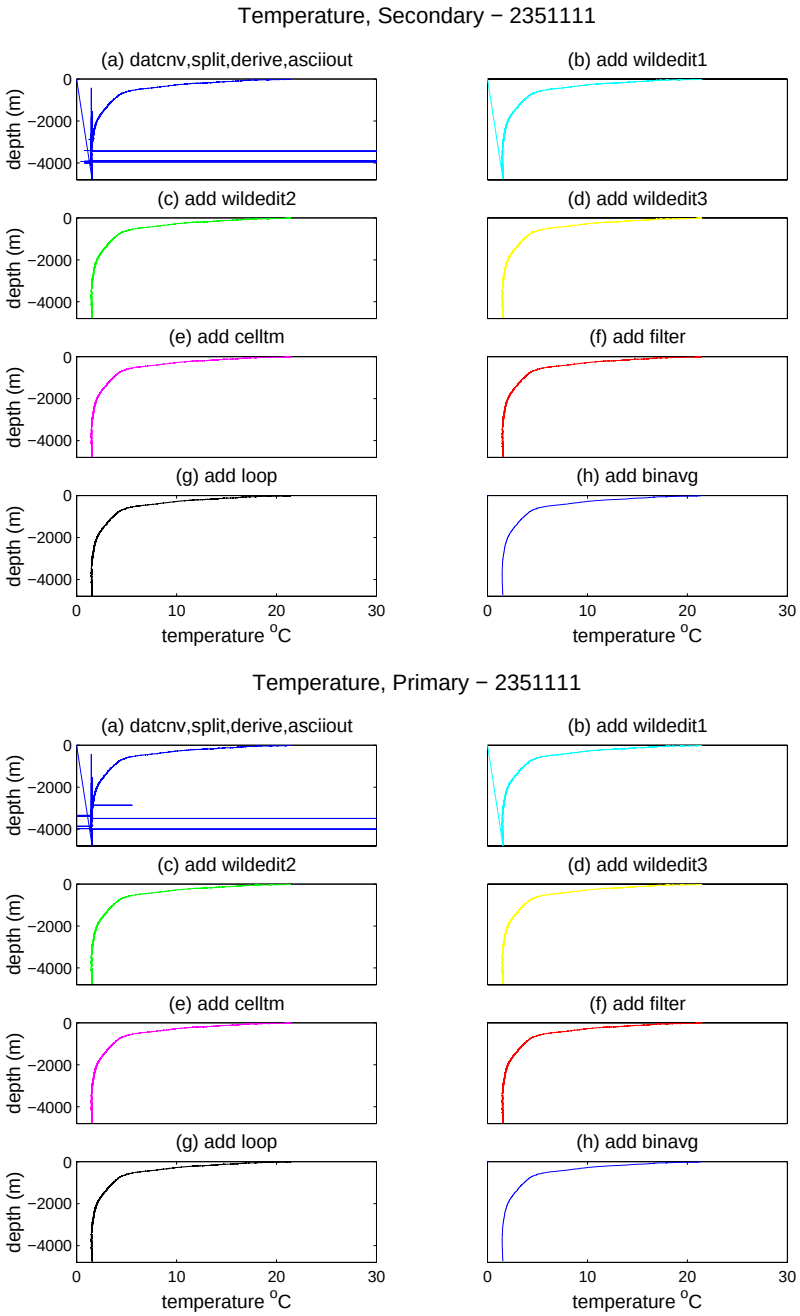

Figure 8. Same as in Figure 7, except for the primary temperature profile (top) and secondary temperature profile (bottom).

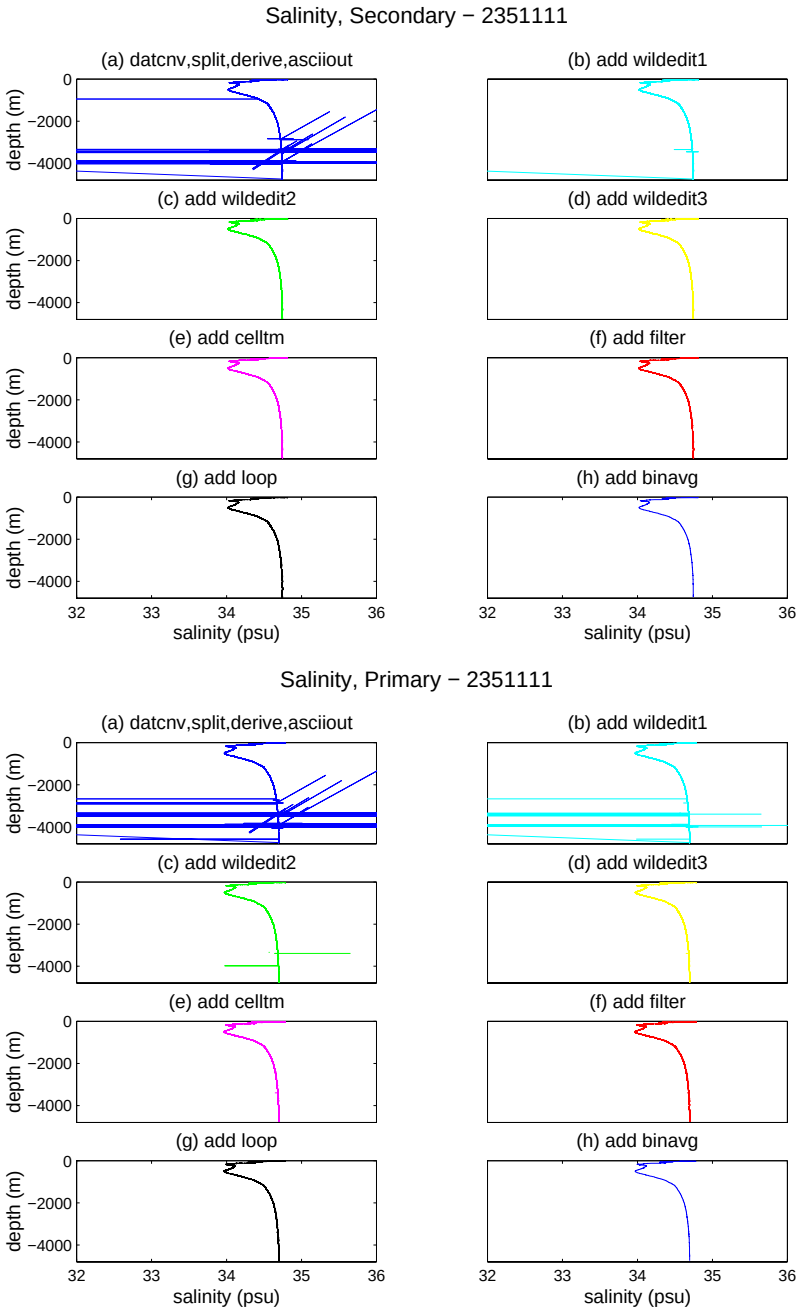

Figure 9. Same as in Figure 7, except for primary salinity profile (top) and secondary salinity profile (bottom).

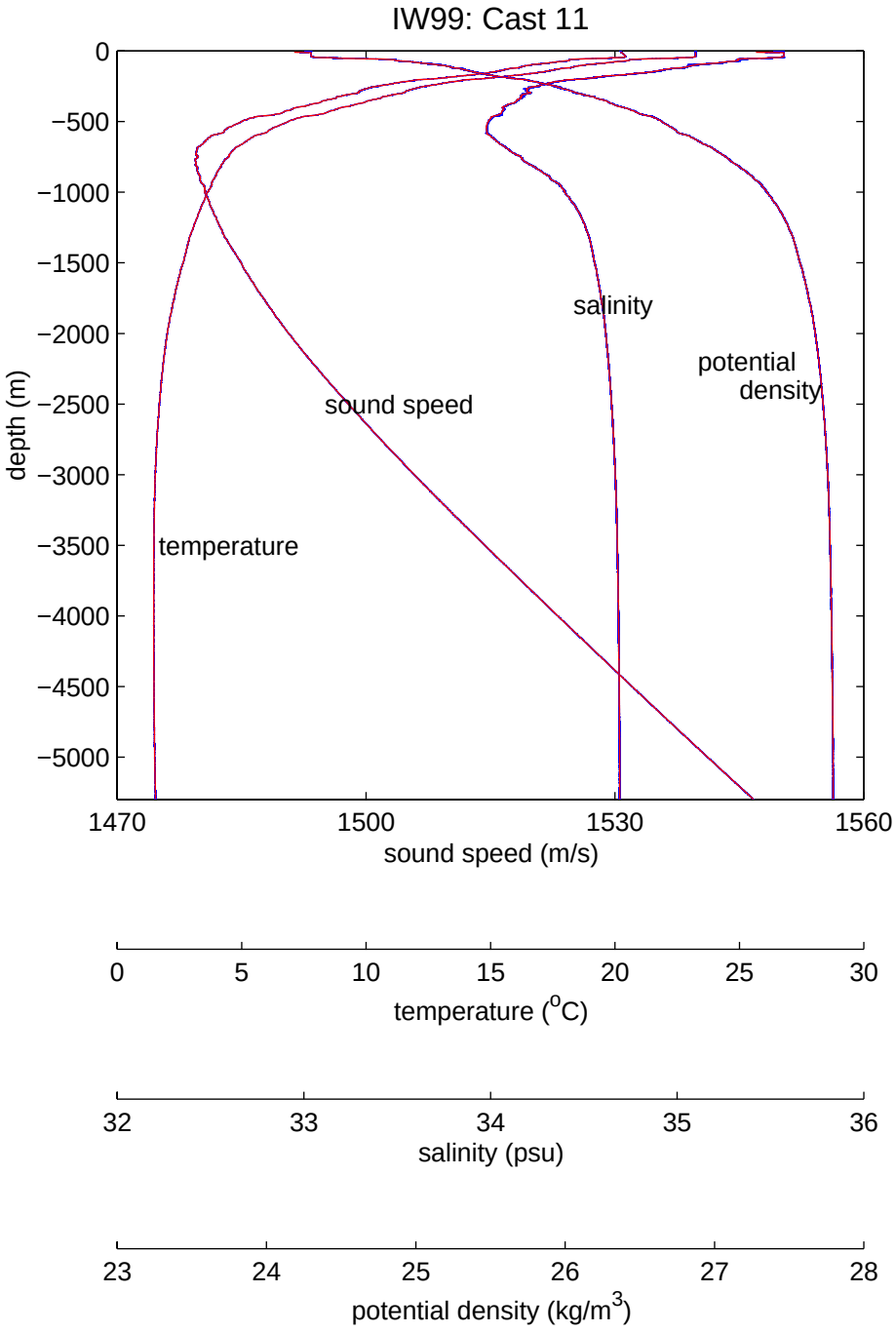

Figure 10. Sound speed, temperature, salinity, and potential density profiles for Cast 11 (1741143) on IW99, pre-processing (blue) and post-processing (red).

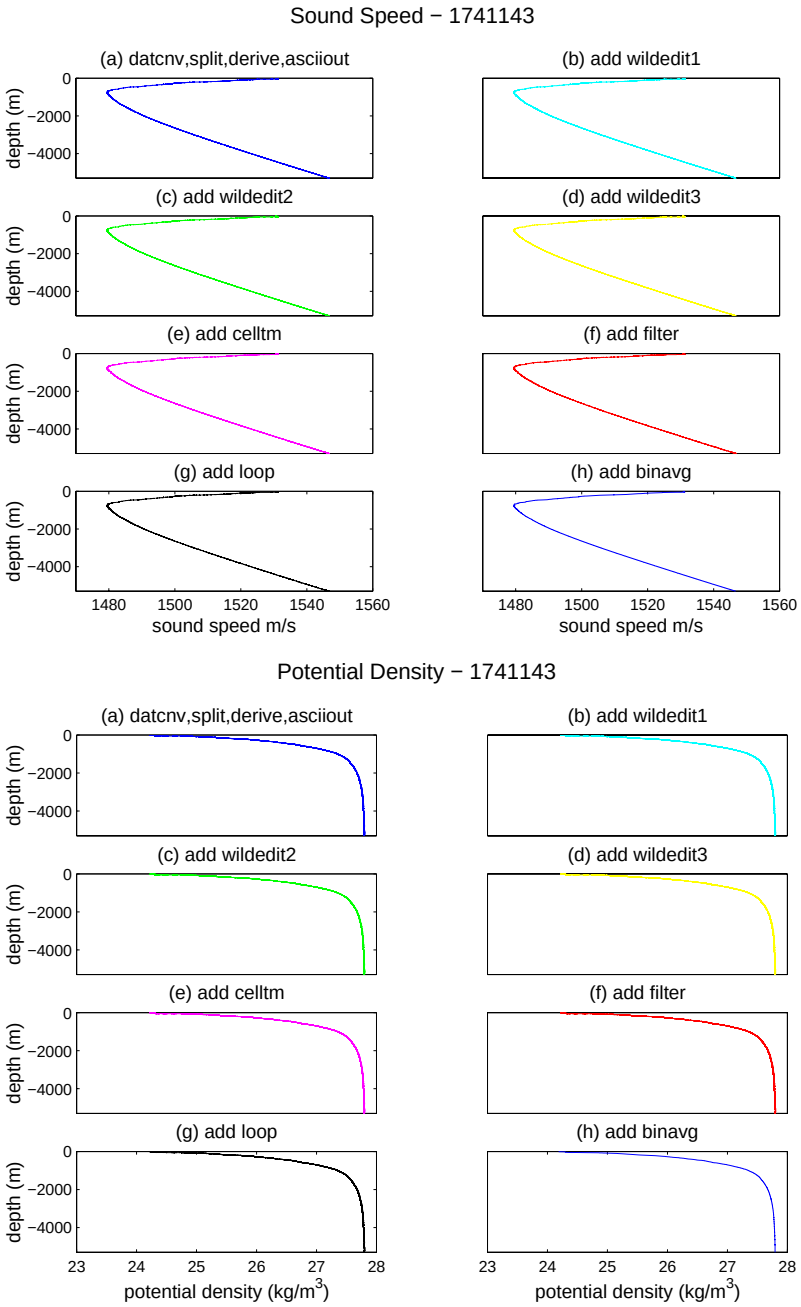

Figure 11. Sound speed and potential density profiles for Cast #11, file name 1741143 of IW99, for each step of the data processing. Top and bottom panels are similar. (a) Raw data after conversion to engineering units. (b), (c), and (d) Data after screening for wild data points, once, twice, and three times, respectively. (e) Data corrected for thermal mass effects. (f) Effect of a low-pass filter, (g) data after removal of slow or reversed downward motion, and (h) data after averaging into two-decibar pressure bins.

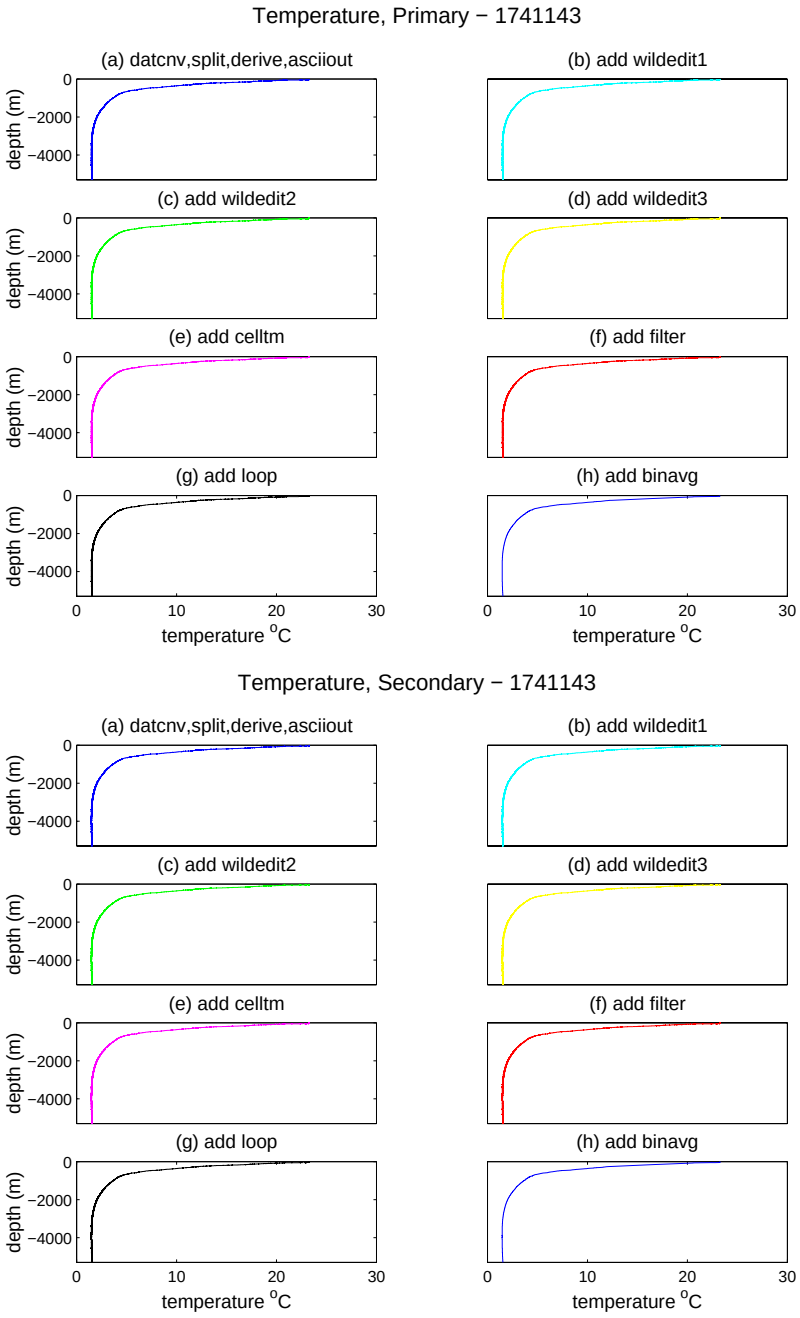

Figure 12. Same as in Figure 11, except for the primary temperature profile (top) and secondary temperature profile (bottom).

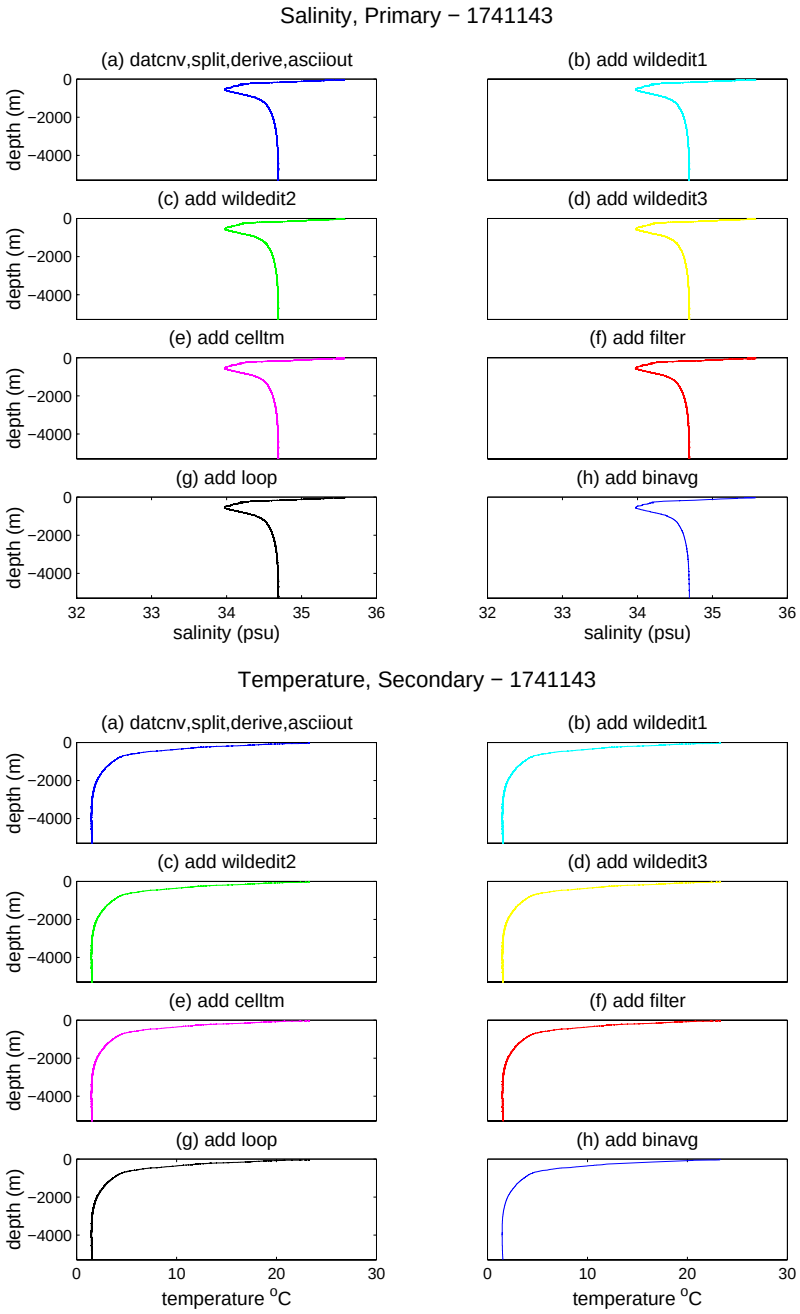

Figure 13. Same as in Figure 11, except for primary salinity profile (top) and secondary salinity profile (bottom). This secondary salinity profile was thrown out.

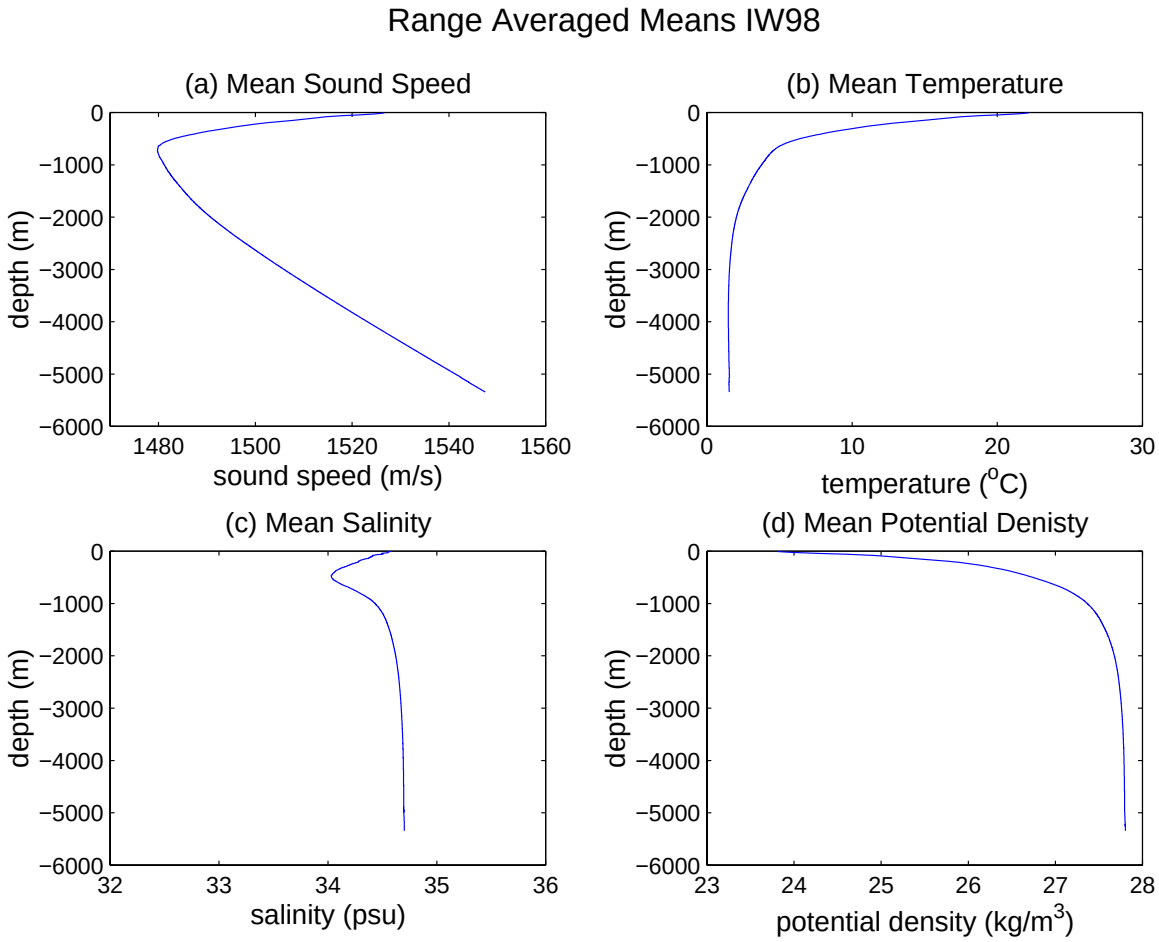

Figure 14. Range-averaged means from IW98 for (a) sound speed in m/s, (b) temperature in °C, (c) salinity in psu, and (d) potential density in kg/m^3.

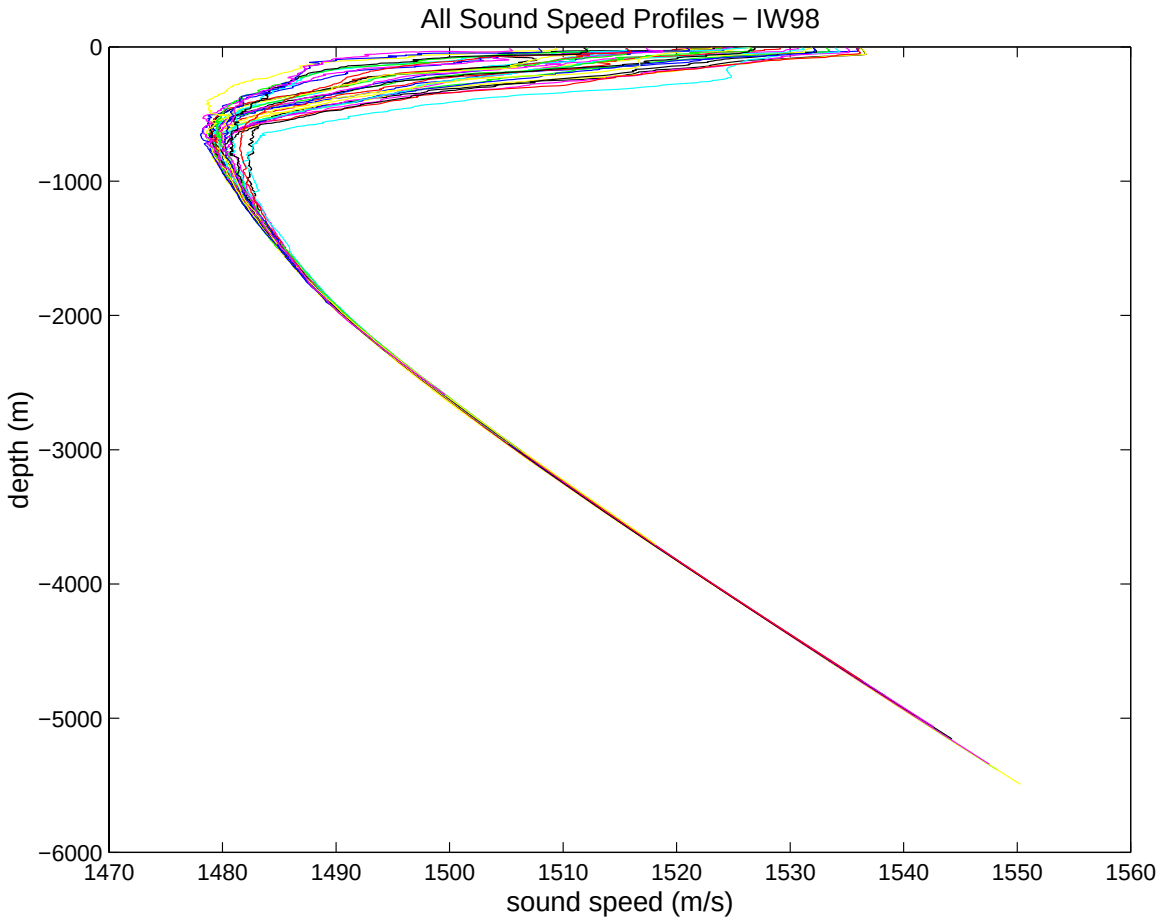

Figure 15. Sound speed profiles from IW98 casts in m/s. The colors are the same as in Figure 36, which shows the profiles separated by 10 m/s.

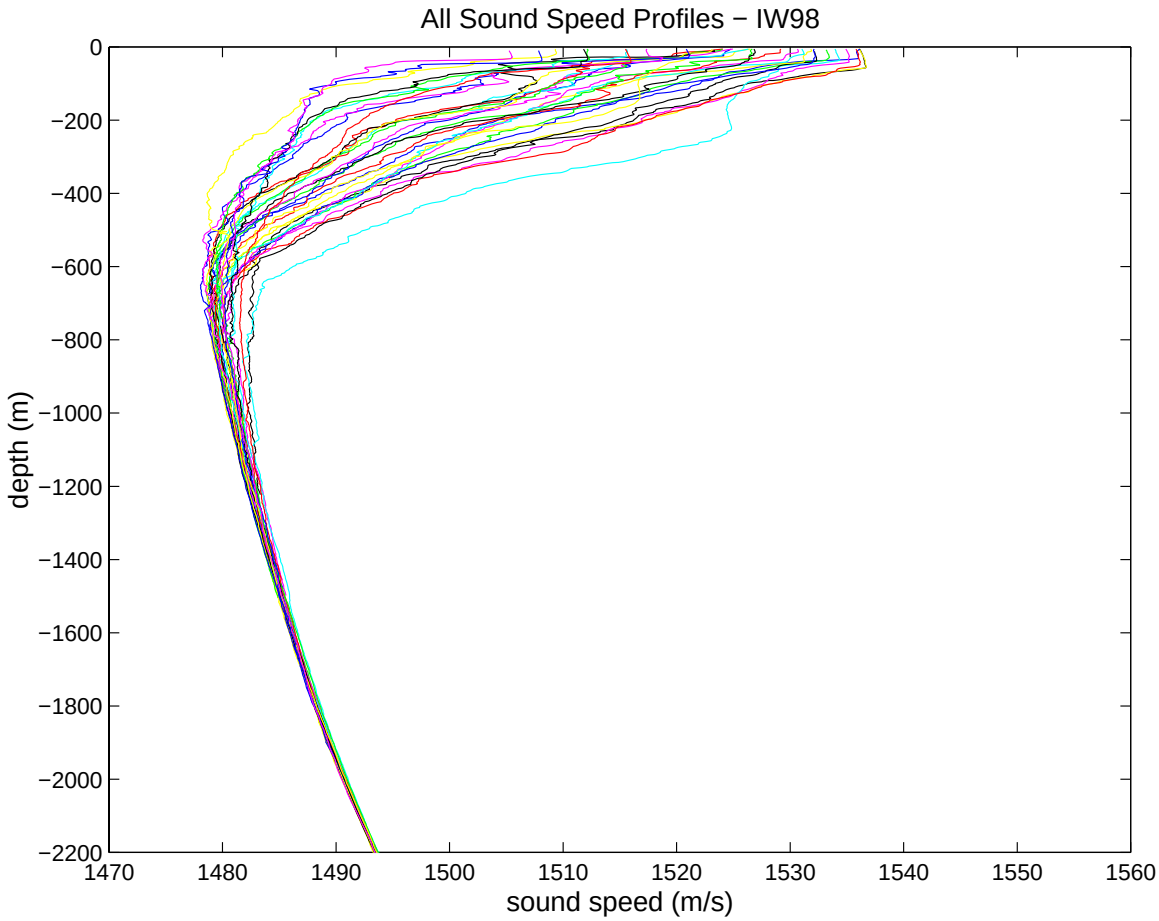

Figure 16. Sound speed profiles from IW98, in m/s, shown from the surface down to 2200 m.

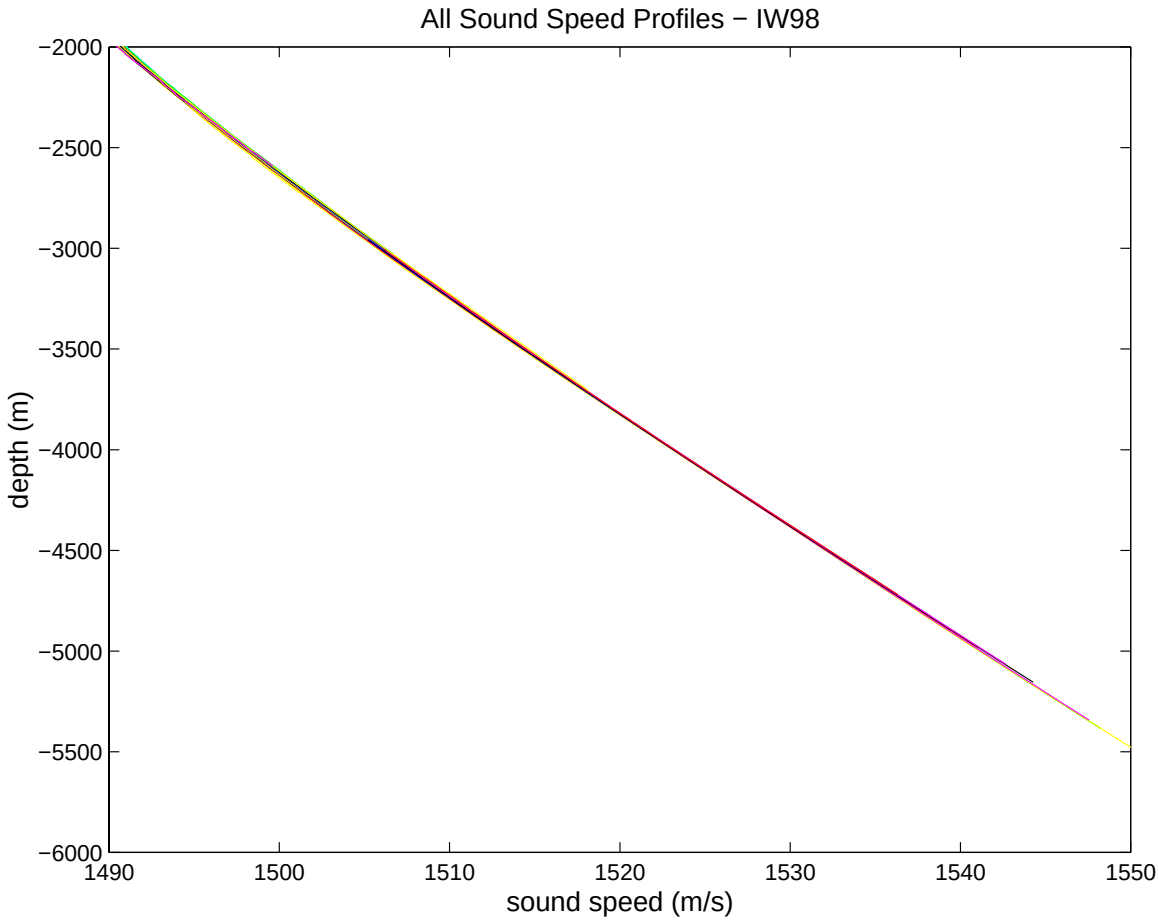

Figure 17. Sound speed profiles from IW98, in m/s, shown from 2000 m to the ocean bottom.

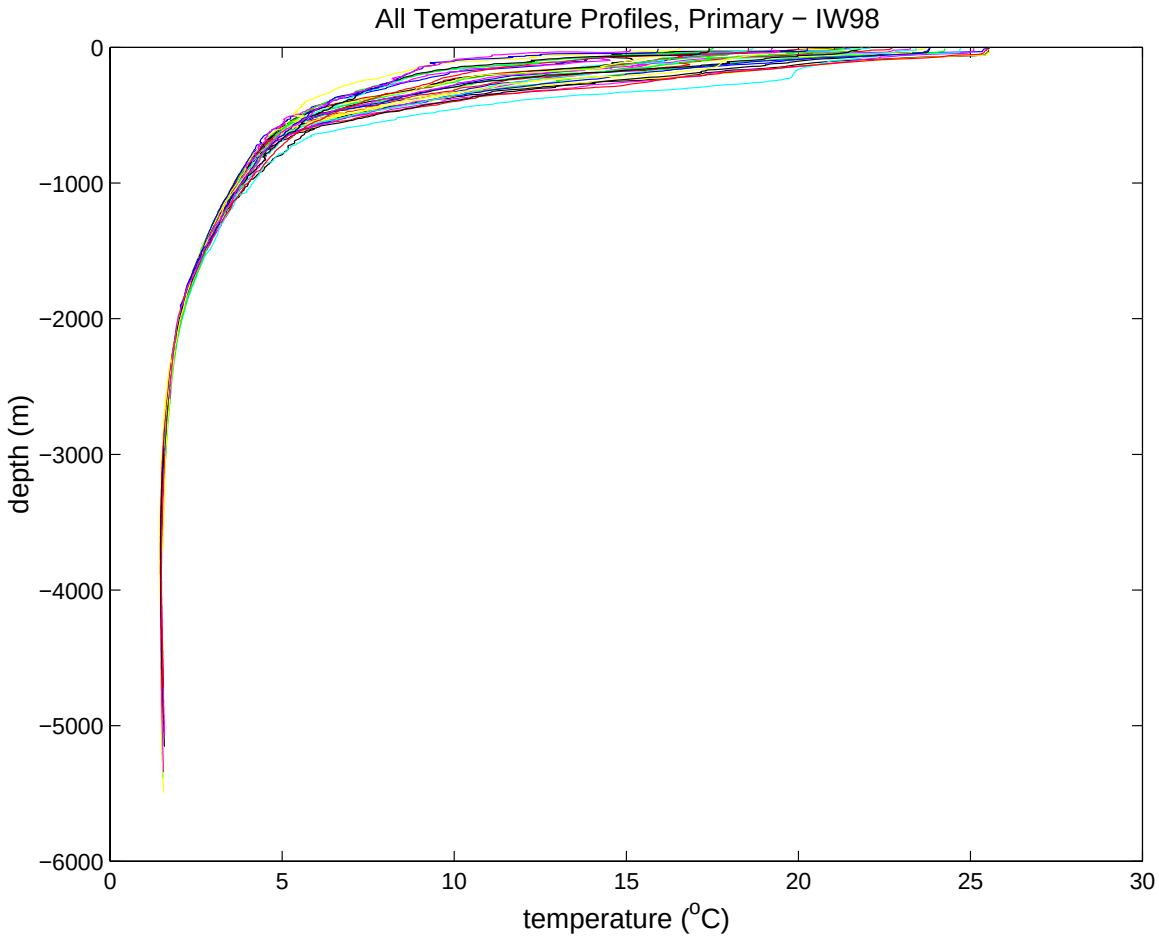

Figure 18. Temperature profiles from the primary sensor on the IW98 cruise in °C.

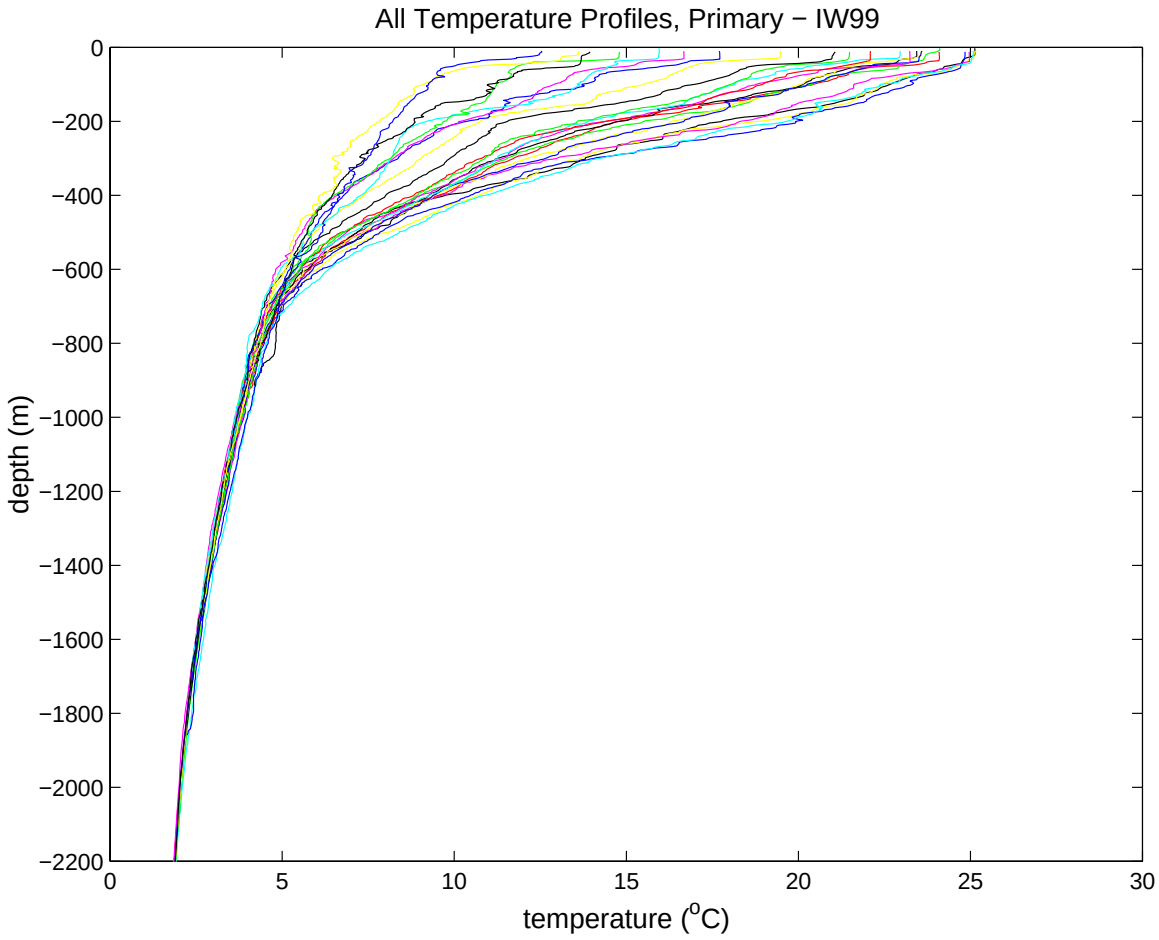

Figure 19. Temperature profiles from the primary sensor on IW98, in °C, from the surface down to 2200 m.

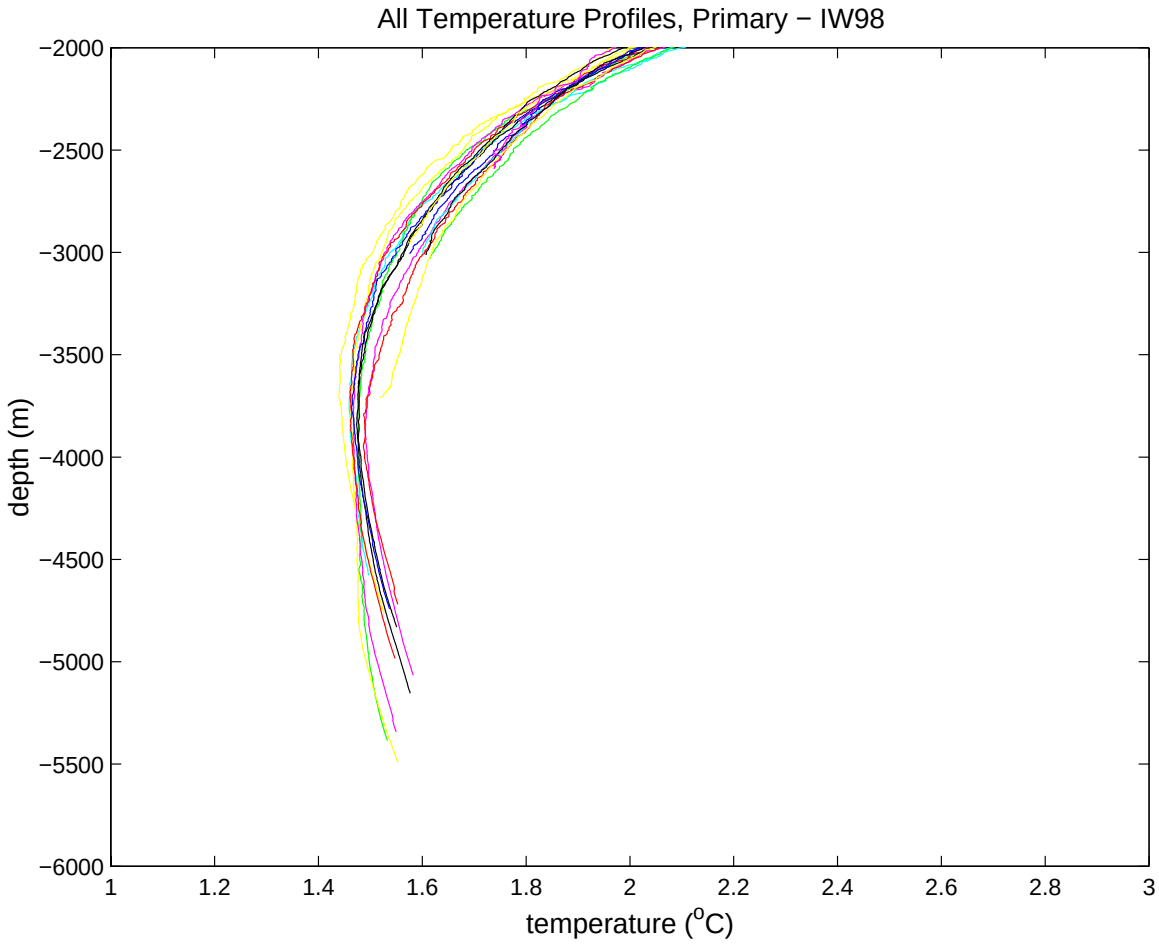

Figure 20. Temperature profiles from the primary sensor on IW98, in °C, from 2000 m down to the ocean bottom.

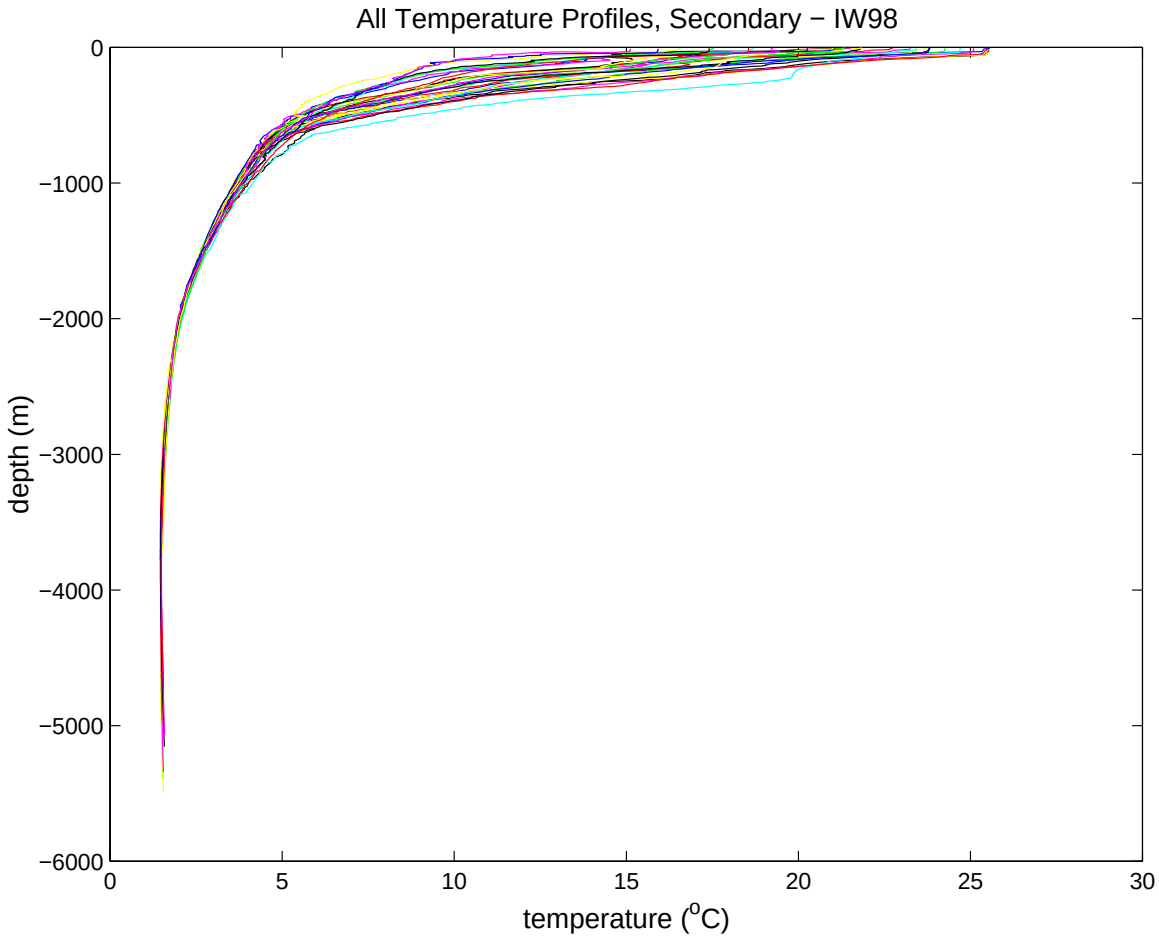

Figure 21. Temperature profiles from the secondary sensor on the IW98 cruise in °C.

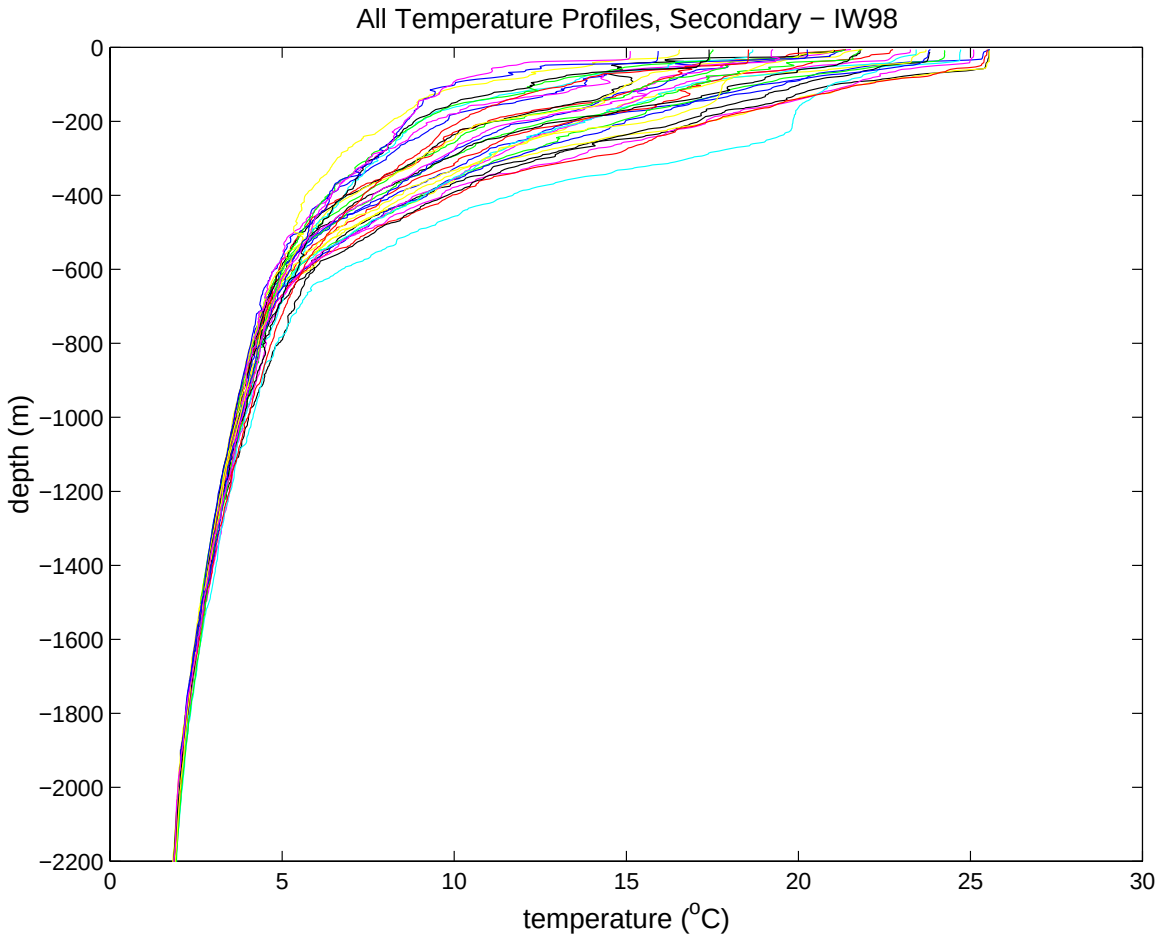

Figure 22. Temperature profiles from the secondary sensor on IW98, in °C, from the surface down to 2200 m.

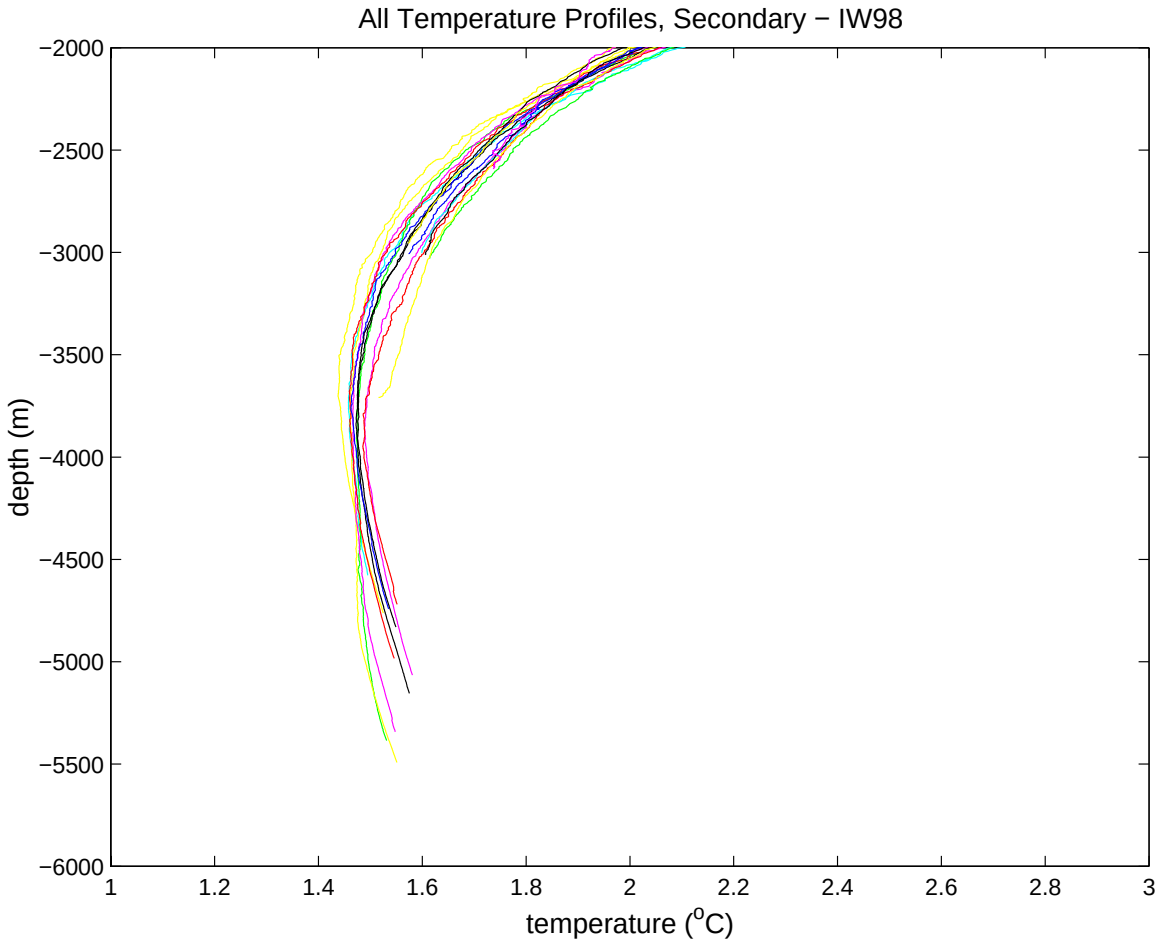

Figure 23. Temperature profiles from the secondary sensor on IW98, in °C, from 2000 m down to the ocean bottom.

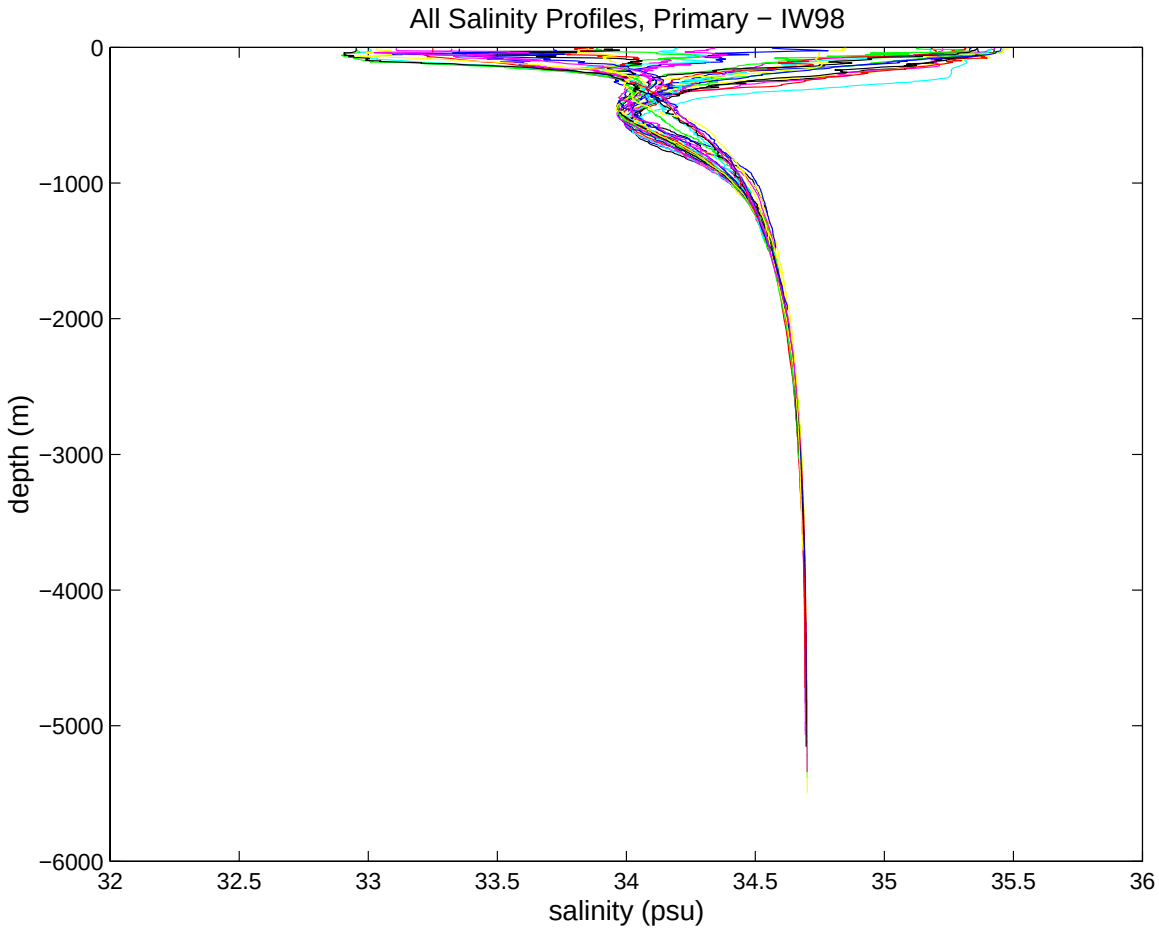

Figure 24. Salinity profiles, in psu, computed from the primary sensor on the IW98 cruise.

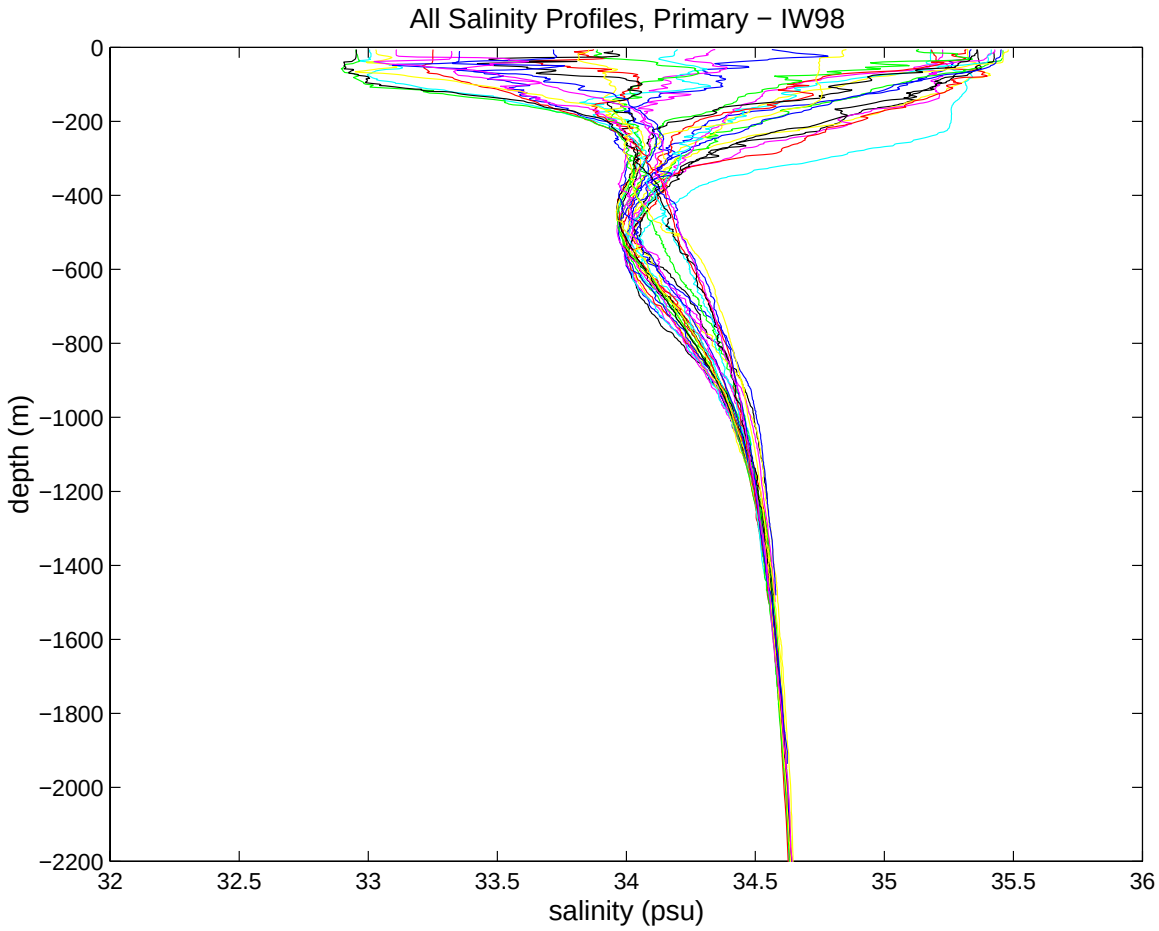

Figure 25. Salinity profiles, in psu, computed from the primary sensor on IW98 from the surface down to 2200 m.

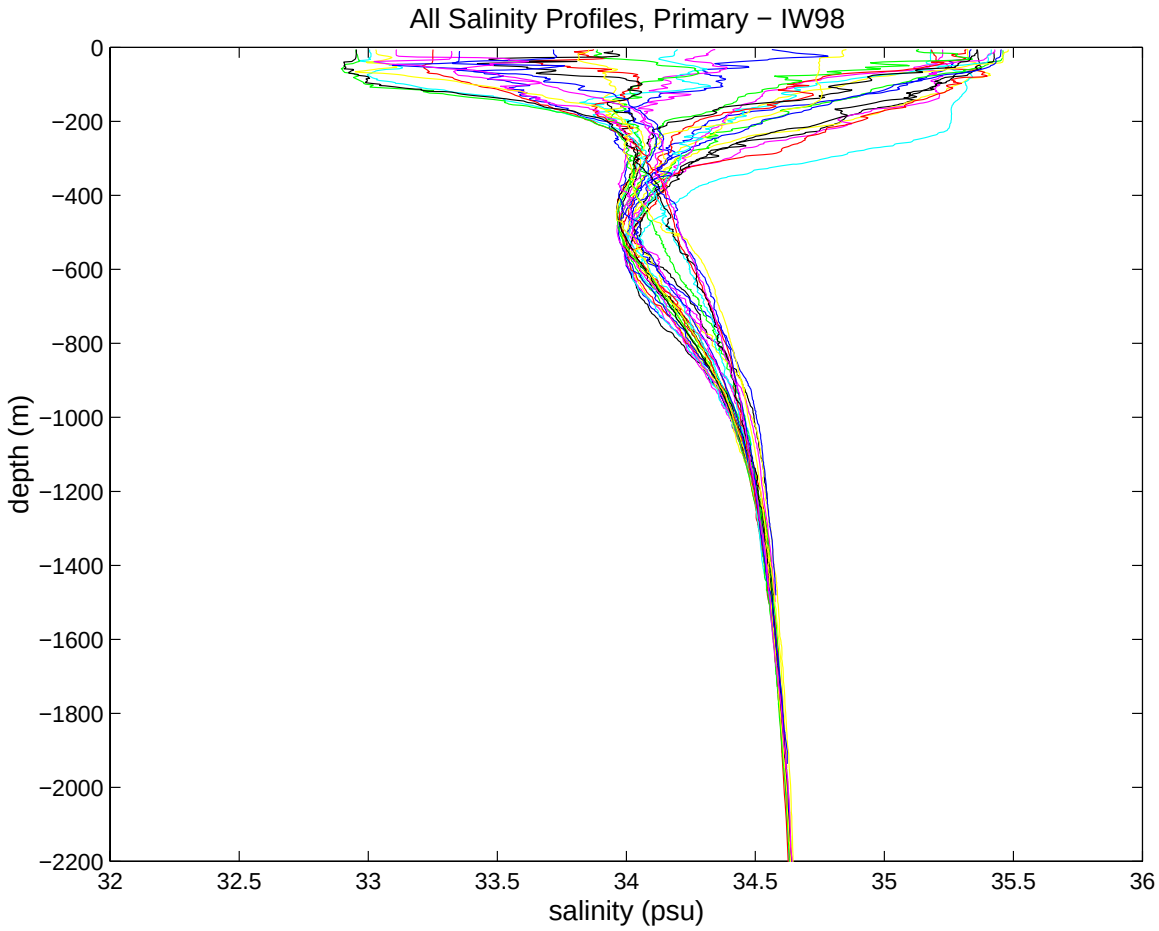

Figure 26. Salinity profiles, in psu, computed from the primary sensor on IW98 from 2000 m down to the ocean bottom.

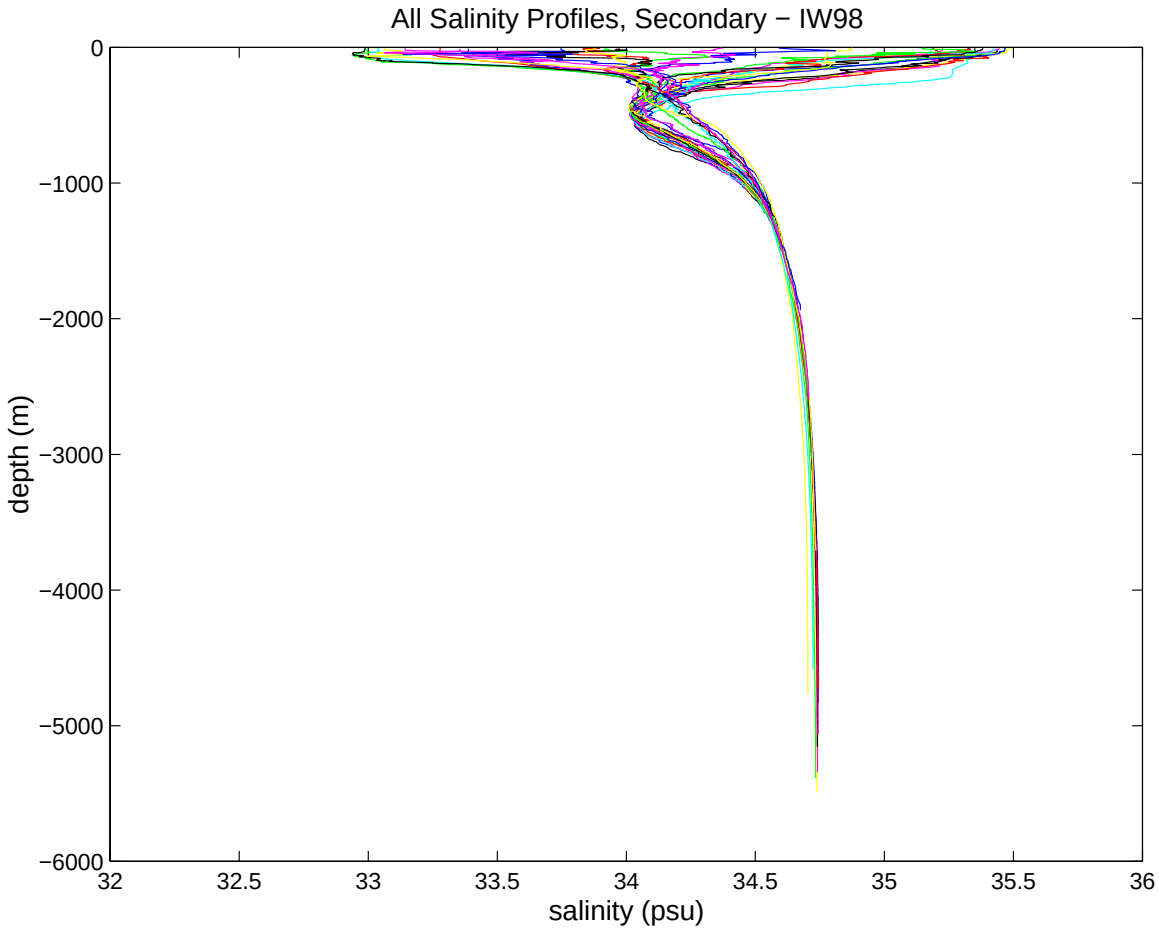

Figure 27. Salinity profiles, in psu, computed from the secondary sensor on the IW98 cruise.

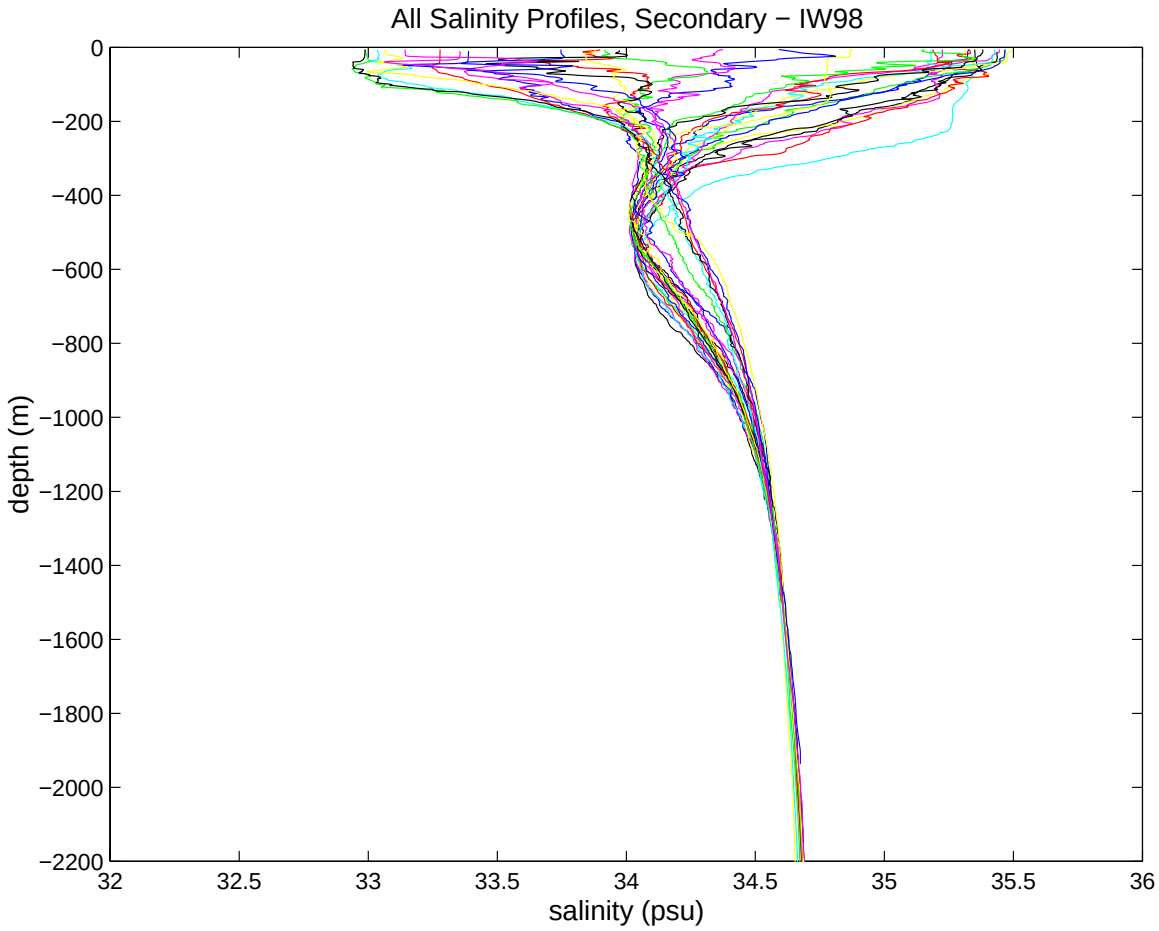

Figure 28. Salinity profile, in psu, computed from the secondary sensor on IW98 from the surface down to 2200 m.

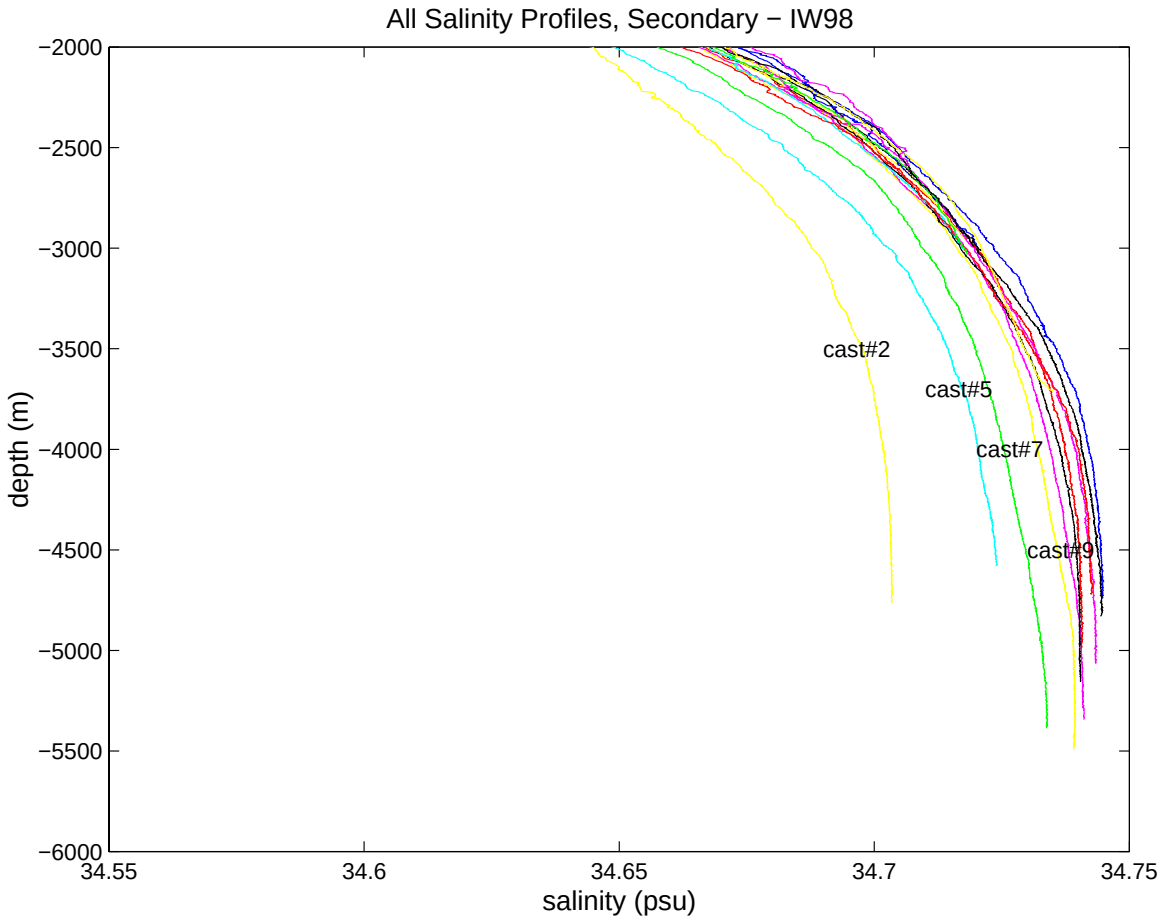

Figure 29. Salinity profiles, in psu, computed from the secondary sensor on IW98 from 2000 m down to the ocean bottom. The first four deep casts on this cruise are labeled.

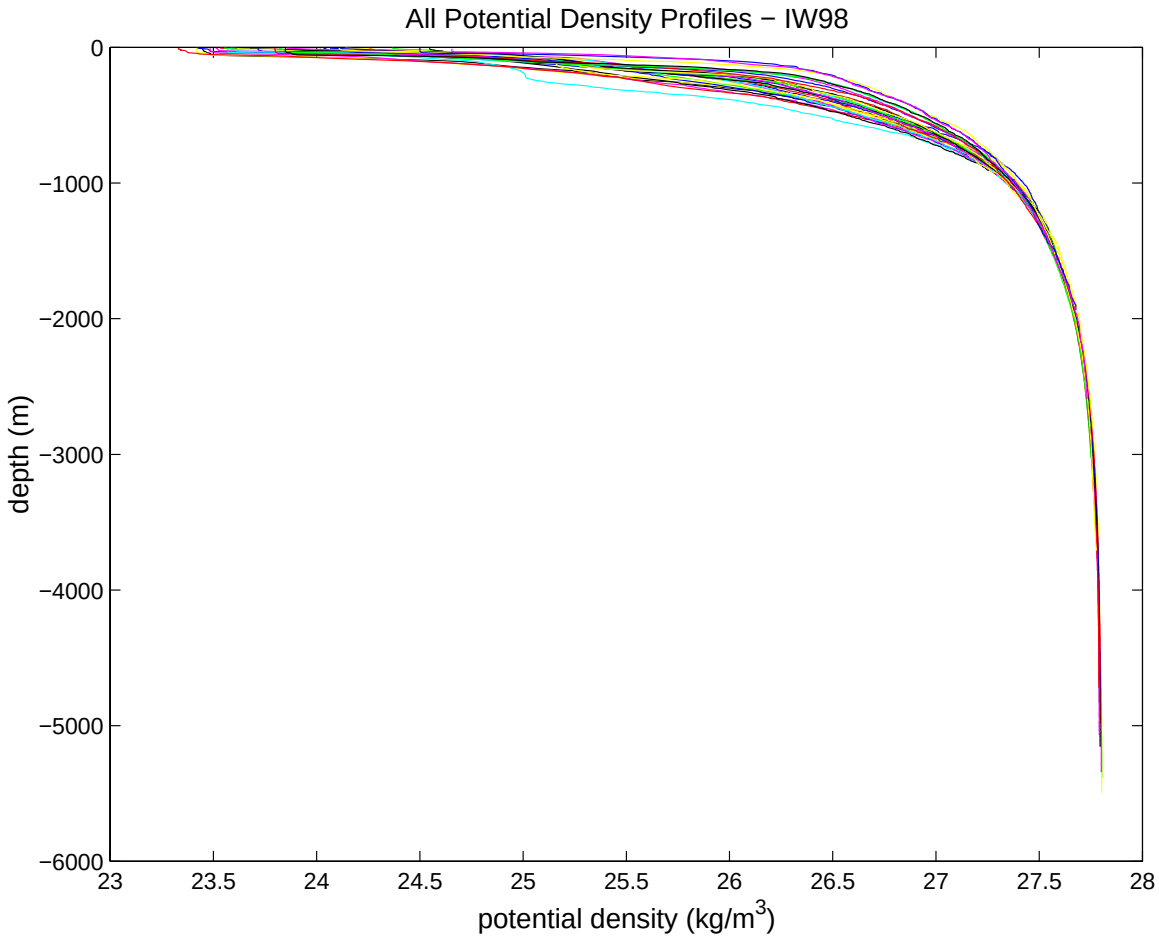

Figure 30. Potential density profiles, kg/m^3, from the IW98 cruise.

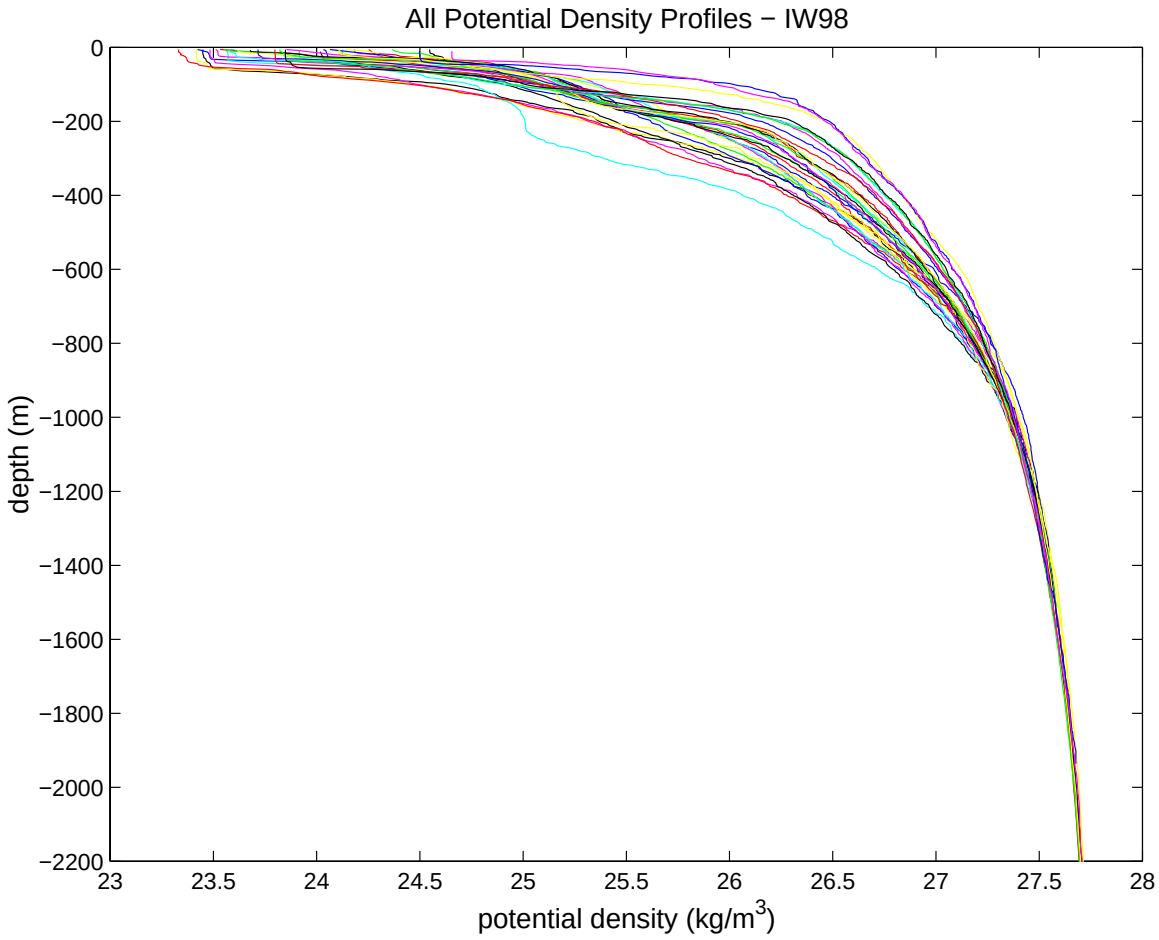

Figure 31. Potential density profiles, in kg/m^3, from the IW98 cruise from the surface down to 2200 m.

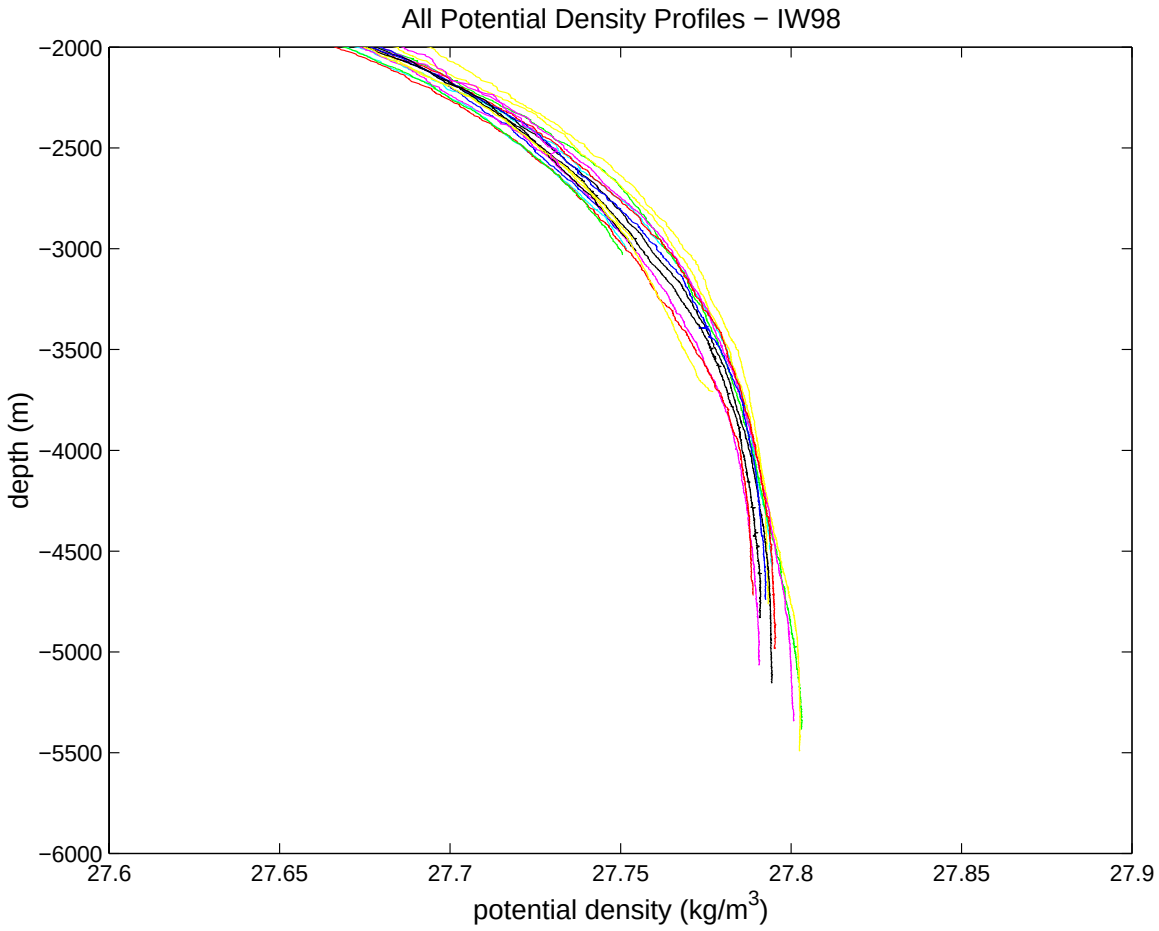

Figure 32. Potential density profiles, in kg/m^3, from the IW98 cruise from 2000 m down to the ocean bottom.

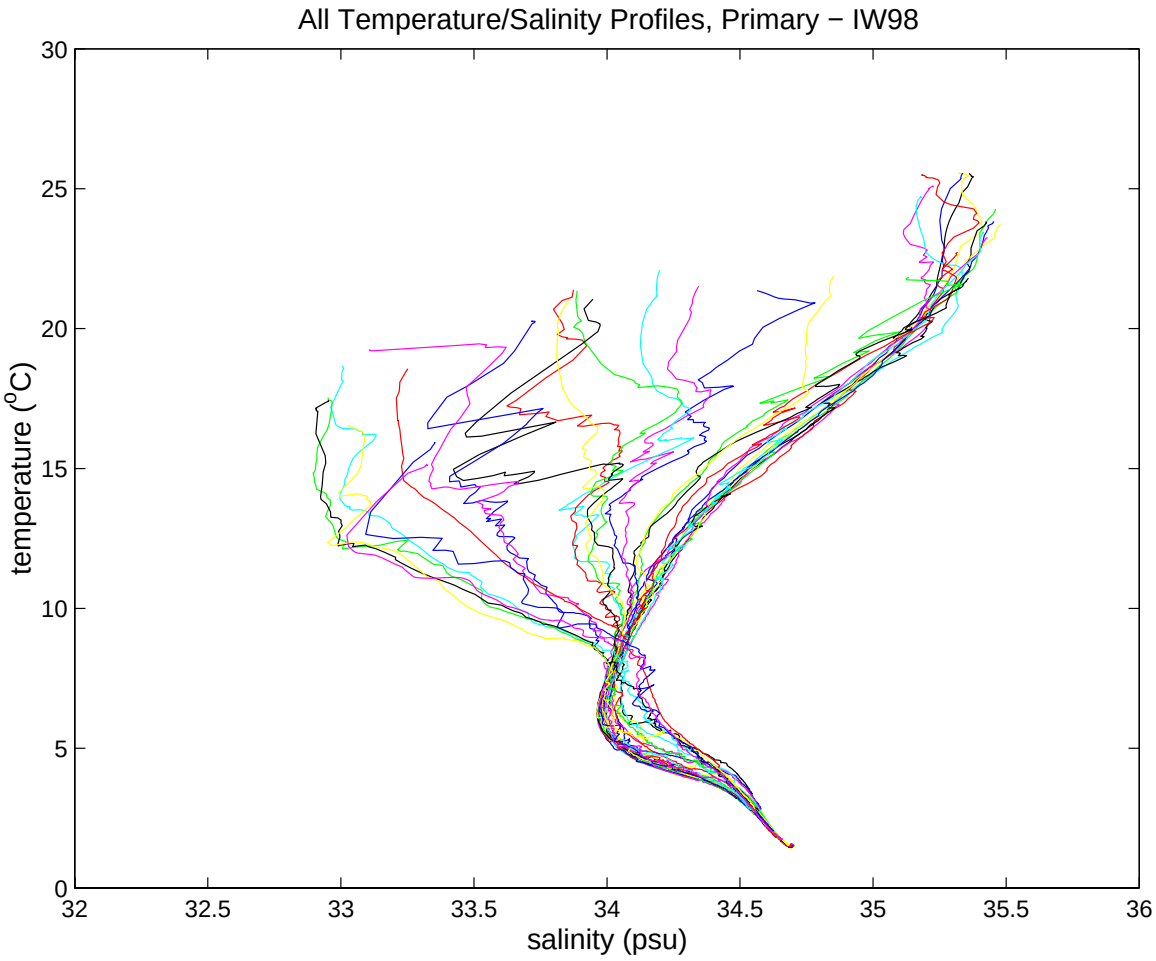

Figure 33. Temperature-salinity profiles from the primary sensors from the IW98 cruise. Temperature in °C and salinity in psu.

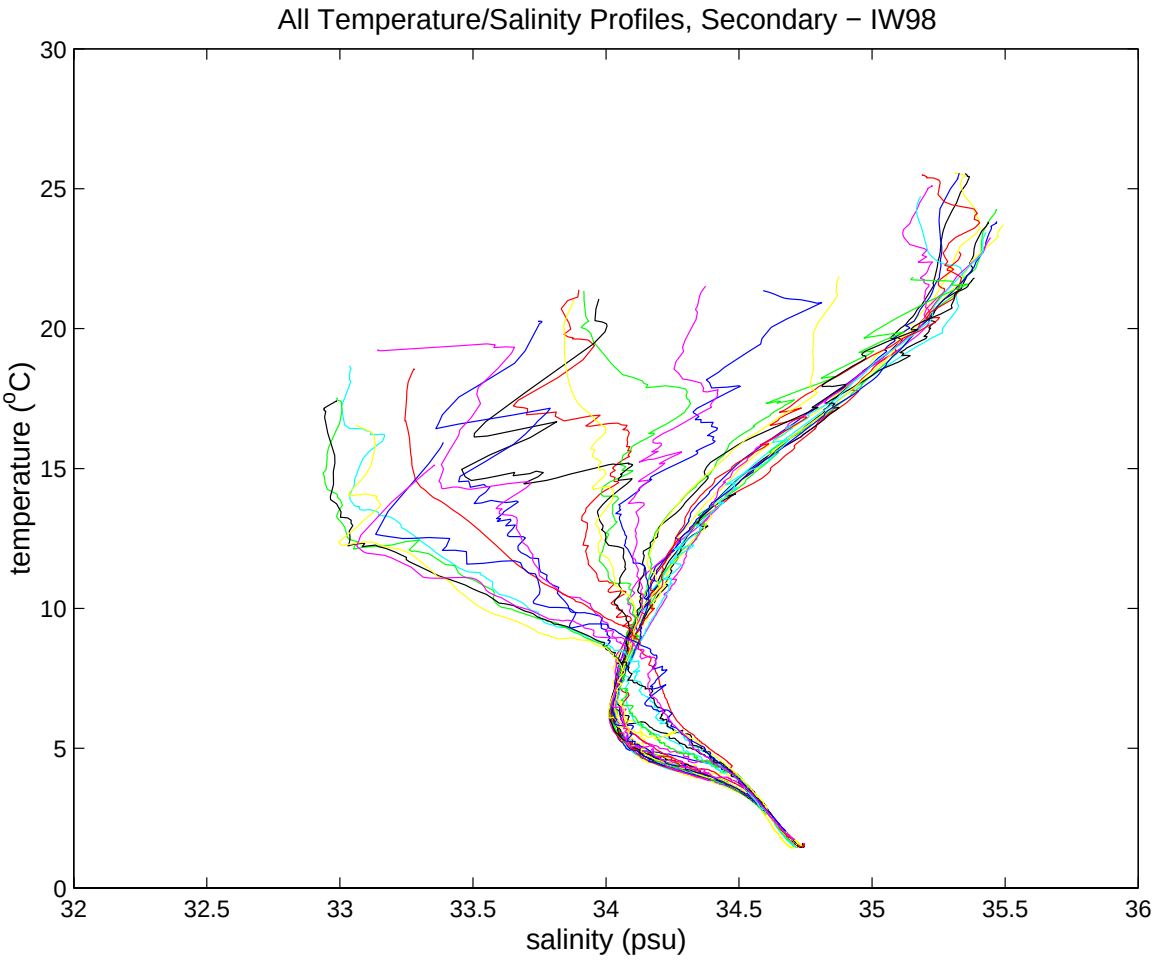

Figure 34. Temperature-salinity profiles from the secondary sensors from the IW98 cruise. Temperature in °C and salinity in psu.

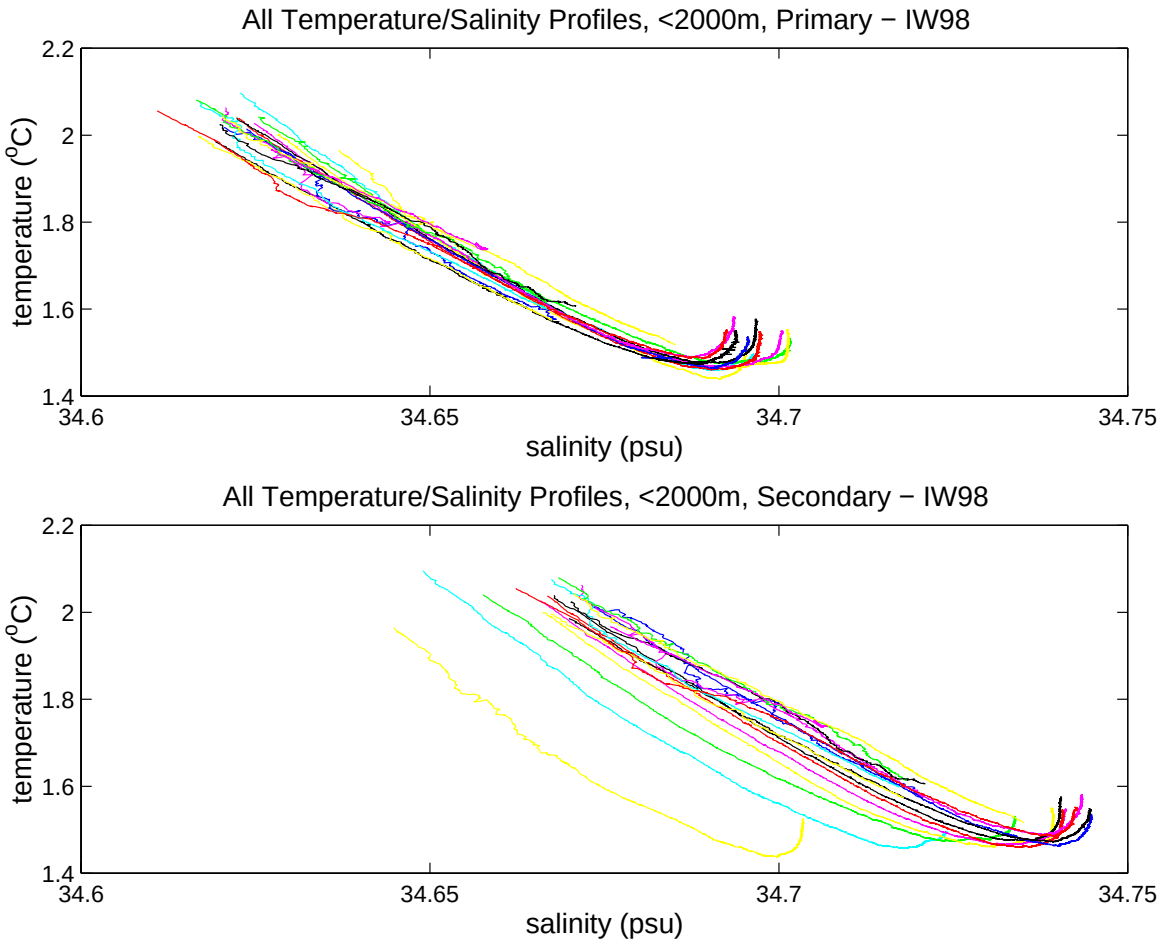

Figure 35. Temperature-salinity profiles below 2000 m from (a) the primary sensors and (b) the secondary sensors from the IW98 cruise. Temperature in °C and salinity in psu.

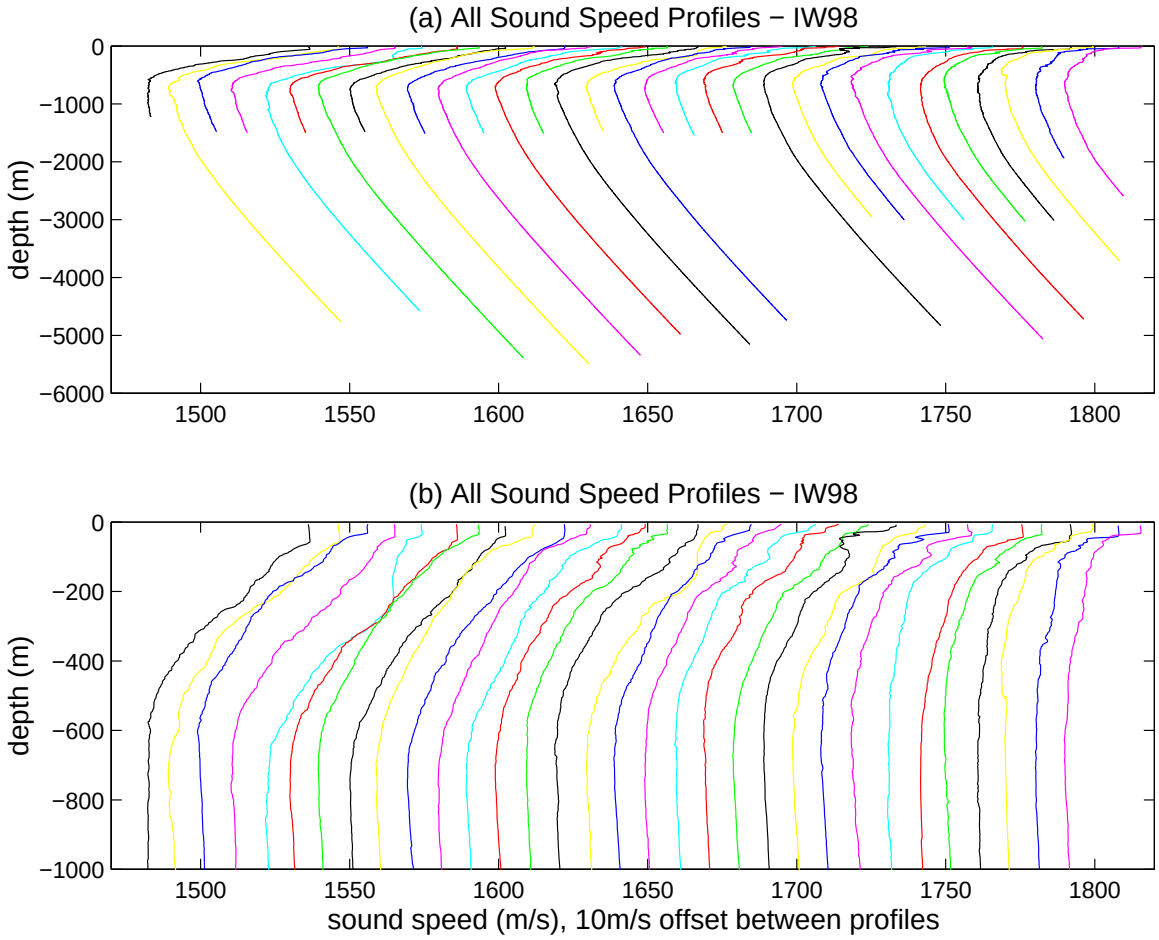

Figure 36. Sound speed profiles from IW98 for (a) the entire depth and (b) the top 1000 m. Velocities are given in m/s. Profiles are separated by 10 m/s.

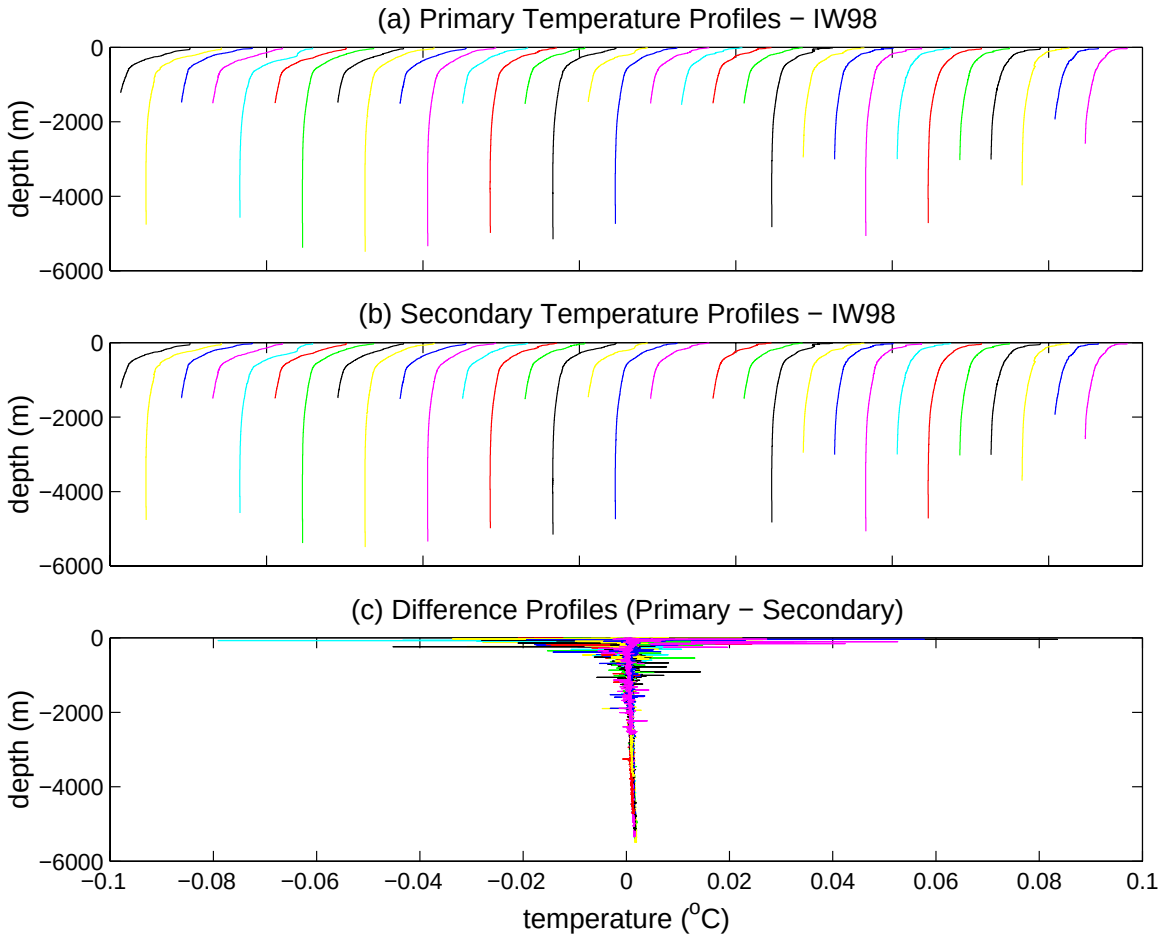

Figure 37. Temperature profiles from IW98 for (a) the primary sensor and (b) the secondary sensor for the entire depth. (c) Primary minus secondary temperatures. Temperatures are given in °C. Profiles are separated by 10°C.

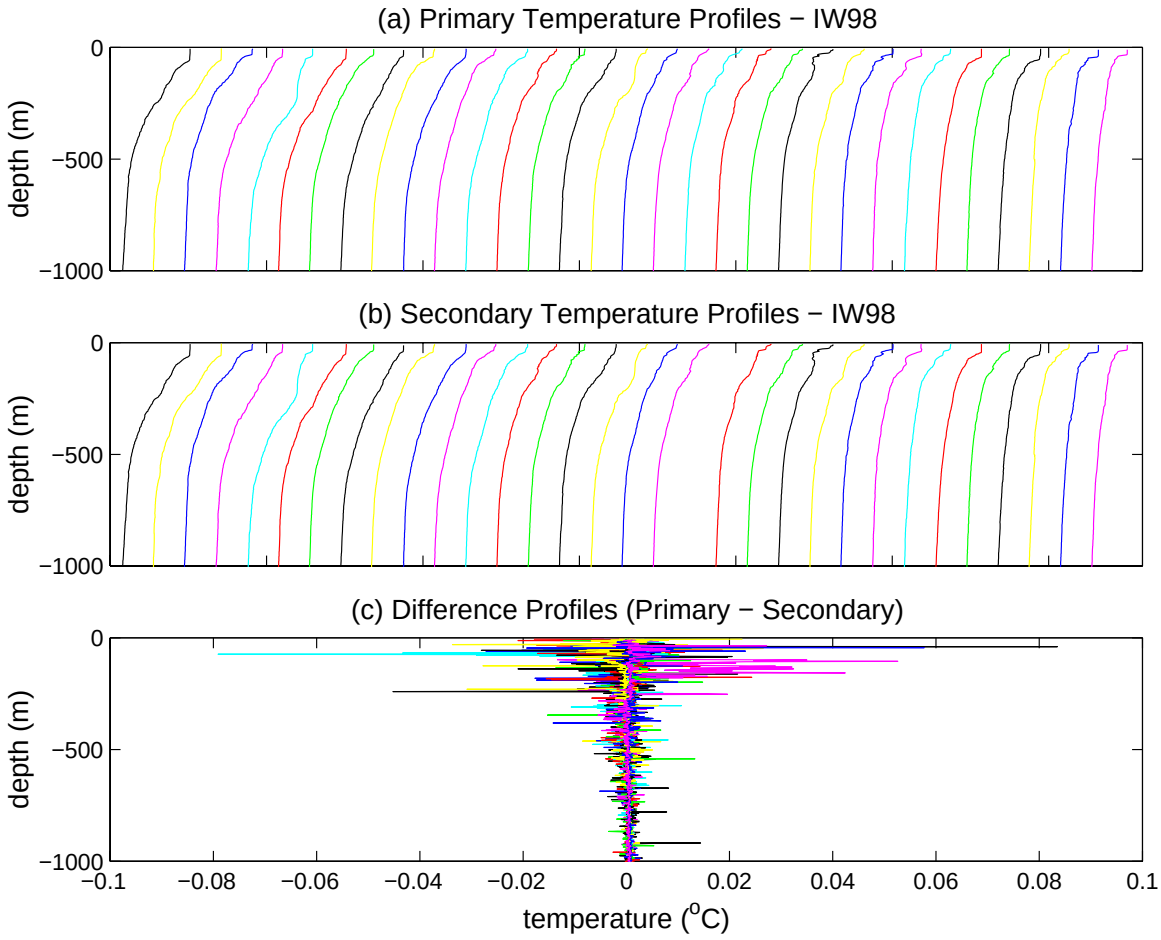

Figure 38. Same as Figure 37, except showing only the top 1000 m.

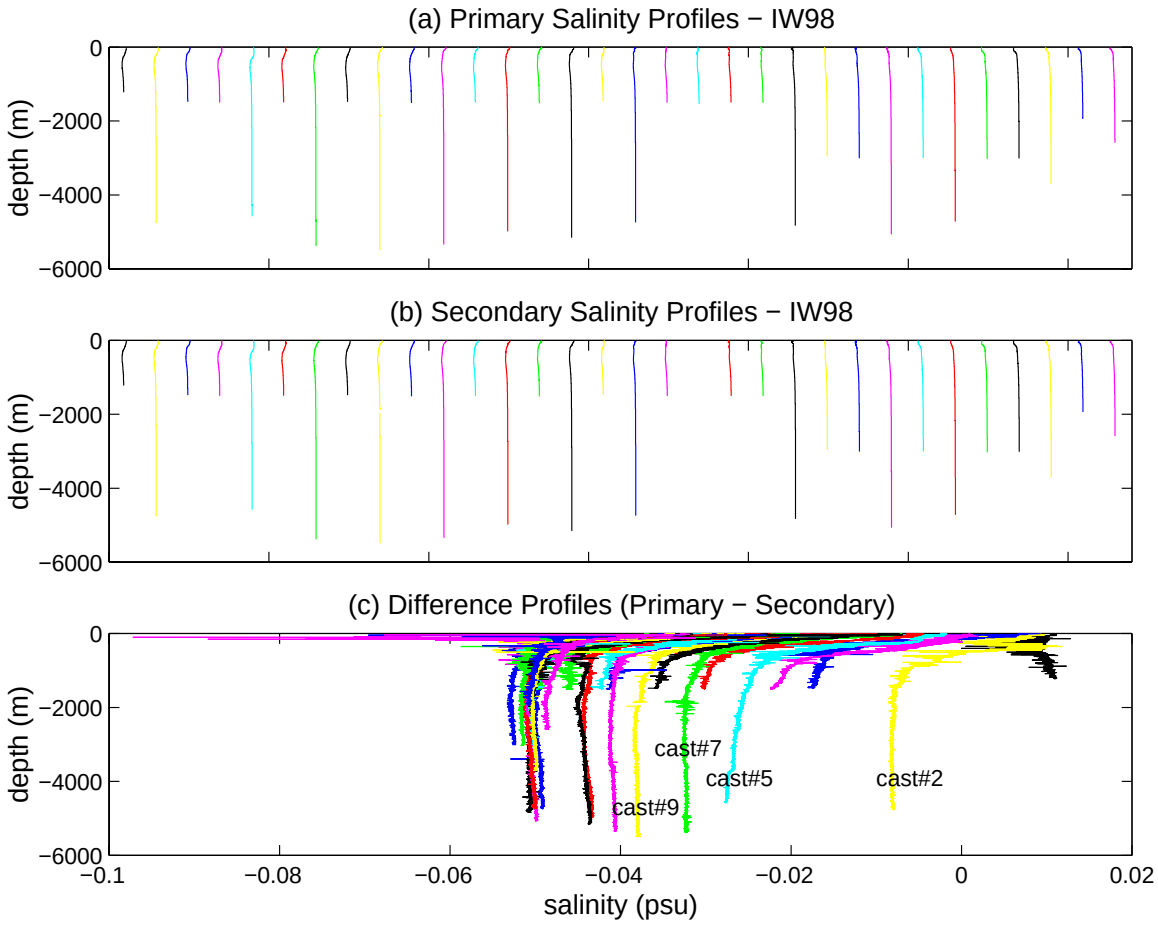

Figure 39. Salinity profiles from IW98 for (a) the primary sensor and (b) the secondary sensor for the entire depth. (c) Primary minus secondary salinities. Salinities are given in psu. Profiles are separated by 10 psu. The first four deep casts are labeled.

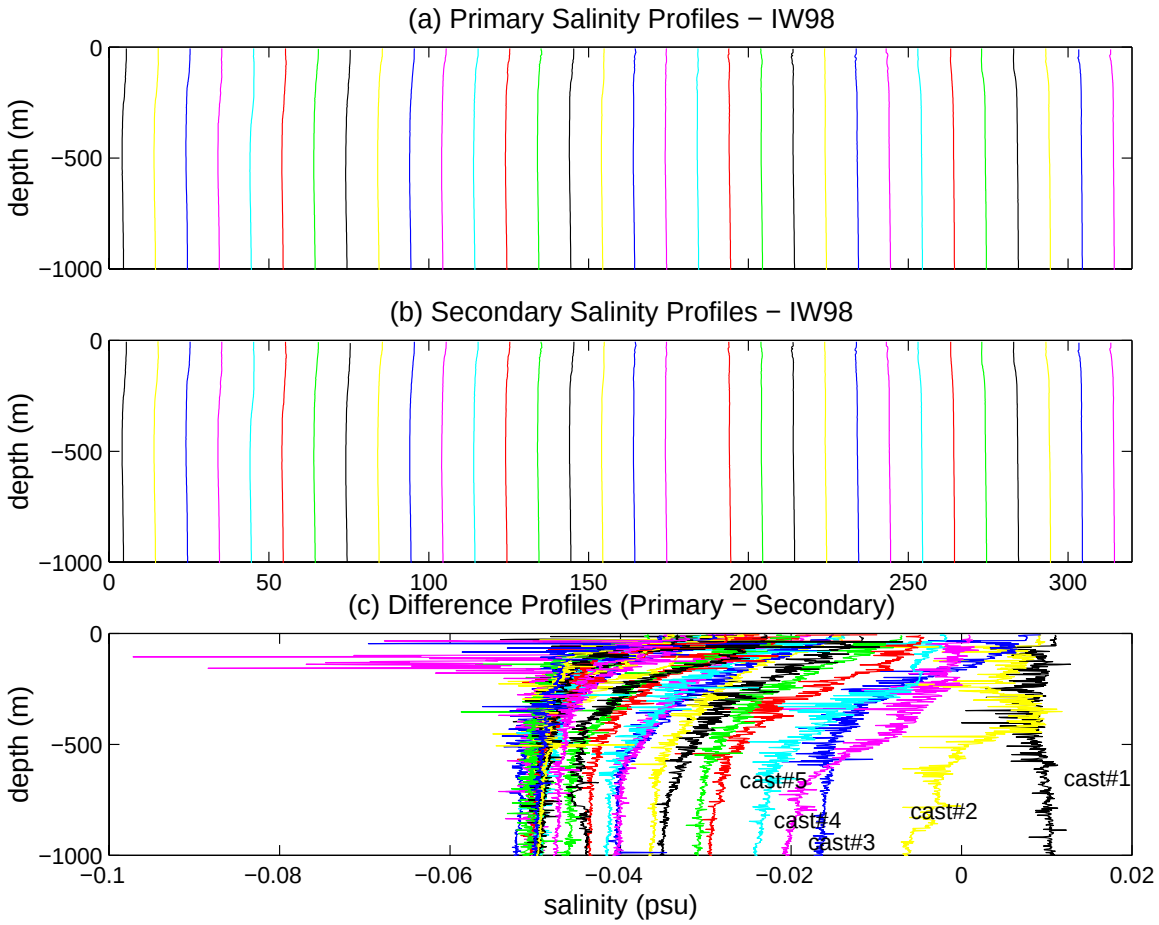

Figure 40. Same as Figure 39, except showing only the top 1000 m. The first five casts are labeled.

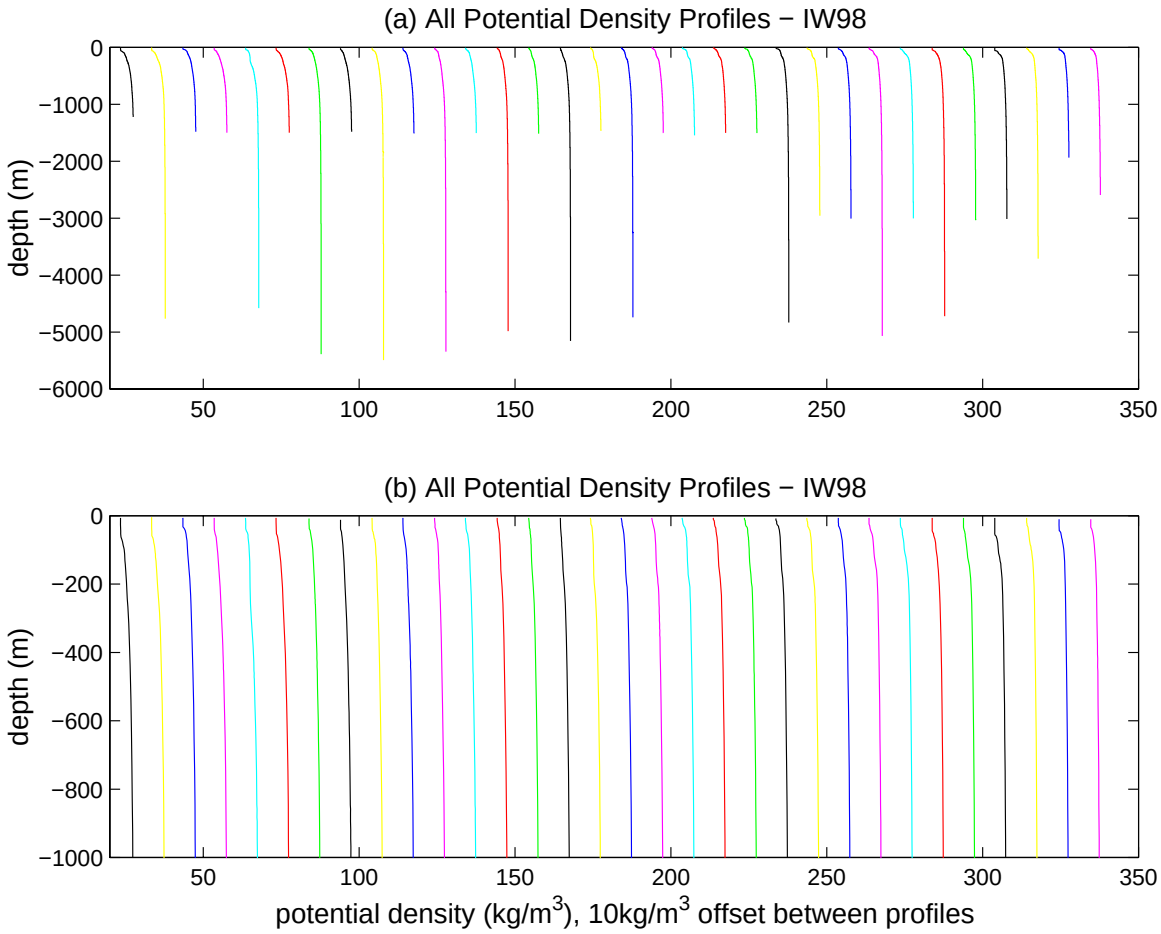

Figure 41. Potential density profiles from IW98 for (a) the entire depth and (b) the top 1000 m. All profiles separated by 10 kg/m^3.

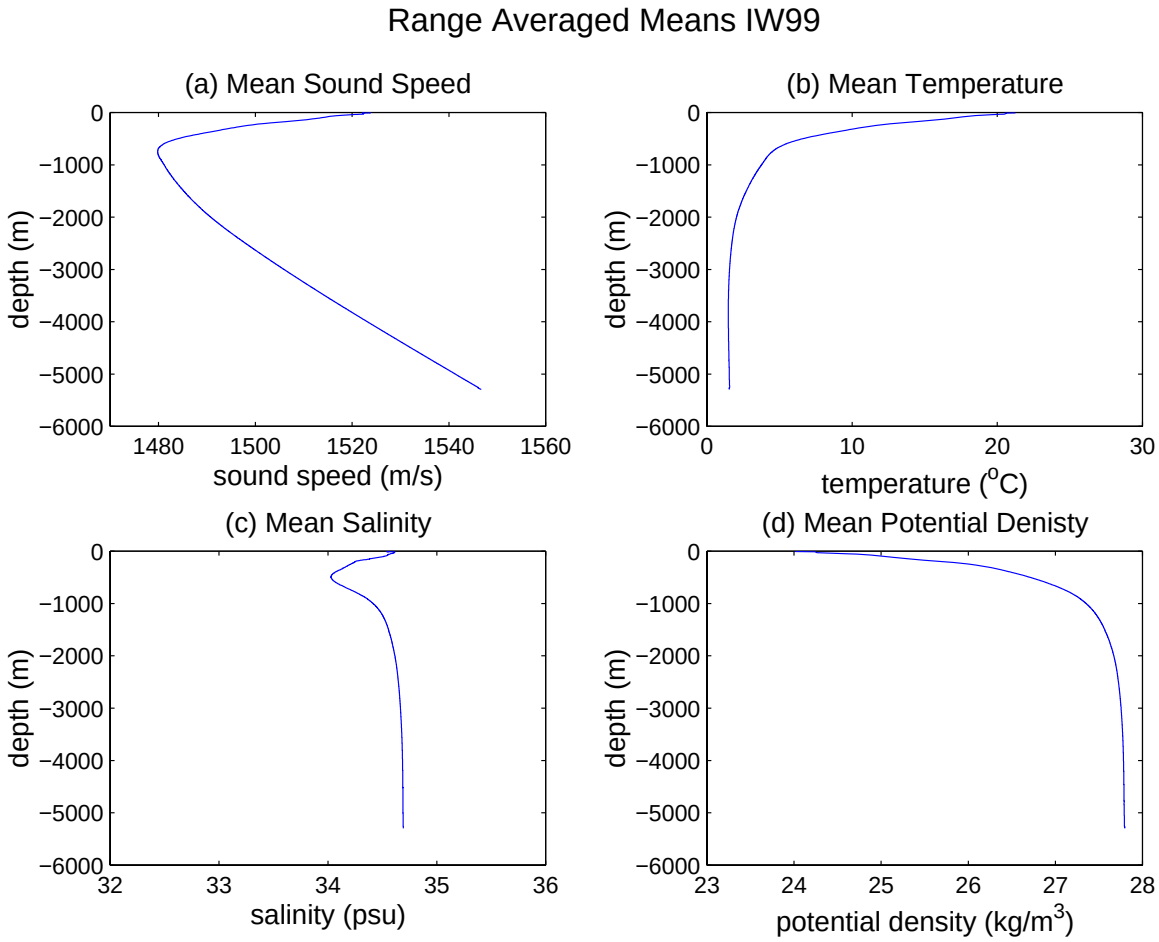

Figure 42. Cruise means for (a) sound speed in m/s, (b) temperature in °C, (c) salinity in psu and (d) potential density in kg/m^3 for IW99.

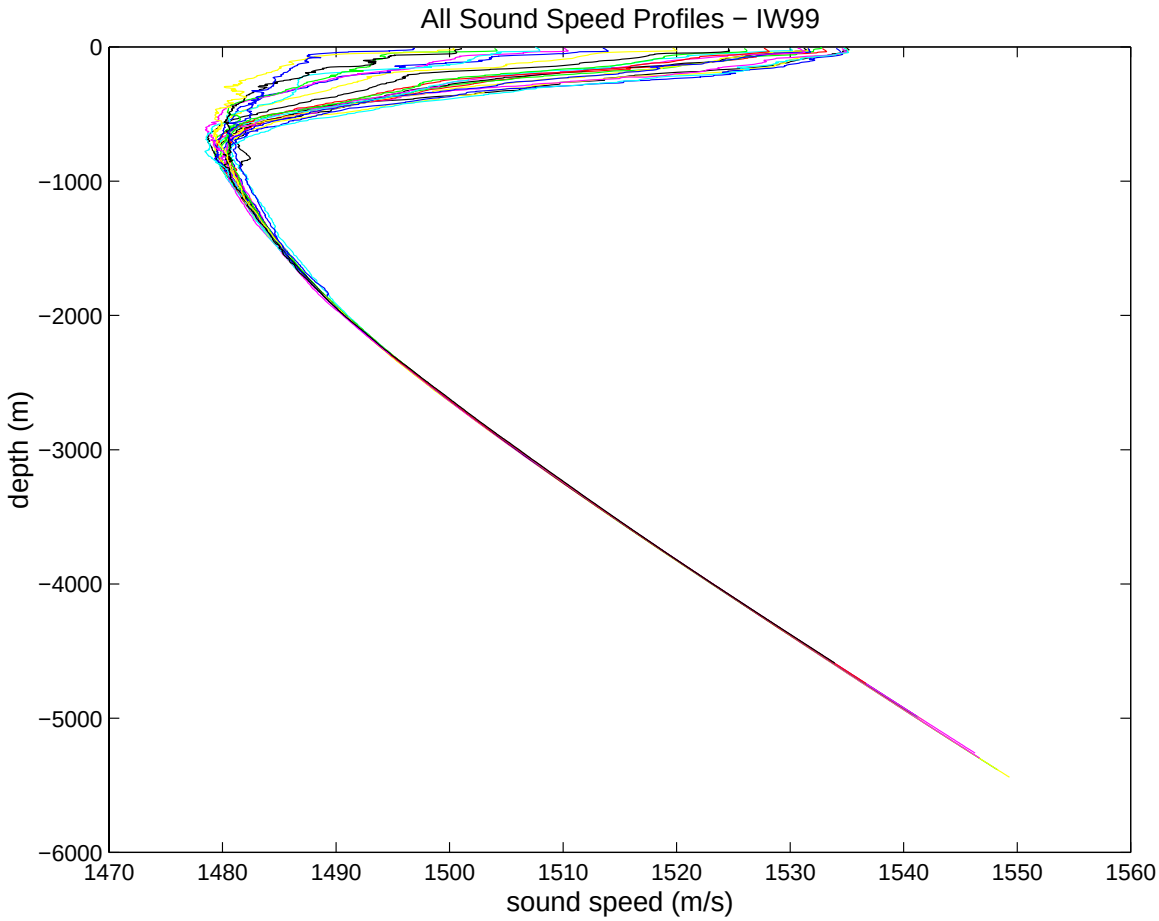

Figure 43. Sound speed profiles from IW99 in m/s.

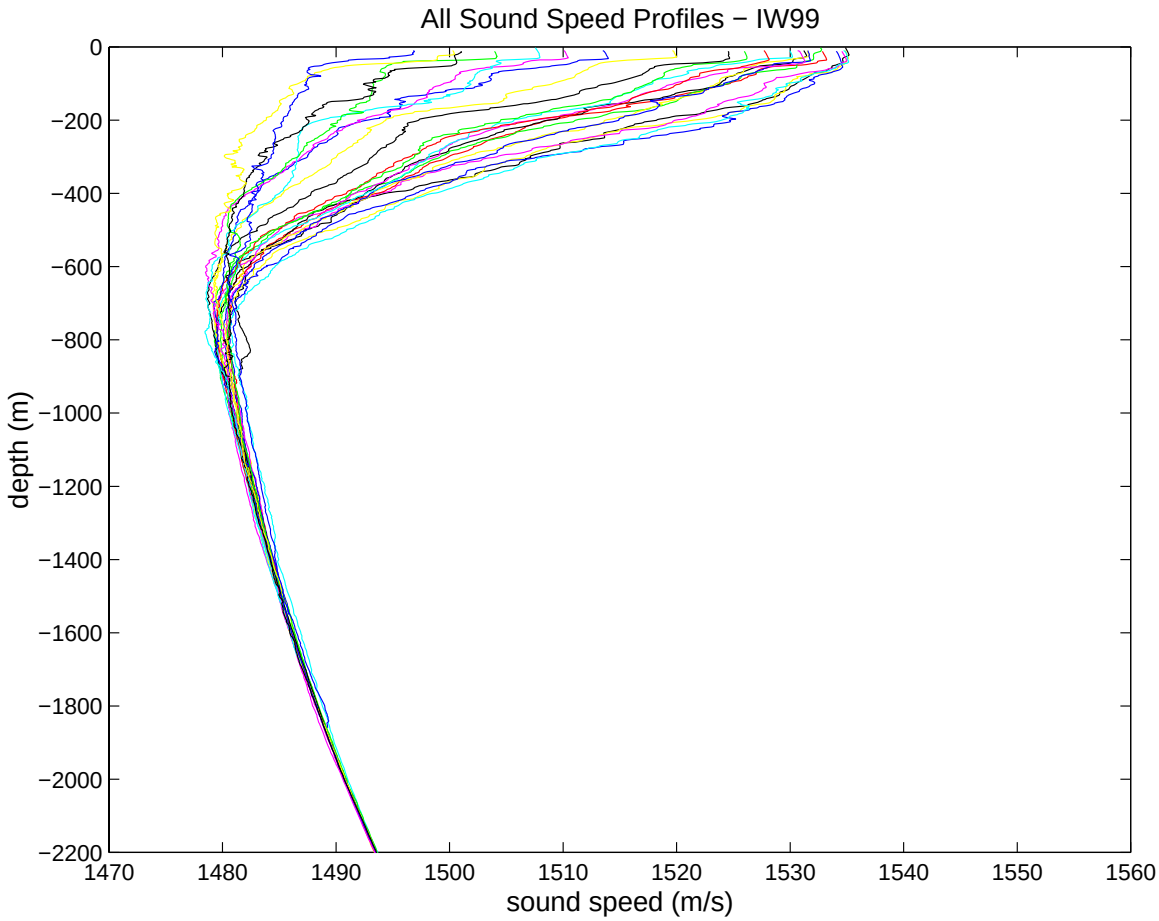

Figure 44. Sound speed profiles from IW99, in m/s, shown from the surface down to 2200 m.

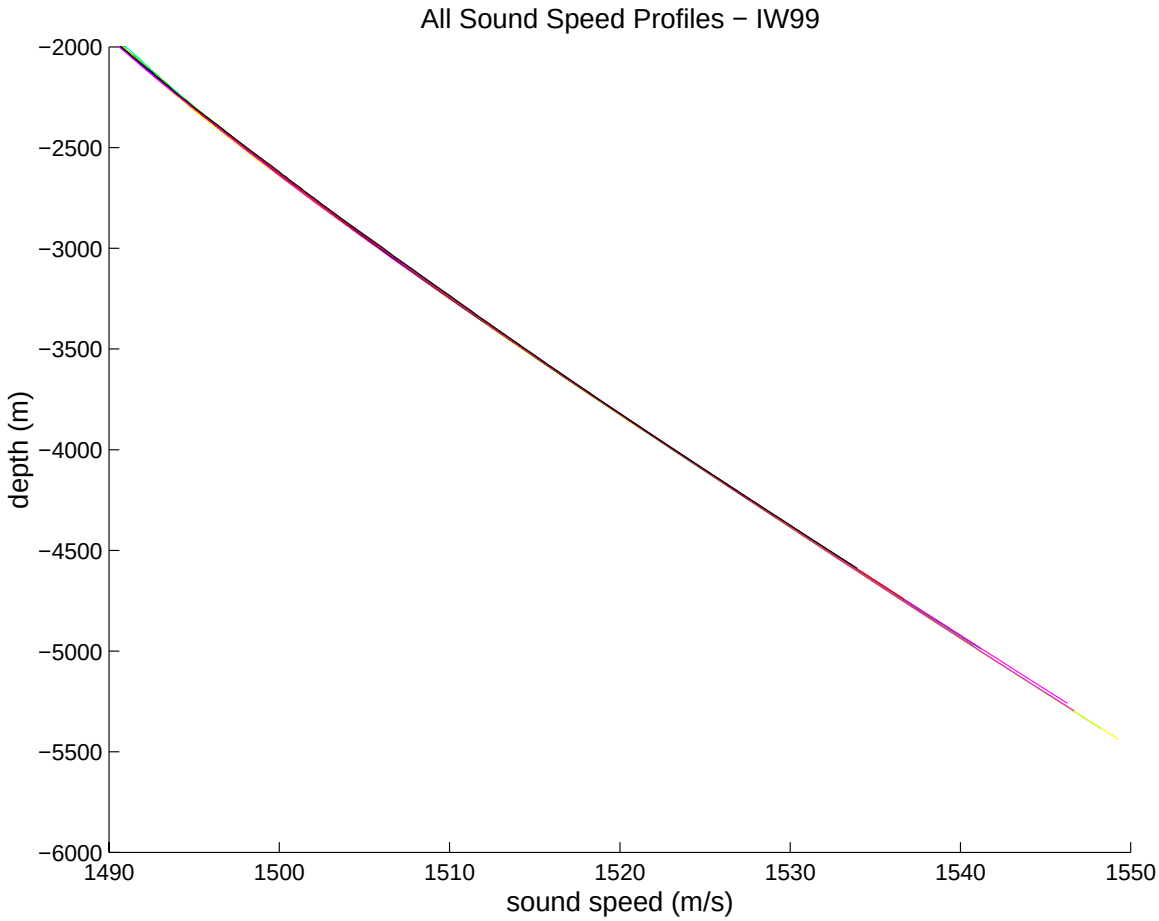

Figure 45. Sound speed profiles from IW99, in m/s, shown from 2000 m down to the ocean bottom.

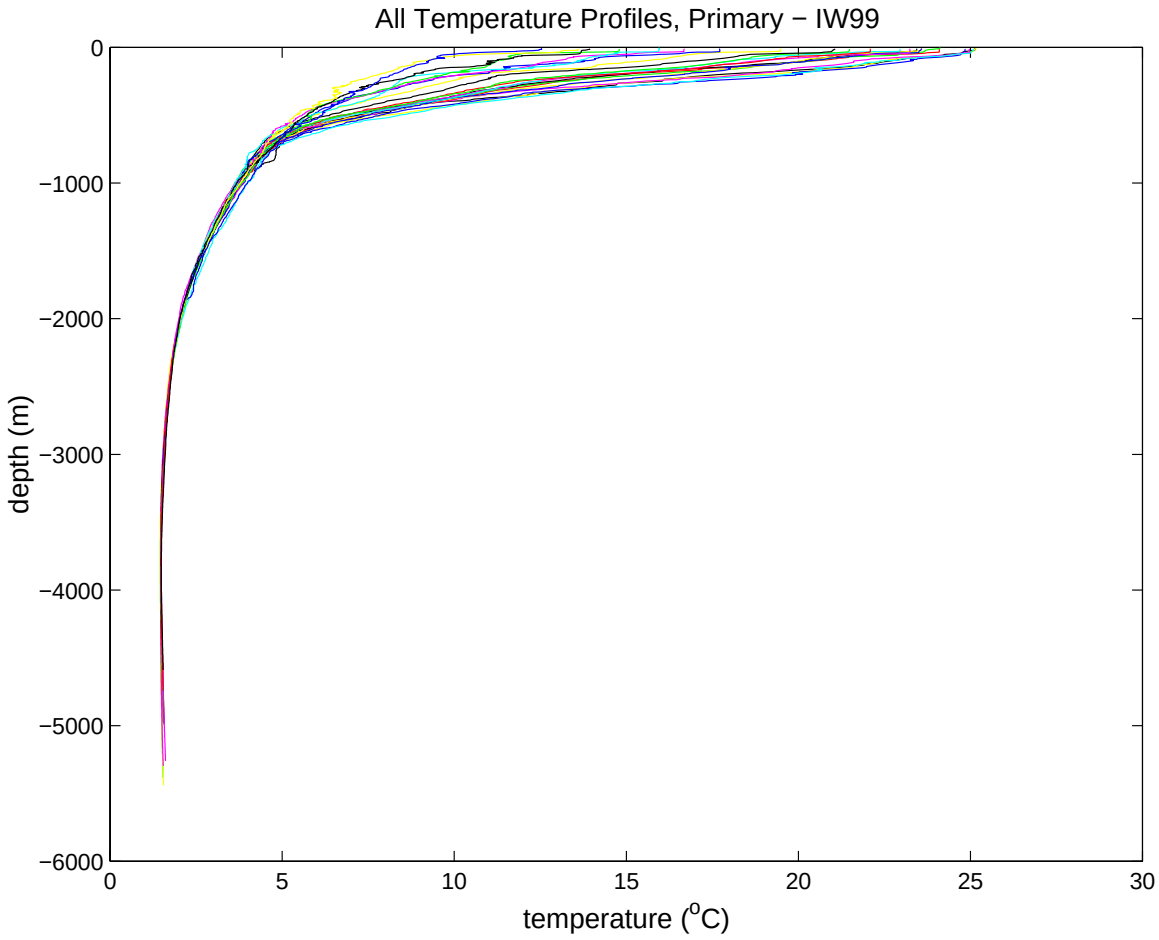

Figure 46. Temperature profiles from the primary sensor on the IW99 cruise in °C.

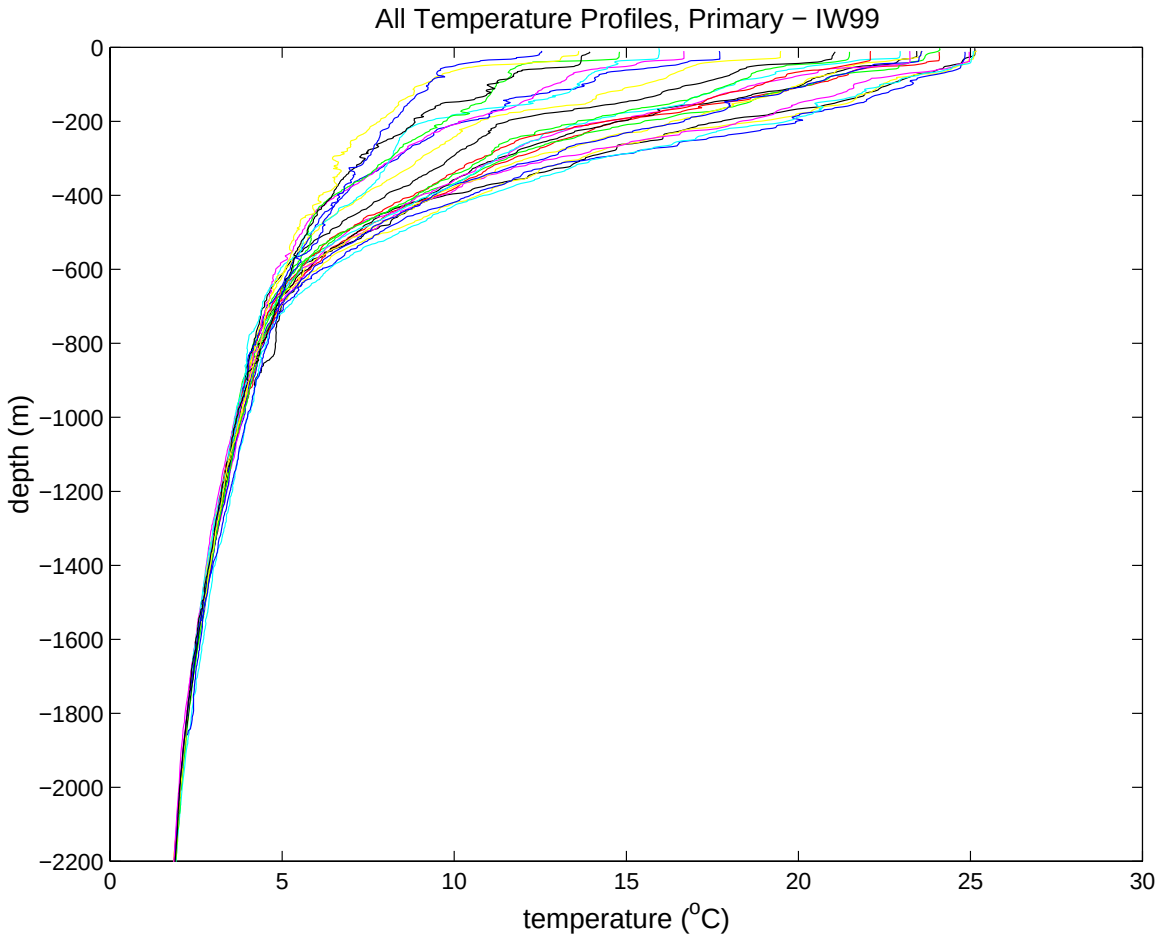

Figure 47. Temperature profiles from the primary sensor on IW99, in °C, from the surface down to 2200 m.

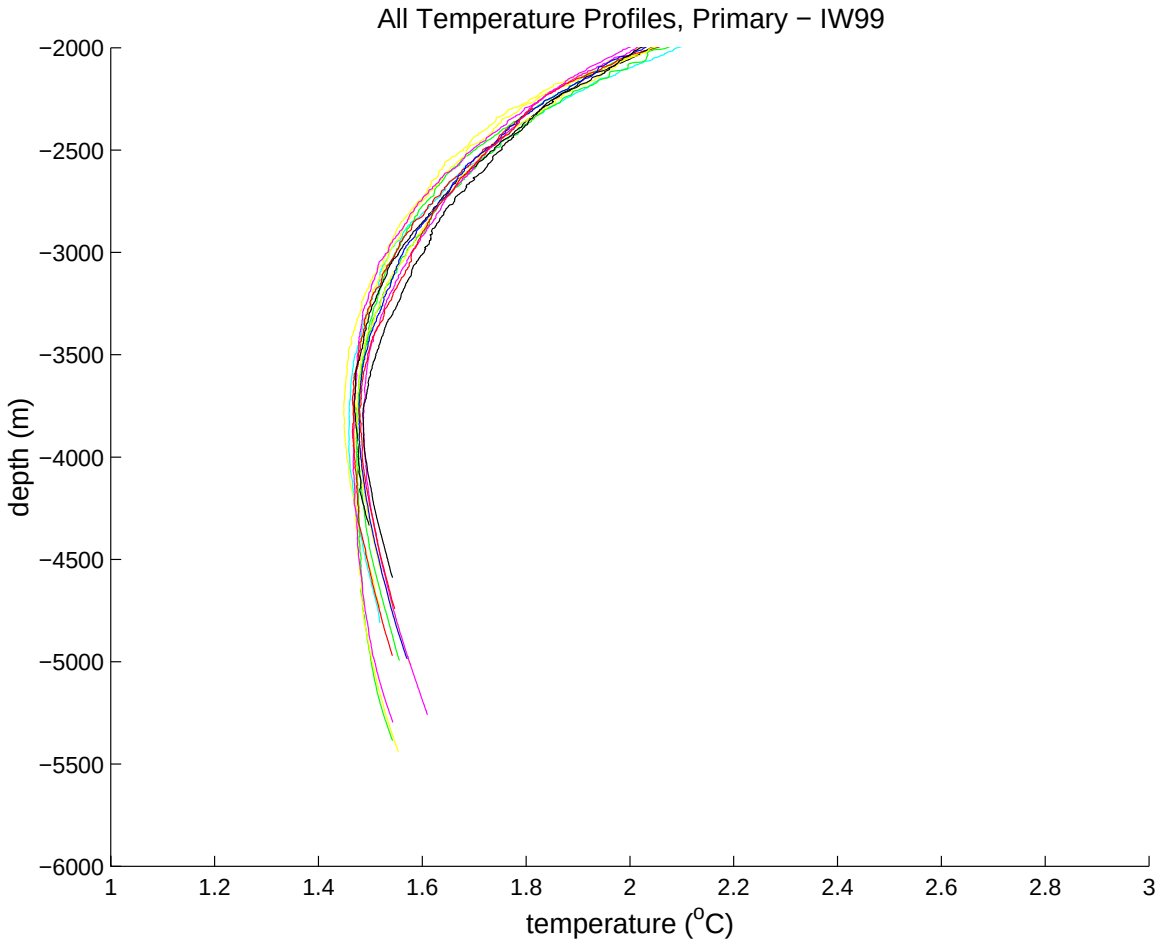

Figure 48. Temperature profiles from the primary sensor on IW99, in °C, from 2000 m down to the ocean bottom.

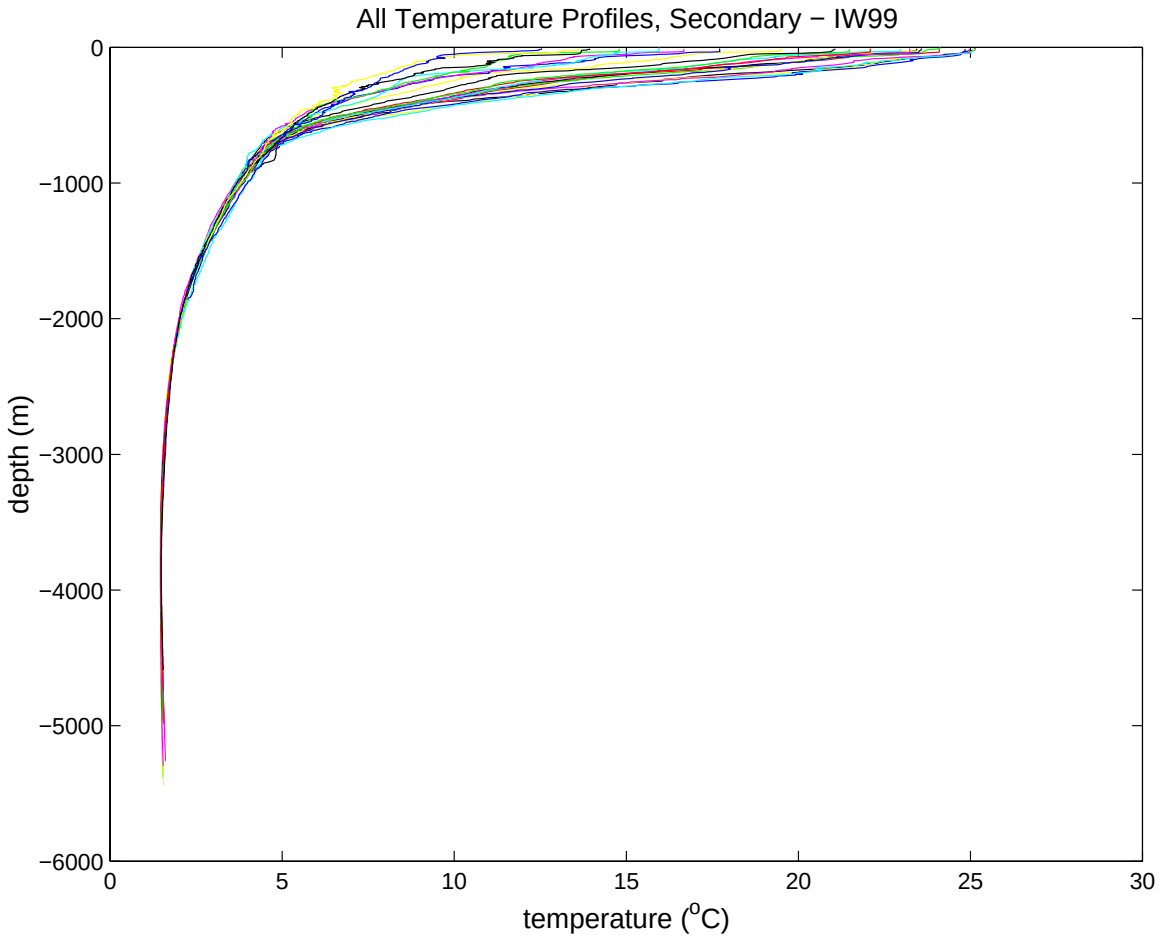

Figure 49. Temperature profiles from the secondary sensor on the IW99 cruise in °C.

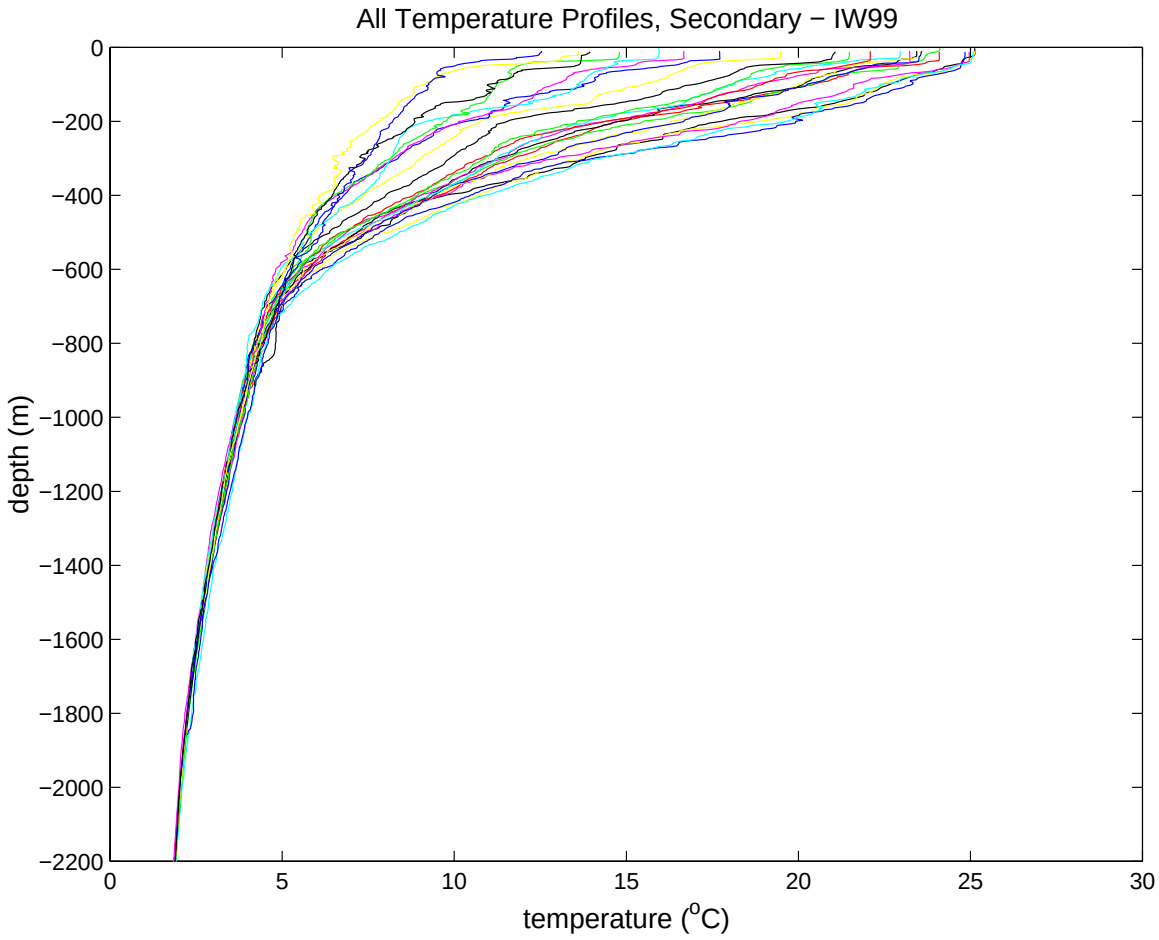

Figure 50. Temperature profiles from the secondary sensor on IW99, in °C, from the surface down to 2200 m.

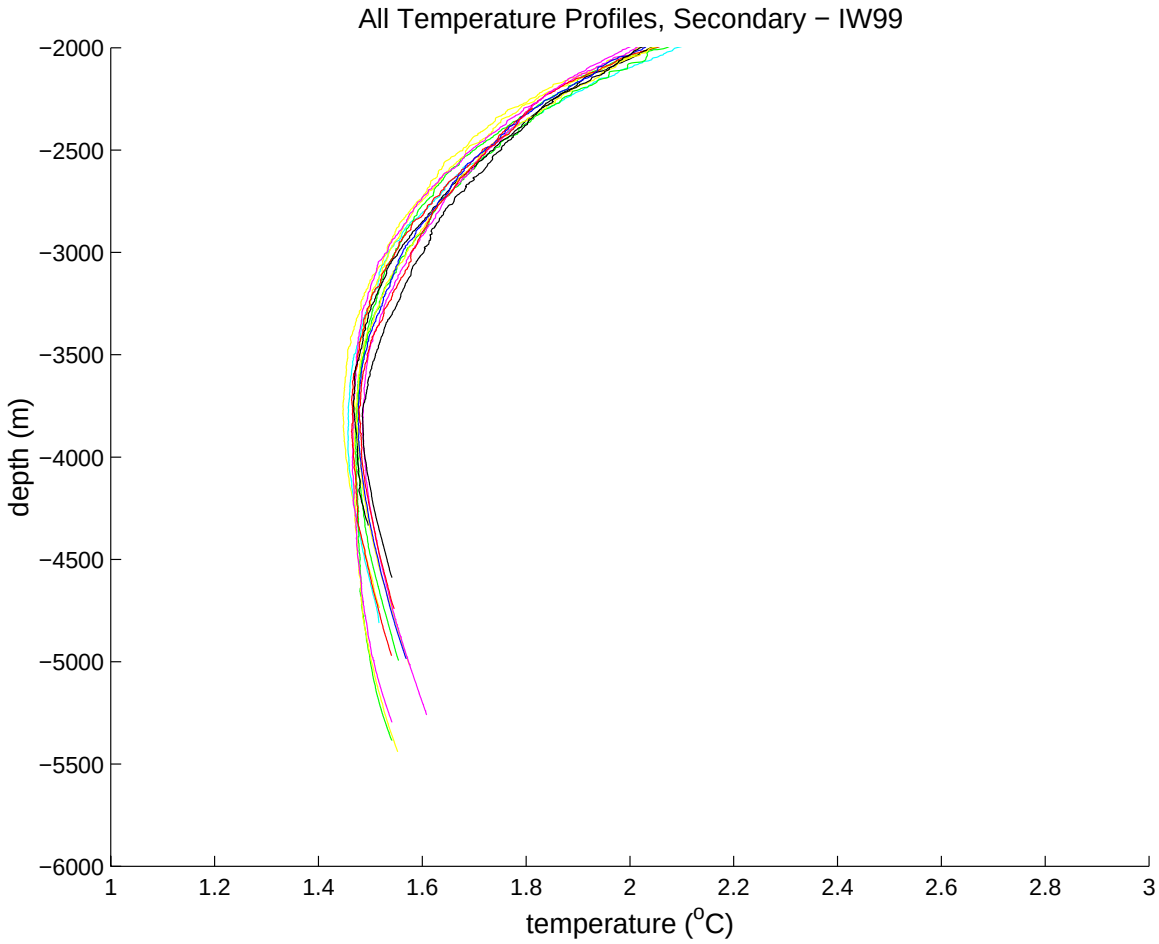

Figure 51. Temperature profiles from the secondary sensor on IW99, in °C, from 2000 m down to the ocean bottom.

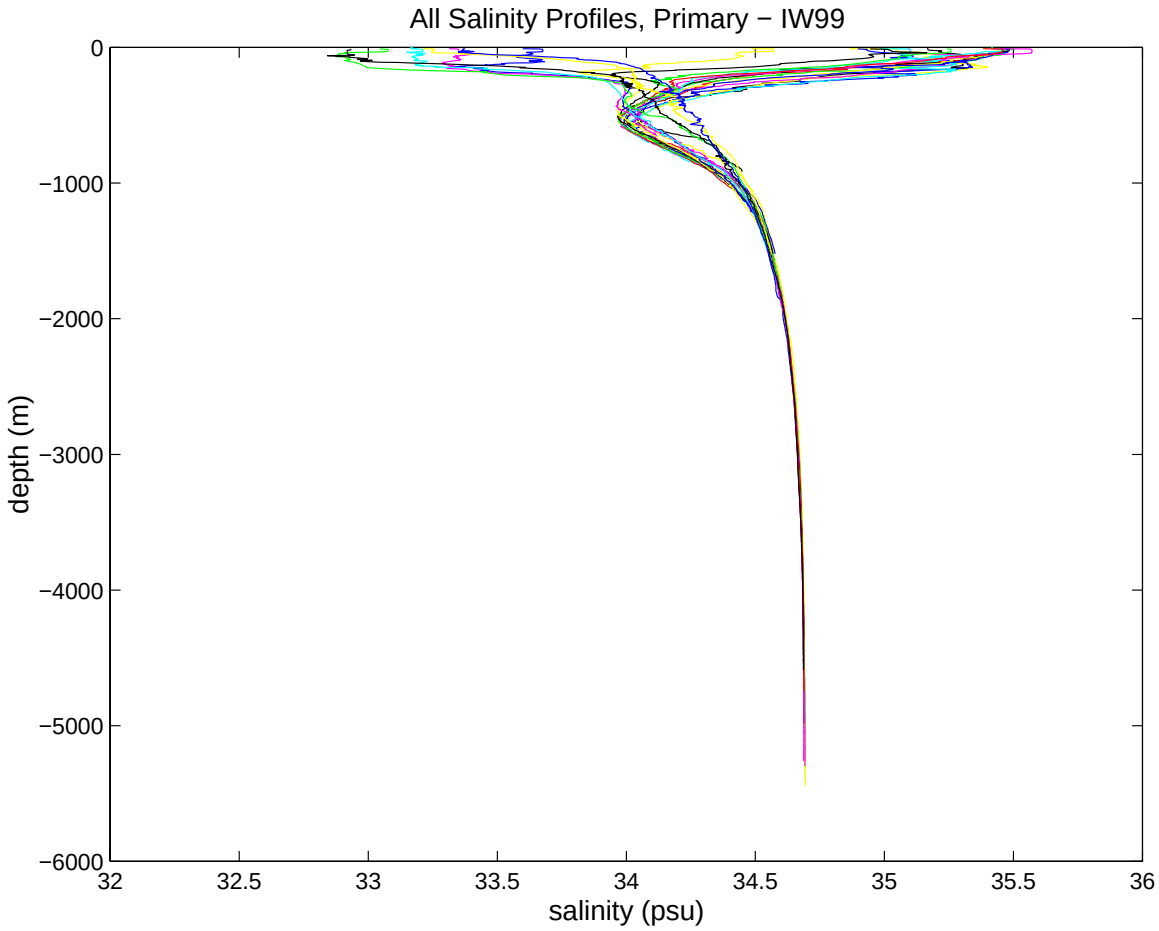

Figure 52. Salinity profiles, in psu, computed from the primary sensor on the IW99 cruise.

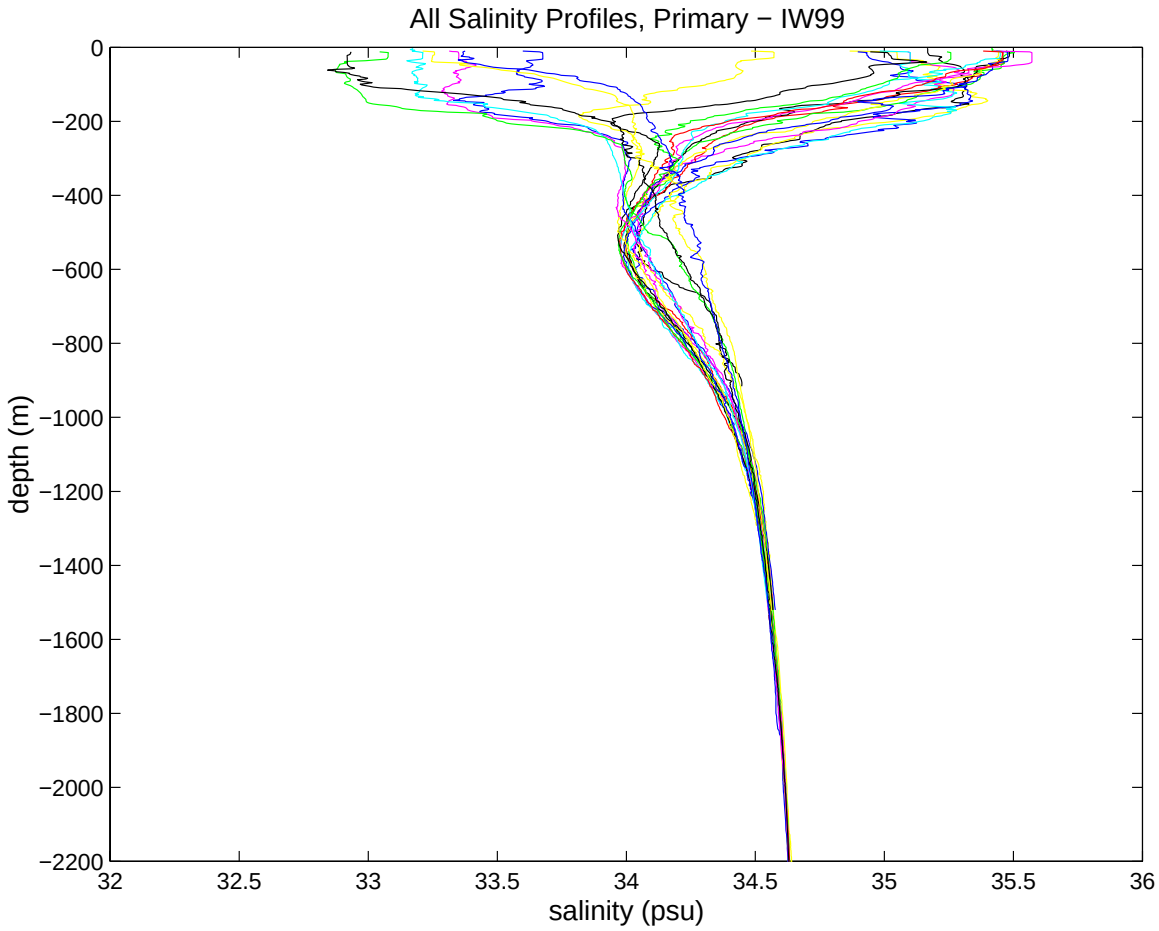

Figure 53. Salinity profiles, in psu, computed from the primary sensor on IW99 from the surface down to 2200 m.

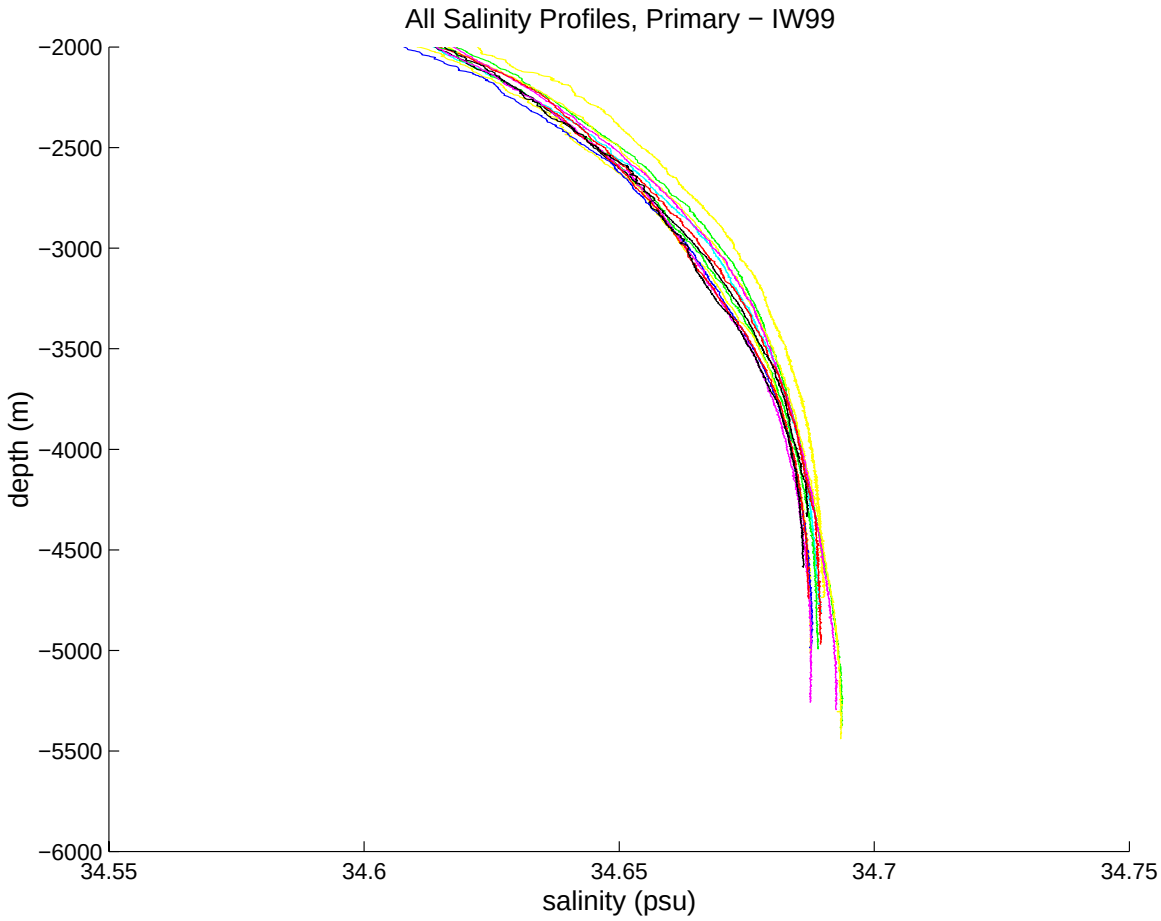

Figure 54. Salinity profiles, in psu, computed from the primary sensor on IW99 from 2000 m down to the ocean bottom.

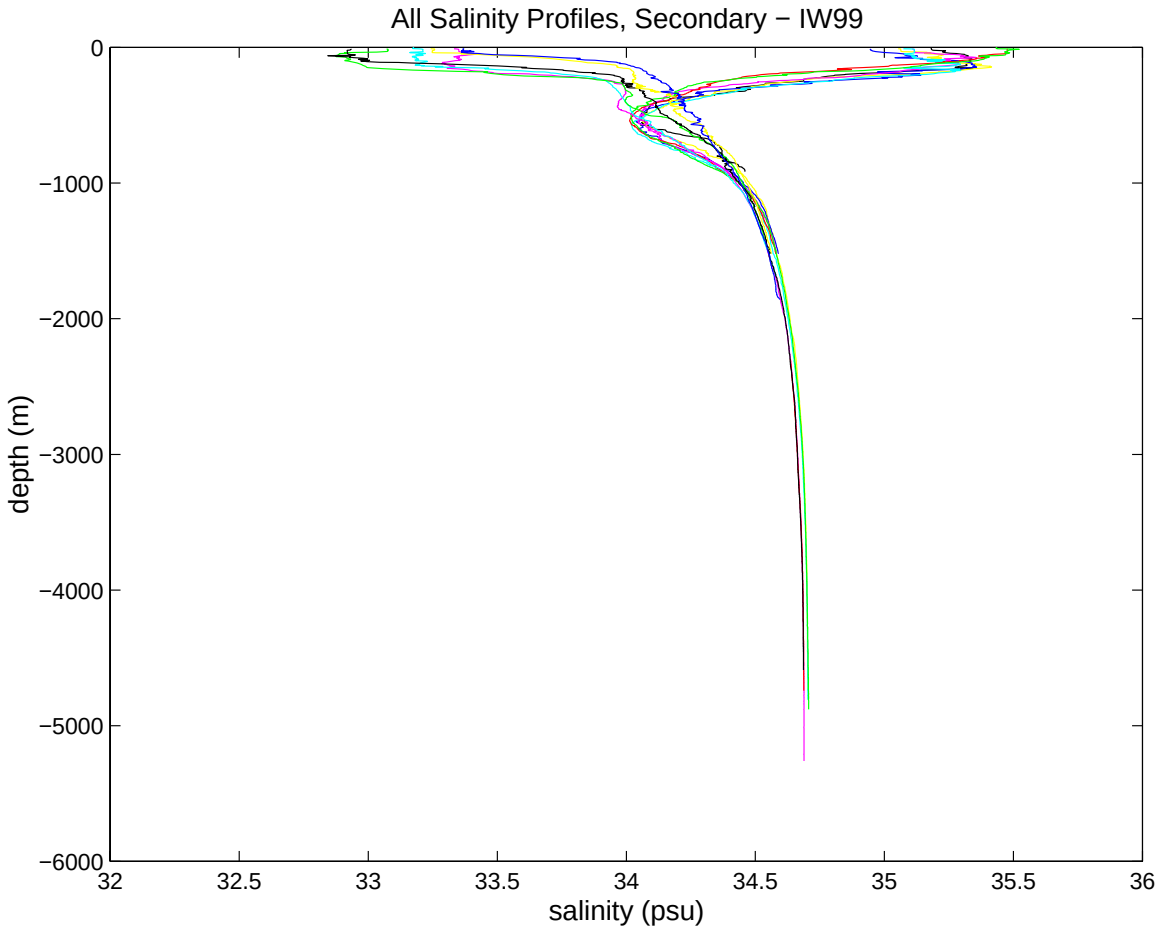

Figure 55. Salinity profiles, in psu, computed from the secondary sensor on the IW99 cruise. Casts #8, 9, 10, 11, 12, 13, 15, 17, 20, and 22 have been removed. See text for details.

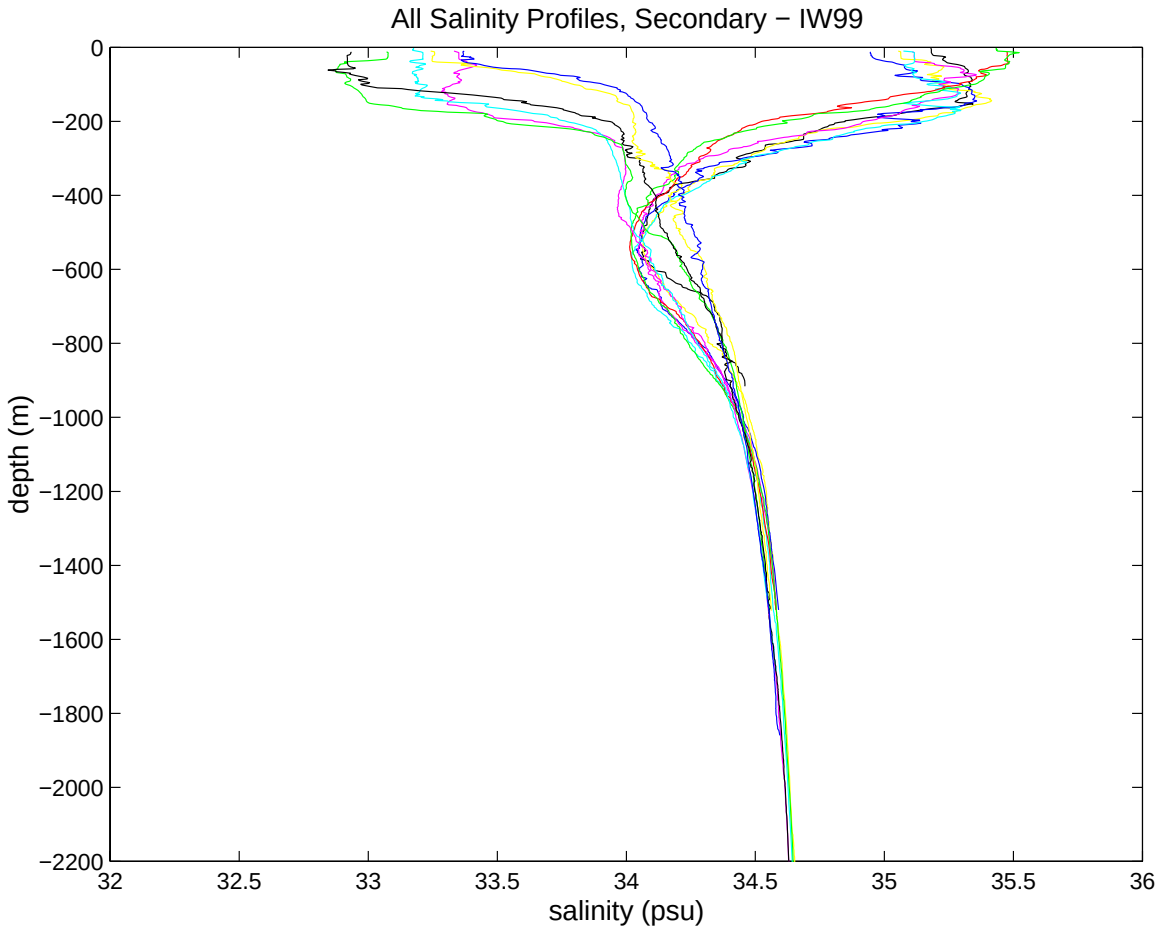

Figure 56. Salinity profiles, in psu, computed from the secondary sensor on IW99 from the surface down to 2200 m.

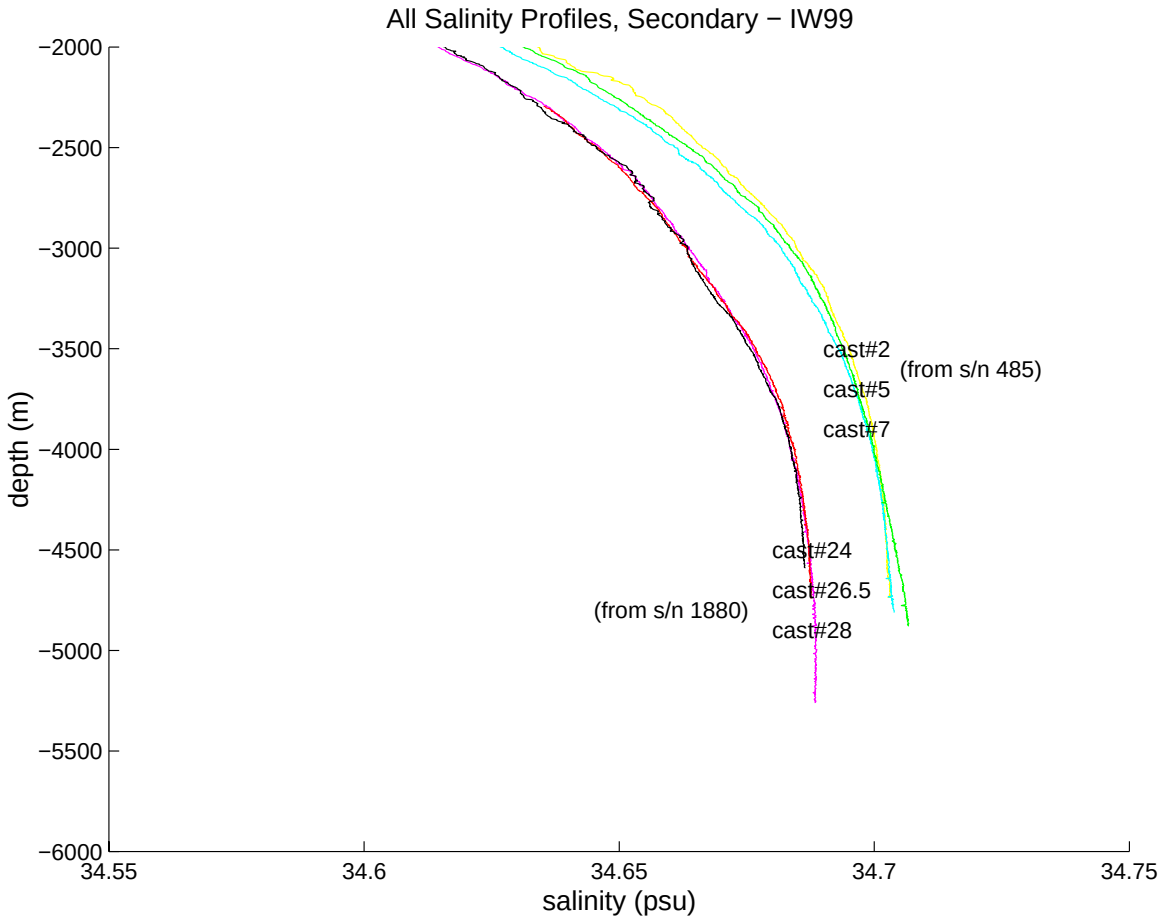

Figure 57. Salinity profiles, in psu, computed from the secondary sensor on IW99 from 2000 m down to the ocean bottom. Casts #2, 5, and 7 are with secondary conductivity sensor number 485. Casts #24, 26.5, and 28 are with secondary conductivity sensor 1880.

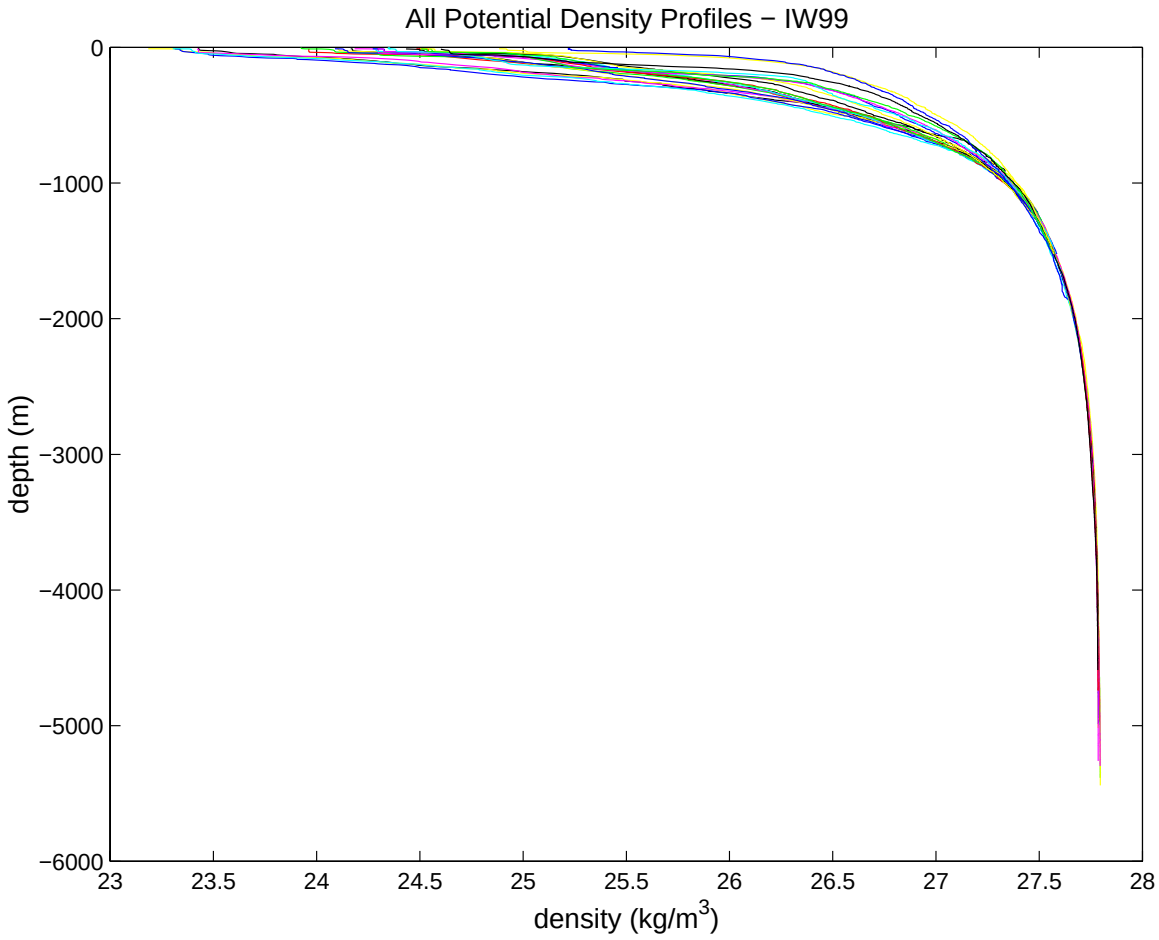

Figure 58. Potential density profiles, in kg/m^3, from IW99 cruise.

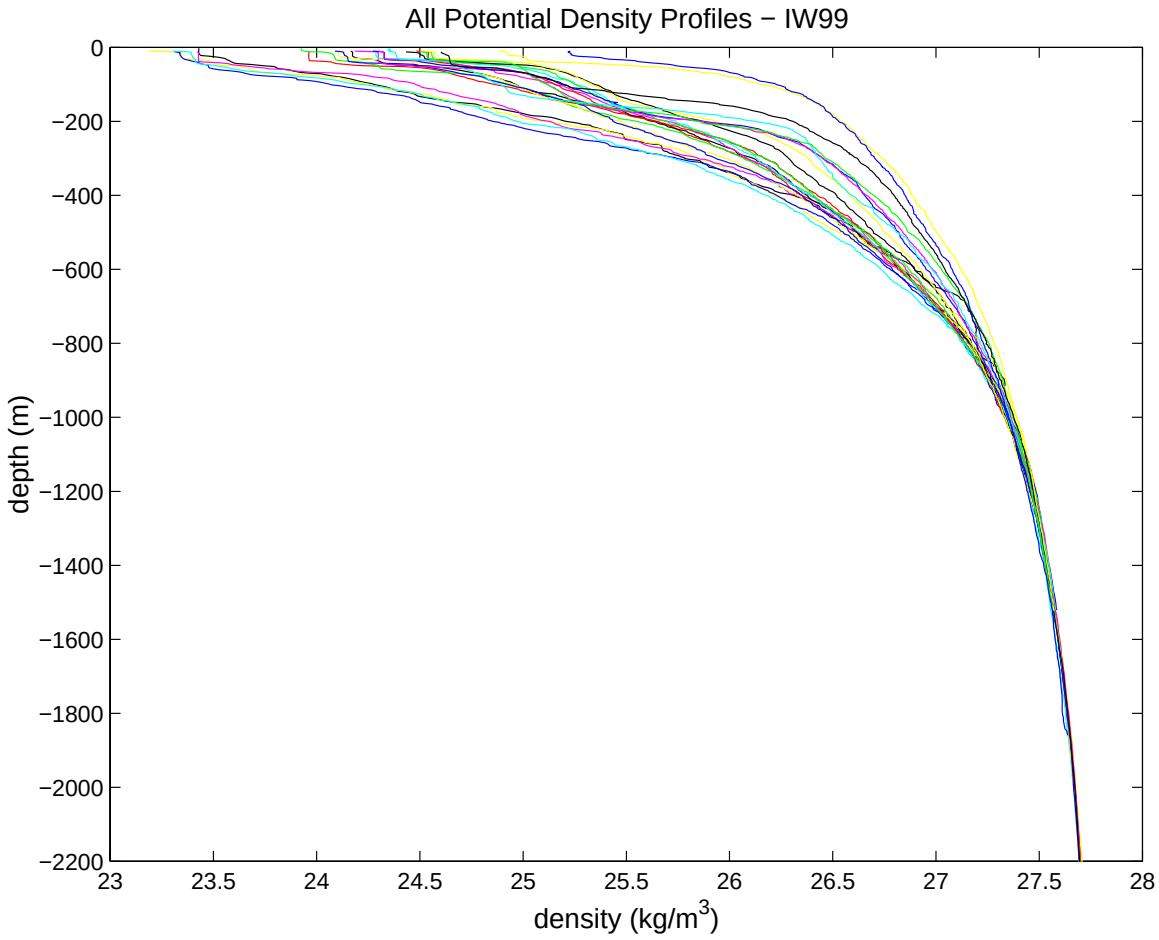

Figure 59. Potential density profiles, in kg/m^3, from the IW99 cruise from the surface down to 2200 m.

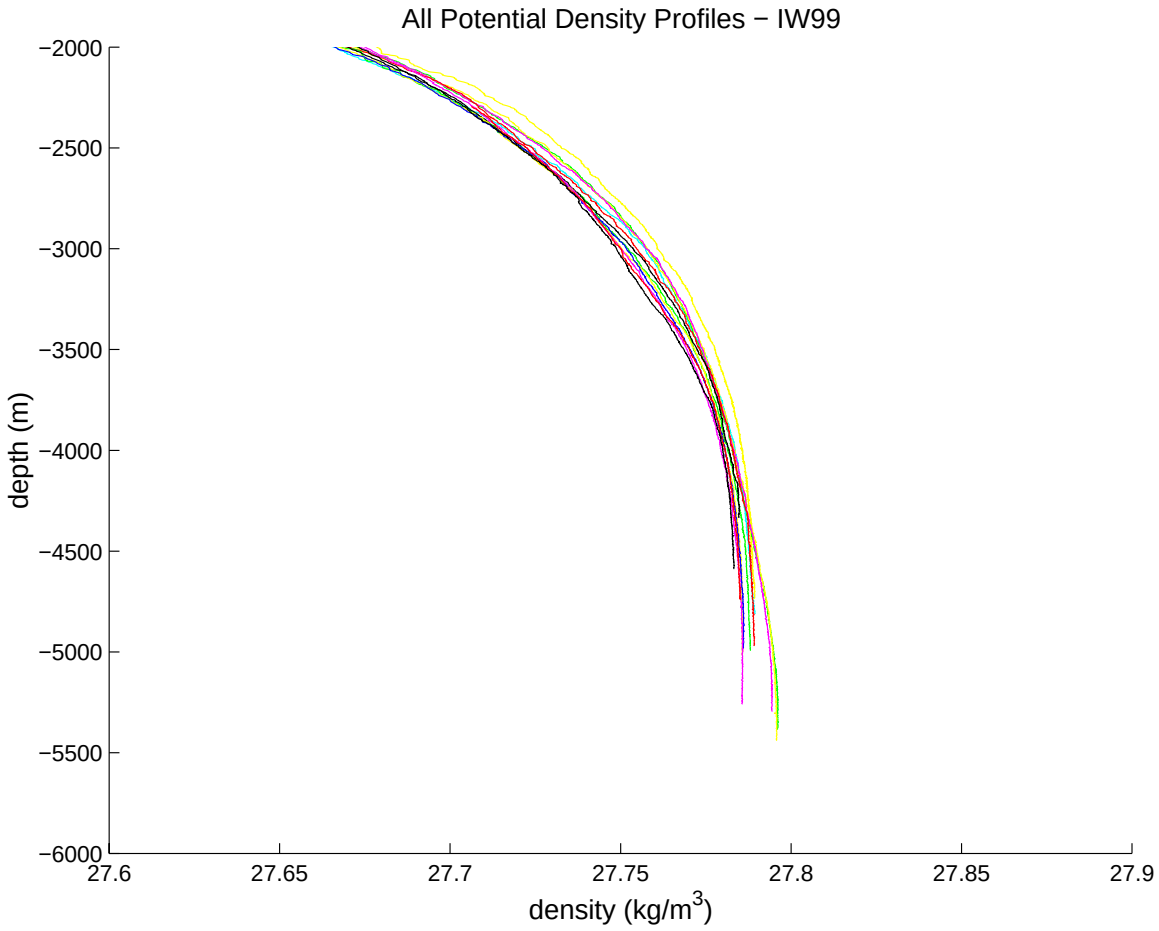

Figure 60. Potential density profiles, in kg/m^3, from the IW99 cruise from 2000 m down to the ocean bottom.

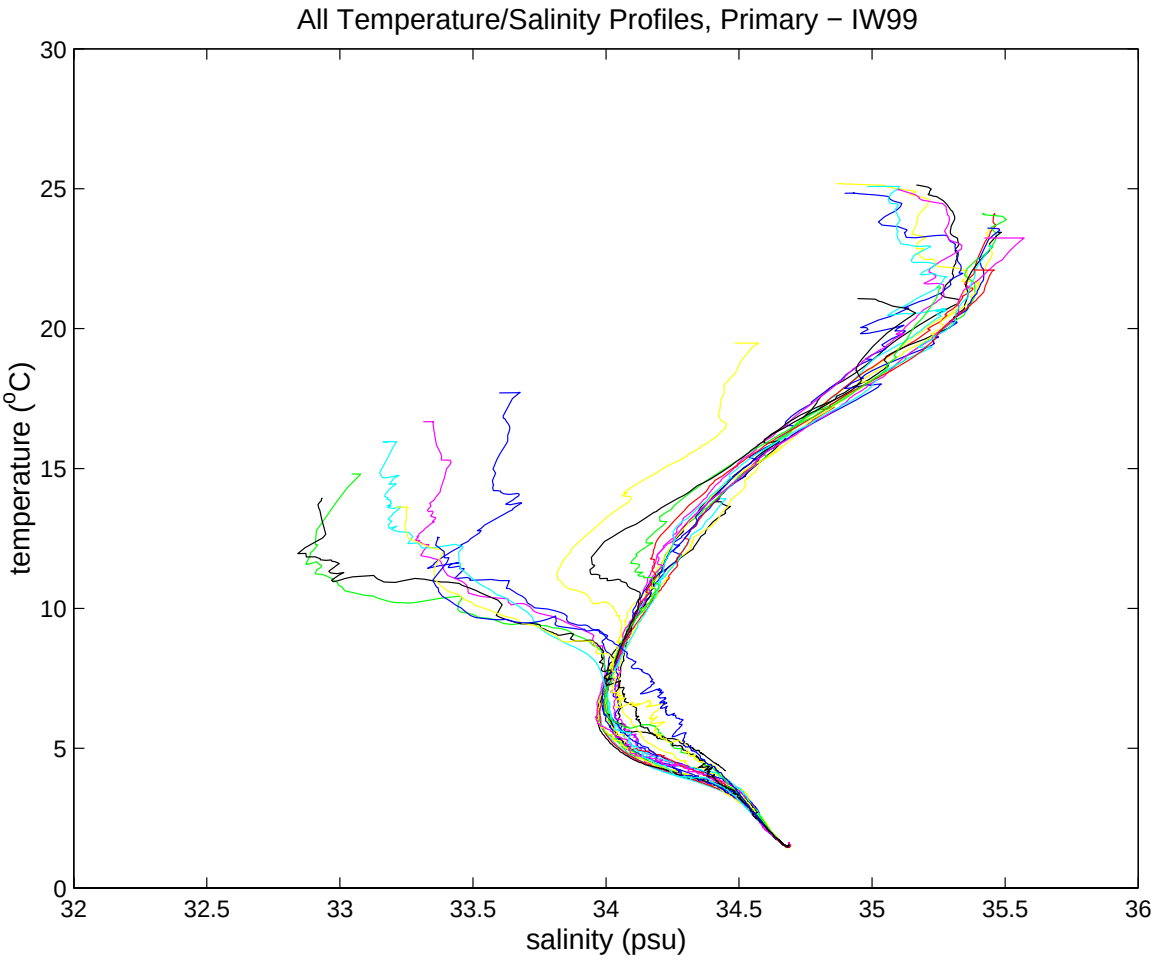

Figure 61. Temperature-salinity profiles from the primary sensors from the IW99 cruise. Temperature in °C and salinity in psu.

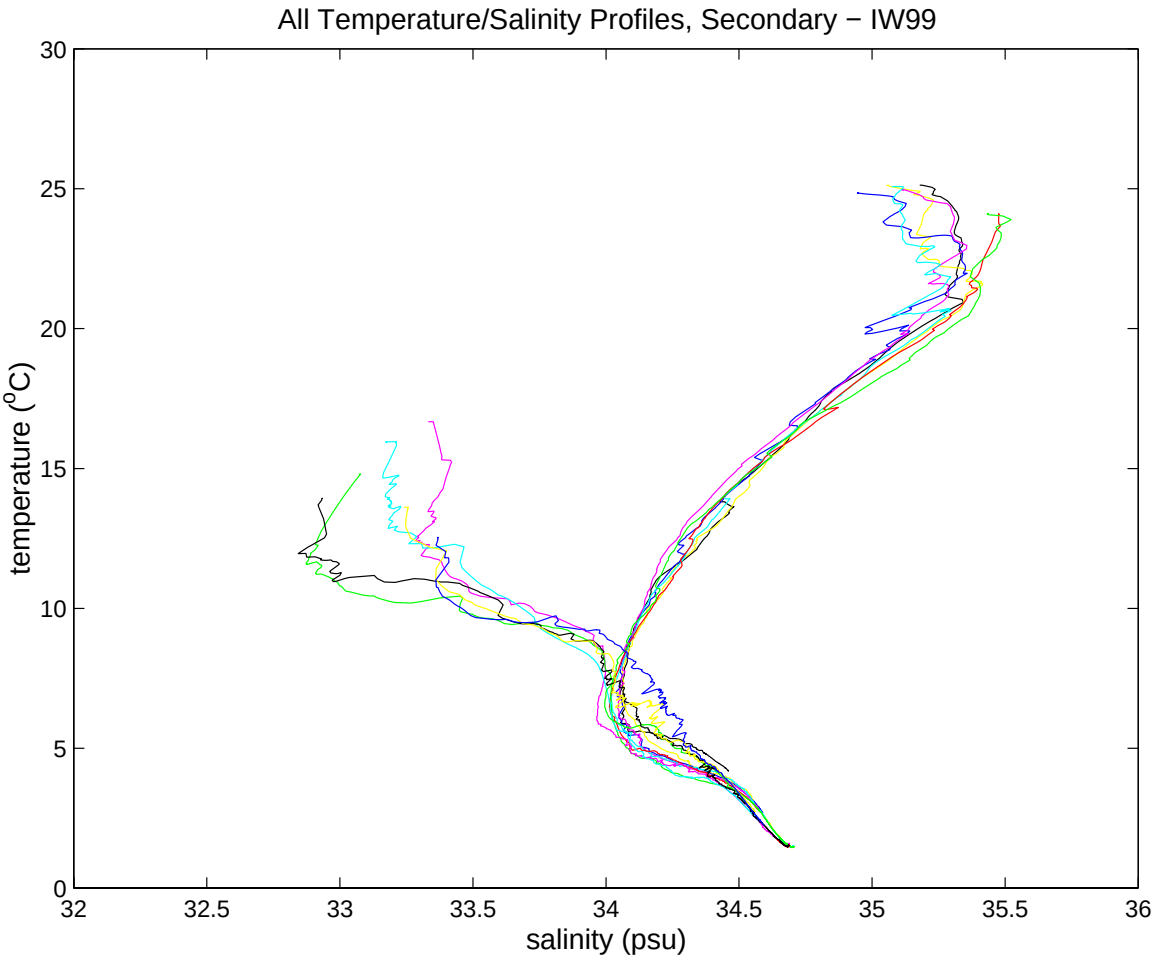

Figure 62. Temperature-salinity profiles from the secondary sensors from the IW99 cruise. Temperature in °C and salinity in psu.

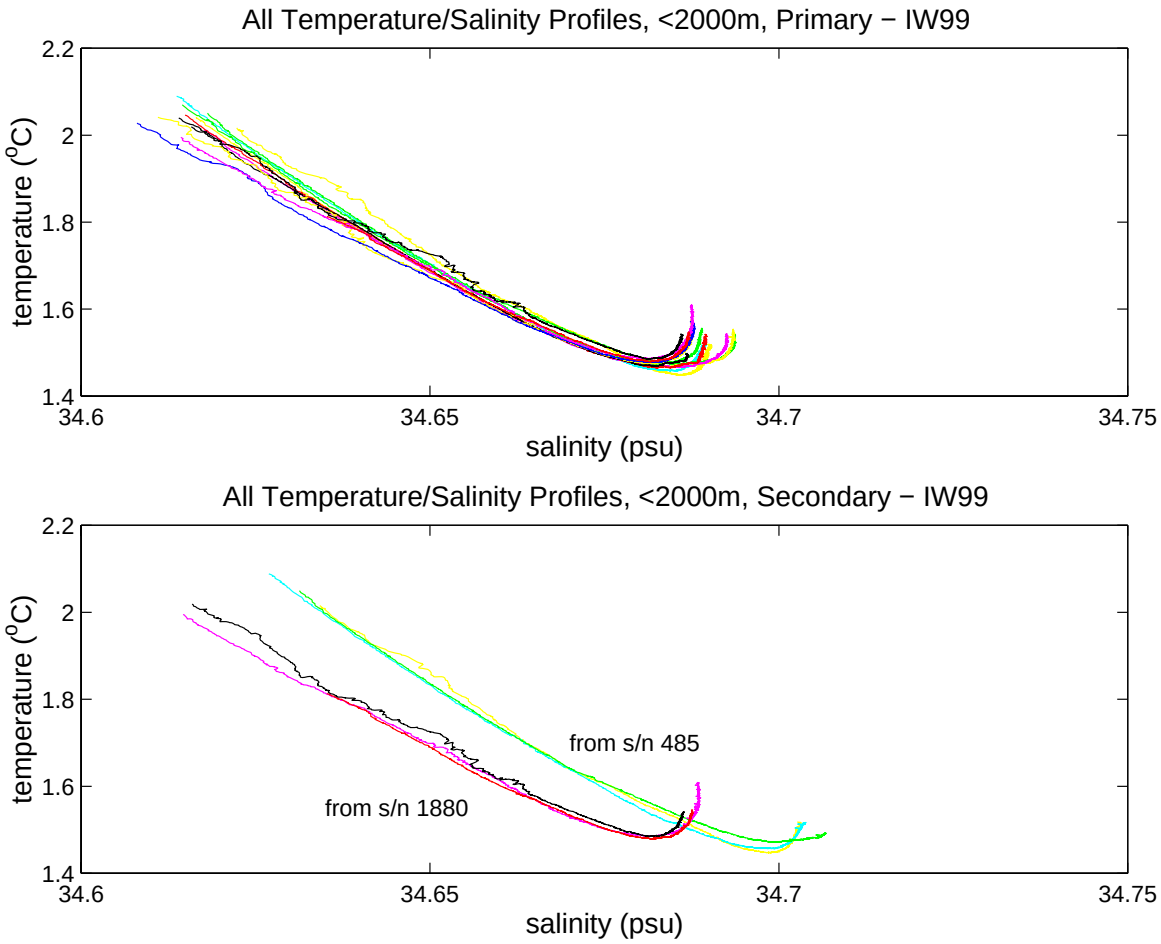

Figure 63. Temperature-salinity profiles below 2000 m from (a) the primary sensors and (b) the secondary sensors from the IW99 cruise. In (b) the serial numbers of the secondary conductivity sensor are shown. Temperature in °C and salinity in psu.

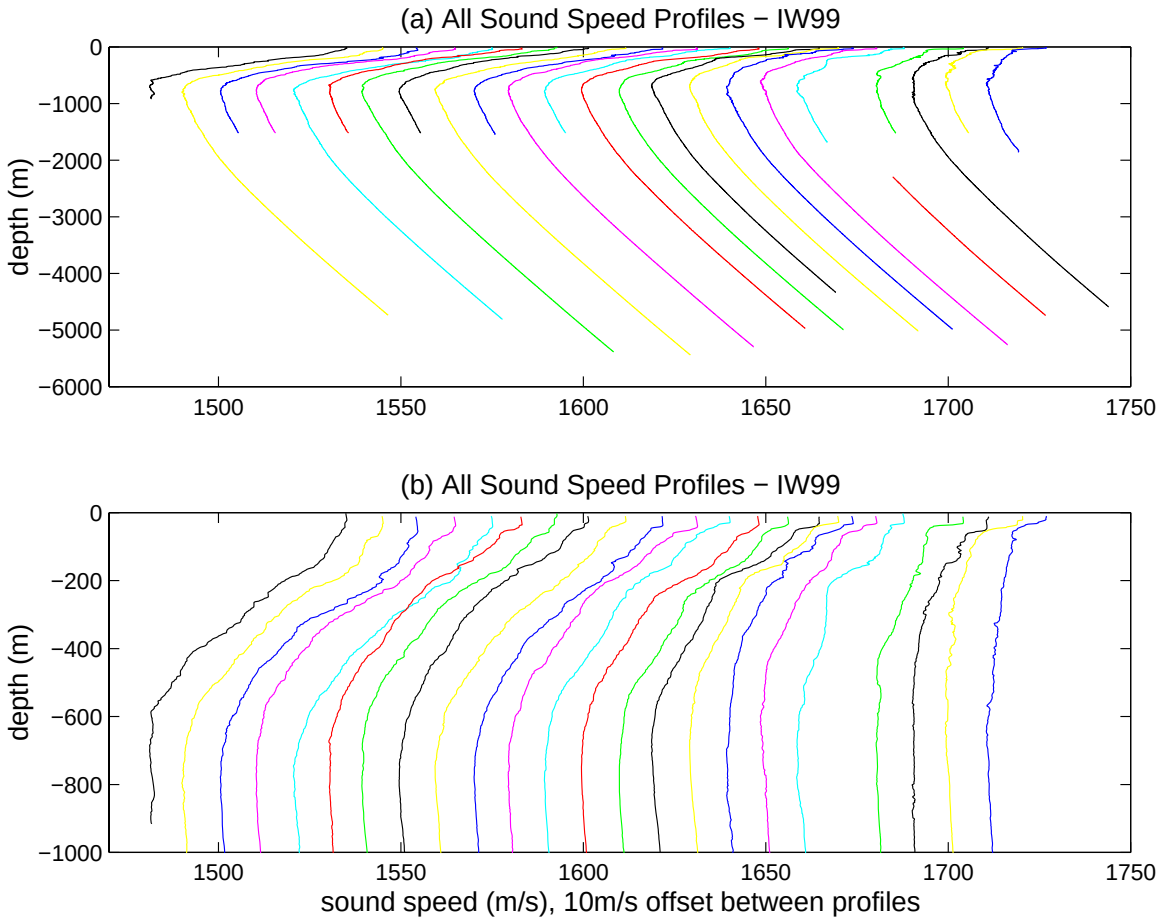

Figure 64. Sound speed profiles from IW99 for (a) the entire depth and (b) the top 1000 m. Velocities are given in m/s. Profiles are separated by 10 m/s.

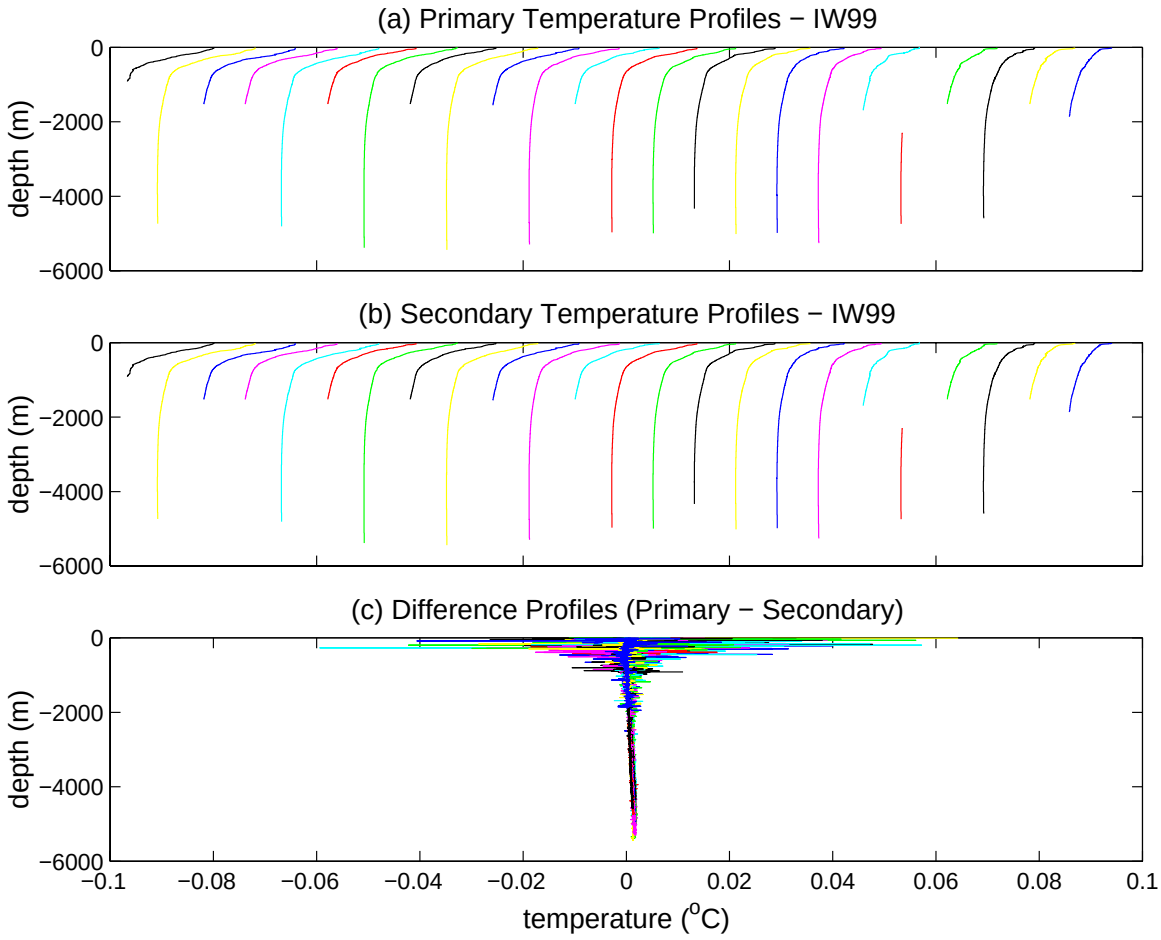

Figure 65. Temperature profiles from IW99 for (a) the primary sensor and (b) the secondary sensor for the entire depth. (c) Primary minus secondary temperatures. Temperatures are given in °C. Profiles are separated by 10°C.

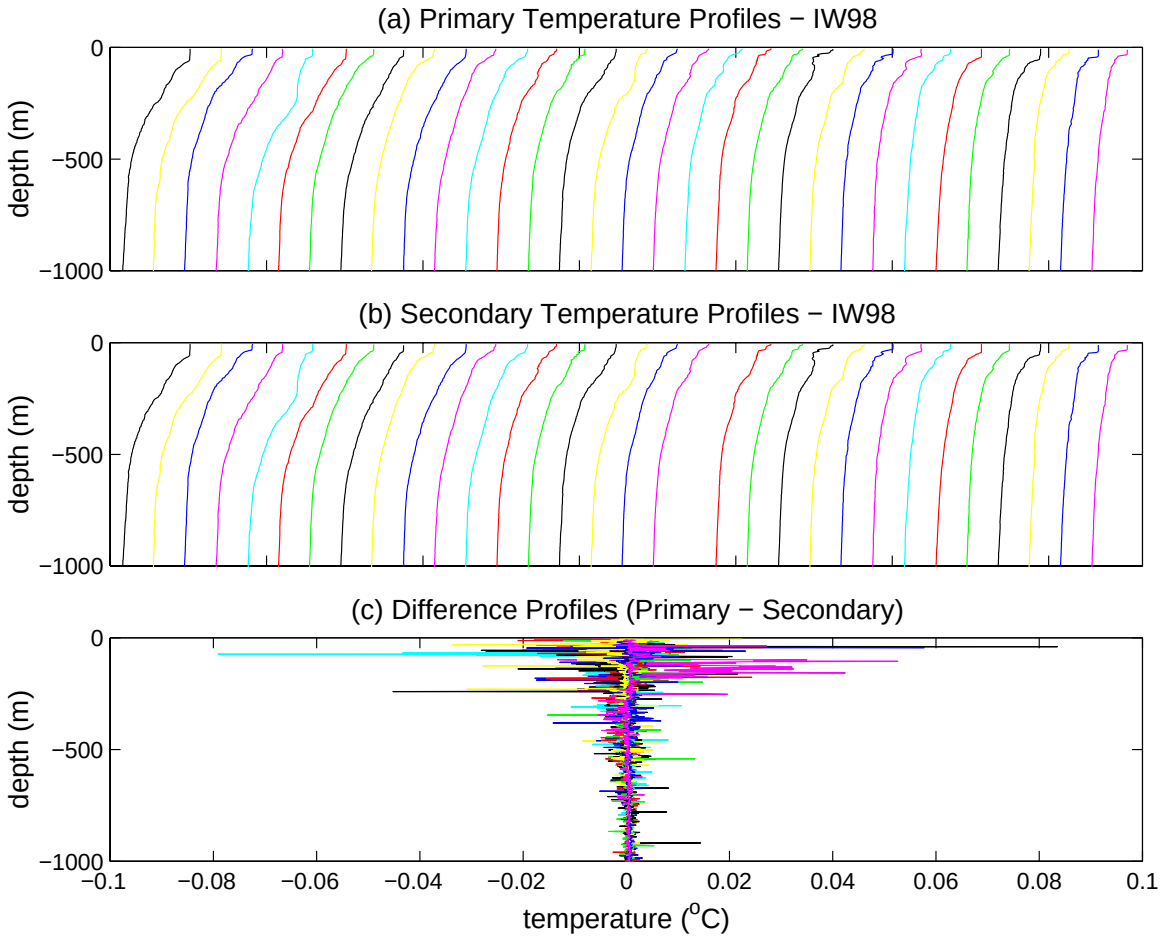

Figure 66. Same as Figure 65, except showing only the top 1000 m.

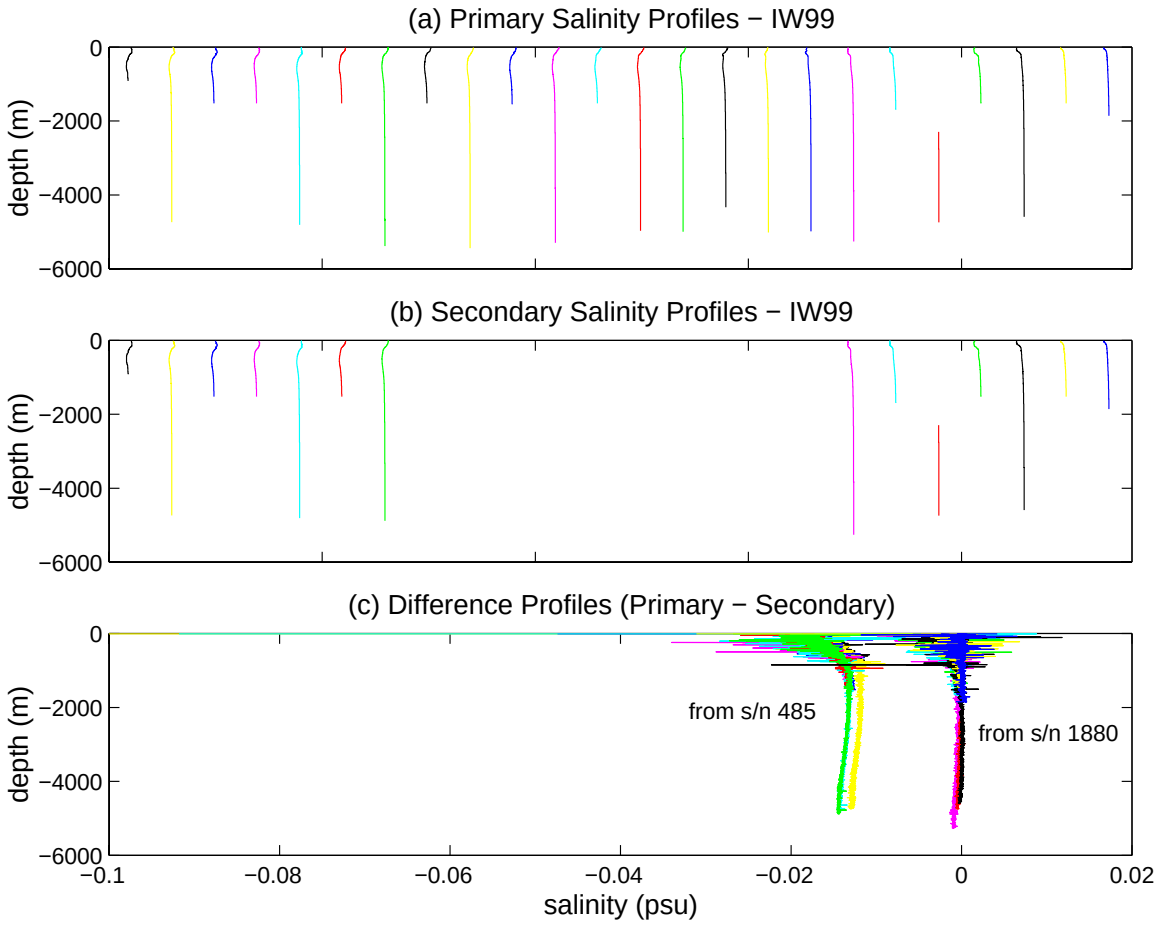

Figure 67. Salinity profiles from IW99 for (a) the primary sensor and (b) the secondary sensor for the entire depth. Casts #8, 9, 10, 11, 12, 13, 15, 17, 20, and 22 were removed due to secondary conductivity sensor serial number 485 being faulty. (c) Primary minus secondary salinities. Note the difference between salinities measured with conductivity sensors, serial number 485 and serial number 1880. Salinities are given in psu. Profiles are separated by 10 psu.

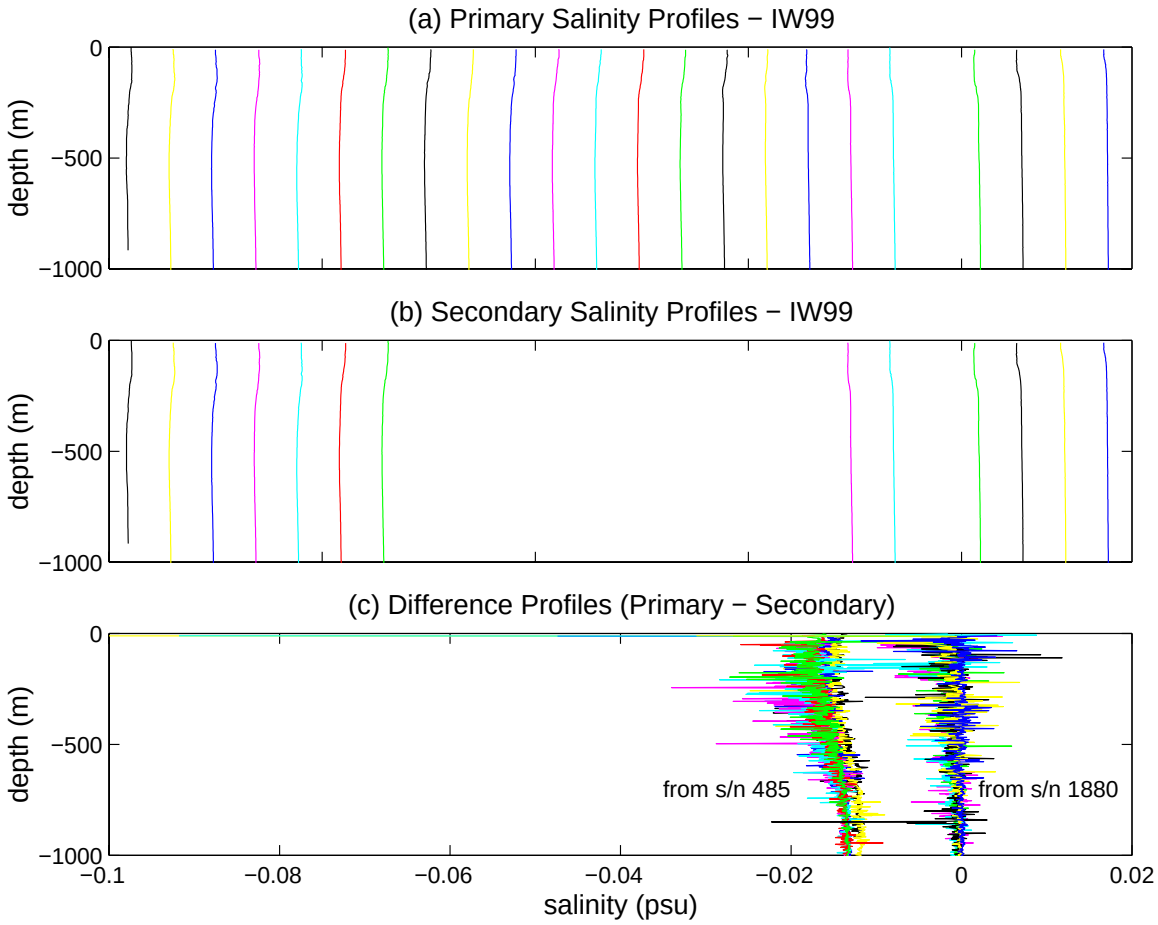

Figure 68. Same as Figure 67, except showing only the top 1000 m.

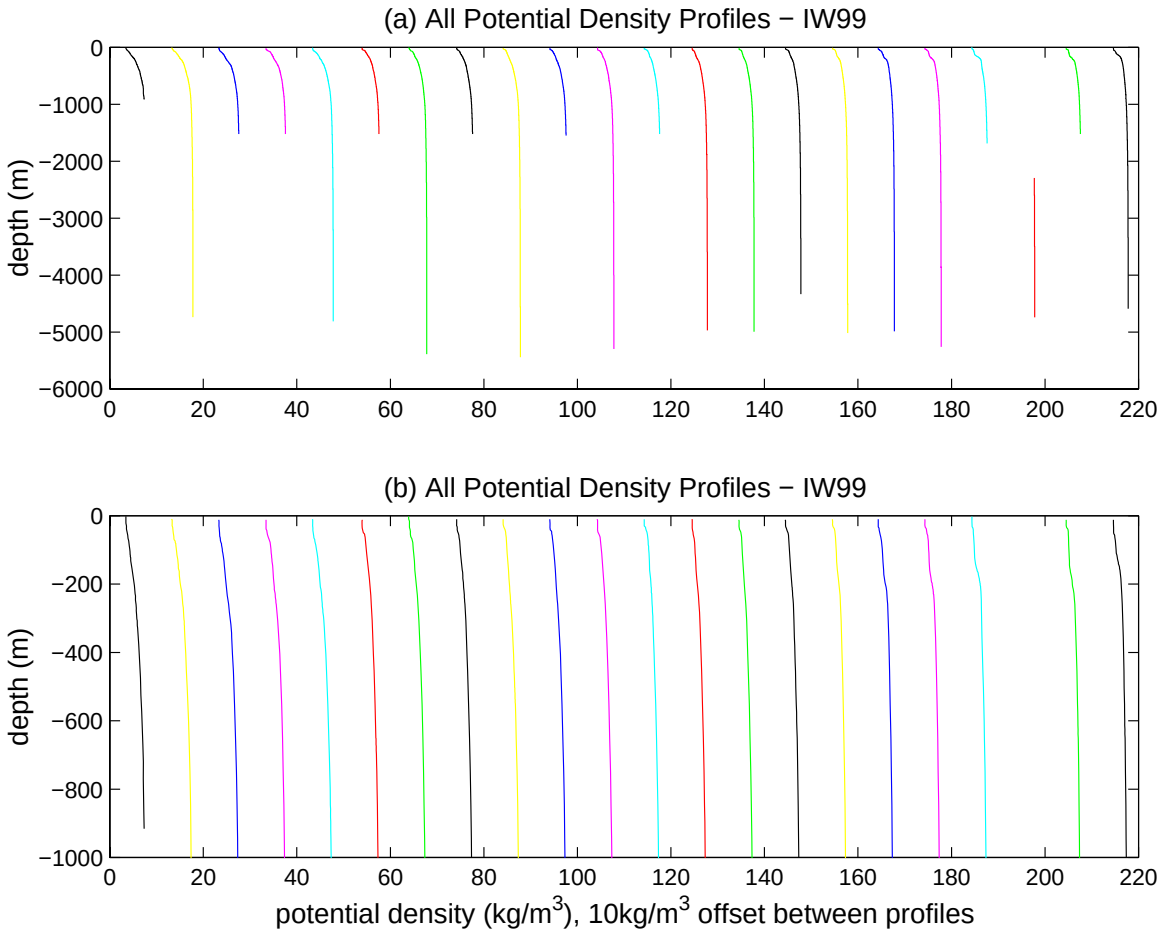

Figure 69. Potential density profiles from IW99 for (a) the entire depth and (b) the top 1000 m. All profiles separated by 10 kg/m^3.

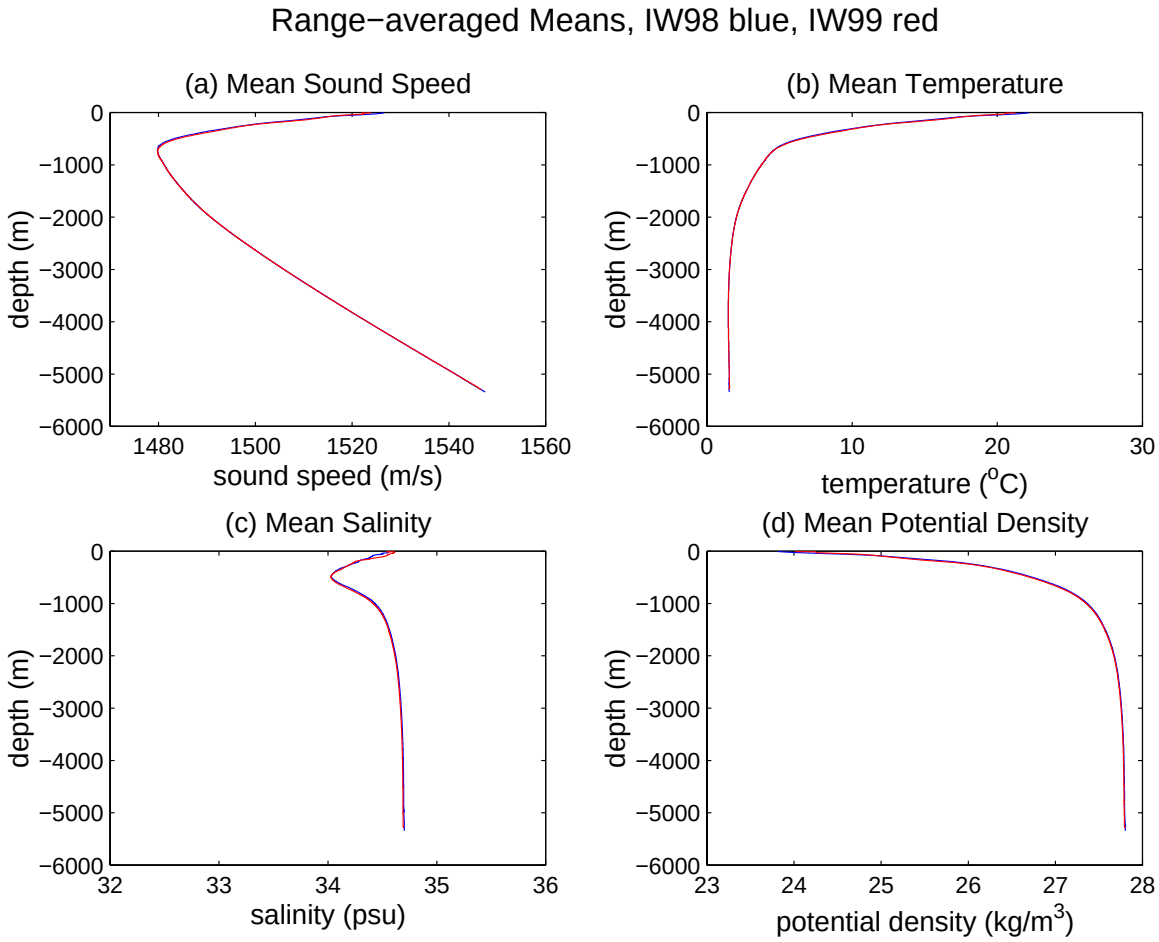

Figure 70. Range-averaged means for IW98 in blue and IW99 in red for (a) sound speed in m/s, (b) primary temperature in °C, (c) primary salinity in psu, and (d) potential density in kg/m^3.

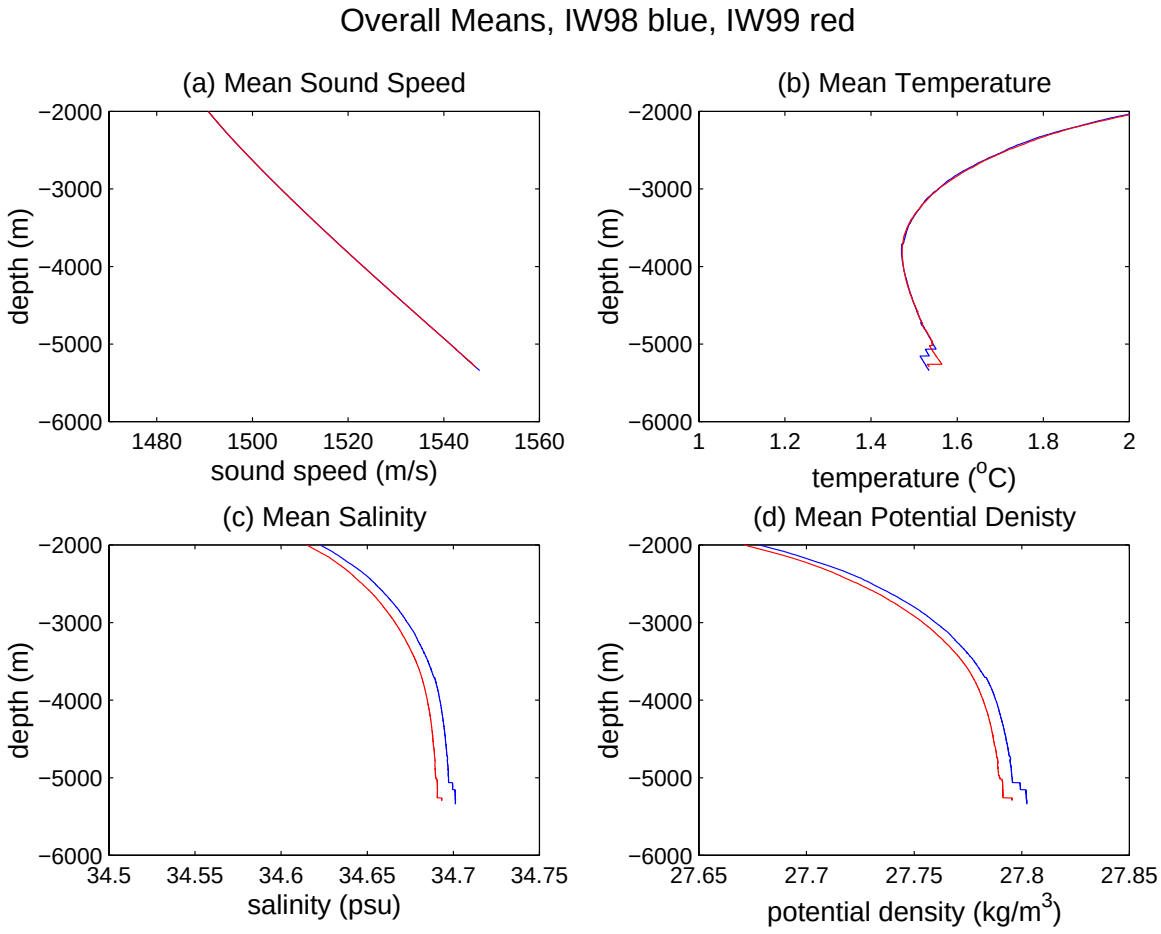

Figure 71. Same as Figure 70, except from 2000 m down to the ocean bottom. The range-averaged primary salinity and potential density means are larger from IW98 than those from IW99.

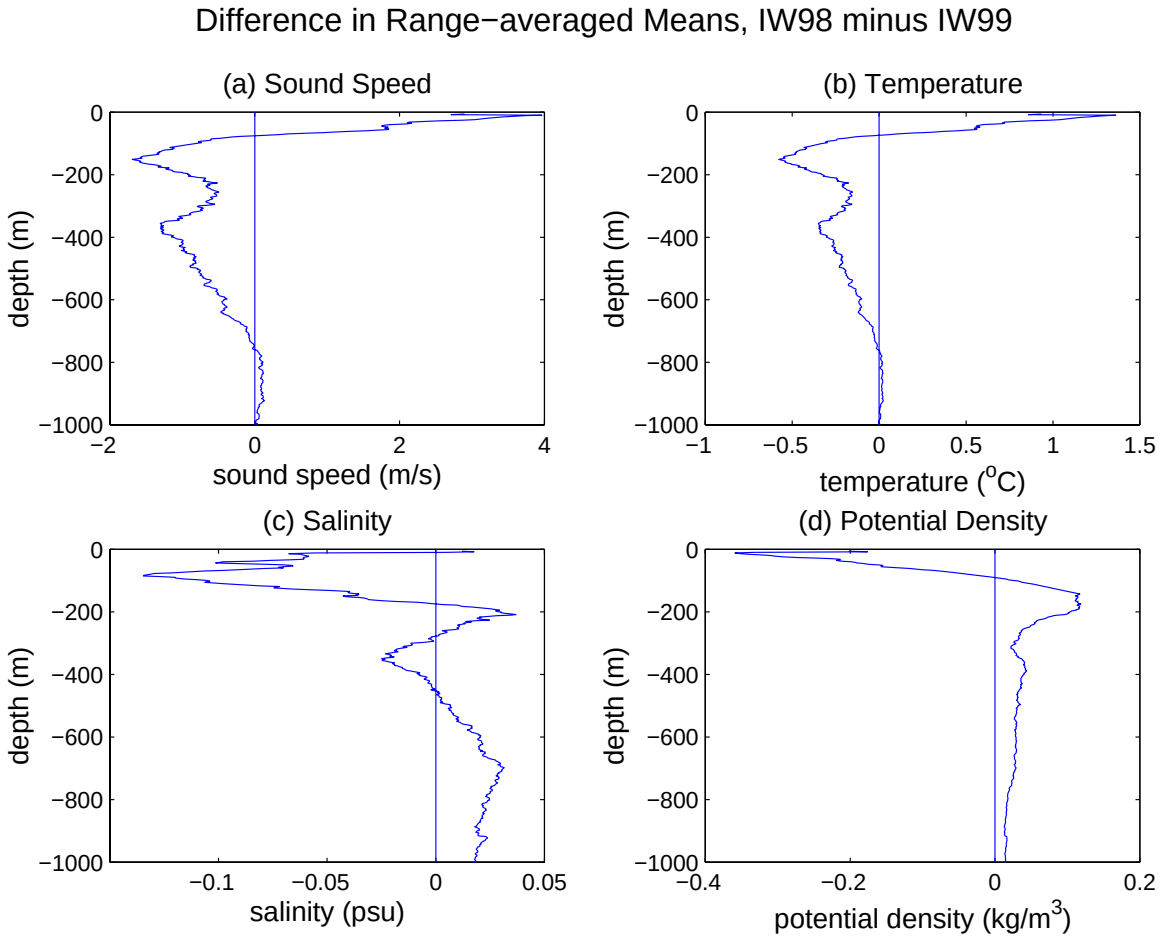

Figure 72. Difference in range-averaged means from IW98 minus IW99 for top 1000 m, for (a) sound speed in m/s, (b) primary temperature in °C, (c) primary salinity in psu, and (d) potential density in kg/m^3.

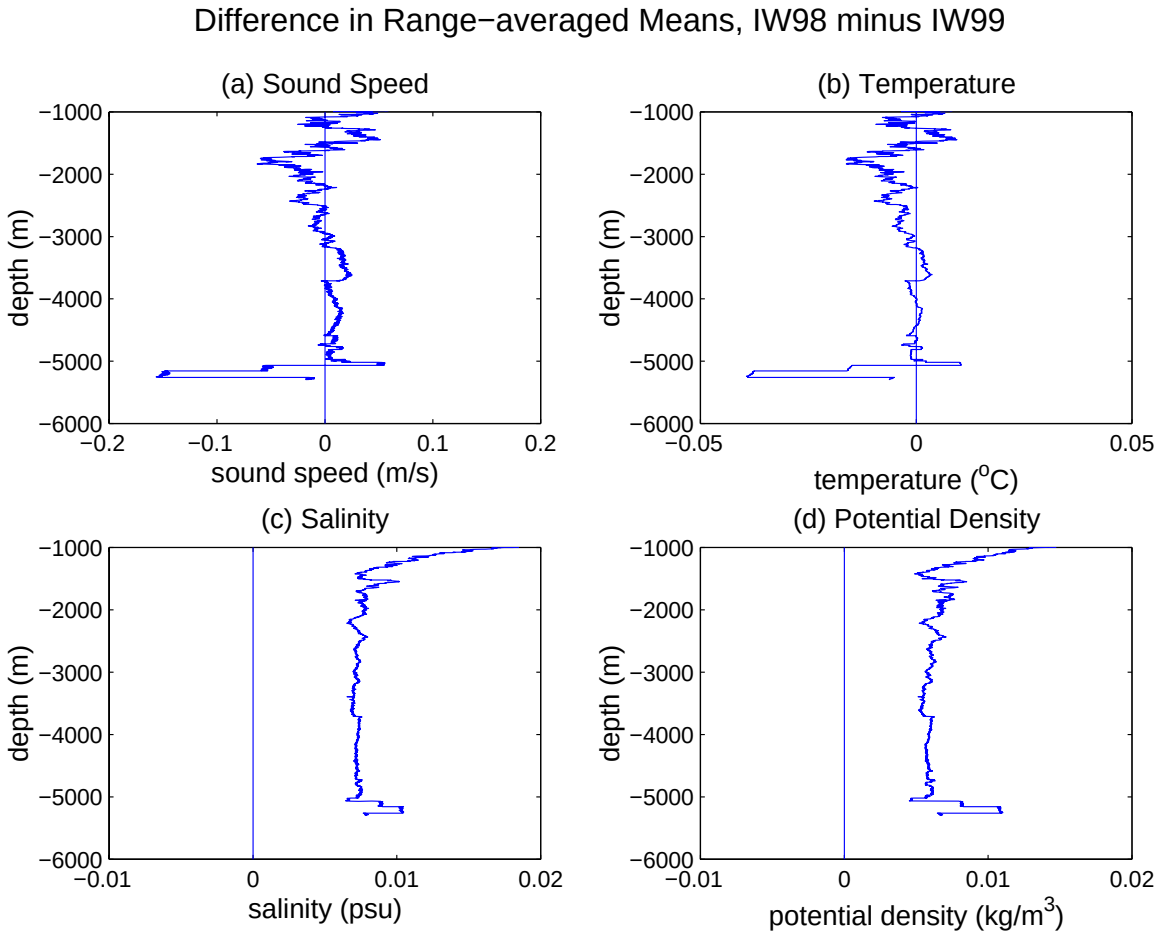

Figure 73. Same as Figure 72, except for 1000 m down to the ocean bottom.

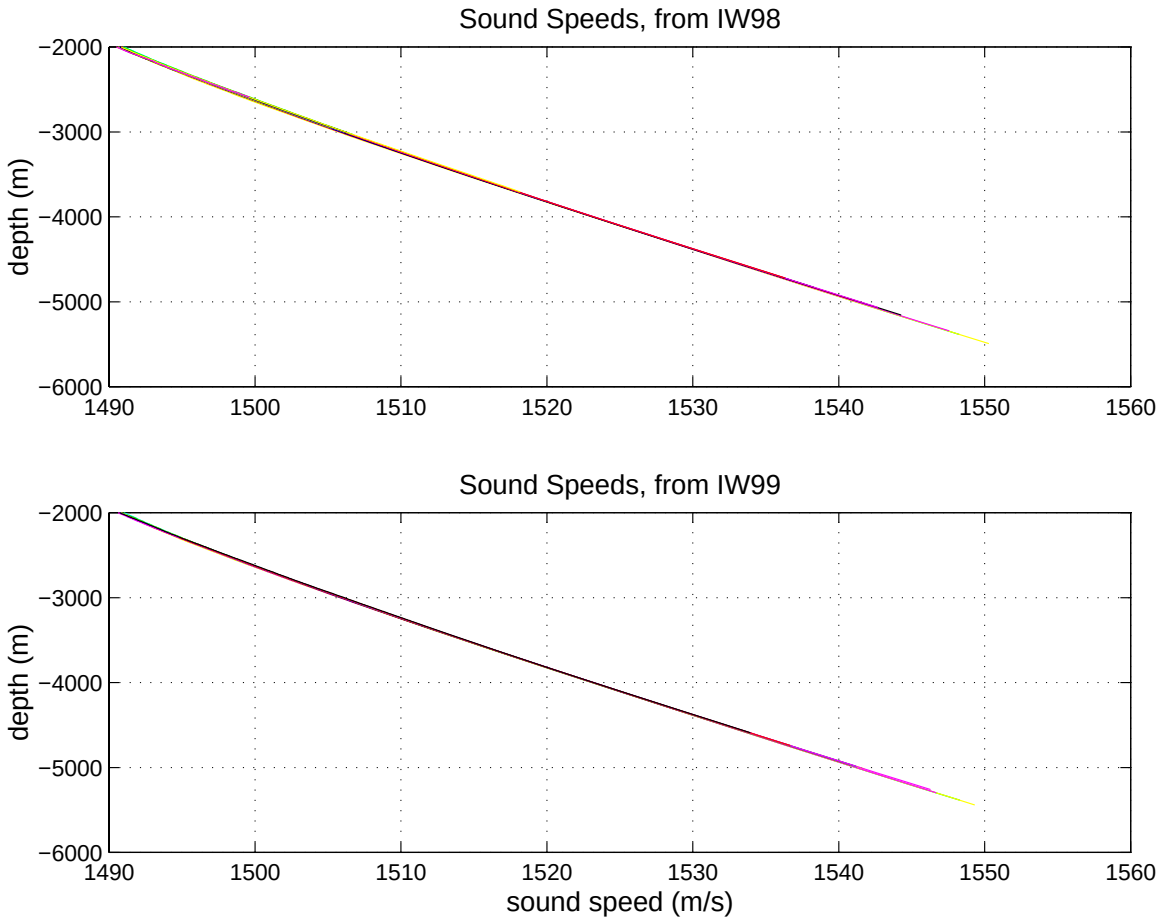

Figure 74. Sound speed profiles below 2000 m from (a) IW98 and (b) IW99 for comparison. Sound speed in m/s.

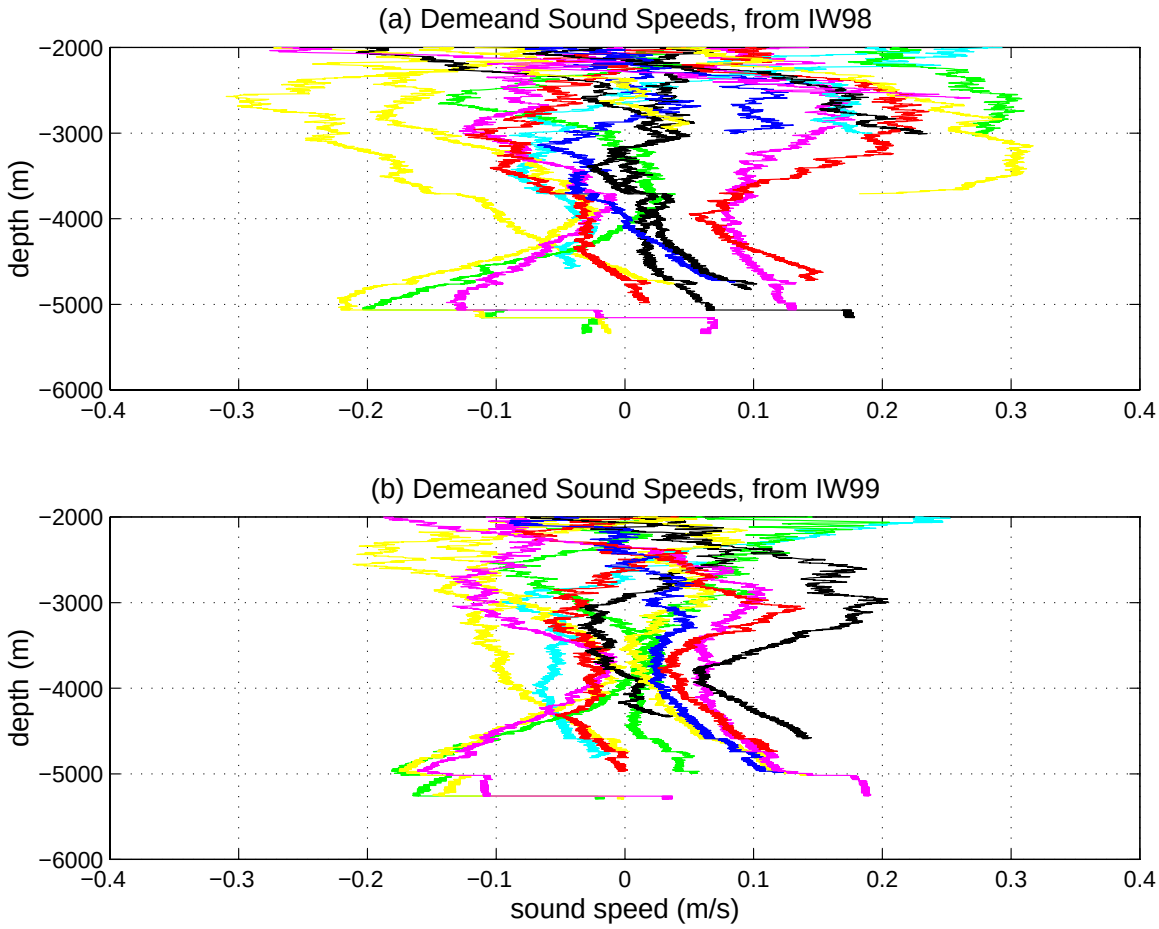

Figure 75. Demeaned sound speed profiles below 2000 m from (a) IW98 and (b) IW99 for comparison. Sound speed in m/s.

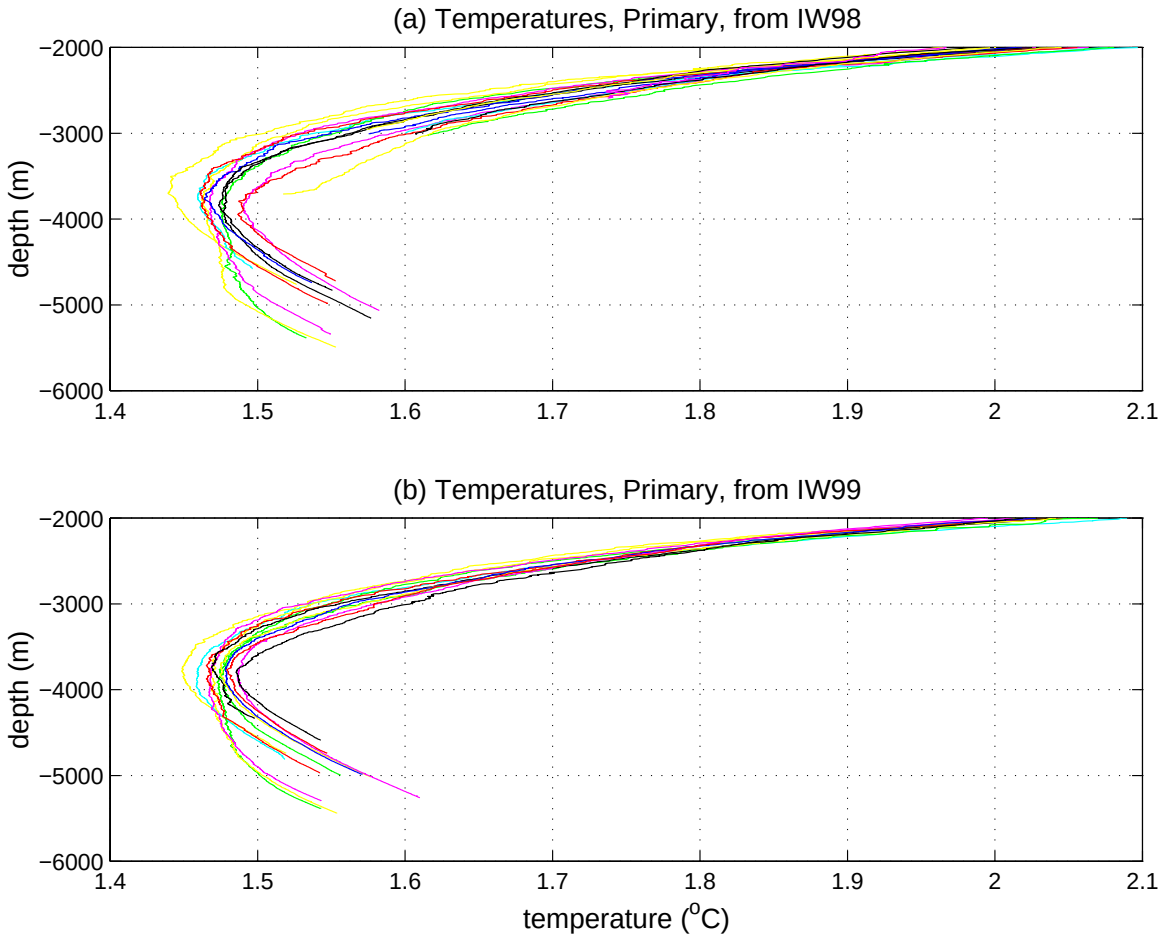

Figure 76. Primary temperature profiles below 2000 m from (a) IW98 and (b) IW99 for comparison. Temperatures in °C.

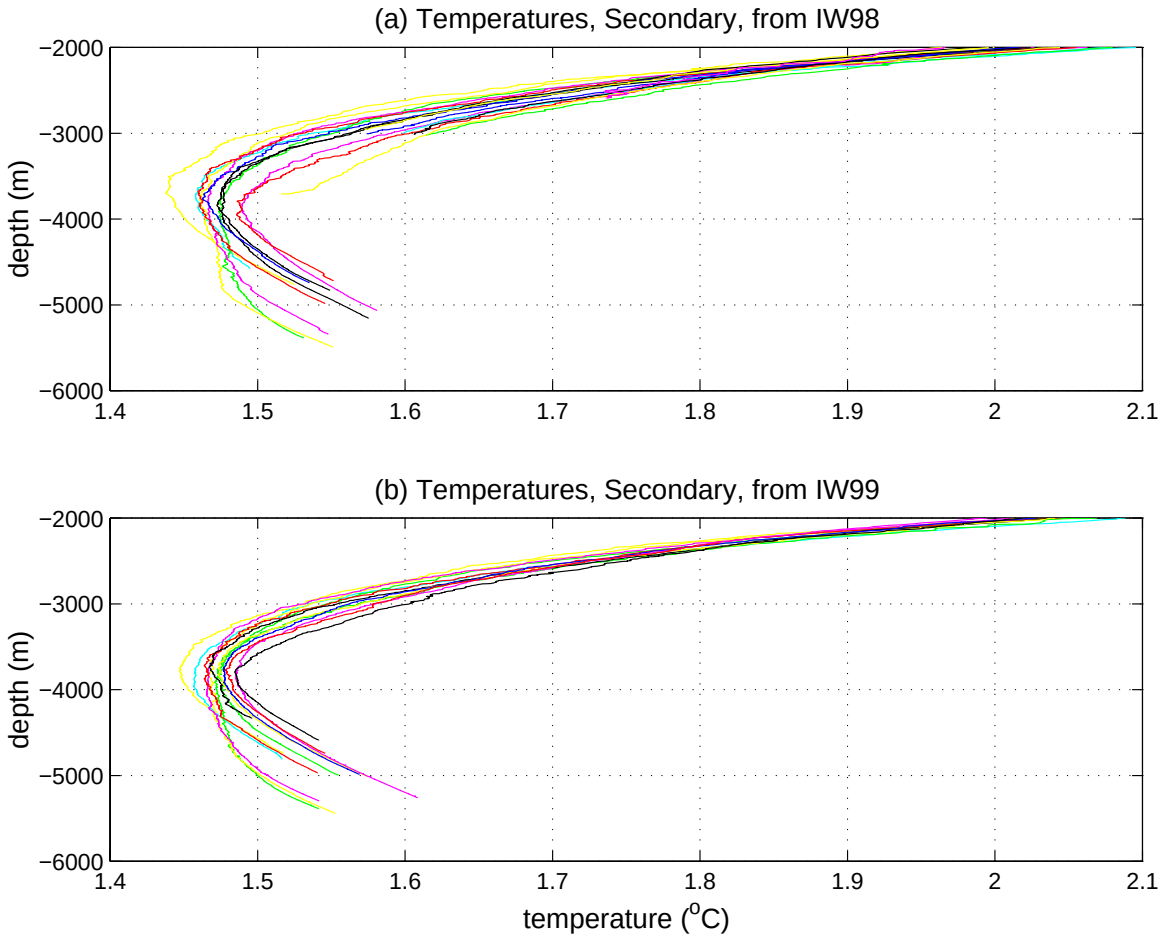

Figure 77. Secondary temperature profiles below 2000 m from (a) IW98 and (b) IW99 for comparison. Temperatures in °C.

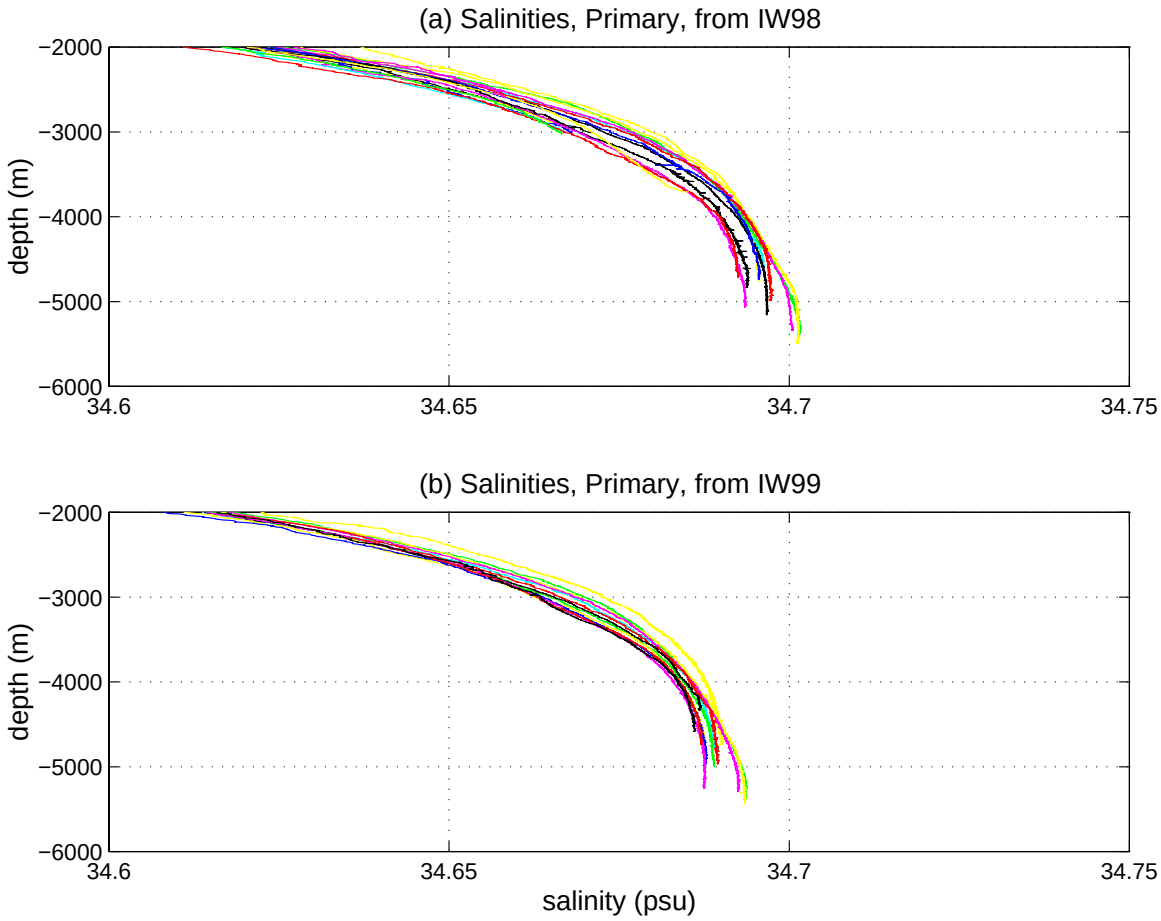

Figure 78. Primary salinity profiles below 2000 m from (a) IW98 and (b) IW99 for comparison. The salinities measured during the IW99 cruise are roughly 0.01 psu smaller than those measured during the IW98 cruise. Salinities in psu.

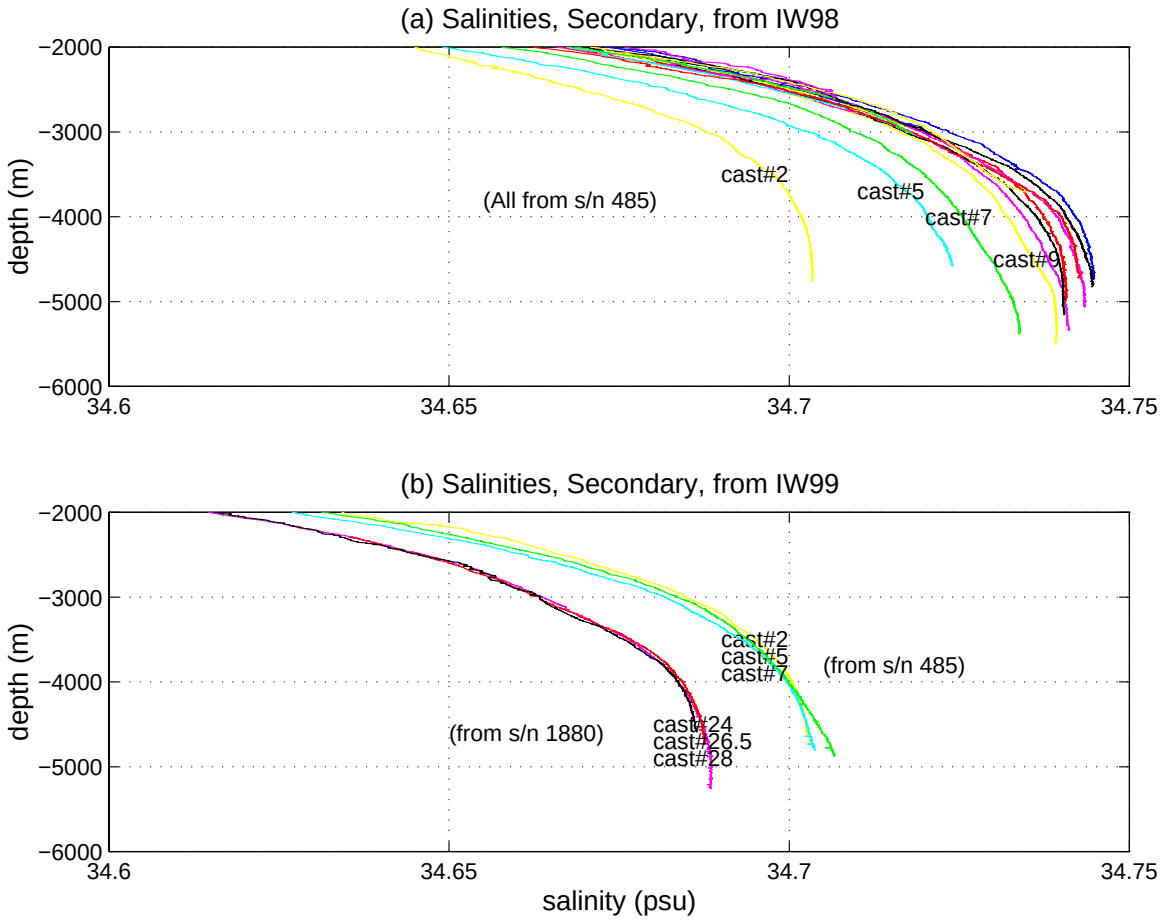

Figure 79. Secondary salinity profiles, in psu, below 2000 m from (a) IW98 and (b) IW99 for comparison. Salinities in psu.

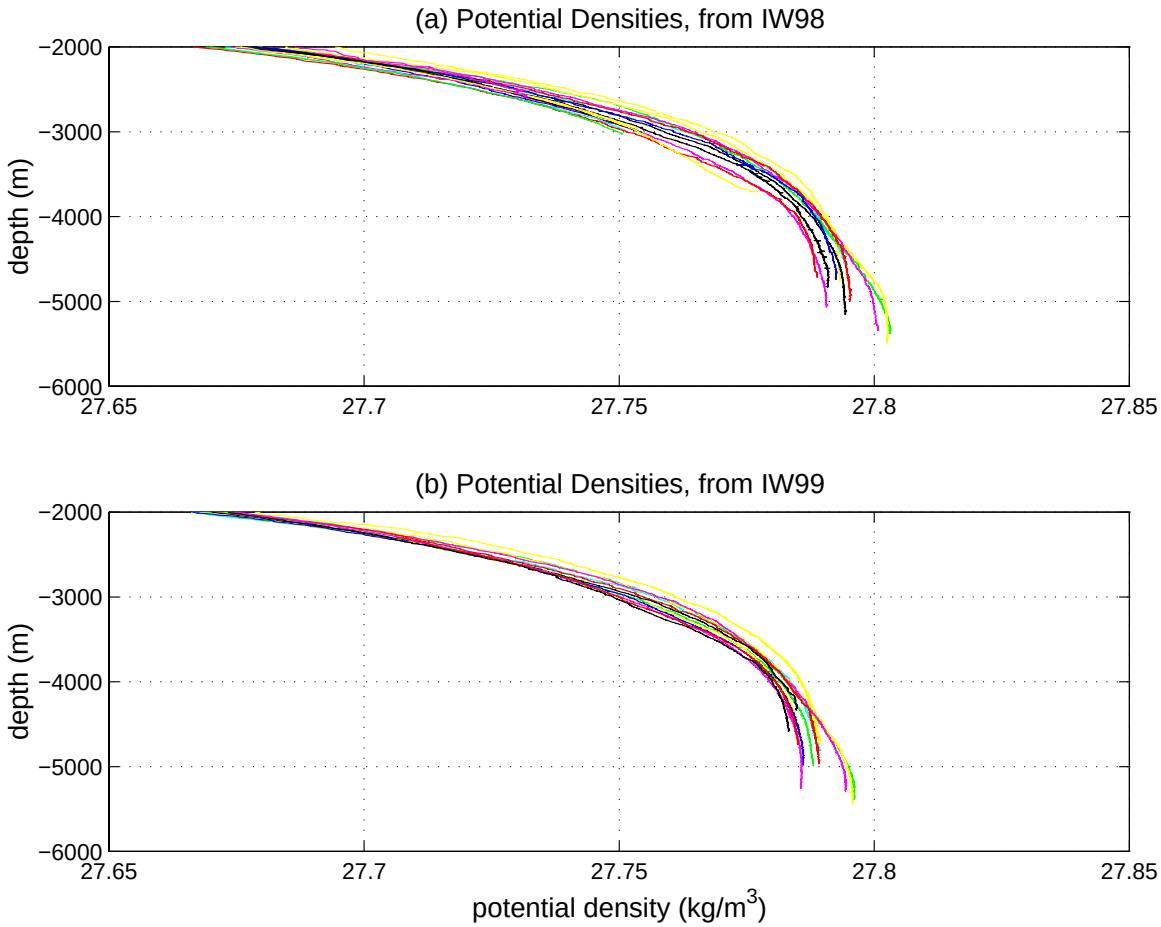

Figure 80. Potential density profiles below 2000 m from (a) IW98 and (b) IW99 for comparison. Potential densities in kg/m^3.

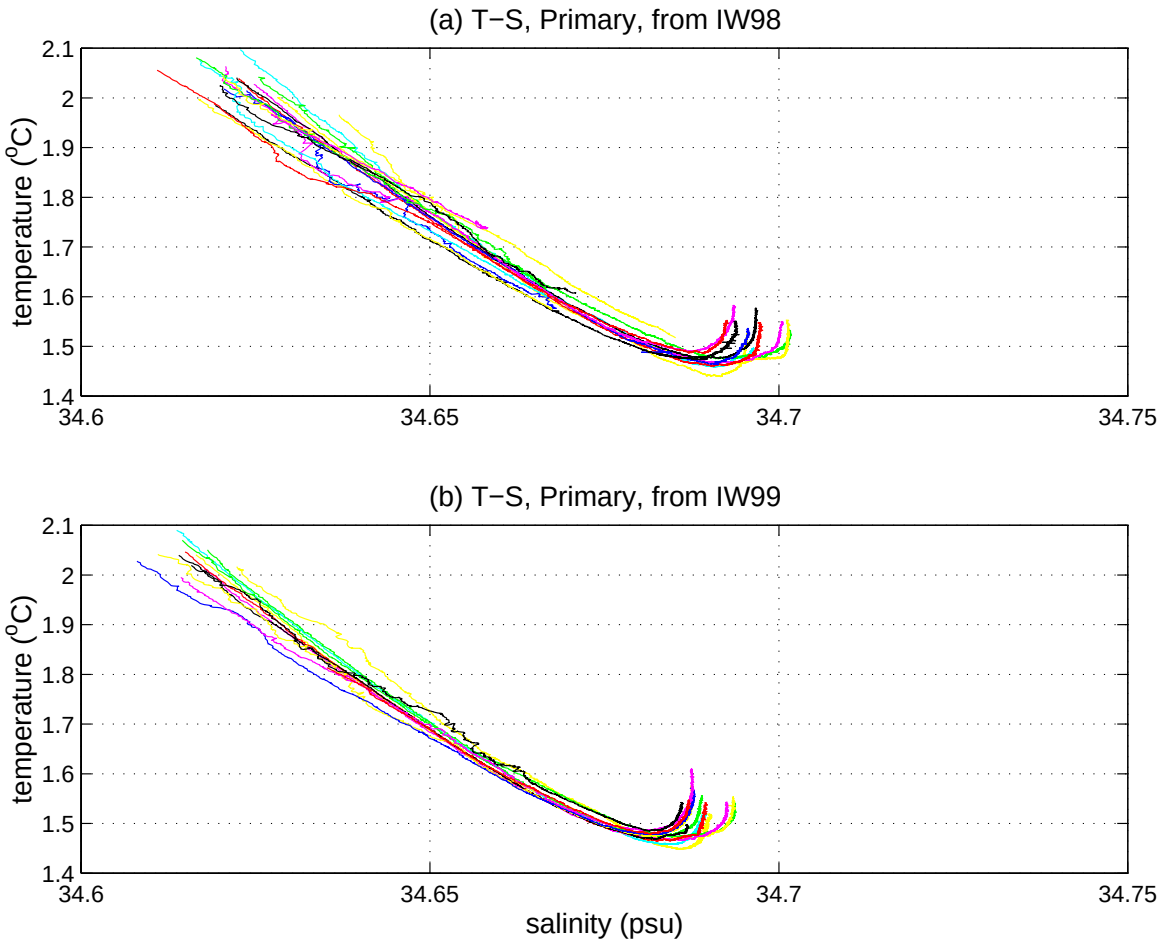

Figure 81. Temperature-salinity plots from the primary sensors for (a) IW98 and (b) IW99. Temperatures in °C and salinities in psu.

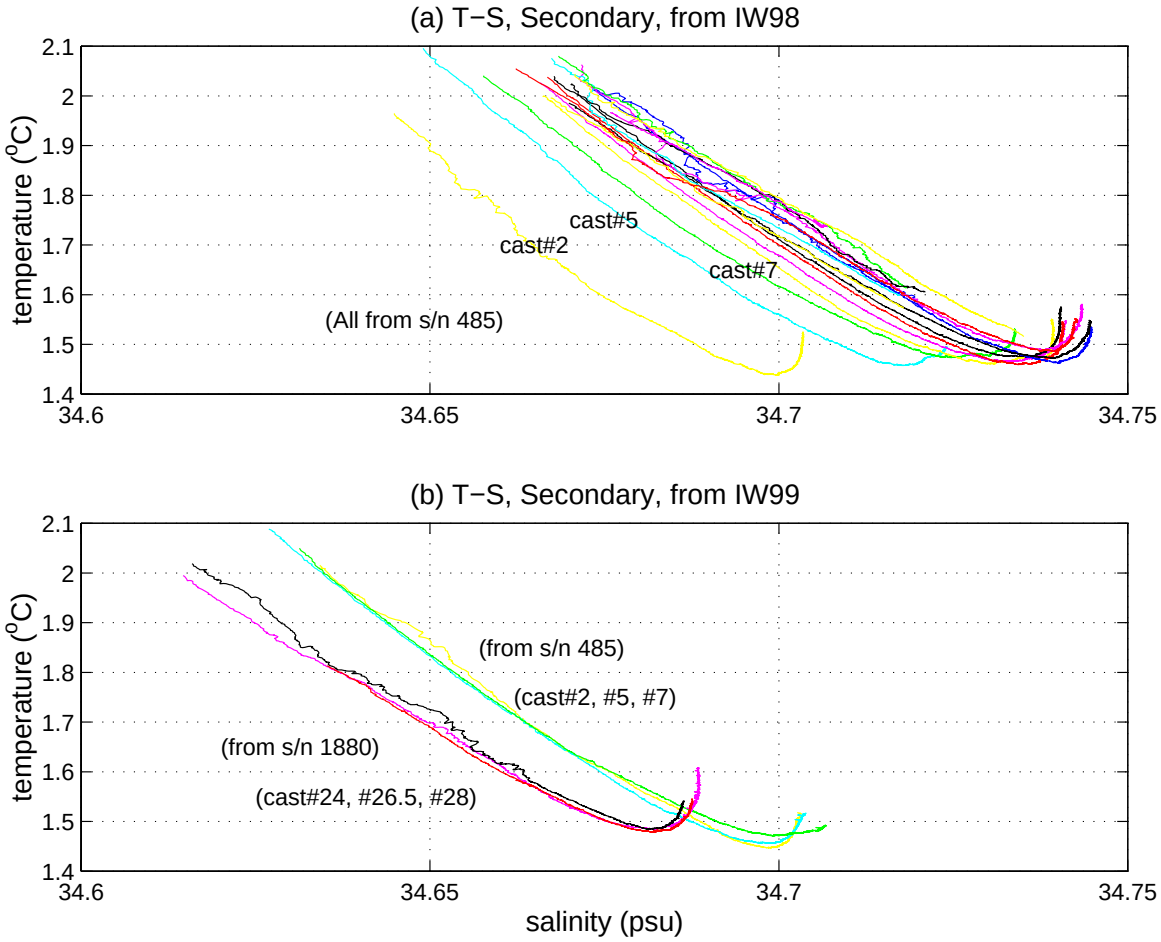

Figure 82. Temperature-salinity plots from the secondary sensors for (a) IW98 and (b) IW99. Temperatures in °C and salinities in psu.

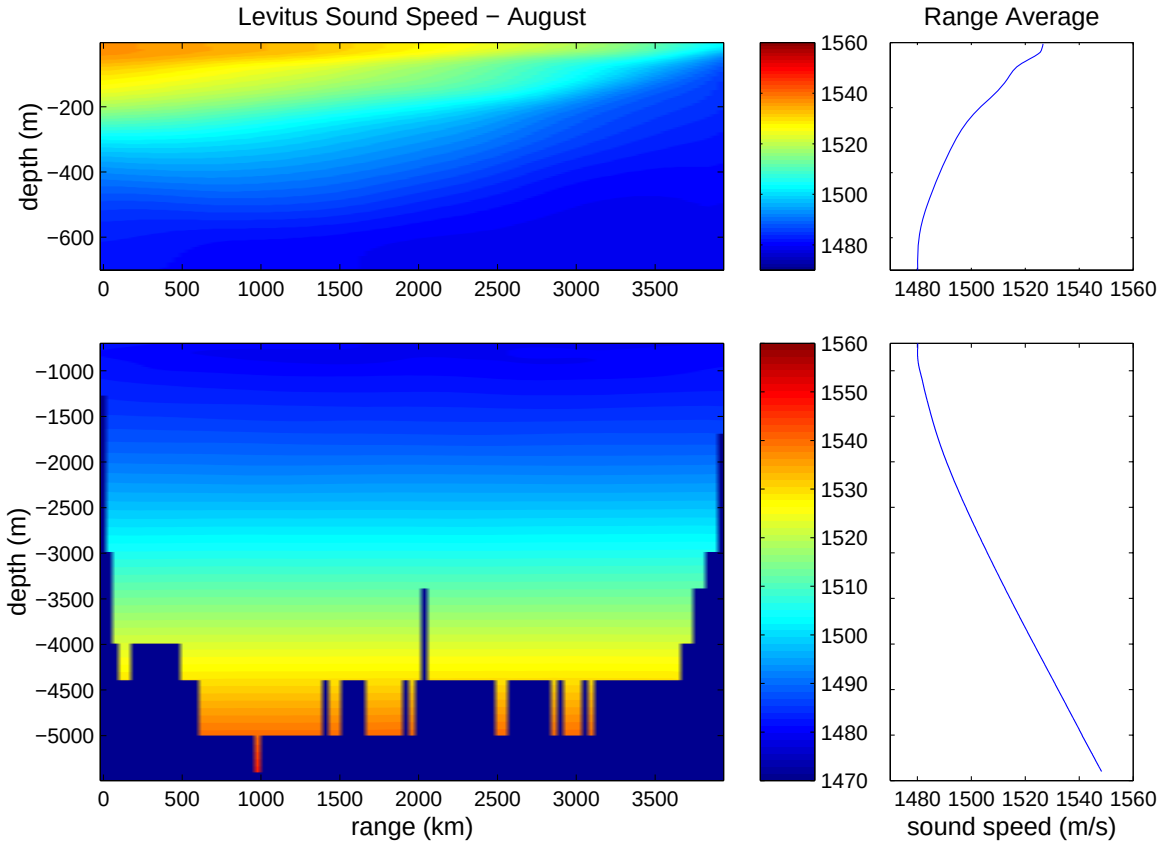

Figure 83. Sound speed from the Levitus climatology for August in m/s. Upper left panel shows sound speed from surface down to 700 m. Lower left panel shows sound speed from 700 m down to the ocean bottom with a different color scale. Both left panels are a slice along the cruise track. Range from the start of the cruise is measured in km. Right panels show range-averaged profiles. (Levitus data courtesy of B. Cornuelle.)

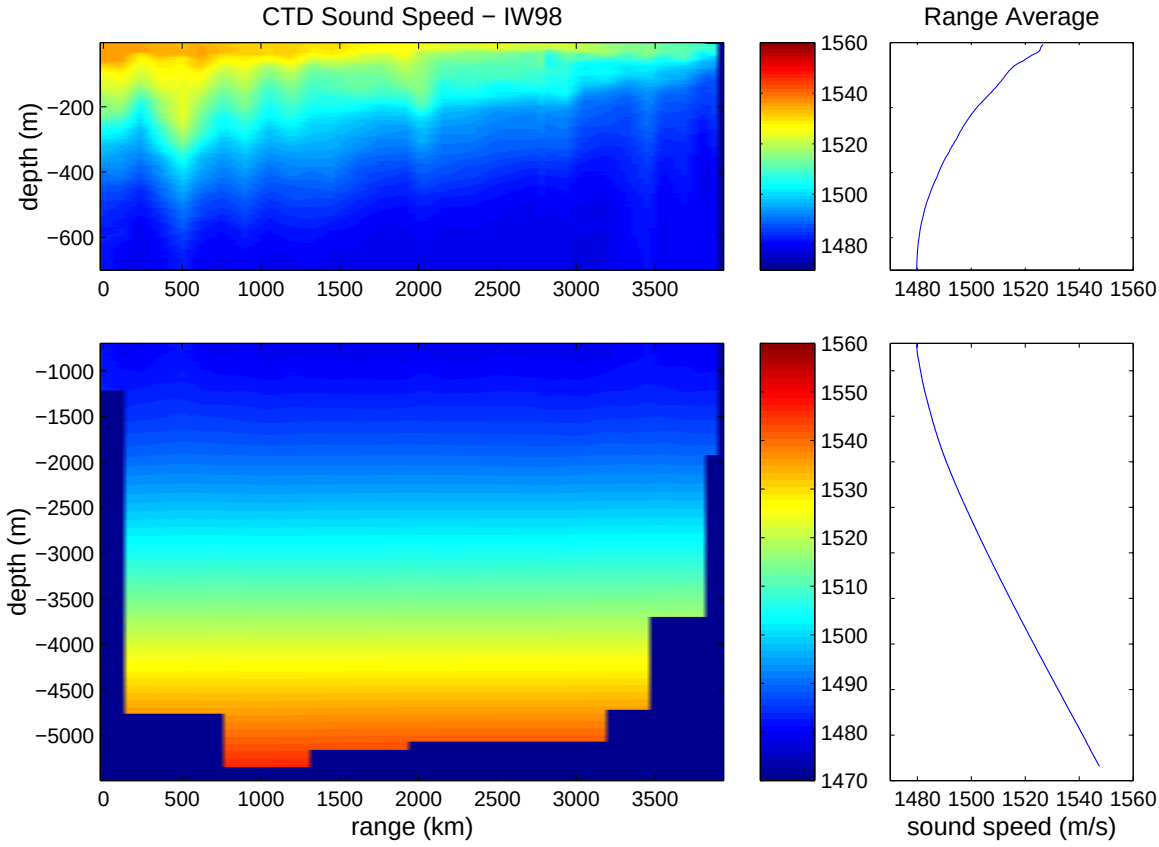

Figure 84. Sound speed from IW98 in m/s. Upper left panel shows sound speed from surface down to 700 m. Lower left panel shows sound speed from 700 m down to the ocean bottom with a different color scale. Both left panels are a slice along the cruise track. Range from the start of the cruise is measured in km. Right panels show range averaged profiles.

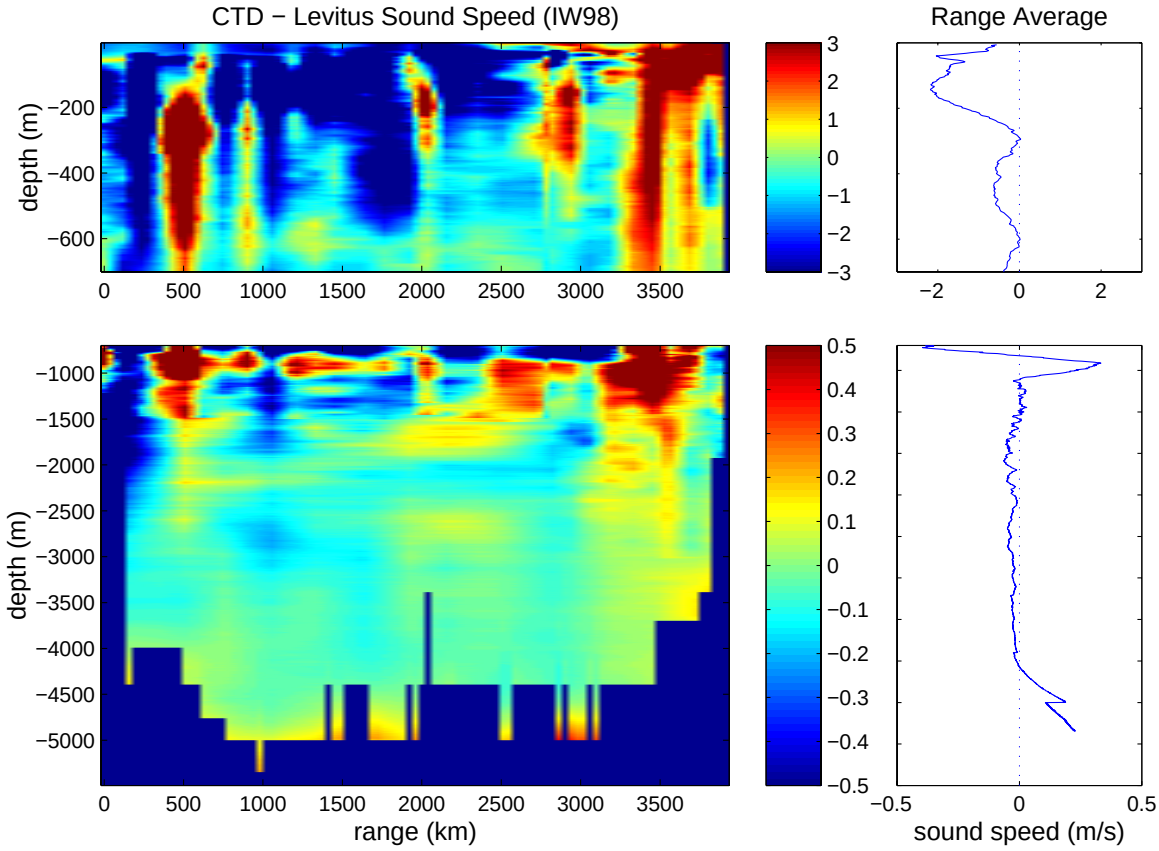

Figure 85. Sound speed differences; CTD data minus Levitus climatology. Panels same as in Figure 83 except for scales.

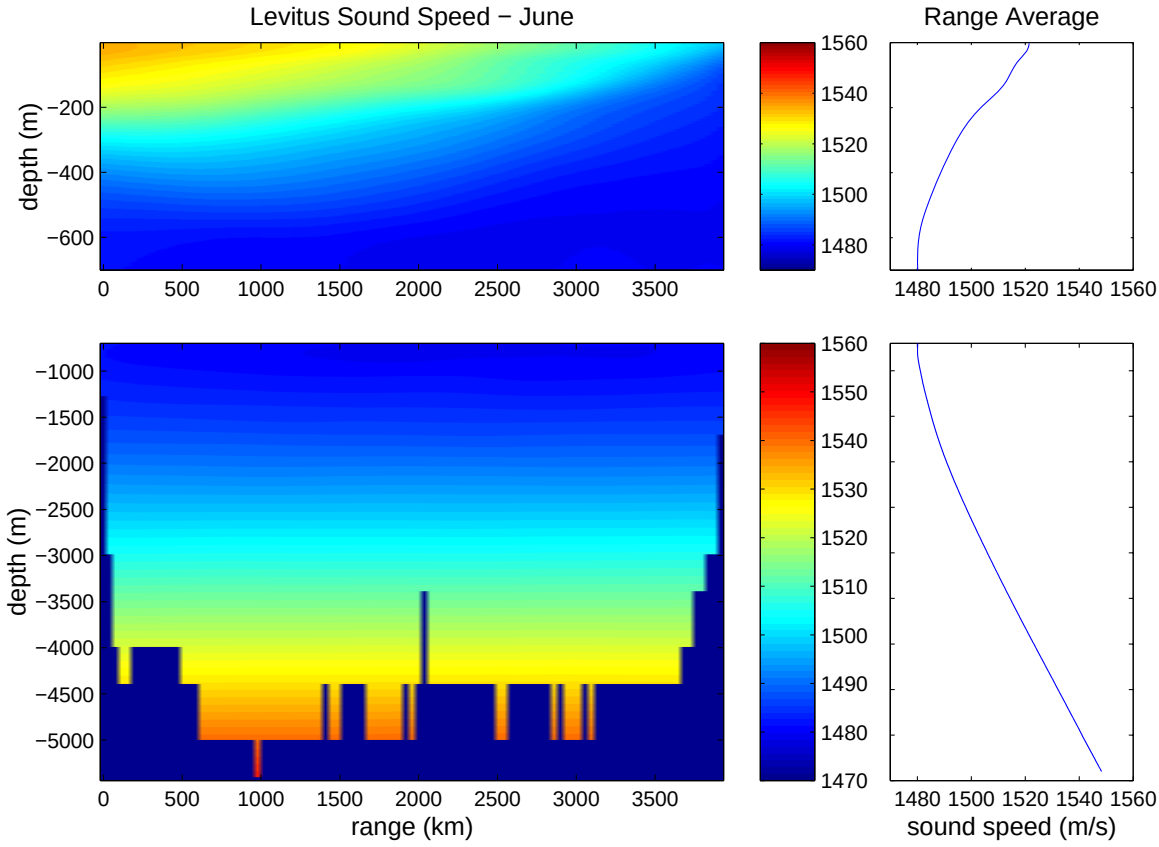

Figure 86. Sound speed from the Levitus climatology for June in m/s. Upper left panel shows sound speed from surface down to 700 m. Lower left panel shows sound speed from 700 m down to the ocean bottom with a different color scale. Both left panels are a slice along the cruise track. Range from the start of the cruise is measured in km. Right panels show range-averaged profiles. (Levitus data courtesy of B. Cornuelle.)

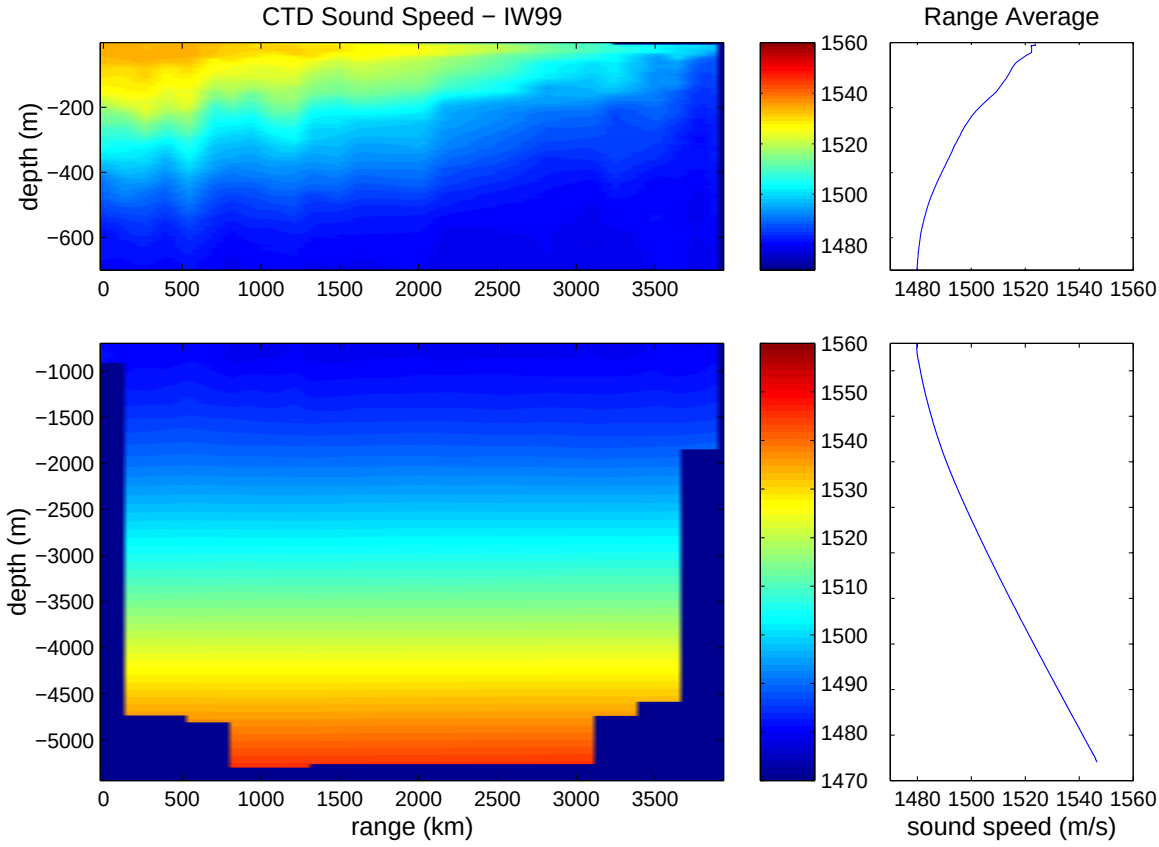

Figure 87. Sound speed from IW99 in m/s. Upper left panel shows sound speed from surface down to 700 m. Lower left panel shows sound speed from 700 m down to the ocean bottom with a different color scale. Both left panels are a slice along the cruise track. Range from the start of the cruise is measured in km. Right panels show range-averaged profiles.

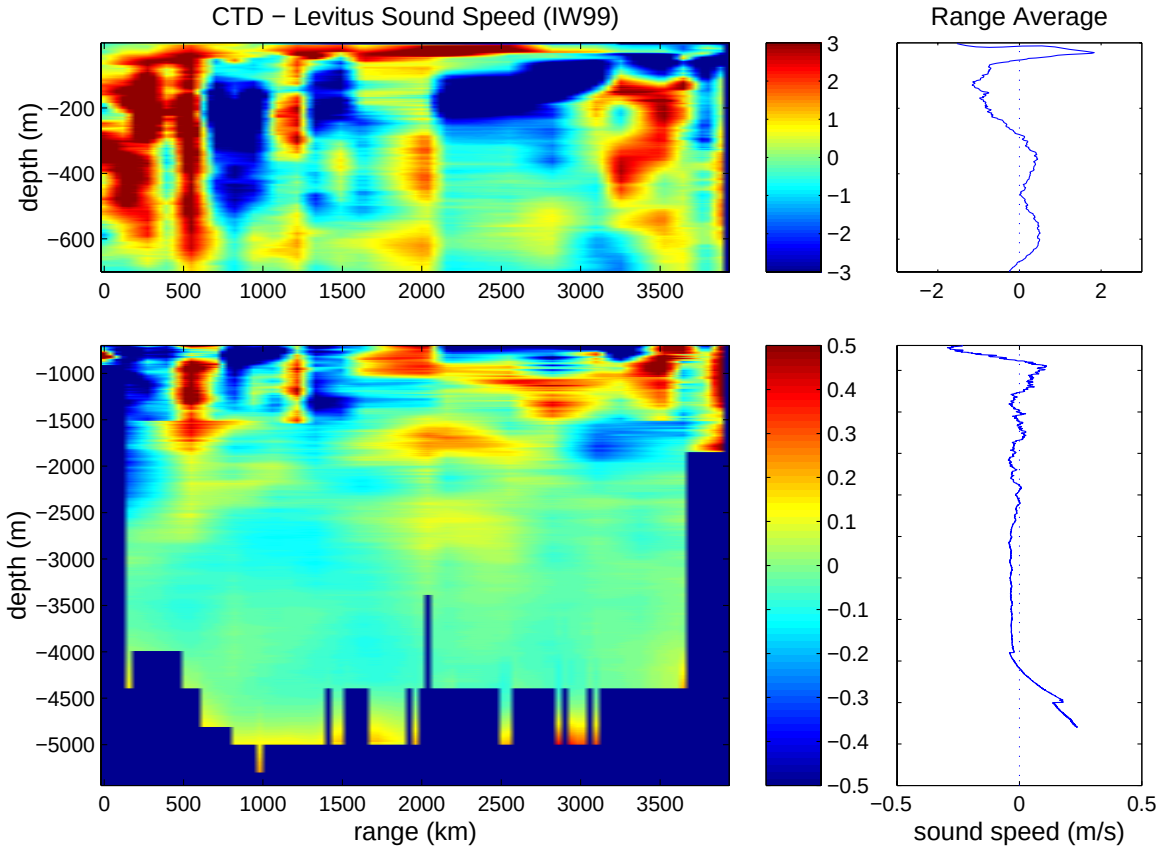

Figure 88. Sound speed differences; CTD data minus Levitus climatology. Panels same as in Figure 86 except for scales.

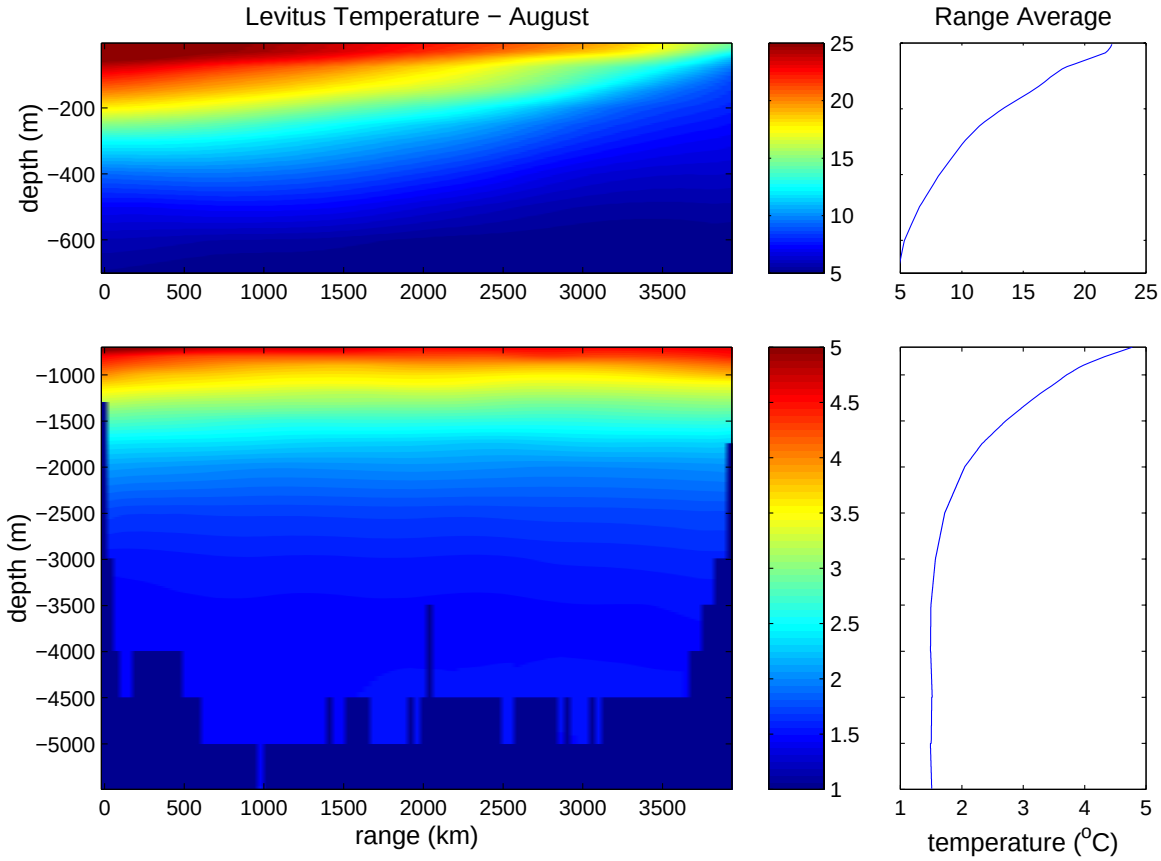

Figure 89. Same as in Figure 83, except for temperature in °C.

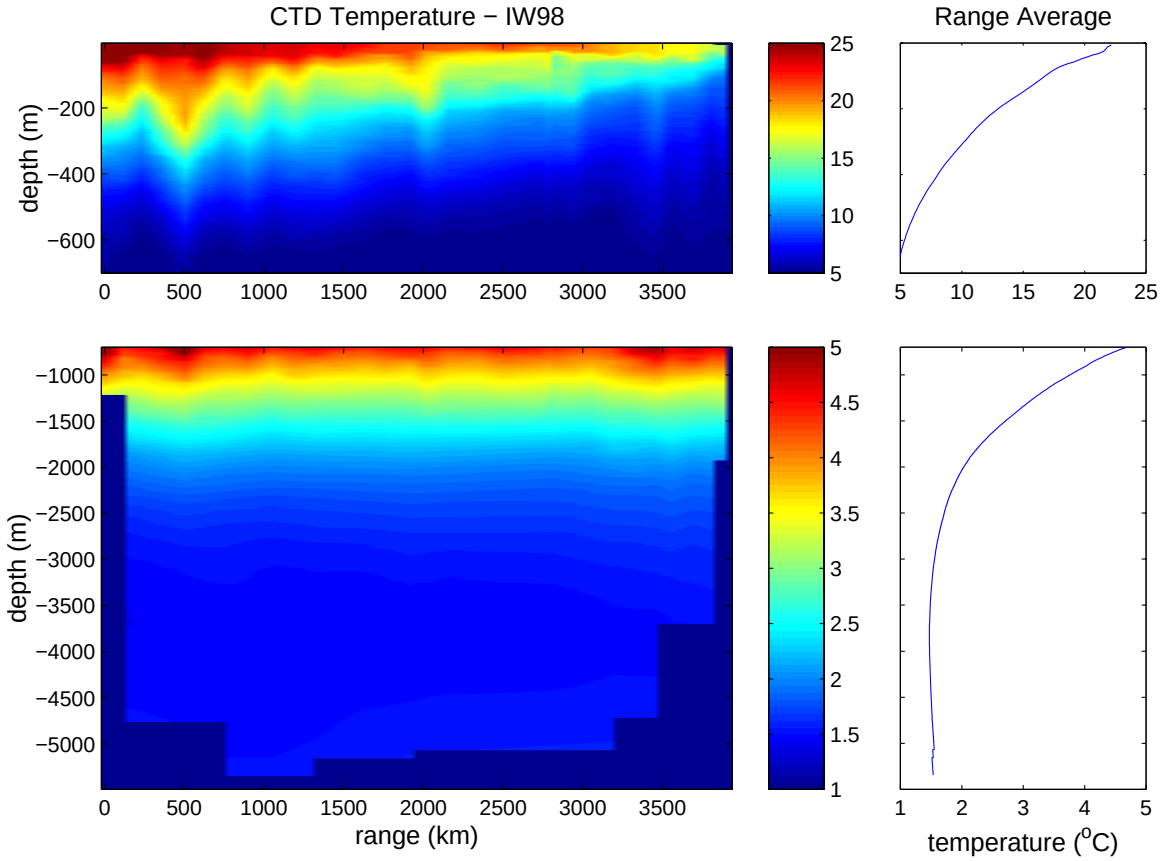

Figure 90. Same as in Figure 84, except for temperature in °C.

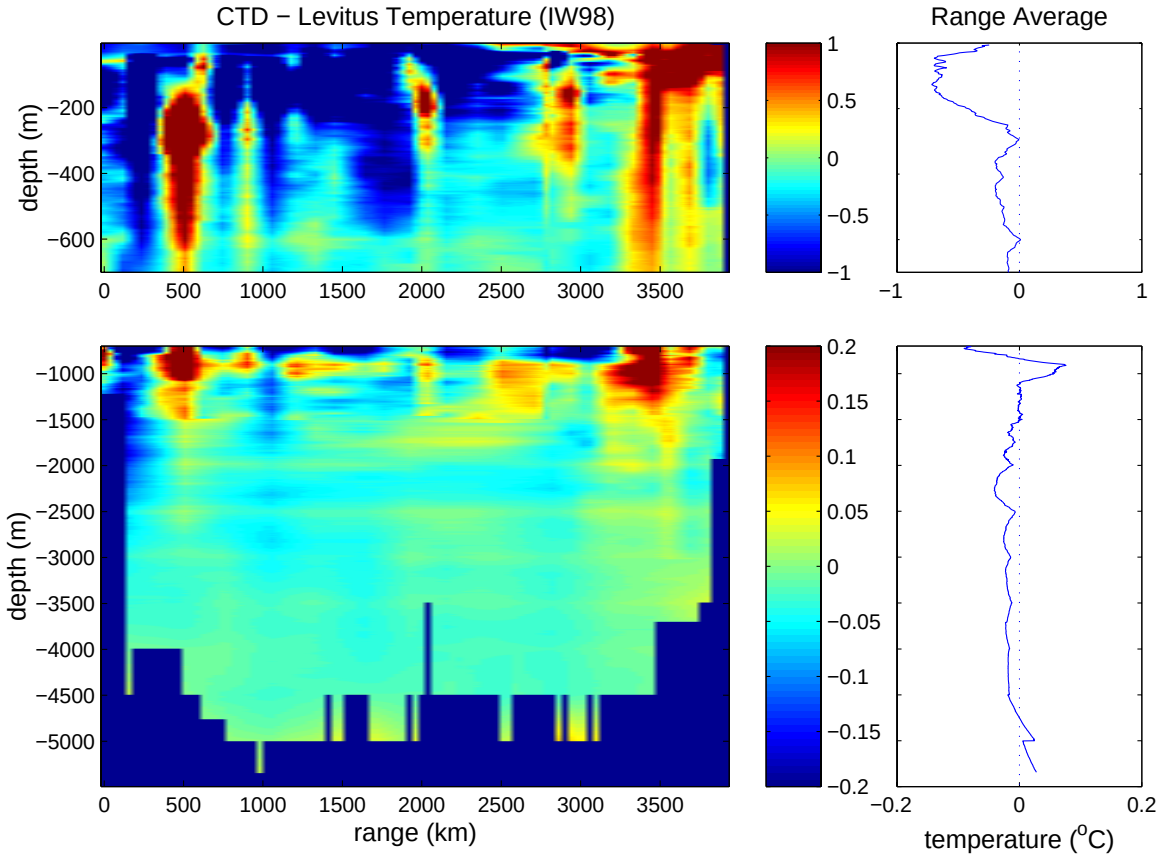

Figure 91. Same as in Figure 85, except for temperature in °C.

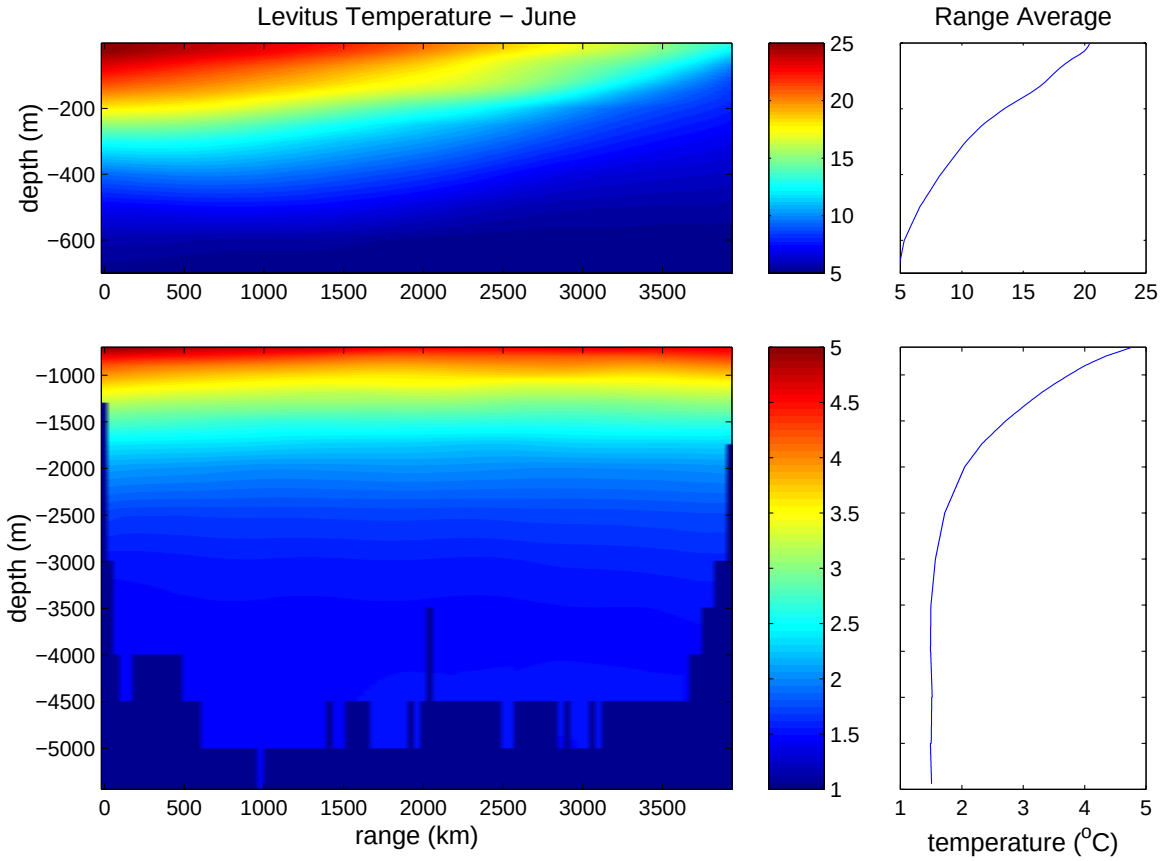

Figure 92. Same as in Figure 86, except for temperature in °C.

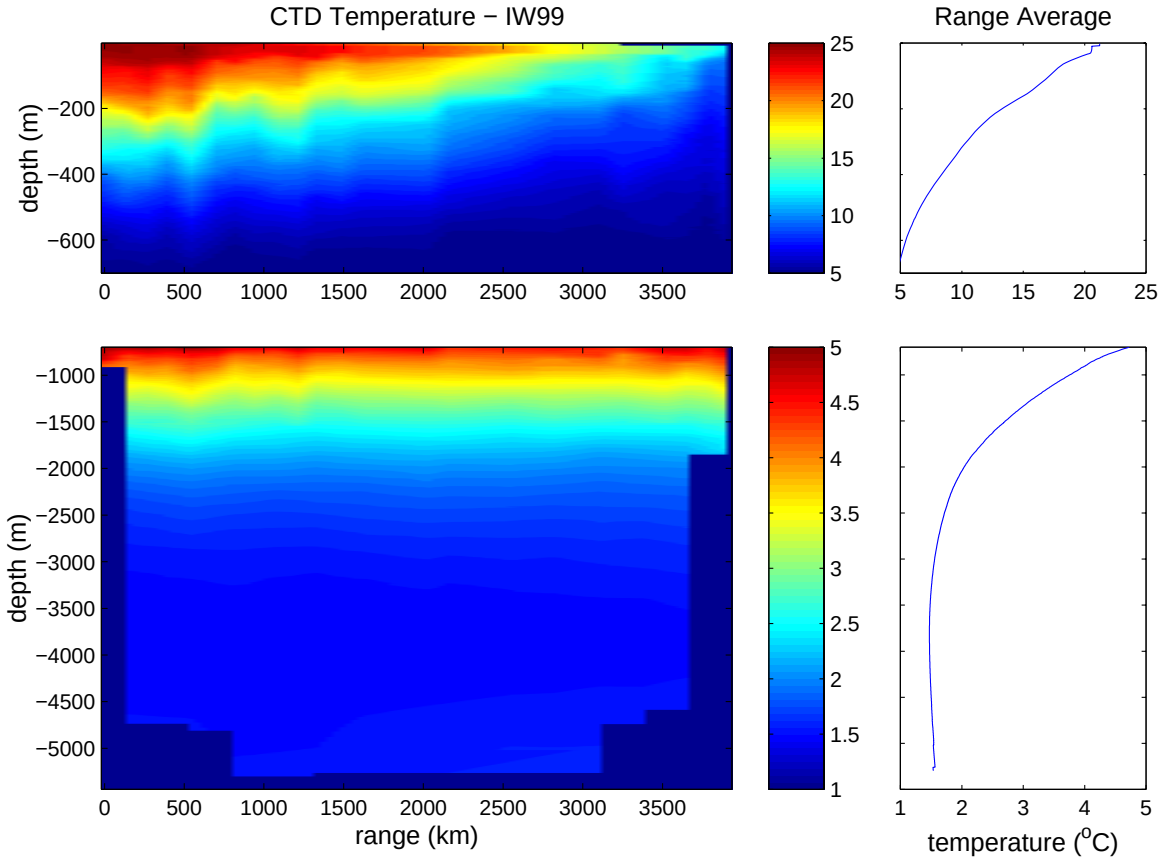

Figure 93. Same as in Figure 87, except for temperature in °C.

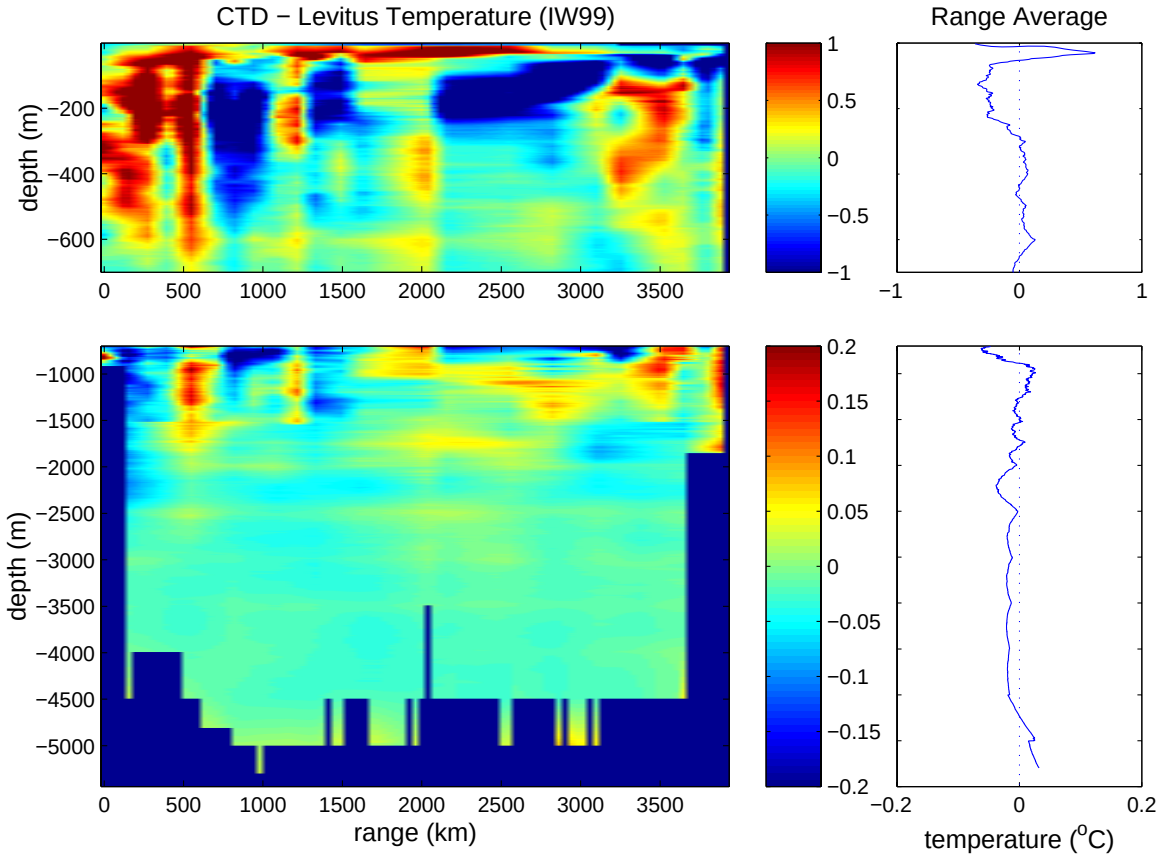

Figure 94. Same as in Figure 88, except for temperature in °C.

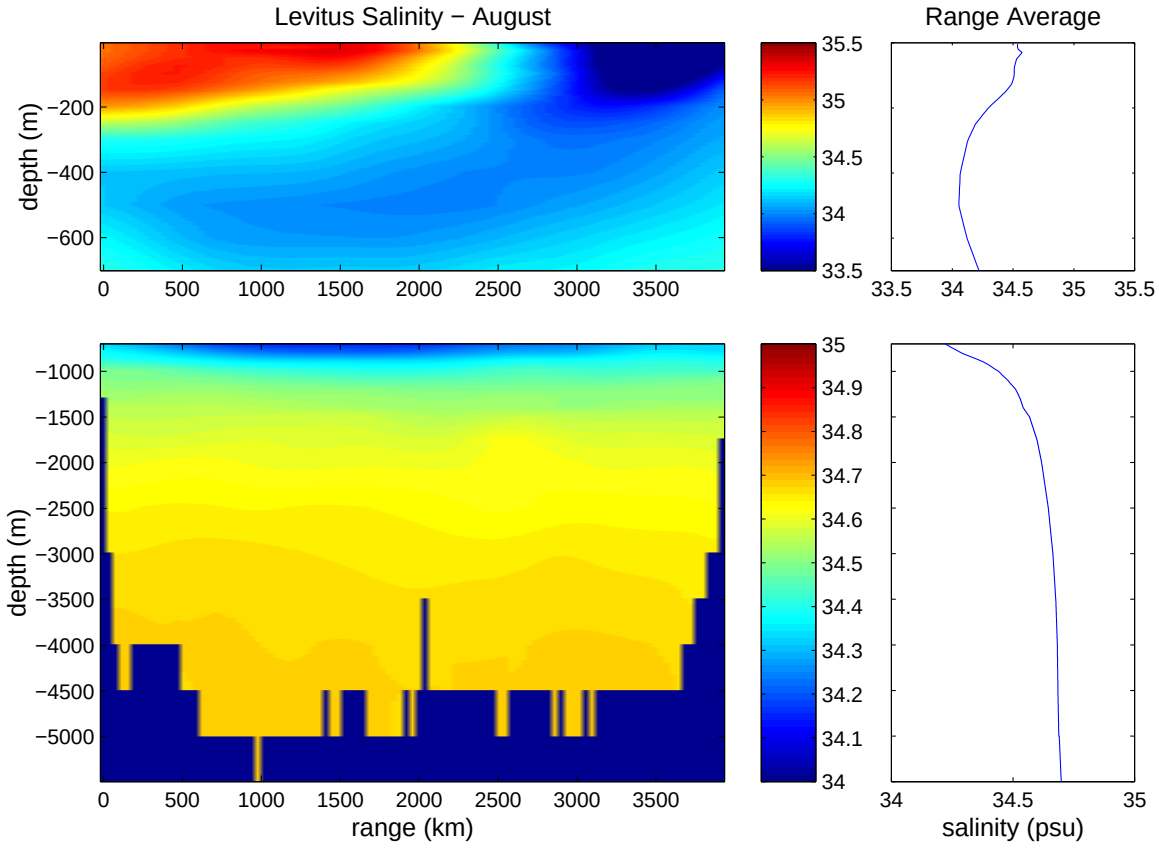

Figure 95. Same as in Figure 83, except for salinity in psu.

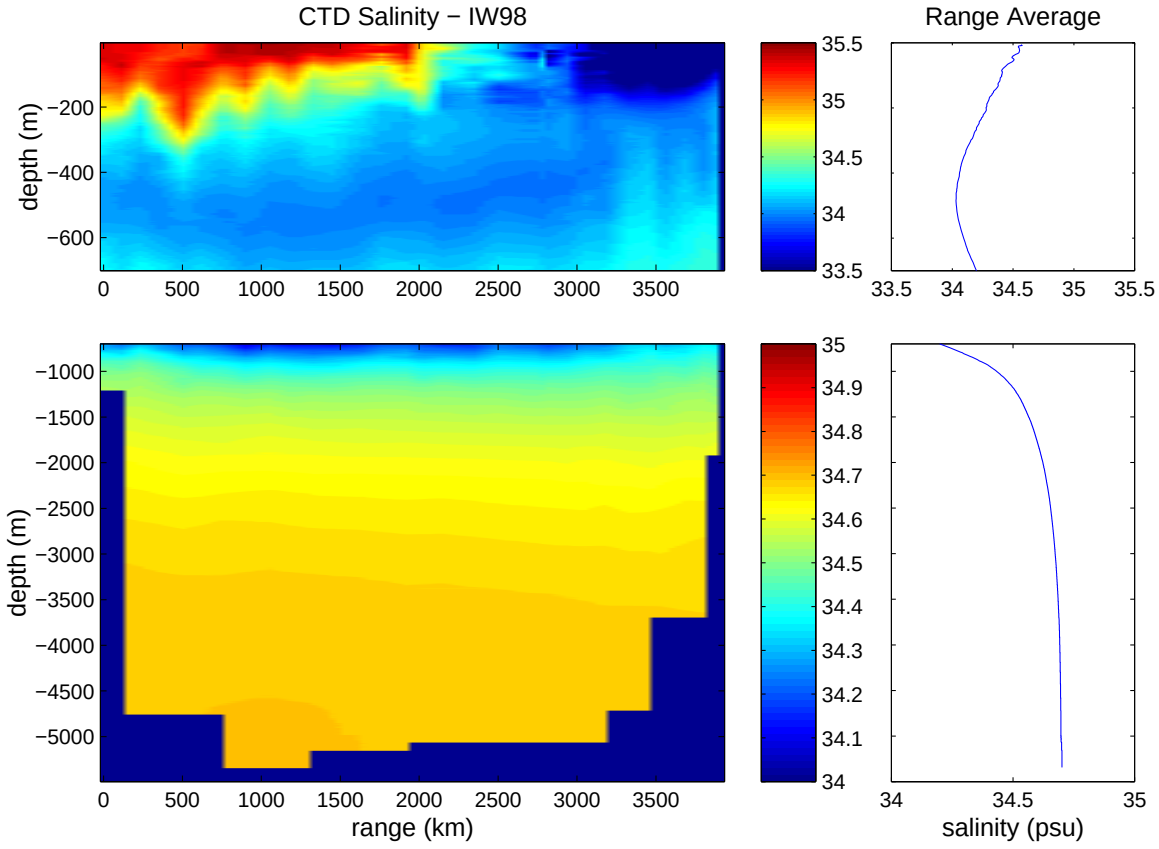

Figure 96. Same as in Figure 84, except for salinity in psu.

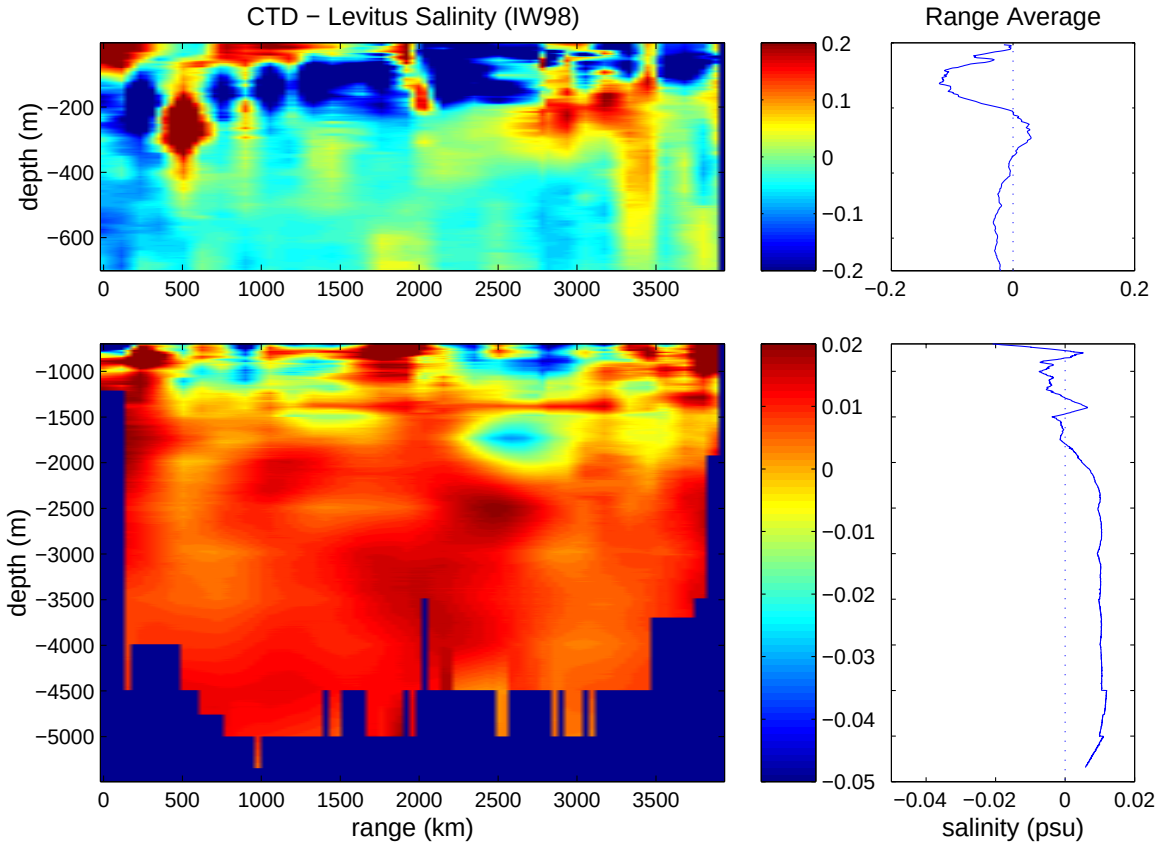

Figure 97. Same as in Figure 85, except for salinity in psu.

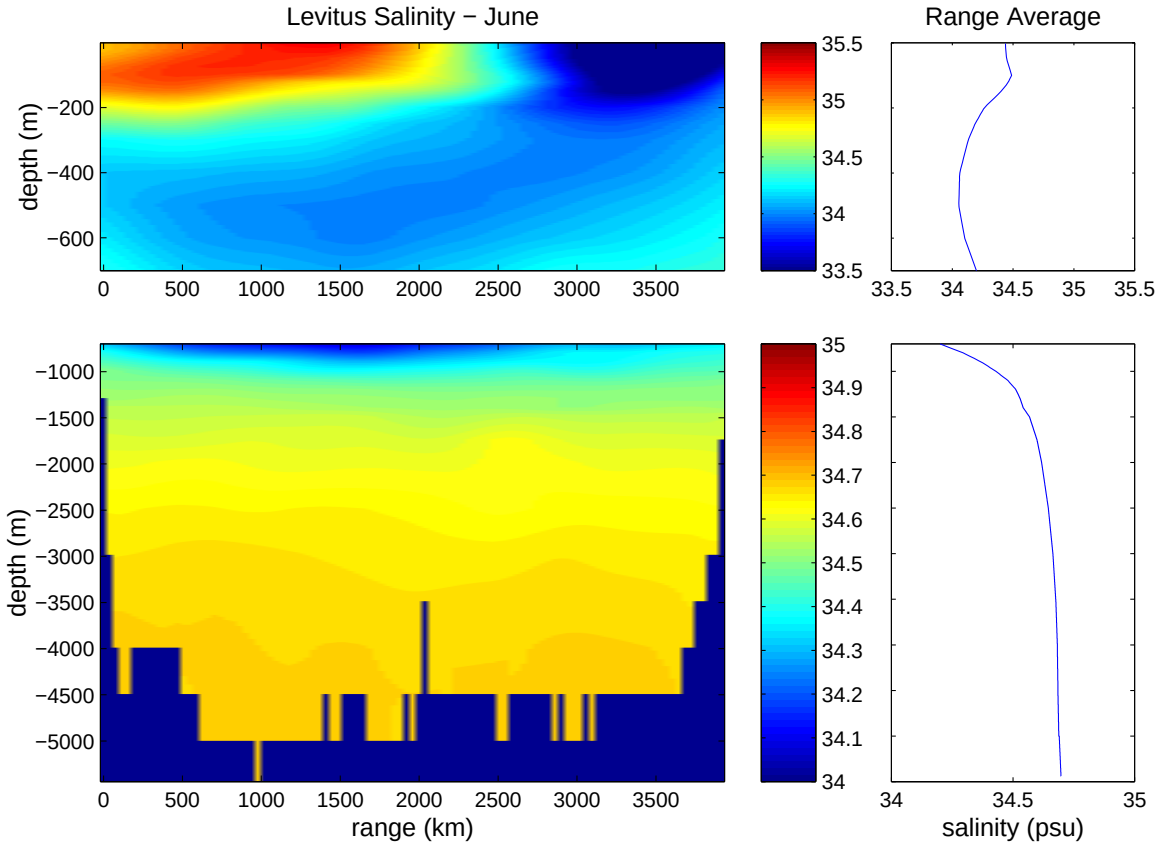

Figure 98. Same as in Figure 86, except for salinity in psu.

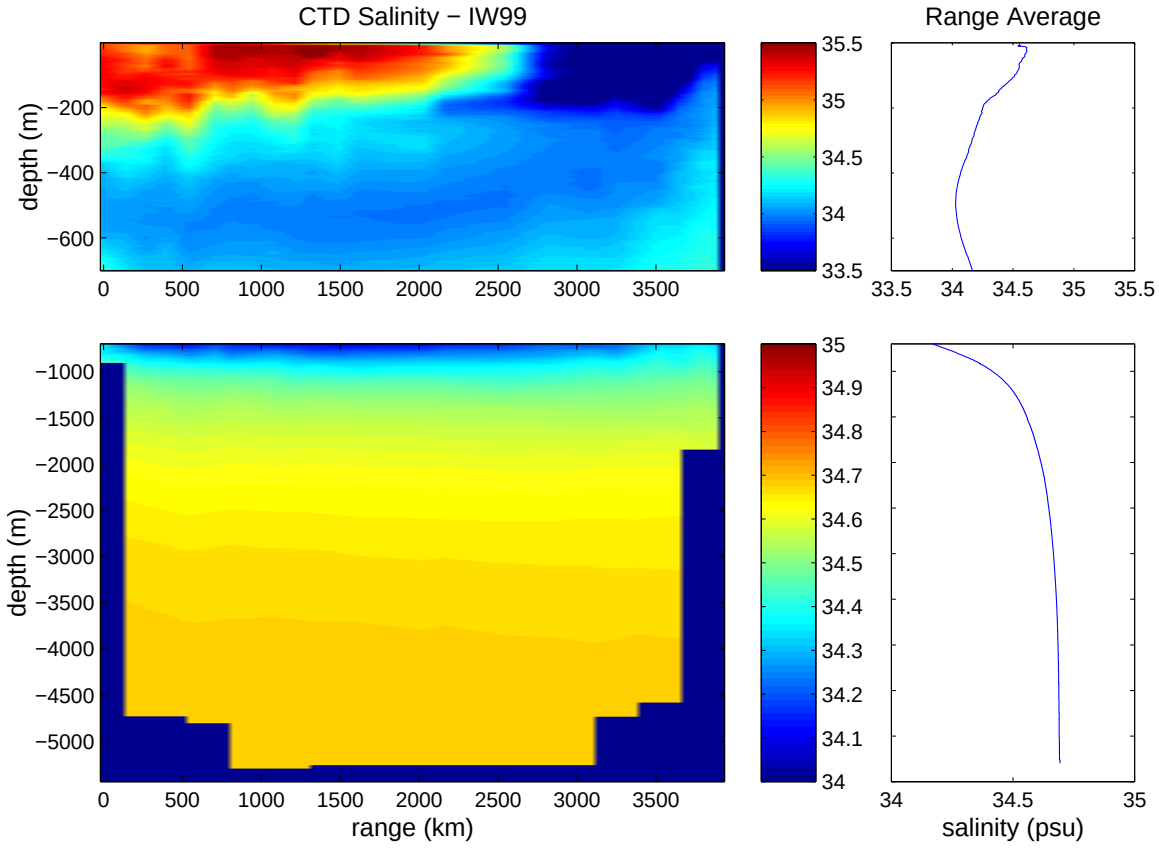

Figure 99. Same as in Figure 87, except for salinity in psu.

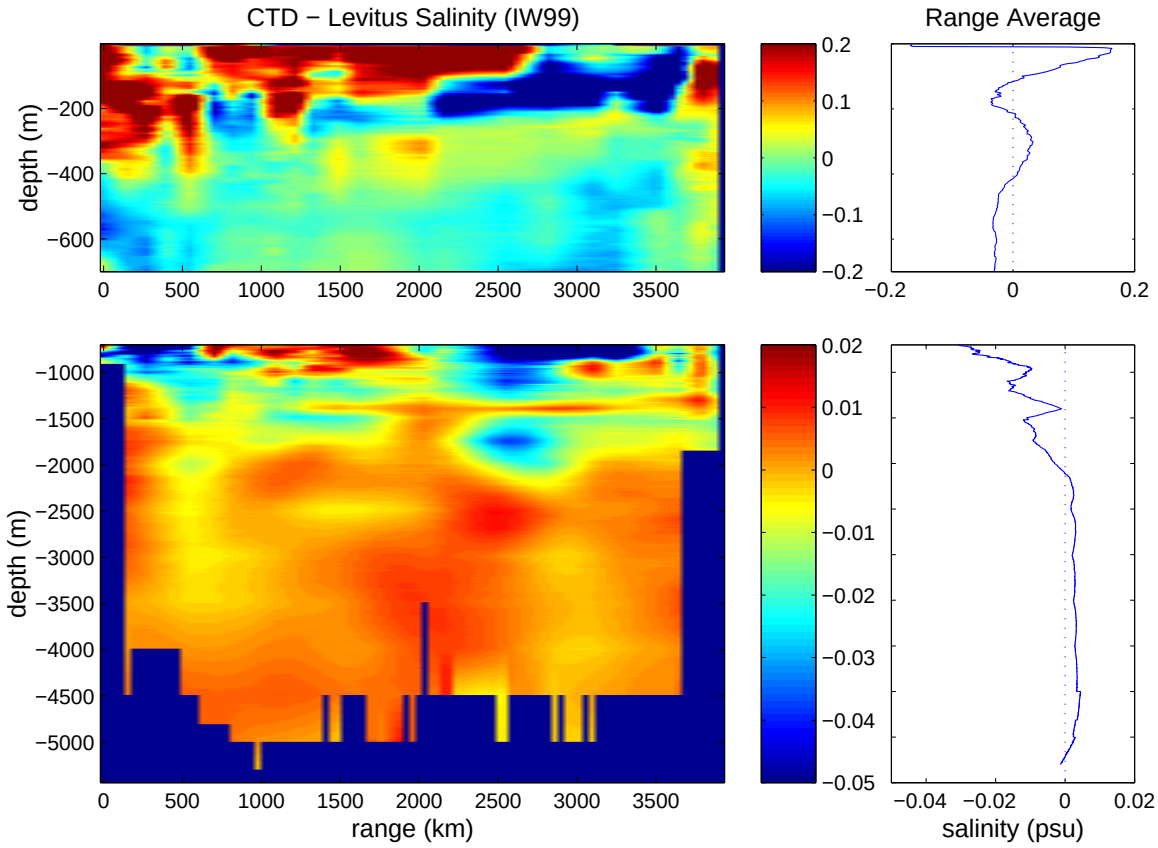

Figure 100. Same as in Figure 88, except for salinity in psu. The large change at the surface is likely due to small sample size at the very highest depth on the CTD data.

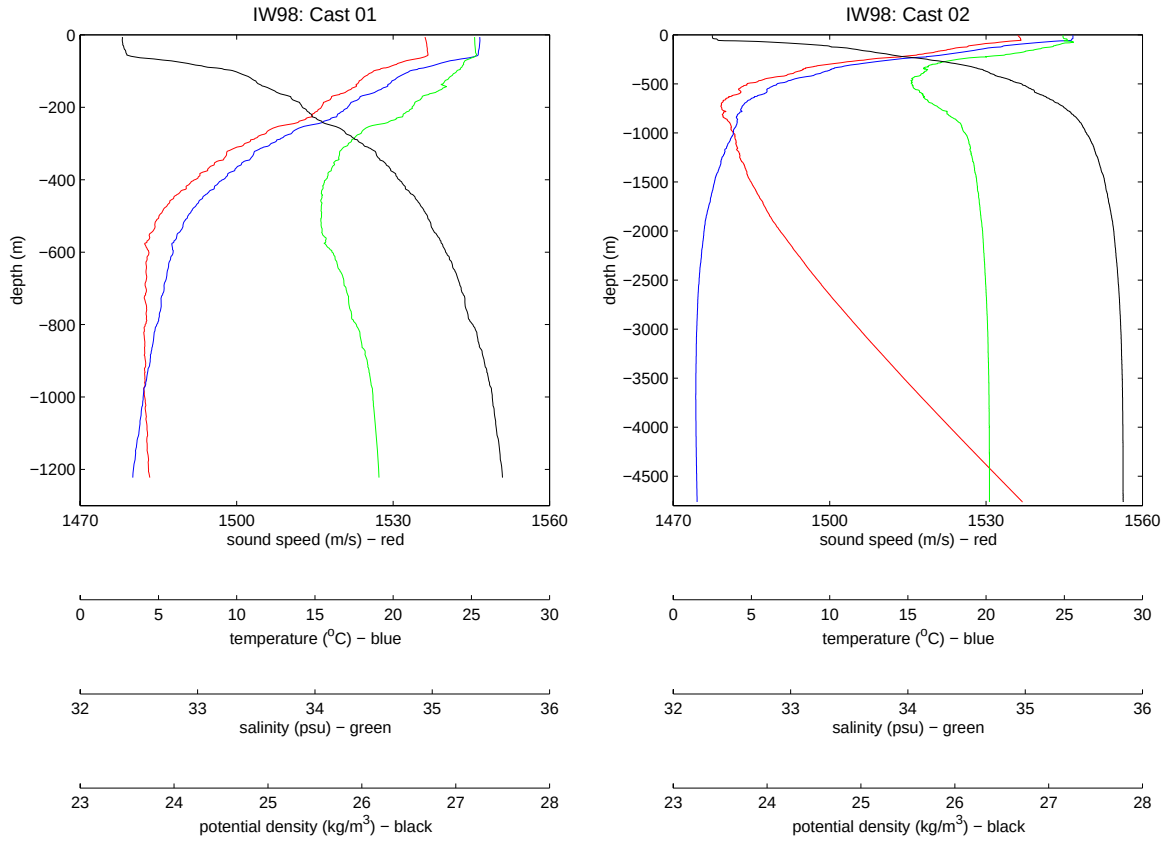

Figure 101. Processed data from Cast no. 1, file name 2280551 (left) and Cast no. 2, file name 2281355 (right) from IW98. Sound speed is in red, temperature is in blue, salinity is in green and density is in black.

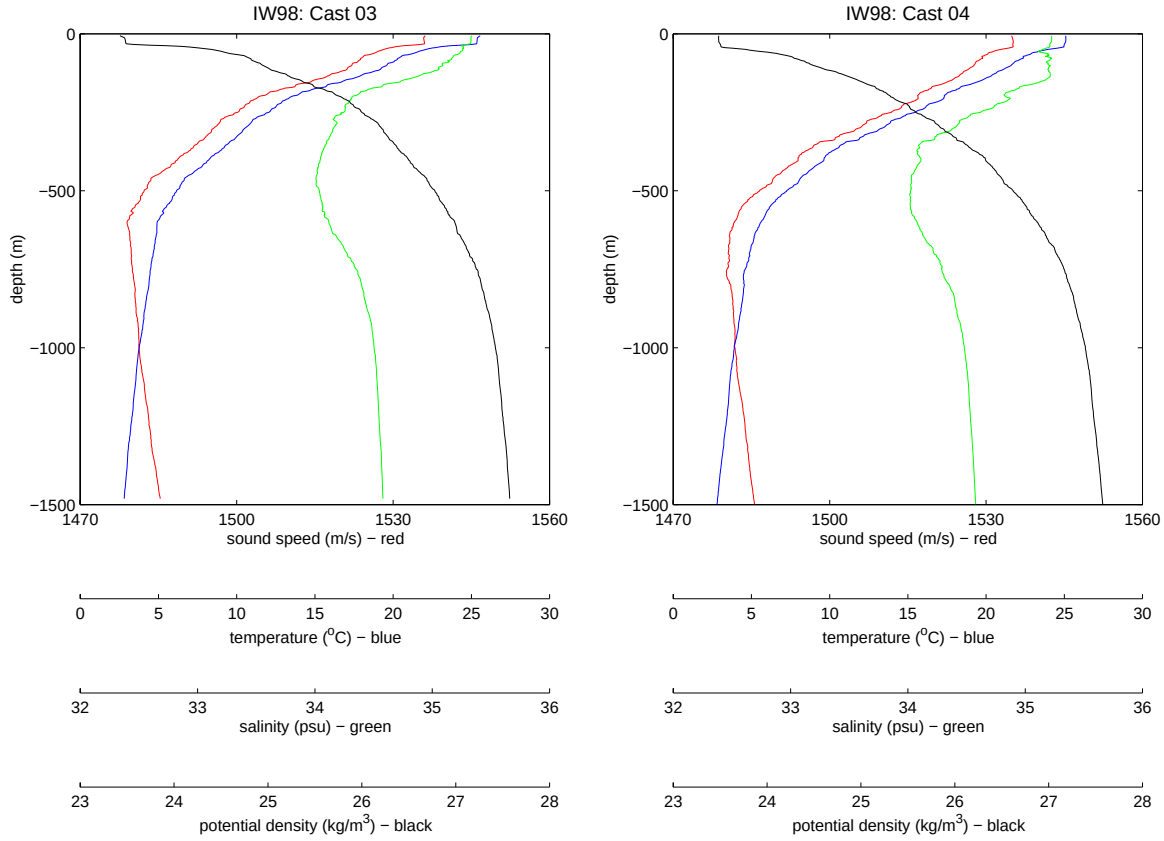

Figure 102. Same as in Figure 101, except for Cast no. 3, file name 2282327 (left) and Cast no. 4, file name 2290939 (right).

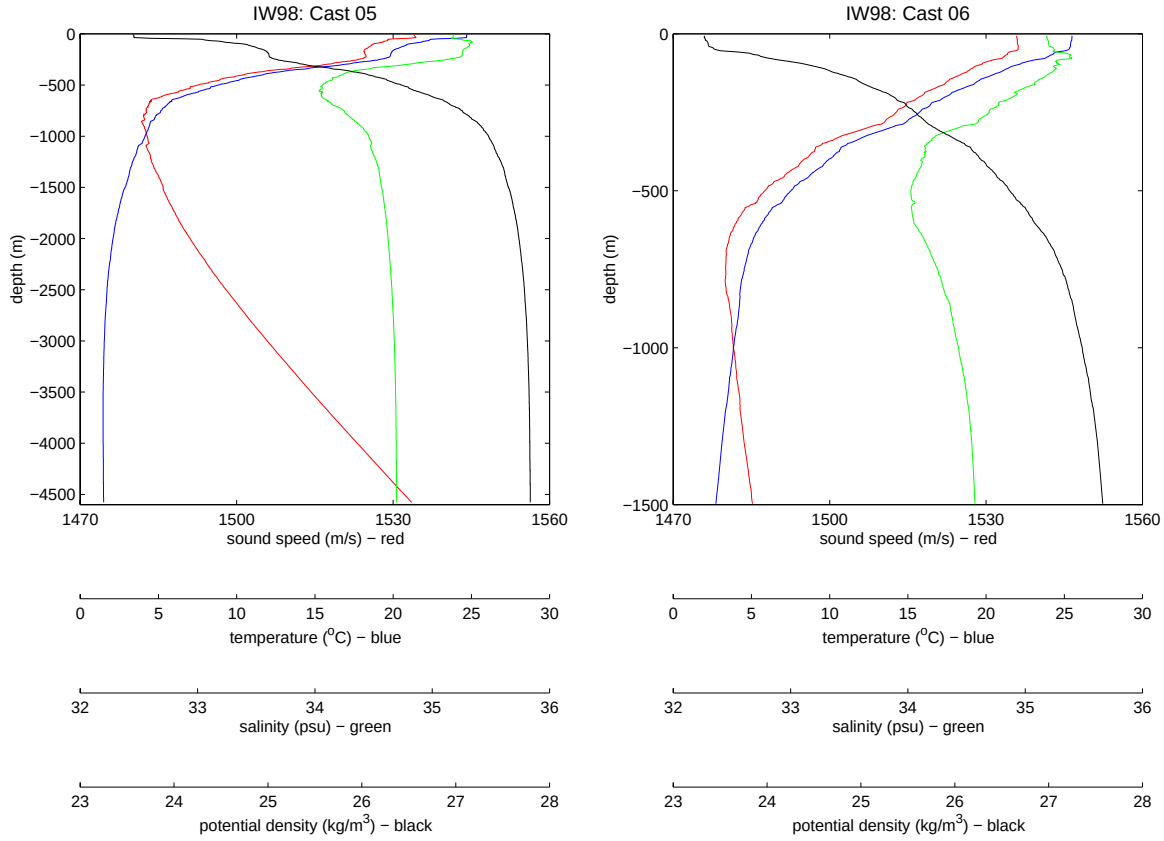

Figure 103. Same as in Figure 101, except for Cast no. 5, file name 2281846 (left) and Cast no. 6, file name 2300405 (right).

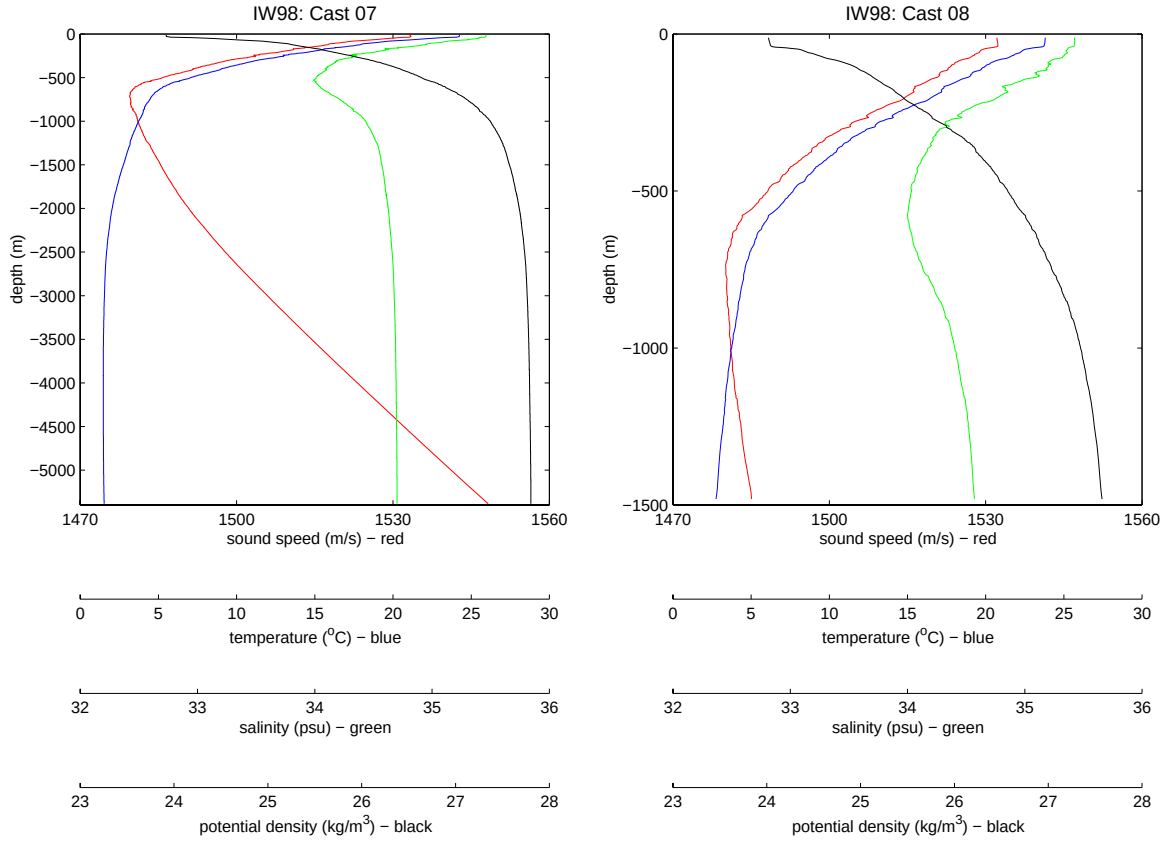

Figure 104. Same as in Figure 101, except for Cast no. 7, file name 2301309 (left) and Cast no. 8, file name 2310026 (right).

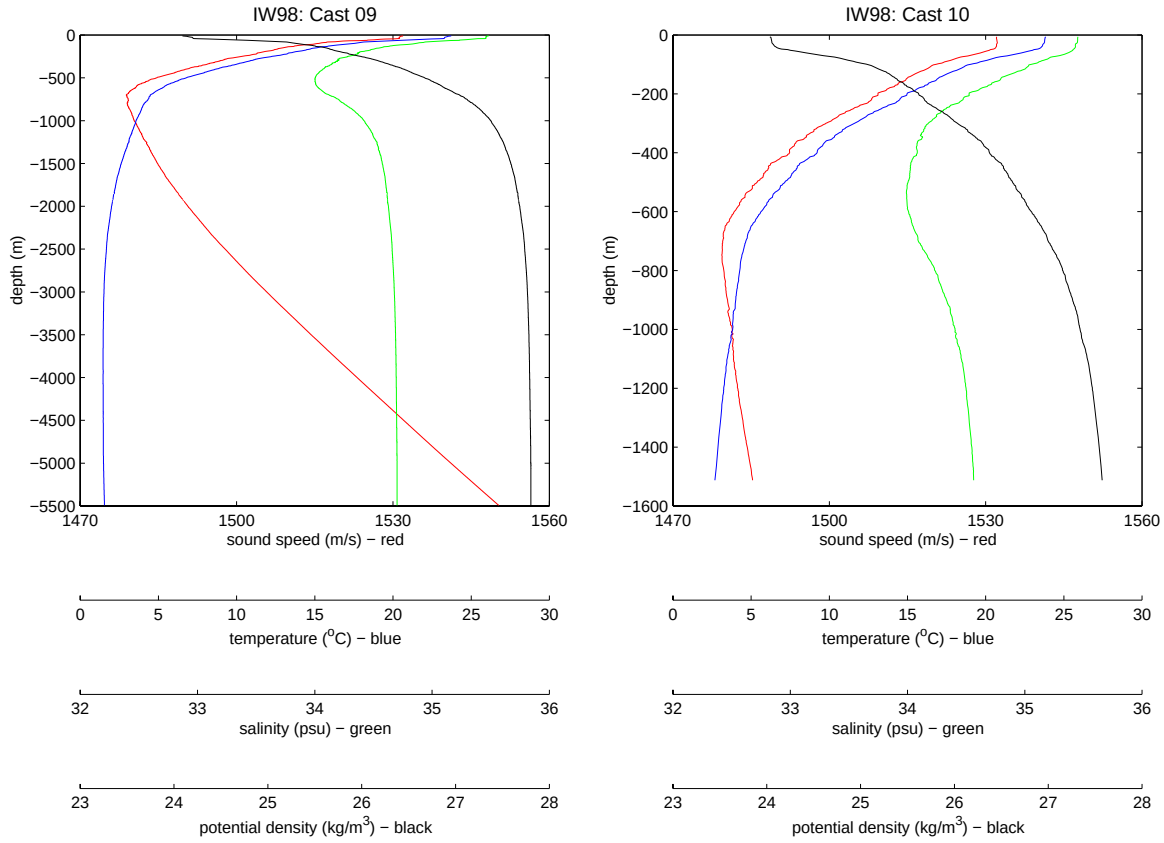

Figure 105. Same as in Figure 101, except for Cast no. 9, file name 2310936 (left) and Cast no. 10, file name 2312011 (right).

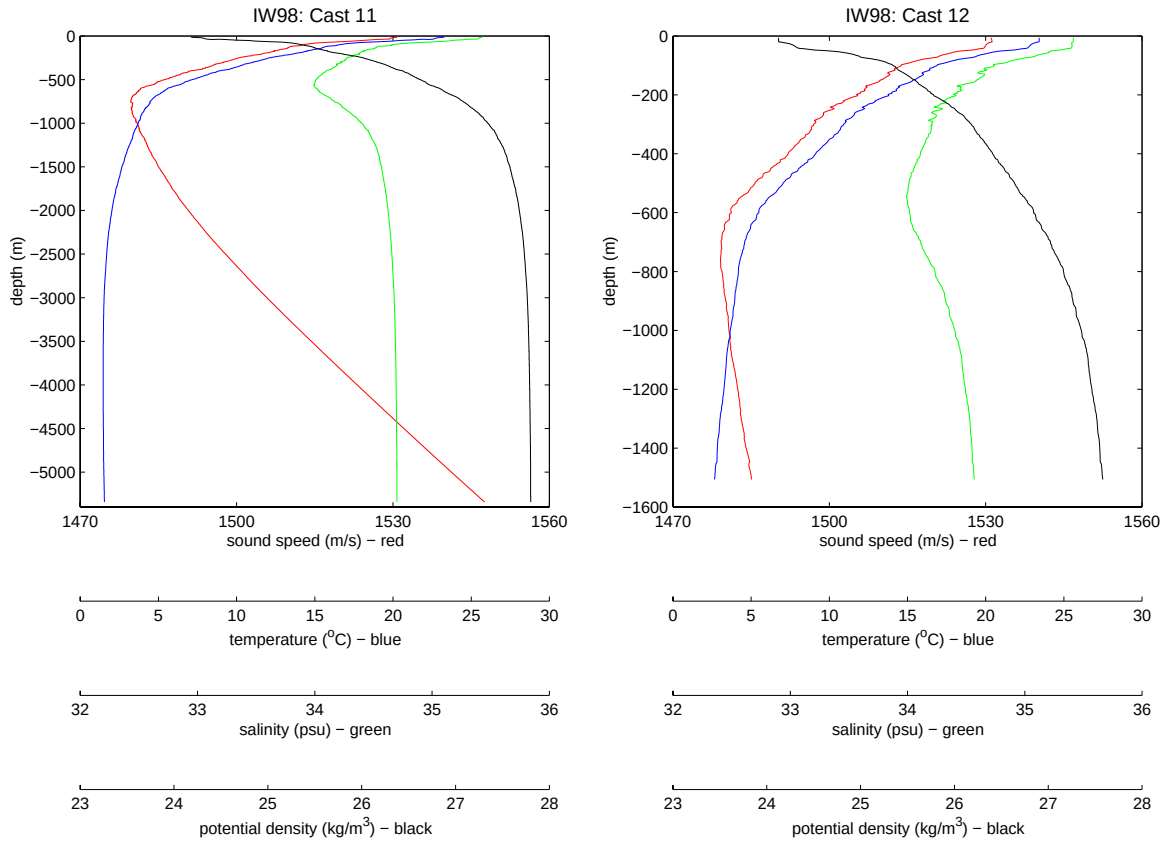

Figure 106. Same as in Figure 101, except for Cast no. 11, file name 2320951 (left) and Cast no. 12, file name 2331127 (right).

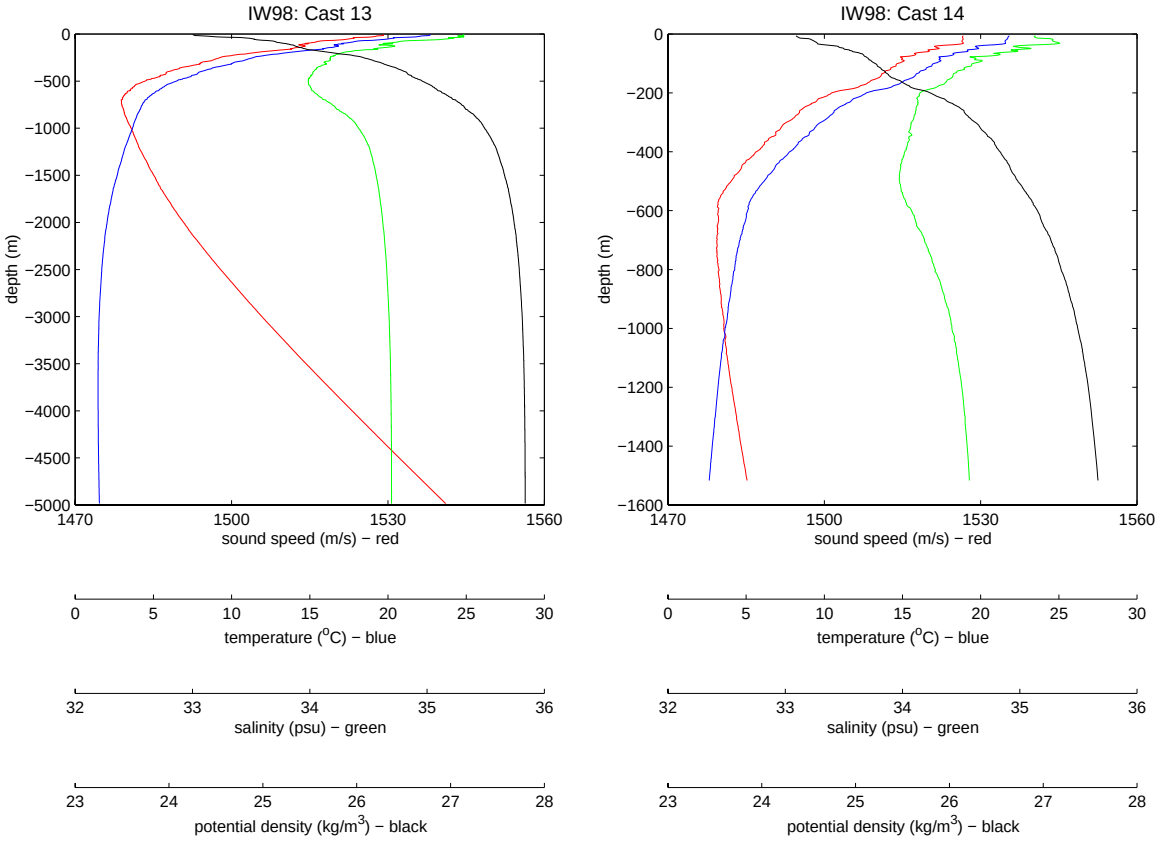

Figure 107. Same as in Figure 101, except for Cast no. 13, file name 2332143 (left) and Cast no. 14, file name 2340750 (right).

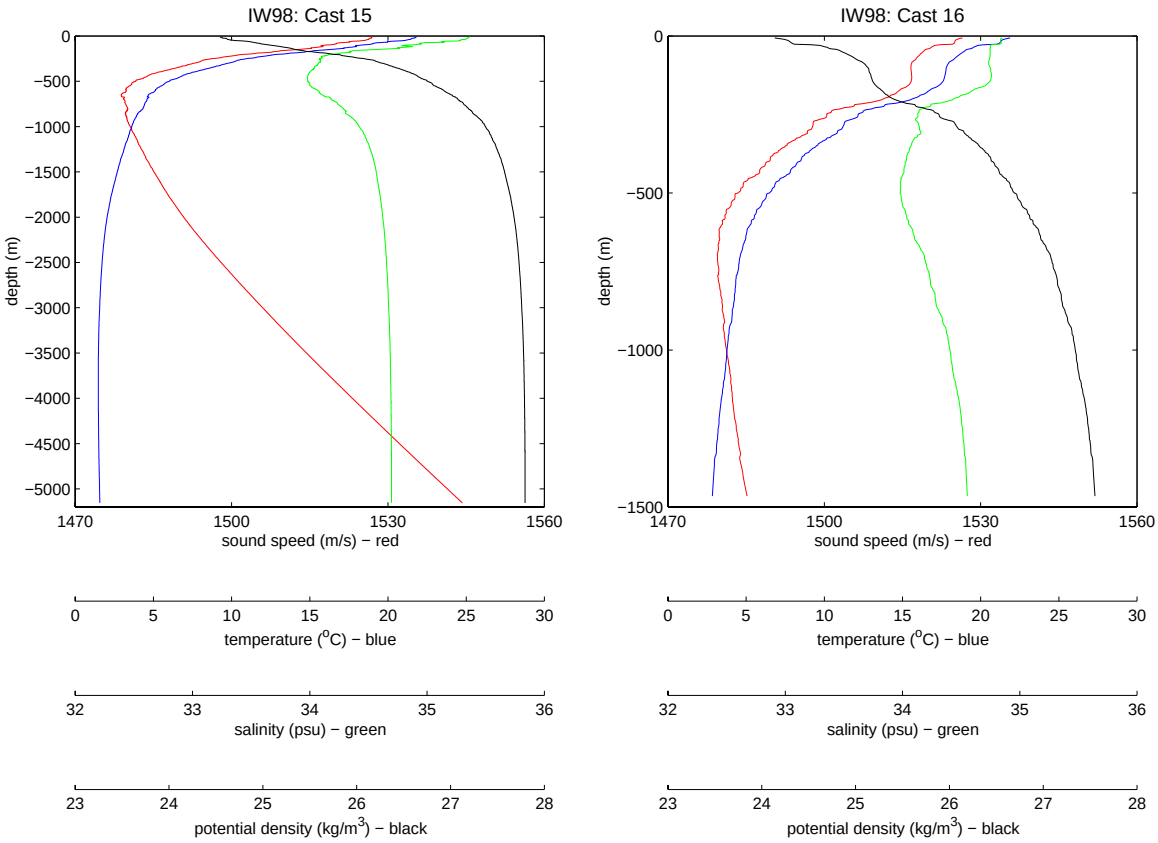

Figure 108. Same as in Figure 101, except for Cast no. 15, file name 2341703 (left) and Cast no. 16, file name 2350129 (right).

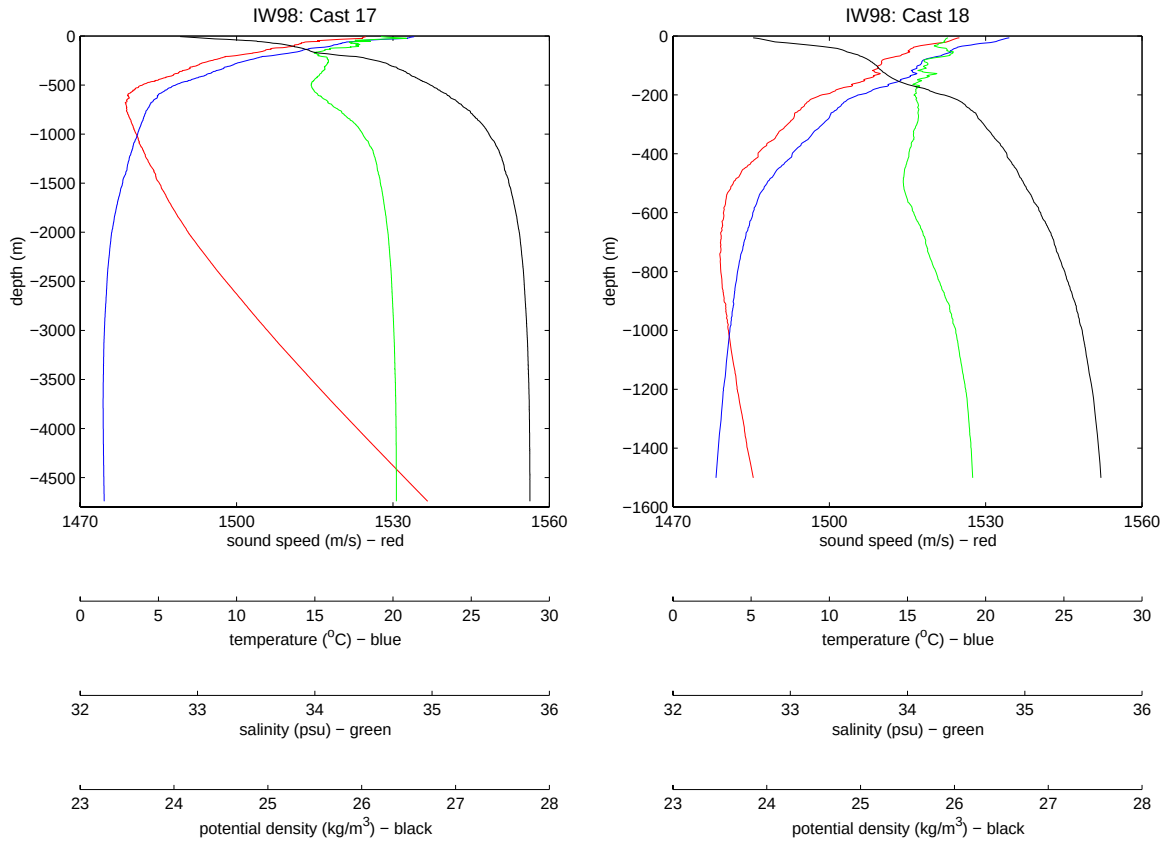

Figure 109. Same as in Figure 101, except for Cast no. 17, file name 2351111 (left) and Cast no. 18, file name 2352157 (right).

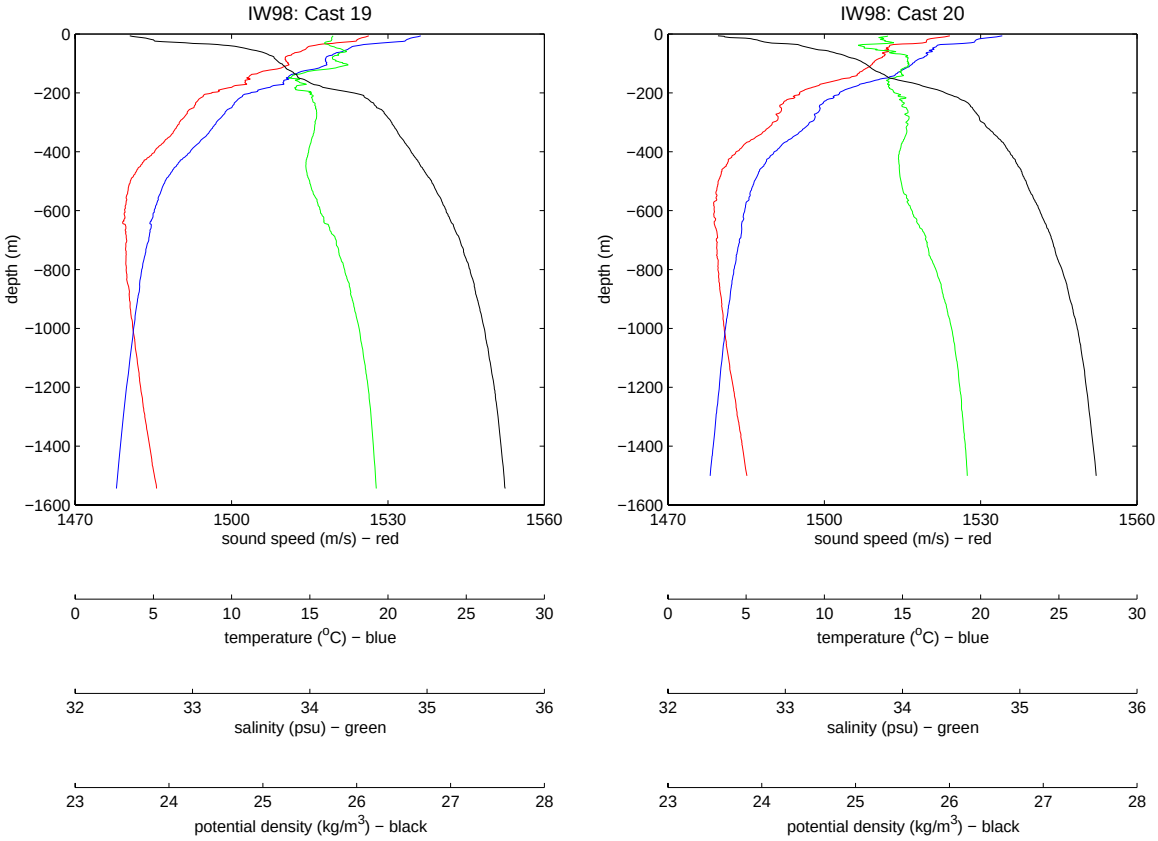

Figure 110. Same as in Figure 101, except for Cast no. 19, file name 2360750 (left) and Cast no. 20, file name 2362029 (right).

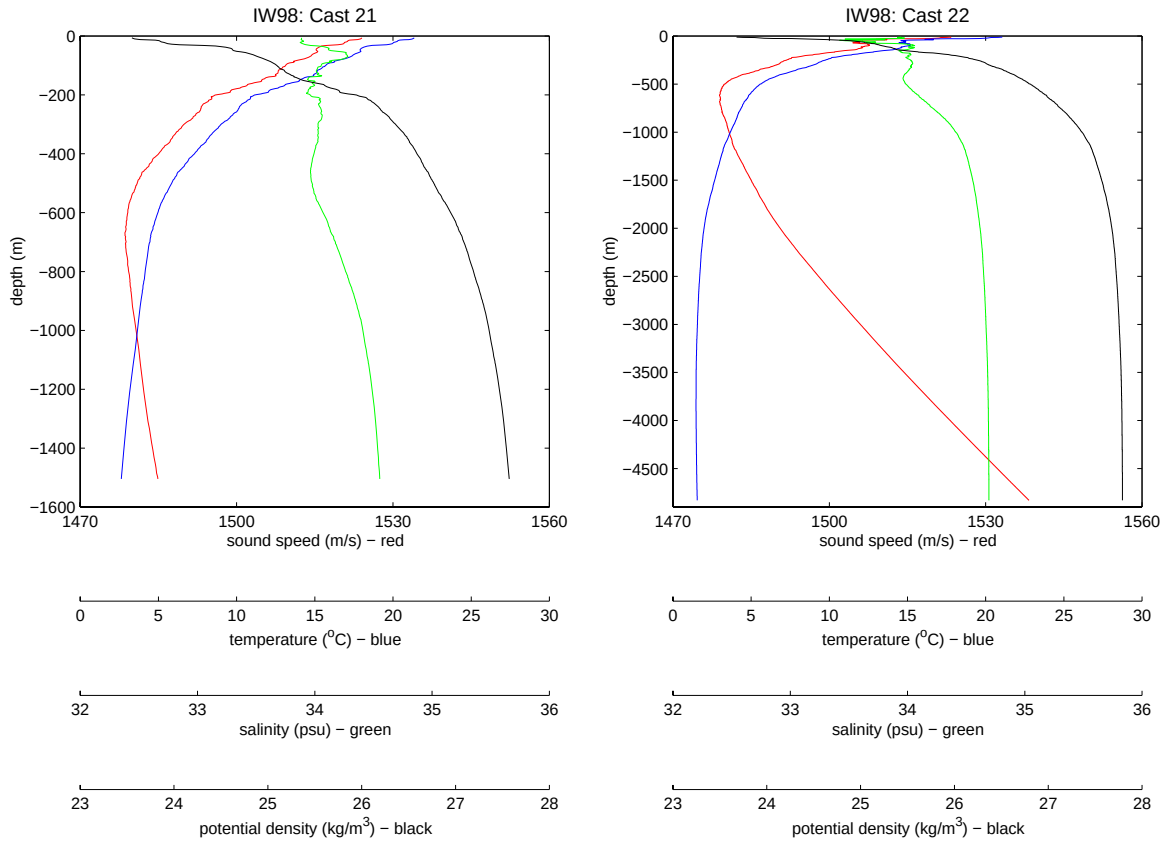

Figure 111. Same as in Figure 101, except for Cast no. 21, file name 2370050 (left) and Cast no. 22, file name 2371313 (right).

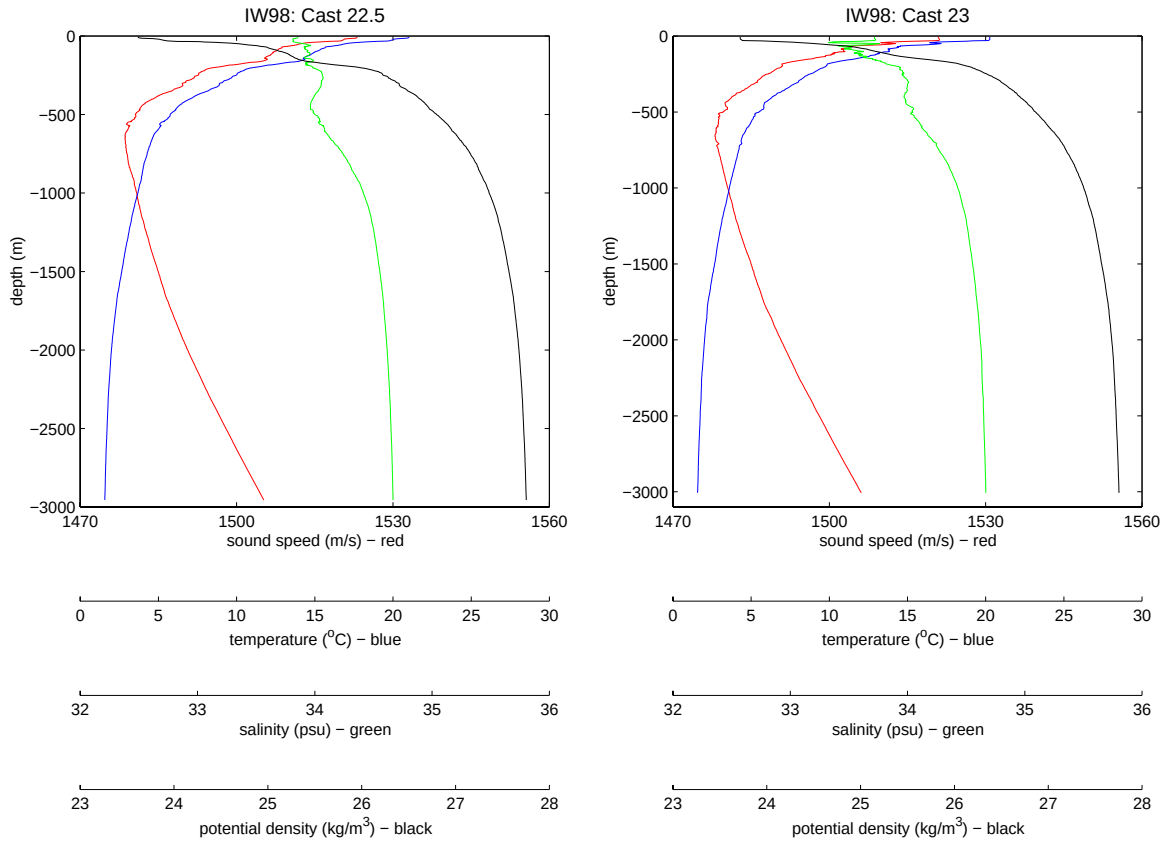

Figure 112. Same as in Figure 101, except for Cast no. 22.5, file name 2380134 (left) and Cast no. 23, file name 2380955 (right).

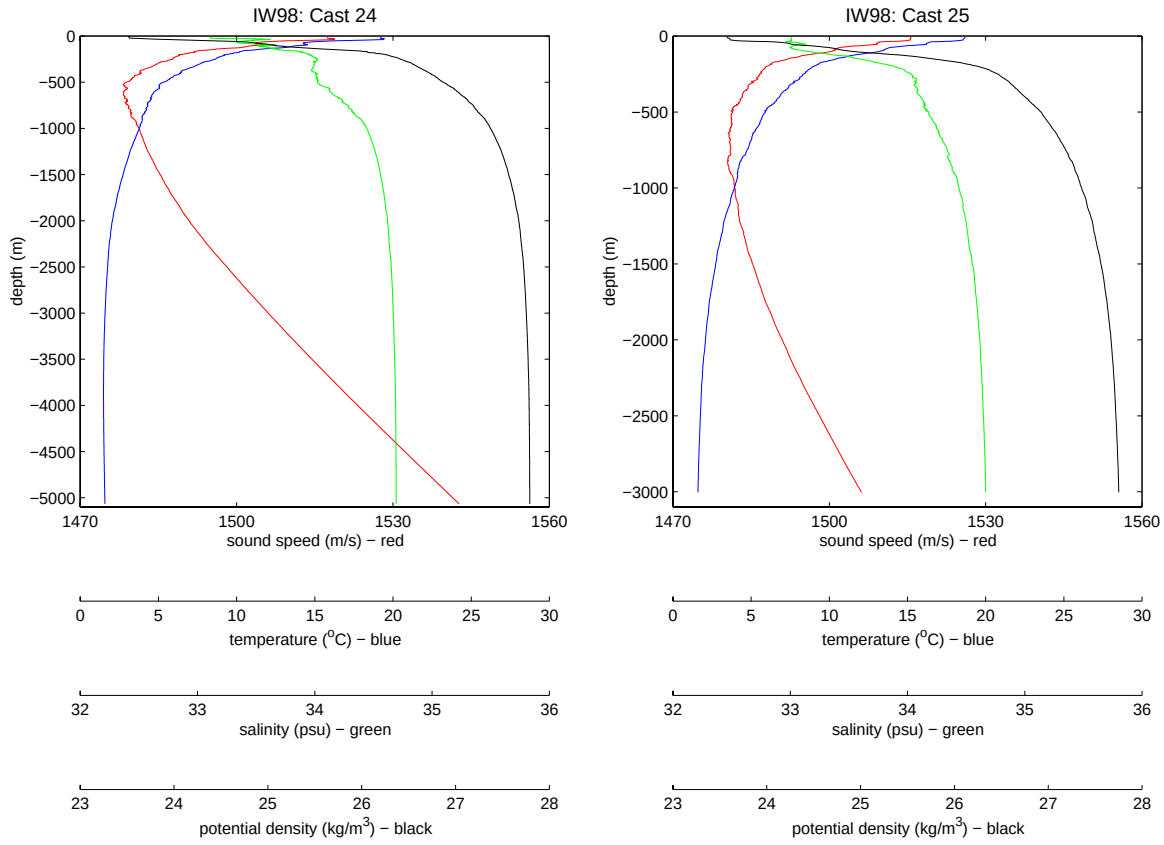

Figure 113. Same as in Figure 101, except for Cast no. 24, file name 2381921 (left) and Cast no. 25, file name 2390650 (right).

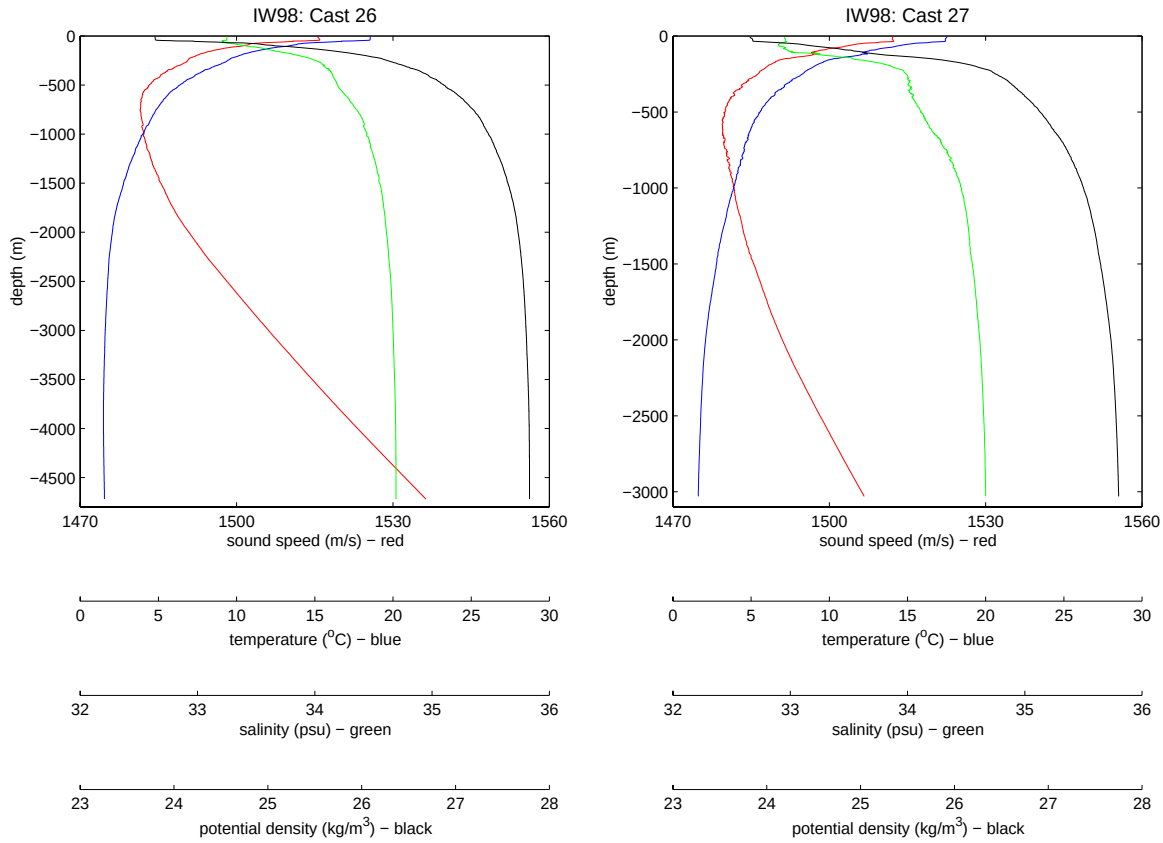

Figure 114. Same as in Figure 101, except for Cast no. 26, file name 2391658 (left) and Cast no. 27, file name 2400036 (right).

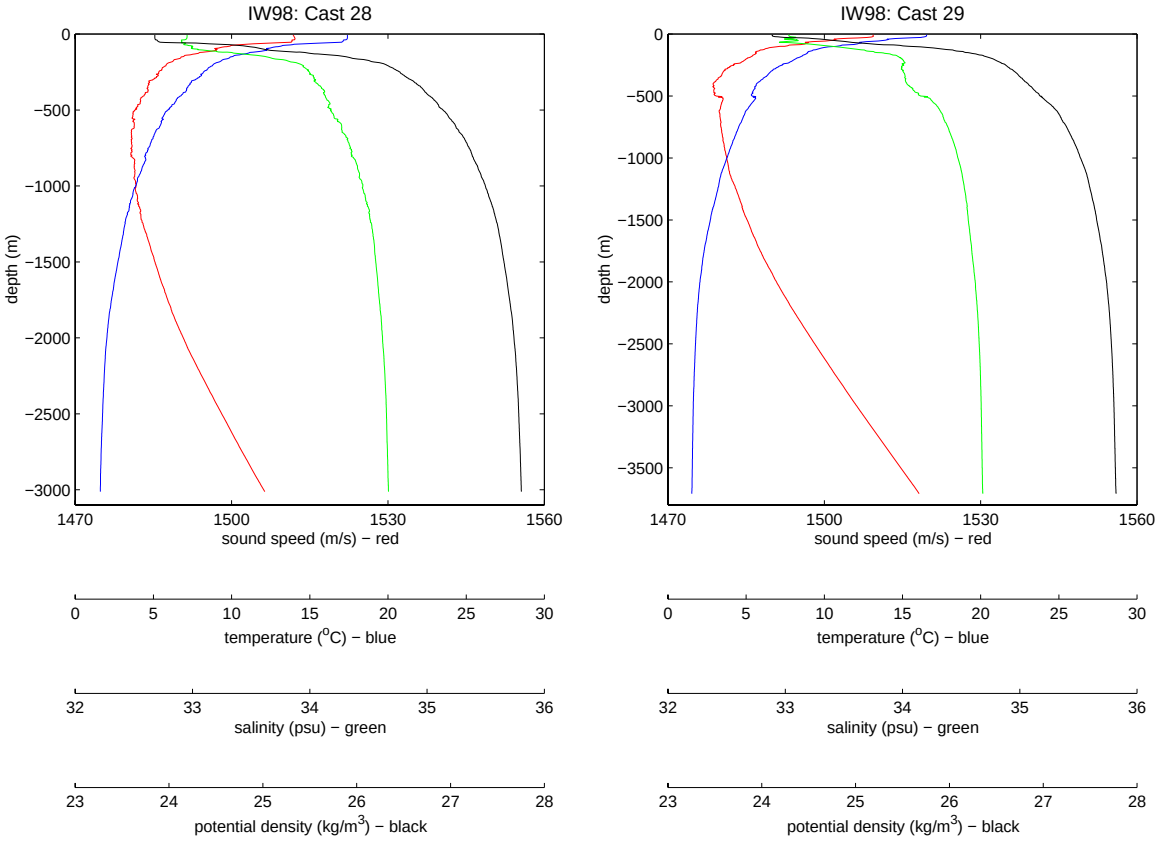

Figure 115. Same as in Figure 101, except for Cast no. 28, file name 2401051 (left) and Cast no. 29, file name 2401956 (right).

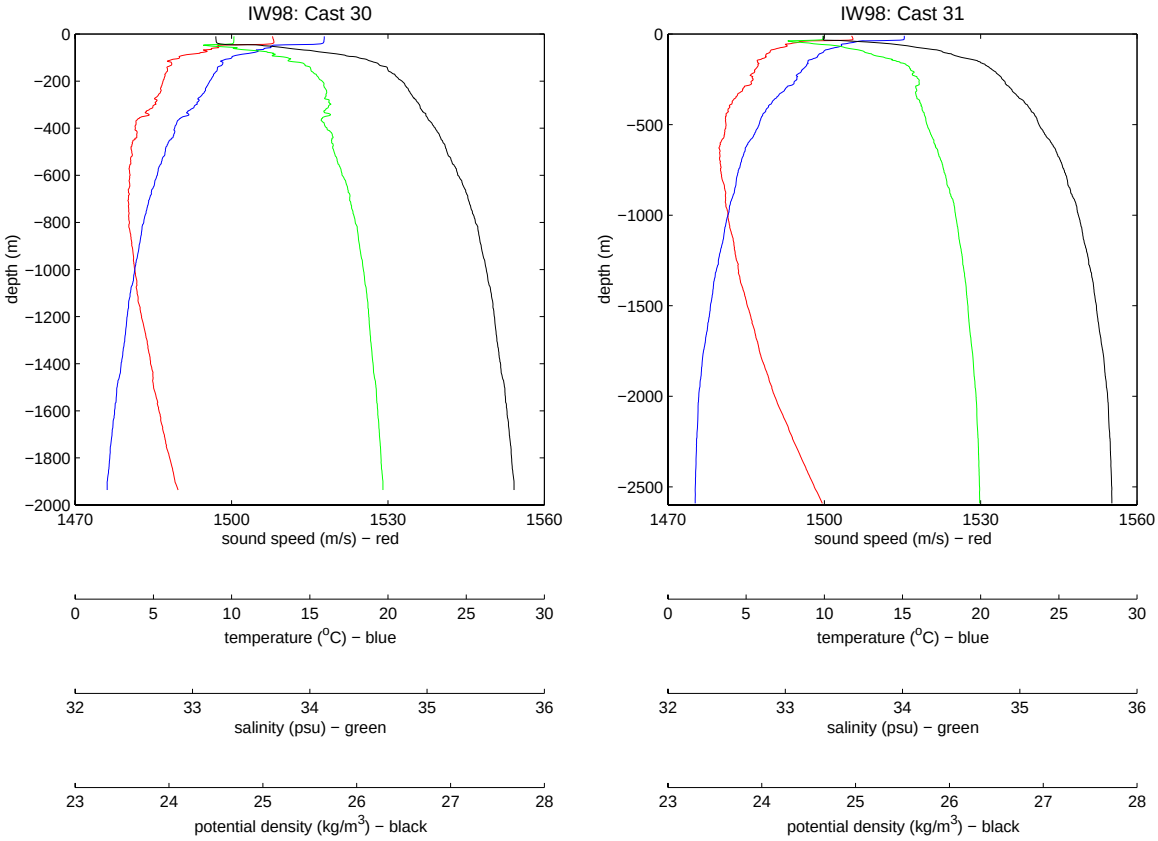

Figure 116. Same as in Figure 101, except for Cast no. 30, file name 2410551 (left) and Cast no. 31, file name 2421143 (right).

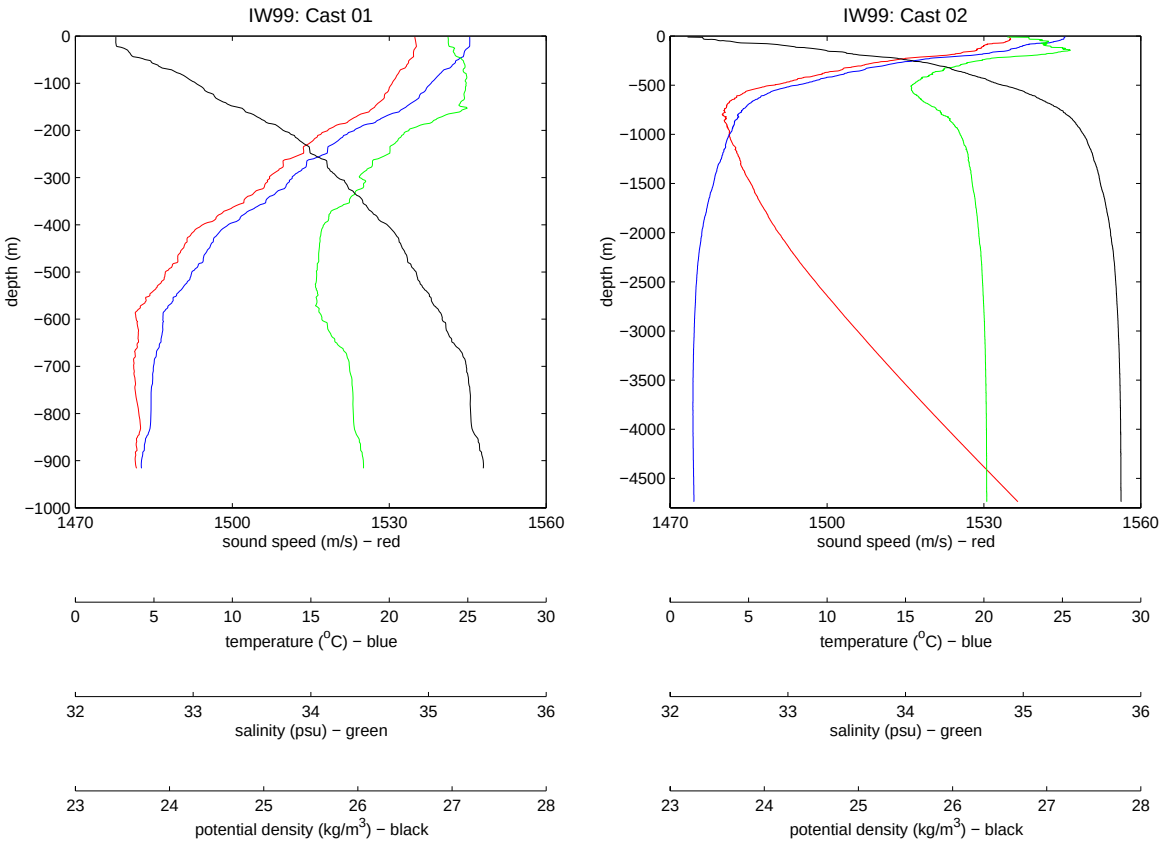

Figure 117. Processed data from Cast no. 1, file name 1701235 (left) and Cast no. 2, file name 1702114 (right) from IW99. Sound speed is in red, temperature is in blue, salinity is in green and density is in black.

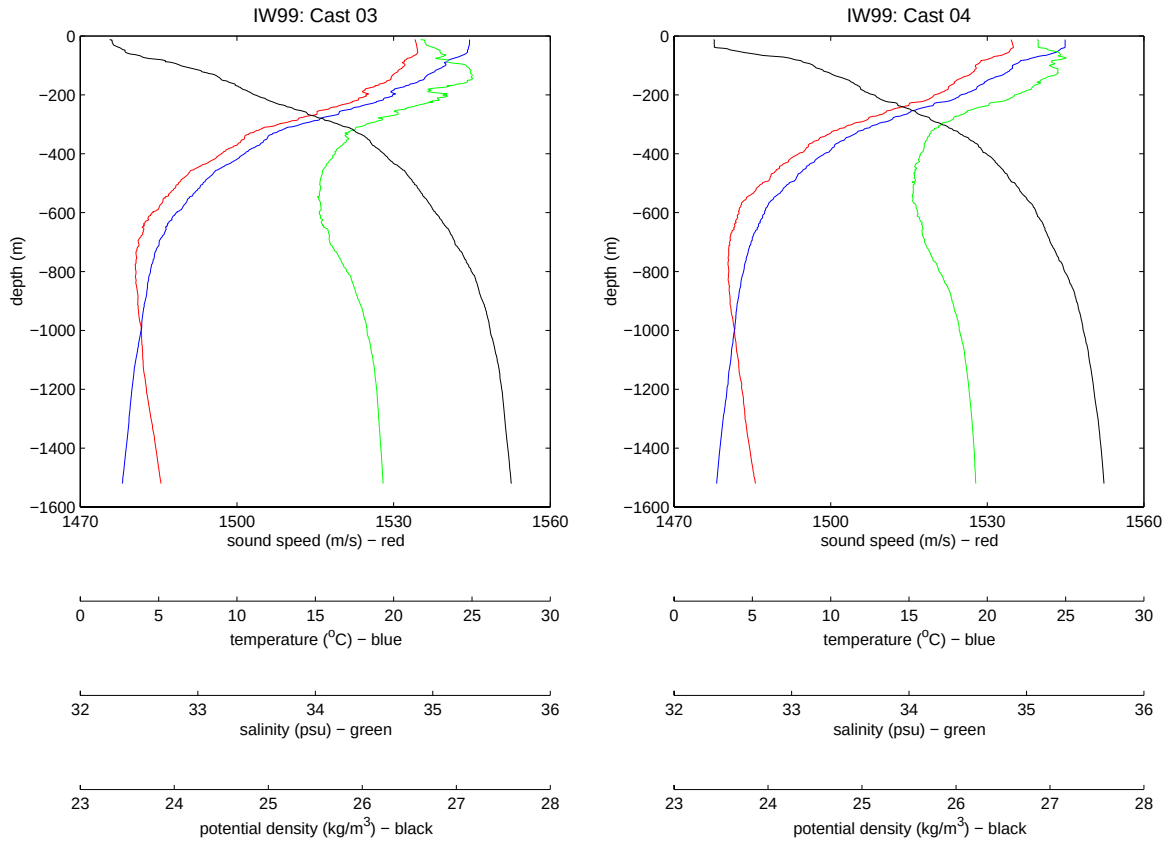

Figure 118. Same as in Figure 117, except for Cast no. 3, file name 1710733 (left) and Cast no. 4, file name 1711653 (right).

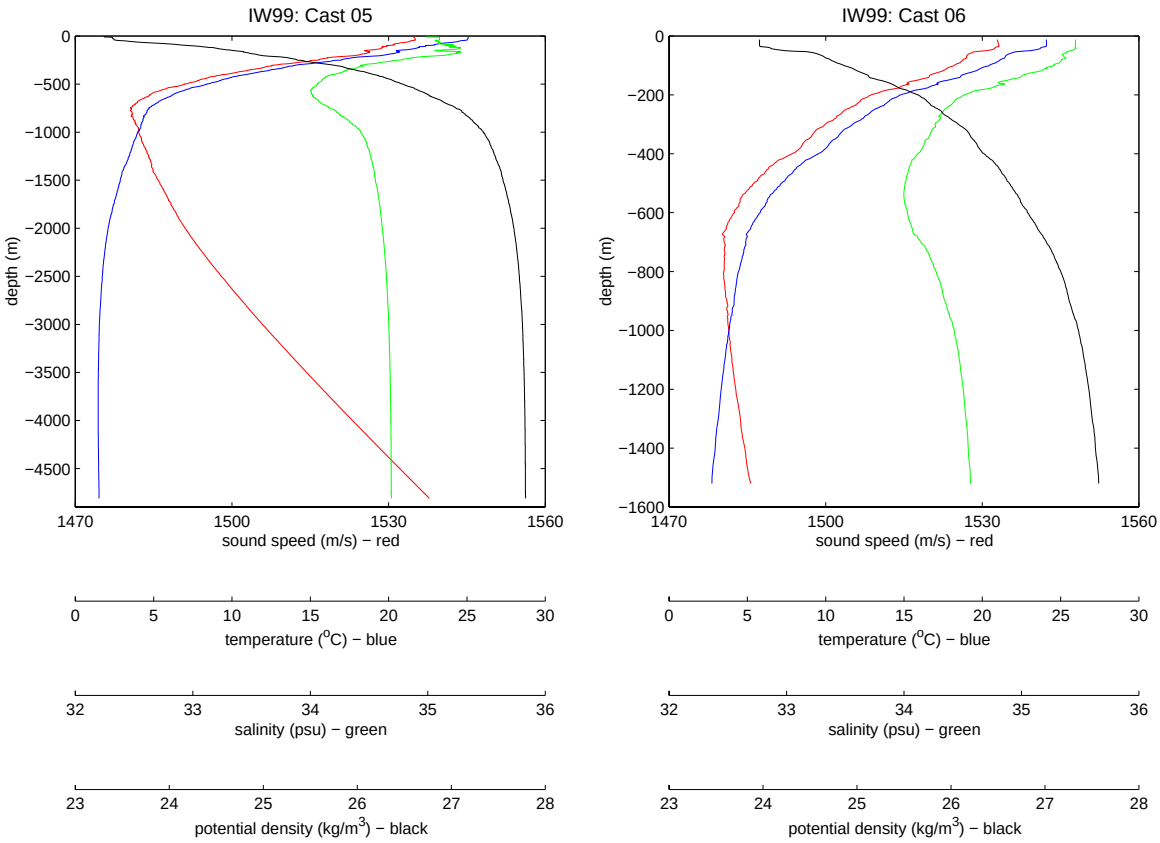

Figure 119. Same as in Figure 117, except for Cast no. 5, file name 1720131 (left) and Cast no. 6, file name 1721556 (right).

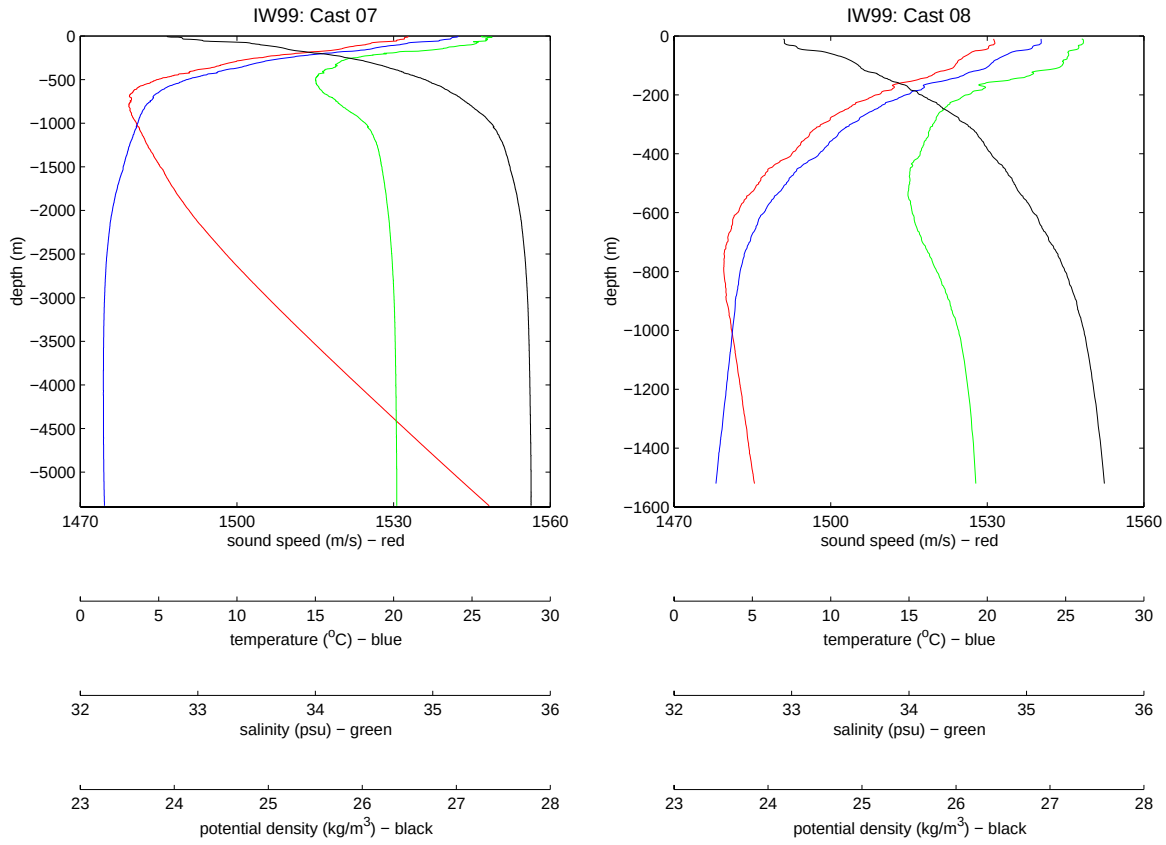

Figure 120. Same as in Figure 117, except for Cast no. 7, file name 1722233 (left) and Cast no. 8, file name 1731008 (right).

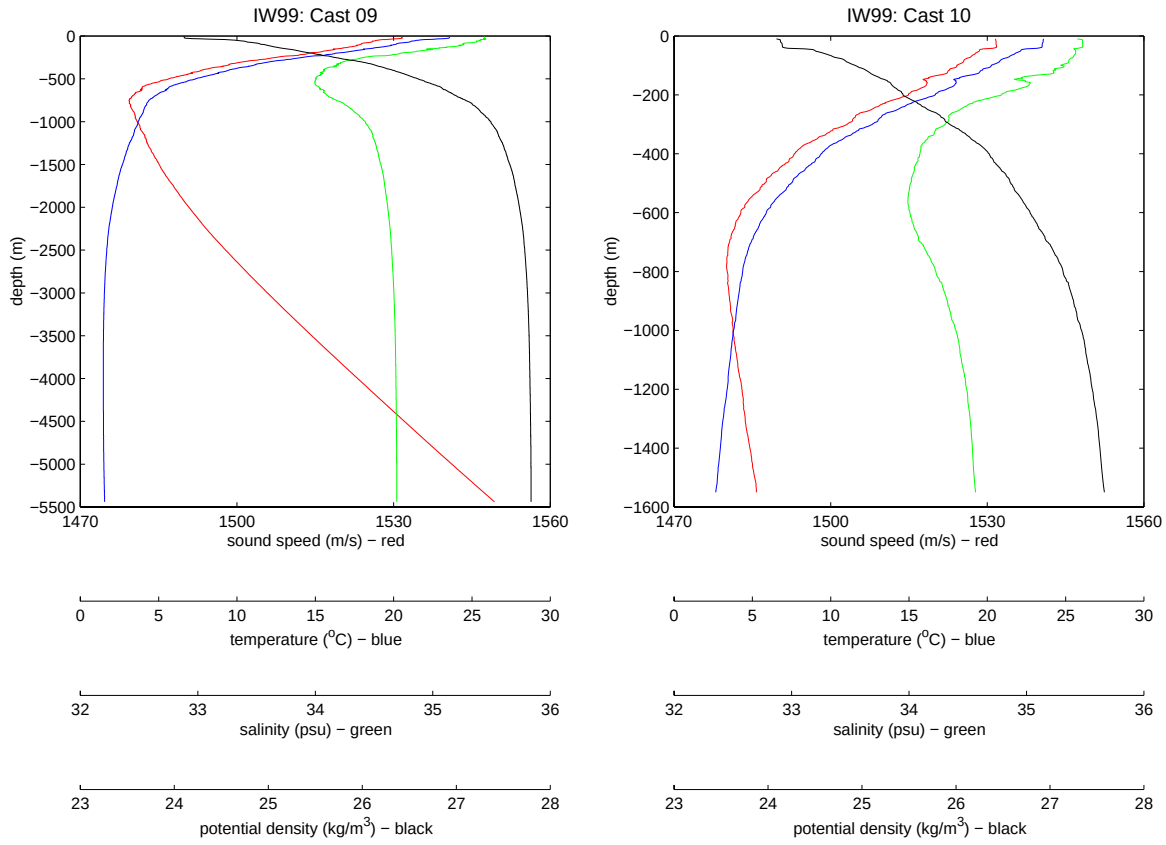

Figure 121. Same as in Figure 117, except for Cast no. 9, file name 1731830 (left) and Cast no. 10, file name 1740409 (right).

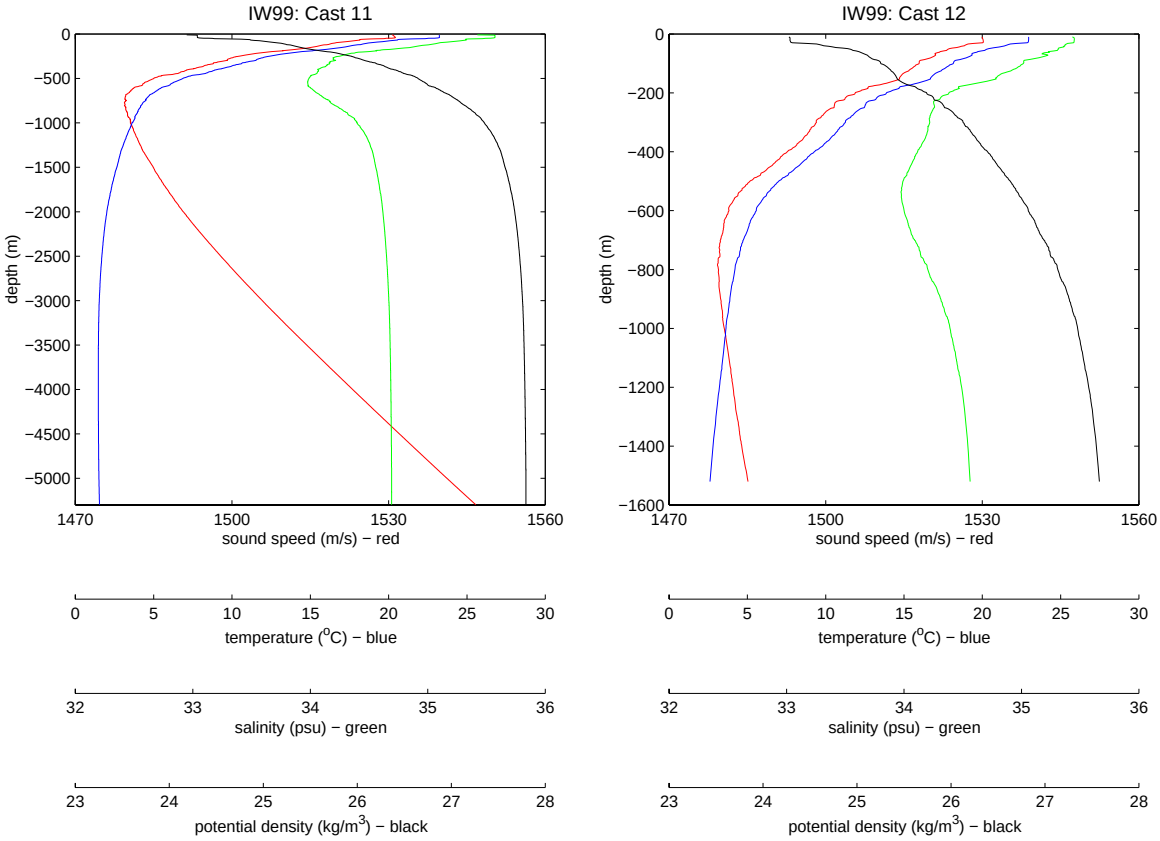

Figure 122. Same as in Figure 117, except for Cast no. 11, file name 1741143 (left) and Cast no. 12, file name 1750626 (right).

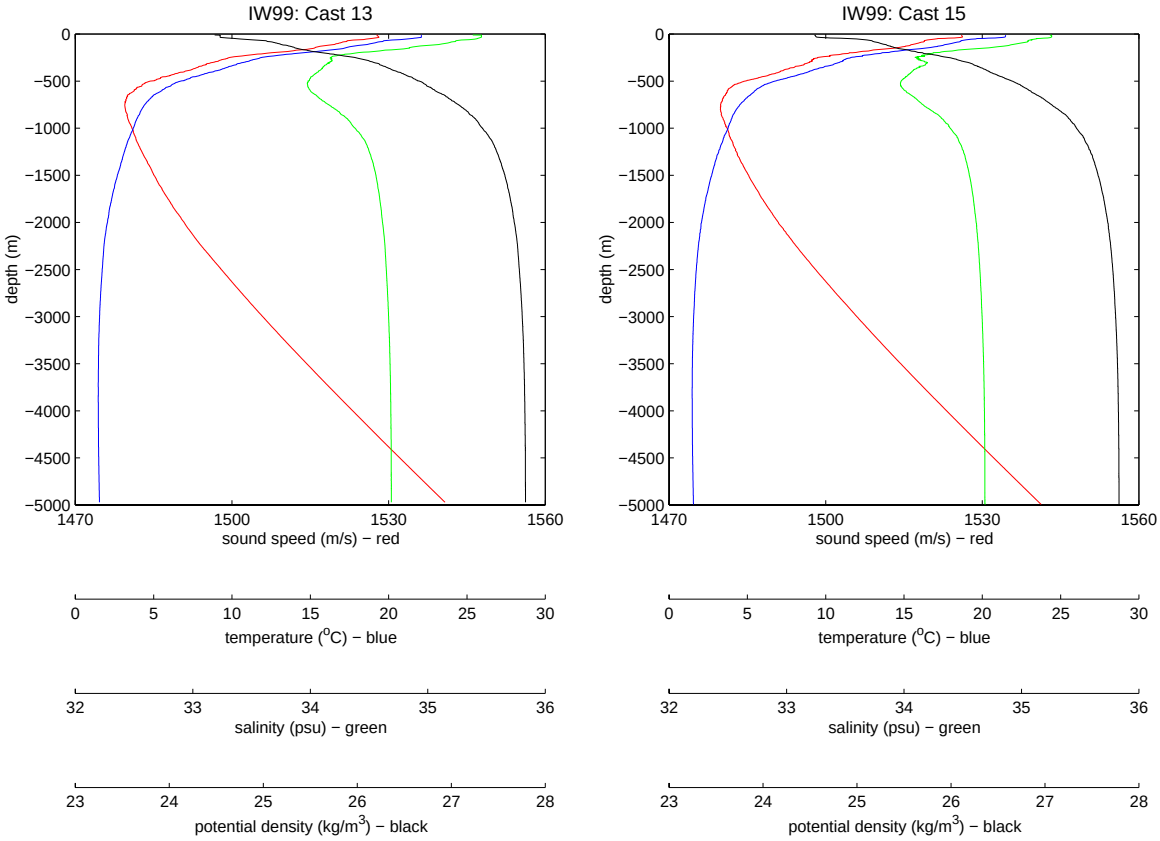

Figure 123. Same as in Figure 119, except for Cast no. 13, file name 1751511 (left) and Cast no. 15, file name 1760815 (right).

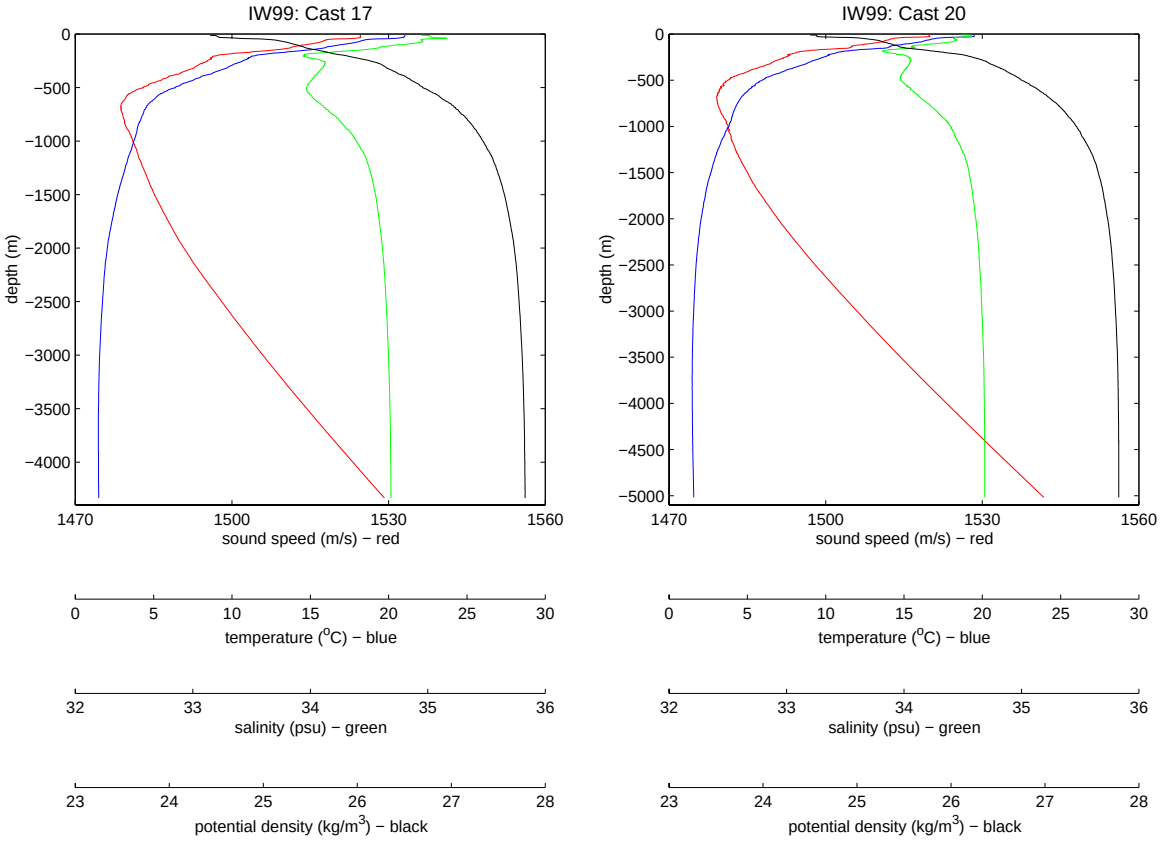

Figure 124. Same as in Figure 117, except for Cast no. 17, file name 1770016 (left) and Cast no. 20, file name 1772306 (right).

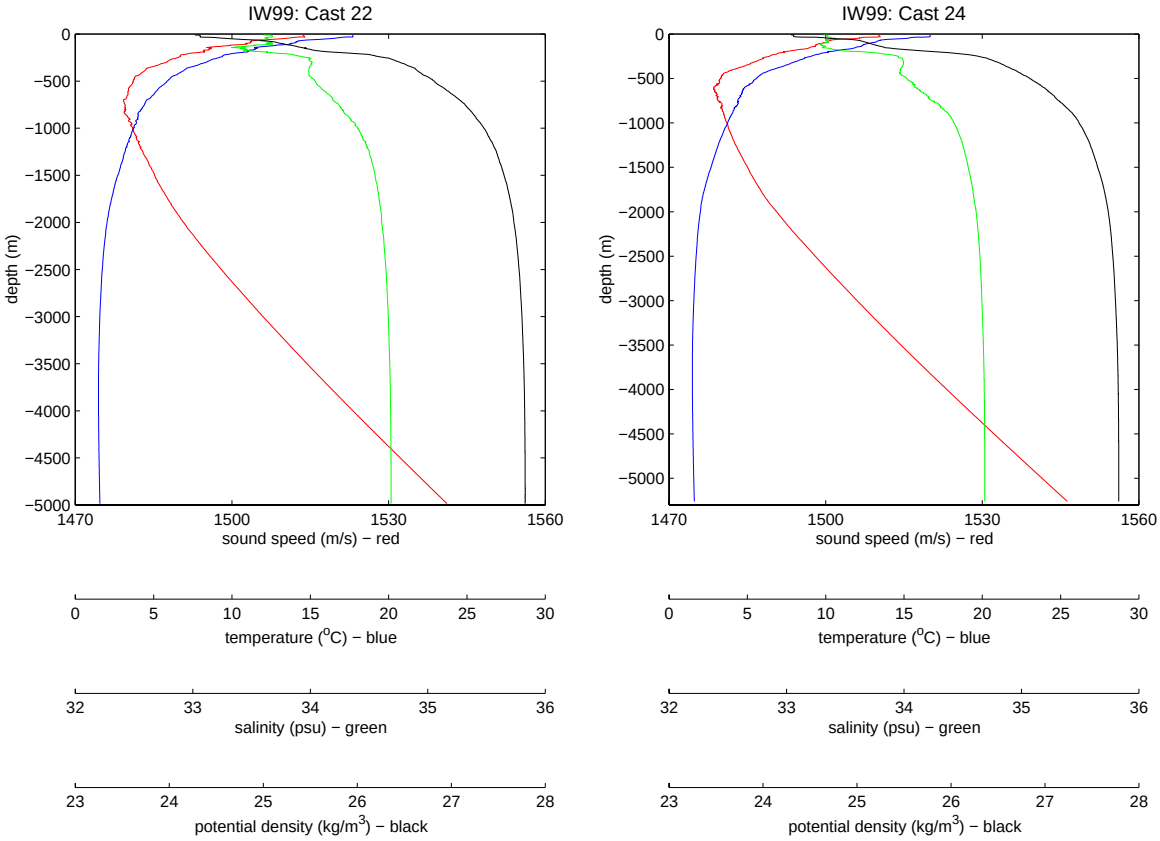

Figure 125. Same as in Figure 117, except for Cast no. 22, file name 1781404 (left) and Cast no. 24, file name 1791204 (right).

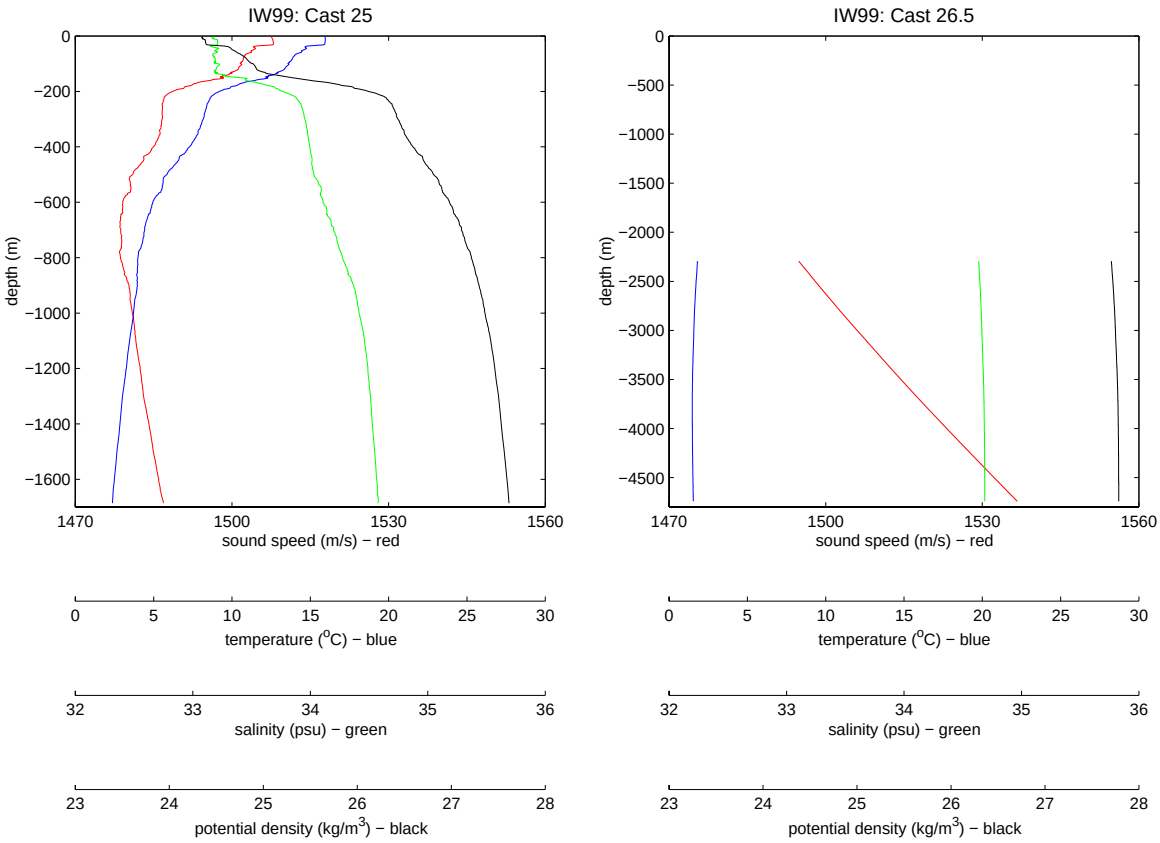

Figure 126. Same as in Figure 117, except for Cast no. 25, file name 1792250 (left) and Cast no. 26.5, file name 1800748 (right).

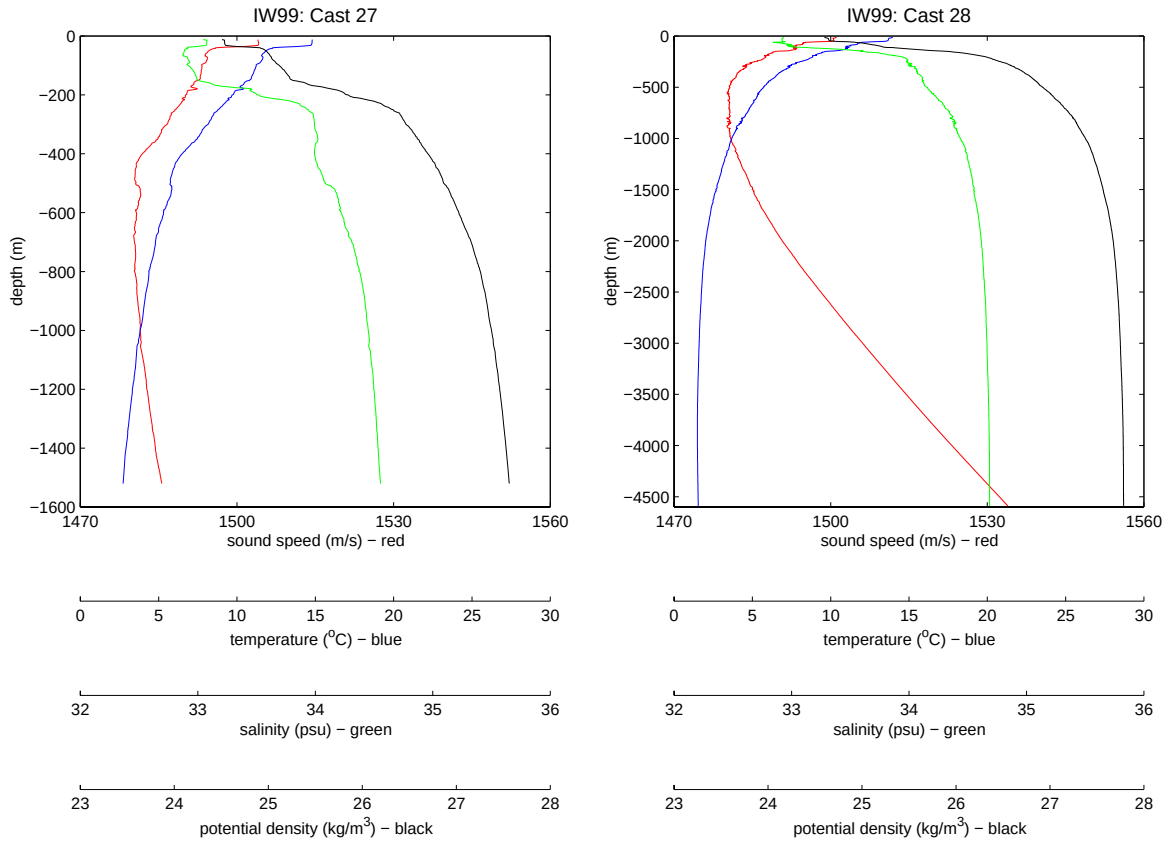

Figure 127. Same as in Figure 117, except for Cast no. 27, file name 1801641 (left) and Cast no. 28, file name 1810030 (right).

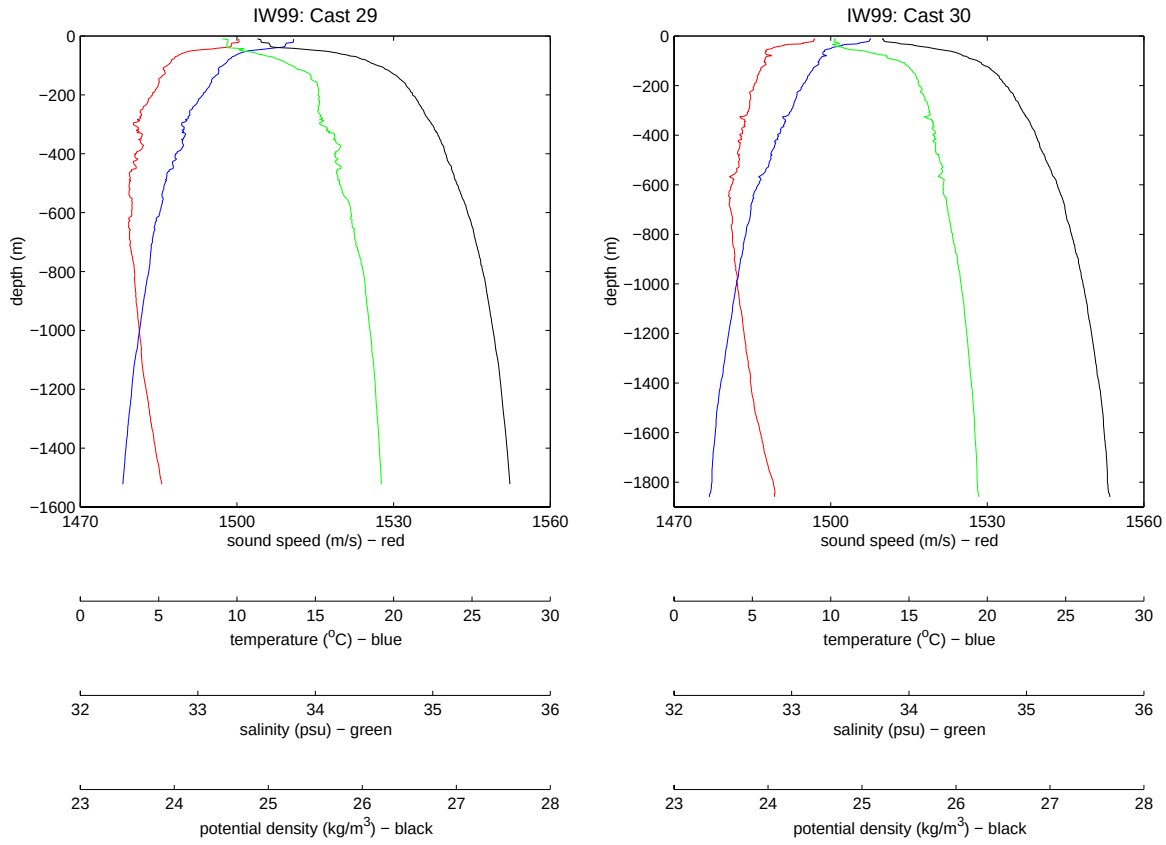

Figure 128. Same as in Figure 117, except for Cast no. 29, file name 1810946 (left) and Cast no. 30, file name 1811715 (right).

Appendix: Respective conductivity and temperature interpolated slopes and offsets

IW98		Sensor		Conductivity, Primary		Conductivity, Secondary		Temperature, Primary		Temperature, Secondary	
		S/N			484		485		843		844
		Pre-cruise cal date			15May98		15May98		14May98		14May98
		Post-cruise cal date			17Sep98		17Sep98		17Sep98		17Sep98
		n			124		124		125		125
					slope		slope		delta T		delta T
		Post-Cruise values			0.999826		1.000483		0.00069		0.00038
cast	file name	date	hr:mn	b	islope	b	islope	b	ioffset	b	ioffset
1	2280551	16Aug98	05:53	92	1.0001291	92	0.9996418	93	0.00051	93	0.00028
2	2281355	16Aug98	13:55	92	1.0001291	92	0.9996418	93	0.00051	93	0.00028
3	2282327	16Aug98	23:29	92	1.0001291	92	0.9996418	93	0.00051	93	0.00028
4	2290939	17Aug98	09:40	93	1.0001305	93	0.9996379	94	0.00052	94	0.00029
5	2291846	17Aug98	18:47	93	1.0001305	93	0.9996379	94	0.00052	94	0.00029
6	2300405	18Aug98	04:06	94	1.0001319	94	0.9996340	95	0.00052	95	0.00029
7	2301309	18Aug98	13:10	94	1.0001319	94	0.9996340	95	0.00052	95	0.00029
8	2310026	19Aug98	00:28	95	1.0001333	95	0.9996301	96	0.00053	96	0.00029
9	2310936	19Aug98	09:37	95	1.0001333	95	0.9996301	96	0.00053	96	0.00029
10	2312011	19Aug98	20:13	95	1.0001333	95	0.9996301	96	0.00053	96	0.00029
11	2320951	20Aug98	09:52	96	1.0001347	96	0.9996262	97	0.00054	97	0.00029
12	2331127	21Aug98	11:28	97	1.0001361	97	0.9996224	98	0.00054	98	0.00030
13	2332143	21Aug98	21:46	97	1.0001361	97	0.9996224	98	0.00054	98	0.00030
14	2340750	22Aug98	07:52	98	1.0001375	98	0.9996185	99	0.00055	99	0.00030
15	2341703	22Aug98	17:04	98	1.0001375	98	0.9996185	99	0.00055	99	0.00030
16	2350129	23Aug98	01:31	99	1.0001389	99	0.9996146	100	0.00055	100	0.00030
17	2351111	23Aug98	11:13	99	1.0001389	99	0.9996146	100	0.00055	100	0.00030
18	2352157	23Aug98	21:58	99	1.0001389	99	0.9996146	100	0.00055	100	0.00030
19	2360705	24Aug98	07:06	100	1.0001403	100	0.9996107	101	0.00056	101	0.00031
20	2362029	24Aug98	20:30	100	1.0001403	100	0.9996107	101	0.00056	101	0.00031
21	2370050	25Aug98	00:48	101	1.0001418	101	0.9996068	102	0.00056	102	0.00031
22	2371313	25Aug98	13:15	101	1.0001418	101	0.9996068	102	0.00056	102	0.00031
22.5	2380134	26Aug98	01:35	102	1.0001432	102	0.9996029	103	0.00057	103	0.00031
23	2380955	26Aug98	09:55	102	1.0001432	102	0.9996029	103	0.00057	103	0.00031
24	2381921	26Aug98	19:23	102	1.0001432	102	0.9996029	103	0.00057	103	0.00031
25	2390650	27Aug98	06:47	103	1.0001446	103	0.9995990	104	0.00057	104	0.00032
26	2391658	27Aug98	16:59	103	1.0001446	103	0.9995990	104	0.00057	104	0.00032
27	2400036	28Aug98	00:37	104	1.0001460	104	0.9995951	105	0.00058	105	0.00032
28	2401051	28Aug98	10:52	104	1.0001460	104	0.9995951	105	0.00058	105	0.00032
29	2401956	28Aug98	19:57	104	1.0001460	104	0.9995951	105	0.00058	105	0.00032
30	2410551	29Aug98	05:53	105	1.0001474	105	0.9995912	106	0.00059	106	0.00032
31	2421143	30Aug98	11:44	106	1.0001488	106	0.9995873	107	0.00059	107	0.00033

IW99		Sensor		Conductivity, Primary		Conductivity, Secondary		Temperature, Primary		Temperature, Secondary	
		S/N			484		485		843		844
		Pre-cruise cal date			06May99		11May99		05May99		05May99
		Post-cruise cal date			13Jul99		13Jul99		13Jul99		13Jul99
		n			67		62		68		68
					slope		slope		delta T		detla T
		Post-Cruise values			0.999967		1.000483		-0.00004		0.00013
		S/N					1880				
		Pre-cruise cal date					25Nov98				
		Post-cruise cal date					13Jul99				
		n					229				
							slope				
		Post-Cruise values					1.000051				
cast	file name	date	hr:mn	b	islope	b	islope	b	ioffset	b	ioffset
1	1701235	19Jun99	12:36	43	1.0000212	38	1.0001208	44	-0.00003	44	0.00008
2	1702114	19Jun99	21:15	43	1.0000212	38	1.0001208	44	-0.00003	44	0.00008
3	1710733	20Jun99	07:36	44	1.0000217	39	1.0001239	45	-0.00003	45	0.00009
4	1711653	20Jun99	16:55	44	1.0000217	39	1.0001239	45	-0.00003	45	0.00009
5	1720131	21Jun99	01:32	45	1.0000222	40	1.0001271	46	-0.00003	46	0.00009
6	1721556	21Jun99	15:58	45	1.0000222	40	1.0001271	46	-0.00003	46	0.00009
7	1722233	21Jun99	22:34	45	1.0000222	40	1.0001271	46	-0.00003	46	0.00009
8	1731008	22Jun99	10:10	46	1.0000227	41	1.0001303	47	-0.00003	47	0.00009
9	1731830	22Jun99	18:32	46	1.0000227	41	1.0001303	47	-0.00003	47	0.00009
10	1740409	23Jun99	04:11	47	1.0000232	42	1.0001335	48	-0.00003	48	0.00009
11	1741143	23Jun99	11:45	47	1.0000232	42	1.0001335	48	-0.00003	48	0.00009
12	1750626	24Jun99	06:29	48	1.0000236	43	1.0001367	49	-0.00003	49	0.00009
13	1751511	24Jun99	15:12	48	1.0000236	43	1.0001367	49	-0.00003	49	0.00009
15	1760815	25Jun99	08:16	49	1.0000241	44	1.0001398	50	-0.00003	50	0.00010
17	1770016	26Jun99	00:18	50	1.0000246	45	1.0001430	51	-0.00003	51	0.00010
20	1772306	26Jun99	23:07	50	1.0000246	45	1.0001430	51	-0.00003	51	0.00010
22	1772306	27Jun99	14:05	51	1.0000251	46	1.0001462	52	-0.00003	52	0.00010
24	1791204	28Jun99	12:46	52	1.0000256	214	0.9999523	53	-0.00003	53	0.00010
25	1792250	28Jun99	22:53	52	1.0000256	214	0.9999523	53	-0.00003	53	0.00010
26.5	1800748	29Jun99	07:49	53	1.0000261	215	0.9999521	54	-0.00003	54	0.00010
27	1801641	29Jun99	16:42	53	1.0000261	215	0.9999521	54	-0.00003	54	0.00010
28	1810030	30Jun99	00:33	54	1.0000266	216	0.9999519	55	-0.00003	55	0.00011
29	1810946	30Jun99	09:47	54	1.0000266	216	0.9999519	55	-0.00003	55	0.00011
30	1811715	30Jun99	17:17	54	1.0000266	216	0.9999519	55	-0.00003	55	0.00011

REPORT DOCUMENTATION PAGE

Form Approved
OPM No. 0704-0188

1. AGENCY USE ONLY *(Leave blank)*	2. REPORT DATE	3. REPORT TYPE AND DATES COVERED
	April 2007	Technical Memorandum

4. TITLE AND SUBTITLE

North Pacific Acoustic Laboratory CTD Data: R/V *Moana Wave* Cruise IW98 (August 15 – 30, 1998) and R/V *Melville* Cruise IW99 (June 18 – July 3, 1999)

5. FUNDING NUMBERS

N00014-97-1-0259

6. AUTHOR(S)

S. Dickinson, B.M. Howe, and J.A. Colosi

7. PERFORMING ORGANIZATION NAME(S) AND ADDRESS(ES)

Applied Physics Laboratory
University of Washington
1013 NE 40th Street
Seattle, WA 98105-6698

8. PERFORMING ORGANIZATION REPORT NUMBER

APL-UW TM 1-07

9. SPONSORING / MONITORING AGENCY NAME(S) AND ADDRESS(ES)

Dr. Ching-Sang Chiu (Code 321OA)
Office of Naval Research
875 North Randolph Street
Arlington, VA 22203-1995

10. SPONSORING / MONITORING AGENCY REPORT NUMBER

11. SUPPLEMENTARY NOTES

12a. DISTRIBUTION / AVAILABILITY STATEMENT

Approved for public release; distribution is unlimited.

12b. DISTRIBUTION CODE

13. ABSTRACT *(Maximum 200 words)*

Two research cruises were conducted in the summers of 1998 and 1999 as part of the North Pacific Acoustic Laboratory (NPAL) project. The cruises' objective was to test the theory that predicts acoustic fluctuations from the internal wave sound speed or temperature fluctuations. Here we discuss the *in situ* profile measurements of temperature, salinity, and derived sound speed taken with conductivity temperature density (CTD) instruments dropped off the side of the ships as they steamed between the NPAL Acoustic Thermometry of Ocean Climate source off Kauai and a billboard receiving array on Sur Ridge off Point Sur, California. The first cruise, IW98, was aboard the University of Hawaii research vessel *Moana Wave* and the second, IW99, was aboard the R/V *Melville*.

14. SUBJECT TERMS

NPAL, ATOC, internal wave, sound speed, CTD, IW98, IW99

15. NUMBER OF PAGES

152

16. PRICE CODE

17. SECURITY CLASSIFICATION OF REPORT	18. SECURITY CLASSIFICATION OF THIS PAGE	19. SECURITY CLASSIFICATION OF ABSTRACT	20. LIMITATION OF ABSTRACT
Unclassified	Unclassified	Unclassified	SAR